Julian D. Perry · Arun D. Singh
Editors

Clinical Ophthalmic Oncology

Orbital Tumors

Second Edition

Springer

Clinical Ophthalmic Oncology

Julian D. Perry • Arun D. Singh
Editors

Clinical Ophthalmic Oncology

Orbital Tumors

Second Edition

Springer

Editors
Julian D. Perry, MD
Division of Opthalmology
Cole Eye Institute
Cleveland Clinic Foundation
Cleveland, OH
USA

Arun D. Singh, MD
Department of Ophthalmic Oncology
Cole Eye Institute
Cleveland Clinic Foundation
Cleveland, OH
USA

ISBN 978-3-642-40491-7 ISBN 978-3-642-40492-4 (eBook)
DOI 10.1007/978-3-642-40492-4
Springer Heidelberg New York Dordrecht London

Library of Congress Control Number: 2013956346

Printed on acid-free paper

Springer is part of Springer Science+Business Media (www.springer.com)

To Clifford, Agnes, Jim, and Cliff for my foundation; to Bob, Norm, and Neil for my education; to Julian, Liam, and Remy for my inspiration. (JDP)

To my parents who educated me beyond their means, my wife Annapurna, and my children, Nakul and Rahul, who make all my efforts worthwhile. (ADS)

Preface

The management of patients with an ophthalmic tumor presents particular challenges. Ophthalmic tumors are rare and diverse so that their diagnosis can be quite complex. Treatment usually requires special expertise and equipment and in many instances is controversial. The field is advancing rapidly because of accelerating progress in tumor biology, pharmacology, and instrumentation. Increasingly, the care of patients with an ocular or adnexal tumor is provided by a multidisciplinary team, comprising of ocular oncologists, general oncologists, radiotherapists, pathologists, psychologists, and other specialists. For all these reasons, we felt that there was a continued need for a textbook of ophthalmic oncology, which would amalgamate knowledge from several different disciplines, thereby helping the various specialists to understand each other better and to cooperate more efficiently eventually moving ophthalmic oncology in the realm of evidence-based medicine.

As several important studies have been published in recent years, the purpose of *Clinical Ophthalmic Oncology* (2nd edition) is to provide up-to-date information of the whole spectrum of the eyelid, conjunctival, intraocular, and orbital tumors including basic principles of chemotherapy, radiation therapy, cancer epidemiology, angiogenesis, and cancer genetics. Several chapters authored by radiation oncologists, medical physicists, pediatric oncologists, hematologist-oncologists, and medical geneticists have been included to provide a broader perspective.

Although each section of *Clinical Ophthalmic Oncology* now represents a stand-alone volume, each chapter has a similar layout with boxes that highlight the key features, tables that provide comparison, and flow diagrams that outline therapeutic approaches. Each chapter has been edited (with author's approval) to present a balanced view of current clinical practice, and special attention has been paid to make the text easily readable.

The authors followed a tight timeline to keep the contents of the book current. As we undertook this ambitious task of editing a multiauthor, multivolume textbook, we were supported and guided by the staff at Springer: Sverre Klemp, Ulrike Huesken, Ellen Blasig, the staff at SPi Global, India. Jennifer Brown kept the seemingly chaotic process under control.

It is our sincere hope that readers will find as much pleasure reading this volume as we had writing and editing it. If you find *Clinical Ophthalmic Oncology* informative, it is because (paraphrasing Isaac Newton), "we have seen further, by standing on the shoulders of the giants."

Cleveland, OH, USA Julian D. Perry, MD
Cleveland, OH, USA Arun D. Singh, MD

Contents

Examination Techniques

1

Sandy X. Zhang-Nunes, Jill A. Foster,
and Julian D. Perry

Contents

S.X. Zhang-Nunes, MD • J.A. Foster, MD (✉)
The Ohio State University Wexner Medical Center,
Columbus, OH, USA

Eye Center of Columbus, Columbus, OH, USA
e-mail: sandyxz@gmail.com; fosterj@jillfoster.com

J.D. Perry, MD
Division of Opthalmology,
Cole Eye Institute,
Cleveland Clinic Foundation,
9500 Euclid Avenue I-32, Cleveland,
OH 44195, USA
e-mail: perryj1@ccf.org

1.1 Introduction

Examination of a patient with orbital disease should begin with a detailed history to discern the chronicity of symptoms, obtain past medical history such as systemic medical conditions or neoplasia, and review any corresponding imaging. Orbital examination techniques in the adult and child will help establish differential diagnoses and direct further studies.

1.2 History

The history aids in establishing a probable diagnosis and in guiding the initial workup and therapy. Important historical elements will be discussed in the following chapters of this section.

1.3 Examination

1.3.1 External Examination

The examiner should inspect the patient visually, assessing the position and symmetry of periocular structures, such as the brows, eyelids, canthi,

J.D. Perry, A.D. Singh (eds.), *Clinical Ophthalmic Oncology*,
DOI 10.1007/978-3-642-40492-4_1,

surrounding soft tissues, and bony structures. Visual inspection should include observation for obvious globe deviation. Grossly visible changes in the periocular skin and preauricular or submandibular lymph nodes are noted.

1.3.2 Pupils

All patients with suspected orbital disease should undergo the swinging flashlight test to determine the presence or absence of a relative afferent pupillary defect. In orbital disease, presence of an afferent pupillary defect may signal optic nerve compression or disruption of the visual system between the optic nerve head and the apex of the orbit. Optic nerve function is further characterized by testing of visual acuity, color plates, and confrontational fields. The efferent pupillary pathway should be tested as well. Anisocoria should be recorded as worse in light (parasympathetic defect) or in dark (sympathetic defect), and pharmacologic testing can be performed.

Tumors of the lateral orbit may impair ciliary ganglion function to produce a parasympathetic defect, whereas cavernous sinus or superior orbital fissure tumors may result in sympathetic dysfunction.

1.3.3 Extraocular Motility

Ductions and versions should be tested in each patient. The cover–uncover test is performed in each cardinal position to measure any phoria or tropia. Patients with suspected restrictive disease may undergo forced duction testing. Classically, after a drop of topical anesthetic is placed, a cotton-tipped applicator soaked in 4 % lidocaine solution is applied to the muscle away from the direction of gaze limitation for approximately 1 min. The anesthetized muscle is then grasped firmly with toothed forceps and rotated toward the direction of gaze limitation. Resistance indicates a restrictive disorder.

If the patient is not amenable to such testing while awake, one can discern restrictive disease from paresis by looking for a "floating" saccade or basically the relative speed and comparison of the simultaneous saccades between the two eyes. Standing approximately 3–4 ft directly in front of the patient, the examiner should ask the patient to look at the examiner's nose and then quickly look at his or her finger on an outstretched arm in the four main positions: left, right, up, and down. For example, if the patient has an abduction deficit on the right from 6th nerve paresis, he or she will have a saccade that "floats" to the right, when compared to the fast adducting saccade on the left. If the abduction deficit is due to restriction, the right eye abducting saccade will be limited by a sudden stop.

Fields of single vision and double vision can be mapped using a penlight; Finoff transilluminator, a.k.a. muscle light; or a kinetic perimeter.

1.3.4 Eyelid Position and Function

Eyelid position is characterized by the marginal reflex distances (MRD). The MRD1 represents the distance from the center of the upper eyelid margin to the corneal light reflex measured in millimeters. The MRD2 represents the distance from the center of the lower eyelid margin to the corneal light reflex. The action of the levator muscle (levator function) is measured as the extent of upper eyelid excursion from downgaze to upgaze with the brows fixated. If present, scleral show is measured from each limbus to the corresponding eyelid margin with the eye in primary position. Upper eyelid ptosis (Fig. 1.1) may imply either mechanical involvement of the levator muscle or palsy, whereas eyelid retraction (Fig. 1.2) suggests proptosis, such as thyroid eye disease, or CNS disorder. The upper eyelid may be everted to inspect the palpebral lobe of the lacrimal gland (Fig. 1.3), especially in the presence of superotemporal fullness. Lymphoma can result in a salmon-colored conjunctival mass that is visible upon inspection of the fornix (Fig. 1.4). Orbicularis strength, Bell's phenomenon, and lagophthalmos should also be evaluated as part of the cranial nerve exam detailed below.

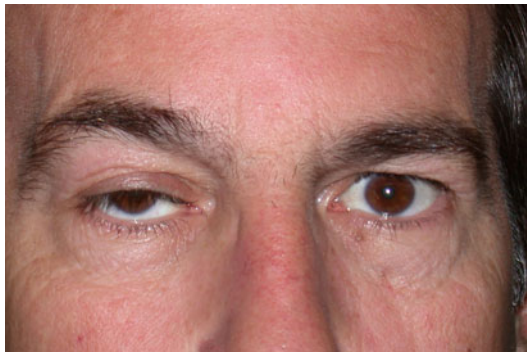

Fig. 1.1 Right upper eyelid with ptosis. Note the right brow is also elevated due to the patient's use of the frontalis muscle in an attempt to lift the ptotic right upper eyelid. The left upper eyelid is also pseudo-retracted and would likely descend to a more normal position with ptosis correction on the right

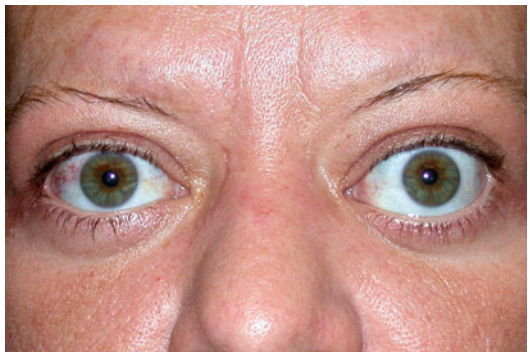

Fig. 1.2 Bilateral upper and lower eyelid retraction, left greater than right from thyroid eye disease

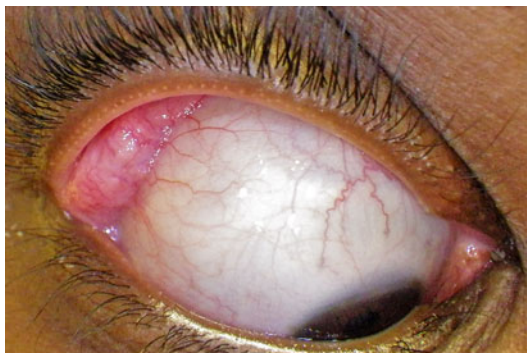

Fig. 1.3 Prominent palpebral lobe of lacrimal gland, visible beneath the upper eyelid

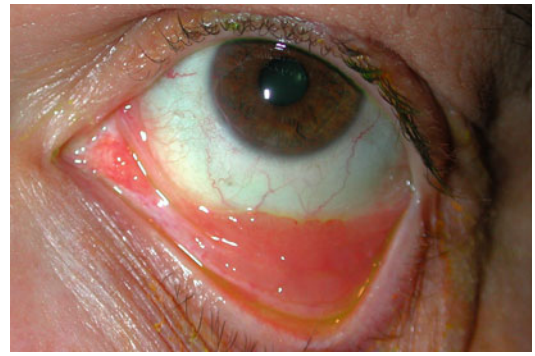

Fig. 1.4 Salmon-colored lymphoma in the inferior fornix

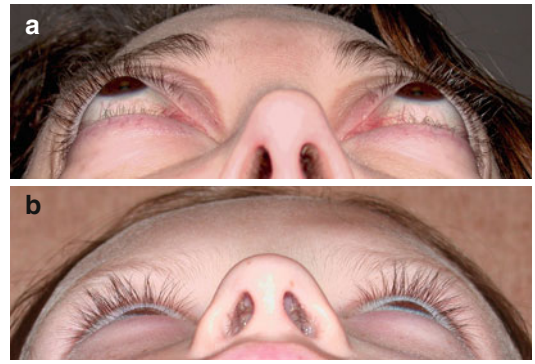

Fig. 1.5 Submental view of proptotic globes from Graves' disease (**a**). Child with left proptosis from orbital dermoid (**b**)

1.3.5 Globe Position

1.3.5.1 Proptosis

By evaluating the patient in the submental view (chin-up position), the examiner can qualitatively look for globe protrusion or retrusion relative to the canthal angle and the nasion (Fig. 1.5). To quantify the degree, three common exophthalmometry tools exist: the Hertel, which is most commonly used (Fig. 1.6); the Naugle, which is useful for patients with abnormal lateral orbital rims (Fig. 1.7); and the Luedde, which is more feasible to use in children (Fig. 1.8).

The Hertel exophthalmometer quantifies the anterior protrusion of the eye by measuring the distance in millimeters from the anterior lateral orbital rim to the front surface of the cornea. The reading is taken with a base measurement of the separation of the positioning arms of the tool to

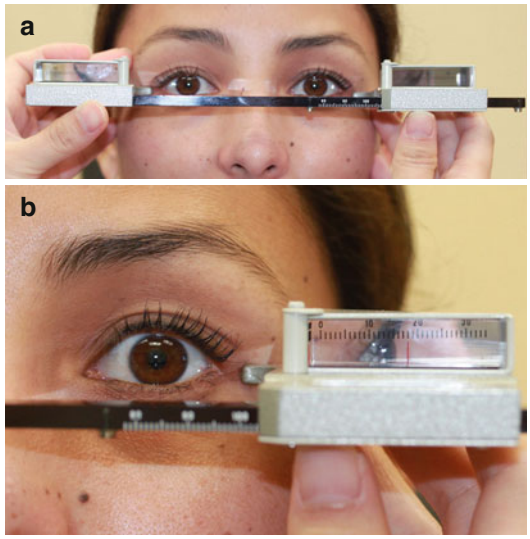

Fig. 1.6 Hertel exophthalmometer. While resting the Hertel instrument on both lateral rims, the base number is recorded on the ruler for consistency (**a**), and the amount of exophthalmos is measured by aligning the *red bars* then recording the number at which one sees the anterior surface of the cornea (**b**)

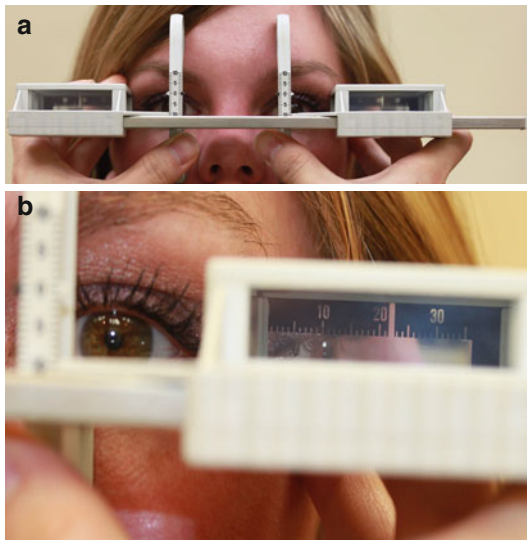

Fig. 1.7 Naugle exophthalmometer. In patients with lateral orbital rim defects, the Naugle can be used by resting the posts on the forehead and the maxillary prominence at the pupillary axis (**a**), aligning the *red mark* with the clear bar, and then recording the number at the anterior surface of the cornea (**b**)

help reference subsequent measurements on the same device. The Naugle exophthalmometer measures anterior globe position relative to the superior and inferior orbital rims. This method

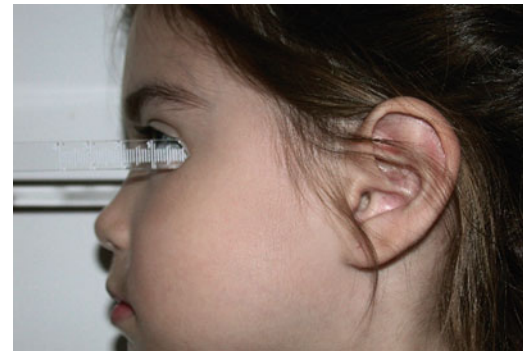

Fig. 1.8 In children, the clear Luedde ruler is placed at the lateral orbital rim, and the distance to the anterior corneal surface is measured

provides a more accurate assessment in those with lateral rim fractures, iatrogenic repositioning of the lateral rim, or orbital rim defects. The Luedde exophthalmometer measures globe protrusion unilaterally from the lateral orbital rim. It consists of a clear bar with millimeter markers. The anterior corneal surface can be visualized through the bar to determine the millimeters of protrusion. This can be positioned on the lateral orbital rim without a device in front of the eyes and is easier to use in children who reflexively more away and close their eyes with the other tools.

1.3.6 Hyperglobus or Hypoglobus

Orbital or periorbital neoplasms often displace the globe. Nonneoplastic conditions such as thyroid eye disease, trauma, and silent sinus syndrome may cause similar examination findings, and further studies, such as maxillofacial computed tomography, may be indicated.

Horizontal and vertical globe displacements are measured in millimeters from the central pupil to vertical midline and horizontal canthal line, respectively.

For vertical displacement, one can draw an imaginary line horizontally across a patient's pupillary axis and determine if the pupil of the other eye is higher or lower, which could suggest hyperglobus (Fig. 1.9) or hypoglobus (Fig. 1.10), respectively. Care must be taken to ensure the patient's head is in primary position, without any tilt, and that the line is parallel to the ground.

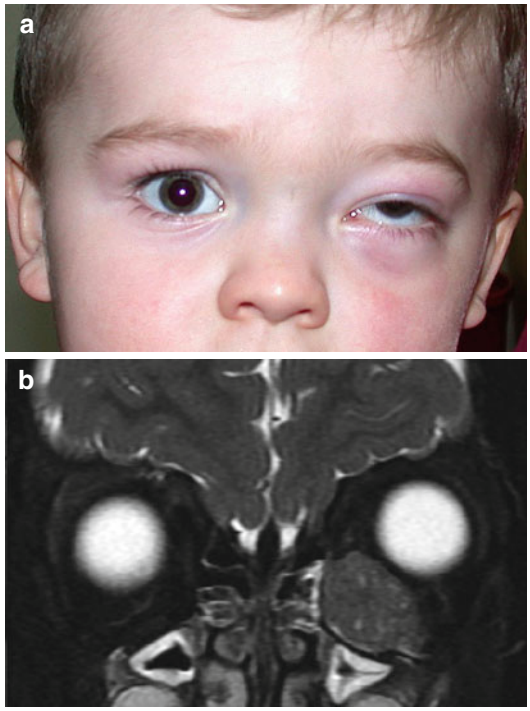

Fig. 1.9 A 23-month-old boy with left hyperglobus from desmoplastic small round cell tumor/round cell sarcoma, grade 3/3. Clinical appearance (**a**) and coronal MRI (**b**)

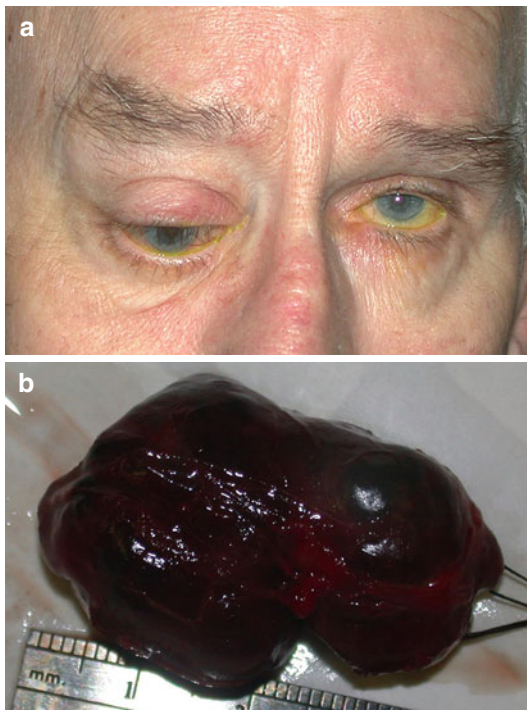

Fig. 1.10 Right hypoglobus from large cavernous hemangioma. Clinical appearance (**a**) and gross resected specimen (**b**)

1.3.7 Palpation

The examiner should palpate any abnormal areas for tenderness or a mass, assess the degree of resistance to retropulsion of each globe, and check for local adenopathy. The lacrimal gland area should be palpated for fullness and tenderness. Sensation to evaluate sensory nerve function is evaluated with tactile stimulation by touch. Areas of reduced sensation or hypesthesia are noted (see below CN V).

1.3.8 Resistance to Globe Retropulsion

The examiner places both forefingers over the anterior portion of the globe with the eyelids closed and gently pushes posteriorly on the globe. The degree of resistance is recorded on a relative scale. Orbital mass lesions often produce increased resistance to manual globe retrodisplacement.

1.3.9 Slit Lamp Examination

The slit lamp examination typically focuses on the corneal surface and the posterior pole in patients with a suspected orbital neoplasm. The corneal surface is evaluated for signs of exposure, and the posterior pole is evaluated for signs of ocular or optic nerve compression or congestion.

1.3.10 Fundus Examination

Orbital mass lesions may result in choroidal folds, optic disc edema, pallor, or shunt vessels (Fig. 1.11).

1.3.11 Cranial Nerves V and VII

Sensation to light touch in each dermatome of the trigeminal nerve, V1–V3, may be tested using a tissue, including testing of the corneal blink reflex. Each motor branch of the facial nerve is also evaluated. Loss of muscle function may be graded on a relative scale comparing the weak side to the normal side. Bell's phenomenon

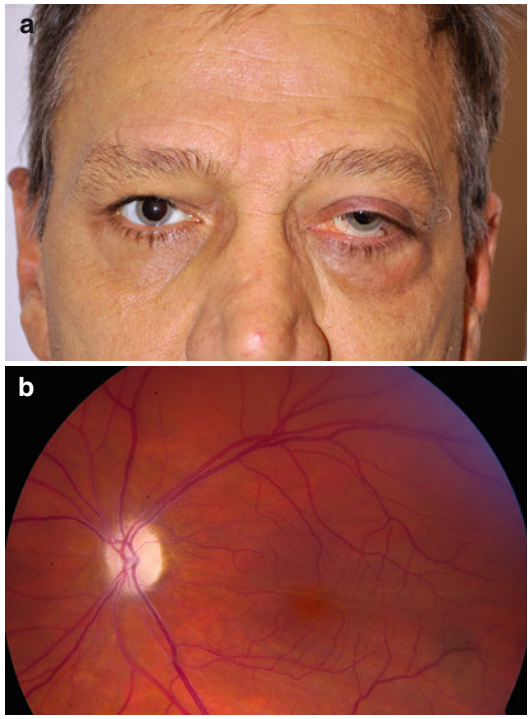

Fig. 1.11 Orbital mantle cell lymphoma. Clinical appearance with hyperglobus on the left (**a**). Note optic atrophy and choroidal folds (**b**)

testing is performed in all patients with lagophthalmos by asking the patient to squeeze his or her eyes shut, while the examiner tries to open them to evaluate if the eye supraducts sufficiently for corneal protection.

1.3.12 Lacrimal System

Attention should be directed to the superotemporal orbit to evaluate for fullness or tenderness of the lacrimal glands. Severe pain and rapidity of onset are more suggestive of a malignant process. The lacrimal secretory function can be measured using Schirmer's testing. This can be performed typically by placing a small strip of filter paper in the lateral conjunctival sac of bilateral lower eyelids for 5 min with the eyes closed. Basal tear secretion can be tested after placing topical anesthetic to prevent tearing from irritation. Normal wetting is 15 mm or more, mild dryness 9–14 mm, moderate 4–8, and severe less than 4 mm.

A tumor or malignancy may also involve the lacrimal drainage system and present as tearing. The excretory drainage patency is determined by irrigation with or without a Jones test. Even in the absence of a tumor, lacrimal outflow obstruction alone can cause enlargement of the lacrimal sac and fullness in the medial canthal region. This more common benign lacrimal pathology usually begins below the medial canthus. Thus, if there is fullness in the medial canthal region that extends above the medial canthal tendon, the examiner should consider an imaging study. Pathology in the lining of the lacrimal sac such as lymphoma or inverted papilloma is difficult to distinguish from benign nasolacrimal duct obstruction in the absence of warning signals like bloody tears. Abnormal mucosa noted at the time of dacryocystorhinostomy warrants biopsy.

1.3.13 Nasal Endoscopy

Intranasal examination using an endoscope can detect intranasal disease causing secondary orbital or lacrimal signs.

1.4 Special Issues in Examination of Children

The examination of the child with orbital pathology requires more creativity and adjustments depending on age and cooperation. Asking the parent to hold or feed an infant often facilitates the physical examination. Usage of small toys to attract the attention of the child is often critical in evaluating ductions and versions. Through observation alone, the evaluator may gather important information regarding skin coloration, eyelid and globe position, external periocular soft tissue changes, ocular motility, and vision. The examination should also include observation of any changes of globe position with crying.

Patient cooperation, however, may limit the ability to perform a complete physical examination in the office. Thus, some children require sedation or general anesthesia to complete the physical examination. Communication with the

pediatrician regarding suspected etiology helps to determine the need for additional systemic evaluation. Systemic workup may include serologic testing, genetic studies, or imaging studies.

1.4.1 Complete Eye Examination

Orbital tumors can affect sensory visual function by producing compressive or glaucomatous optic neuropathy, refractive errors, or keratopathy. Any cause of visual dysfunction in the pediatric group may produce amblyopia. Detailed visual assessment can help localize an orbital tumor and determine whether amblyopia needs to be acutely addressed. In children, assessment requires a cycloplegic retinoscopy and refraction. Eyelid position and pupillary testing should be evaluated prior to placing drops for dilation. Versions, ductions, and strabismus measurements should be noted.

In older children, color plates and visual fields may help to better characterize optic nerve function, especially if the examiner is considering an underlying glioma. In younger children, measurement of visual evoked potential (VEP or VER) may be helpful in assessing optic nerve function. This test is one of many tools used to monitor optic nerve compression in fibrous dysplasia. Evaluation of stereopsis may help distinguish a long-standing tropia from strabismus due to a new orbital process. Comparison with old photos and history from the parents can be utilized.

A standard or portable slit lamp allows for the most detailed anterior segment evaluation. However, a penlight with or without a 20D lens for magnification may be used. Conditions such as lymphangioma, neurofibromatosis, or capillary hemangioma may present with anterior segment findings. Posterior pole examination follows and may reveal findings such as choroidal folds due to an orbital mass effect, optic disc pallor due to a glioma or other tumor compression, or orbital invasion from a primary intraocular tumor.

1.4.2 Orbital Examination

1.4.2.1 Globe Displacement

The examiner assesses globe position qualitatively with the child in the chin-up position. Although an exophthalmometer may provide an objective measure, patient cooperation may limit its accuracy. The Luedde device is particularly valuable for evaluation of globe position in children, who often find it less intimidating because it is smaller and placed on the side (Fig. 1.8). The Luedde instrument offers accurate measurements with the patient in the supine position and can be used during an examination under anesthesia.

1.5 Summary

Each step of the examination aids in disease localization and characterization to ultimately help formulate a treatment plan.

Classification of Orbital Tumors

2

Bryan R. Costin, Julian D. Perry, and Jill A. Foster

Contents

B.R. Costin, MD • J.D. Perry, MD (✉)
Division of Ophthalmology, Cole Eye Institute, Cleveland Clinic Foundation, 9500 Euclid Avenue I-32, Cleveland, OH 44195, USA
e-mail: perryj1@ccf.org

J.A. Foster, MD
The Ohio State University Wexner Medical Center, Columbus, OH, USA

Eye Center of Columbus, Columbus, OH, USA

2.1 Introduction

Orbital tumors represent approximately 0.1 % of all body tumors and approximately one-fifth of all orbital diseases. Classification schemes vary and stratify orbital tumors based on demographics, site of origin, anatomic location within the orbit, histopathologic features, clinical course, and imaging findings. Defining orbital neoplasia presents difficulties, as choristomas, hamartomas, and inflammatory lesions can present as space-occupying lesions and behave as benign and even malignant, neoplasms. In general, neoplasms of the orbit may be classified as primary, secondary (infiltration from an adjacent structure), or metastatic (from distant structures). Orbital neoplasia can be divided into histological categories that include benign, benign but locally aggressive, and malignant. In some cases, especially lymphoproliferative lesions, a spectrum from benign to malignant exists.

This chapter aims to classify orbital tumors on clinical grounds in order to provide a framework to conceptualize space-occupying orbital lesions to determine an evaluation and treatment algorithm.

2.2 Differential Diagnosis of Orbital Tumors

Masquerading processes, such as infectious and inflammatory diseases, can resemble an orbital tumor and must be excluded during the workup

J.D. Perry, A.D. Singh (eds.), *Clinical Ophthalmic Oncology*,
DOI 10.1007/978-3-642-40492-4_2, © Springer-Verlag Berlin Heidelberg 2014

Box 2.1: Lesions That May Simulate an Orbital Neoplasm

Infectious
- Acute bacterial orbital cellulitis
- Invasive fungal infection
- Mycobacterial infection

Inflammatory
- Idiopathic orbital inflammation
- Dysthyroid orbitopathy
- Systemic vasculitides

Other
- Amyloidosis

of a space-occupying orbital lesion. Many non-neoplastic processes can be excluded based on a combination of demographic, clinical, and imaging characteristics (Box 2.1).

2.3 Clinicopathological Classification of Orbital Tumors

2.3.1 Cystic Lesions

Dermoid cysts are the most common cystic lesions of the orbit [1]. They represent congenital lesions that form from epithelial cells trapped beneath the surface epithelium during embryogenesis. They often occur along the orbital rim superotemporally at the zygomaticofrontal suture, but they can occur at other bony sutures or in deeper orbital tissues. Other orbital cystic lesions include colobomatous cyst, congenital cystic eye, meningocele, and teratoma. Several other orbital neoplasms may present with cystic components (Table 2.1).

2.3.2 Vascular Lesions

Tumors arising from, or containing, significant vascular components may be divided into no-flow (type 1), low-flow (type 2), and high-flow (type 3) lesions. Significant overlap exists within these lesions, and current classification schemes describe lower-flow lesions as venous or venous-lymphatic malformations containing microcysts or macrocysts. Treatment is based upon imaging and flow characteristics (Table 2.2).

Table 2.1 Orbital cystic tumors

Aneurysmal bone cyst	Meningoencephalocele
Colobomatous cyst	Mucocele
Congenital cystic eye	Optic nerve sheath cyst
Conjunctival epithelial cyst	Parasitic cysts (e.g., hydatid cyst)
Dermoid cyst	Respiratory cyst
Ductal cyst of the lacrimal gland	Teratoma
Meningocele	

Table 2.2 Orbital vascular lesions

More common	Less common
Capillary hemangioma	Angiosarcoma
Cavernous hemangioma	Cholesterol granuloma
Hemangiopericytoma	Hemangioendothelioma
Lymphangioma (type 1)	Hemangiosarcoma
Varix (type 2)	Kaposi's sarcoma
AVM (type 3)	Kimura's disease
	Vascular leiomyoma
	Vascular leiomyosarcoma

2.3.3 Myogenic Tumors

Rhabdomyosarcoma represents the most common myogenic orbital tumor and the most common primary orbital malignant neoplasia of childhood. It accounts for 4 % of all biopsied orbital masses in children [1]. Rhabdomyosarcoma is believed to arise from primitive orbital mesenchymal elements.

2.3.4 Lipomatous and Myxomatous Tumors

Lipomas are benign tumors of adipose tissue that occur only rarely within the orbit. Dermolipoma is a benign congenital lesion that often occurs as a part of Goldenhar's syndrome. Liposarcoma, the most common soft tissue sarcoma in adults, has widespread distribution but occurs rarely in the orbit.

Table 2.3 Tumors of the lacrimal gland

Epithelial	Nonepithelial
Adenoid cystic carcinoma	Ductal cyst
Pleomorphic adenocarcinoma	Lymphoproliferative
Pleomorphic adenoma	Plasmacytoma
Mucoepidermoid carcinoma	
Myoepithelioma	
Oncocytoma	
Warthin's tumor	

2.3.5 Primary Melanocytic Tumors

Primary melanocytic tumors of the orbit include melanoma, melanocytic hamartoma, and melanotic neuroectodermal tumor of infancy. Accounting for less than 1 % of primary orbital neoplasms, primary orbital melanoma arises from native orbital melanocytes that are located along ciliary nerves, optic nerve leptomeninges, and scleral emissary vessels. Approximately one-half of primary orbital melanomas are associated with pigmentary disorders, including nevus of Ota, ocular melanocytosis, and blue nevi [2].

2.3.6 Tumors of the Lacrimal Gland

Classically, approximately one-half of all lacrimal gland tumors represent epithelial proliferations, and the remainder represents lymphoproliferative lesions. Of the epithelial proliferations, roughly half are pleomorphic adenomas (benign mixed tumors), and the remainder consists of malignant carcinomas, which include adenoid cystic carcinoma, malignant mixed cell tumor, and mucoepidermoid carcinoma. Nonepithelial lacrimal gland tumors consist of ductal cyst, lymphoma, and plasmacytoma (Table 2.3).

2.3.7 Tumors of the Lacrimal Sac

Epithelial tumors are the most common neoplasms of the lacrimal sac [3]. The most common benign and malignant epithelial tumors of the lacrimal sac are the papilloma and squamous cell carcinoma, respectively [3]. Malignant tumors outnumber benign tumors in this region [3].

2.3.8 Lymphoproliferative Tumors

Lymphoid and leukemic tumors represent a common group of orbital neoplasm, and they may arise anywhere within the orbit (Chap. 12).

2.3.9 Peripheral Nerve Tumors

Tumors arising from orbital peripheral nerves include neurilemmoma (schwannoma), neurofibroma, alveolar soft-part sarcoma, granular cell tumor, amputation neuroma, and malignant peripheral nerve sheath tumor. These tumors theoretically can arise from branches of orbital cranial nerves, sympathetic and parasympathetic fibers, and the ciliary ganglion, but most seem to arise from the ophthalmic division of the trigeminal nerve. The vast majority of orbital peripheral nerve sheath tumors are benign; only a few well-documented cases of malignant peripheral nerve sheath tumors have been reported [4].

2.3.10 Optic Nerve, Meningeal, and Other Neural Tumors

Optic nerve and meningeal tumors consist mainly of optic nerve glioma, malignant optic nerve astrocytoma, and meningioma. Optic nerve glioma presents with progressive visual loss and axial proptosis in childhood. Neurofibromatosis (NF) affects children in up to 50 % of cases. Conversely, only a minority of patients with NF develop optic nerve glioma.

Meningioma represents a benign neoplasm arising from the arachnoid layer of the meninges. Other neural tissue tumors include primitive neuroectodermal tumor, primary orbital neuroblastoma, and primary orbital carcinoid.

2.3.11 Fibrous Connective Tissue (Fibrohistiocytic Lesions)

These mass lesions, composed mainly of fibroblastic cells, may present with similar clinical

and histological features. Examples include fibroma, fibrosarcoma, and fibrous histiocytoma.

2.3.12 Histiocytic Tumors

Proliferative disorders of histiocytes comprise a spectrum of disease ranging from solitary inflammatory lesions to widely disseminated lesions that may exhibit malignant behavior. Variants include Langerhans' cell histiocytosis, juvenile xanthogranuloma, Erdheim-Chester disease, sinus histiocytosis, and multinucleate cell angiohistiocytoma.

Langerhans' cell histiocytosis consists of three disorders formerly referred to as eosinophilic granuloma, Hand-Schuller-Christian disease, and Letterer-Siwe disease. Eosinophilic granuloma typically occurs in the orbital region as a solitary lesion of bone.

2.3.13 Primary Bone Tumors

Primary bone tumors of the orbit are a heterogeneous group of conditions that constitute less than 1 % of all orbital tumors.

2.3.13.1 Benign Fibro-osseous Lesions

Osteomas are benign proliferations of bony tissue that occur most commonly in the paranasal sinus bone, calvarium, and other facial bones. Orbital involvement typically results from invasion from a tumor within the adjacent paranasal sinus bone and occurs most frequently in the ethmoidal, frontoethmoidal, and frontal regions.

Fibrous dysplasia represents a benign proliferation of fibrous tissue and woven bone. It has been described in three forms: monostotic, polyostotic, and McCune-Albright syndrome. McCune-Albright syndrome consists of a triad of polyostotic fibrous dysplasia, precocious puberty, and cutaneous pigmentation occurring mainly in girls. The majority of cases with orbital involvement occur in the setting of monostotic fibrous dysplasia, with the frontal bone followed by the sphenoid and ethmoid being bones most commonly affected. The disease presents with longstanding facial asymmetry, proptosis, and globe displacement. Slow growth often continues into adult life.

2.3.13.2 Benign Cartilaginous Tumors

This rare group of tumors includes chondroma, osteochondroma, enchondroma, and fibrochondroma.

2.3.13.3 Reactive Bone Lesions

Reactive bone lesions include cholesterol granuloma, aneurysmal bone cyst, giant cell granuloma, and brown tumor of hyperparathyroidism.

Cholesterol granuloma represents a foreign body reaction to cholesterol deposition following the breakdown of blood products. More commonly seen in the middle ear and temporal bone, it can rarely occur in the orbit, almost exclusively in the superolateral frontal bones.

2.3.13.4 Bone Neoplasms

Orbital bone neoplasms consist of a variety of entities. Osteosarcoma is the most common primary bone neoplasm; however, orbital involvement is rare and the lesion usually has a maxillary focus. Most arise de novo, but some are secondary to Paget's disease, fibrous dysplasia, or radiotherapy. Patients with familial retinoblastoma can develop osteosarcoma, even without a history of radiation.

Multiple myeloma and solitary plasmacytoma may involve the orbital bone. These lesions typically present with subacute pain and proptosis in patients over 50 years of age.

Most frequently occurring in the tongue and subcutaneous tissues, granular cell tumors may rarely involve the orbit, extraocular cell muscles, periorbital, and lacrimal sac [5]. Grossly, the lesions are well-encapsulated tumors composed of round- to oval-shaped cells with granular eosinophilic cytoplasm.

2.3.13.5 Bone Vascular Tumors

Orbital intraosseous hemangioma presents as a slowly evolving painful mass. Malignant vascular tumor of orbital bone is also rare.

2.3.13.6 Miscellaneous Bone Tumors

Other neoplasms, including intramedullary lipoma, intraosseous myxomas, and cartilaginous hamartoma can rarely affect the orbital bones.

2.3.14 Metastatic Tumors to the Orbit

Metastatic cancers to the orbit spread to the orbit hematogenously, as there are no significant lymphatics in the orbit. Metastatic orbital lesions account for approximately 12 % of orbital neoplasms, depending on age, and up to 3.3 % of all orbital lesions [6]. Nearly all systemic malignancies have been reported to metastasize to the orbit.

2.3.14.1 Adult Metastatic Disease

In adults, carcinomas that arise from the epithelial structures of organs most commonly metastasize to the orbit [6]. Breast cancer may account for 42 % of all metastatic orbital lesions, followed by lung (11 %), unknown primary (11 %), prostate (8.3 %), melanoma (5.2 %), gastrointestinal tract (4.4 %), and kidney (3.2 %) [6]. Orbital metastatic disease may occur in the setting of both recognized and unrecognized systemic malignancy. In general, the more indolent systemic malignancies are diagnosed prior to orbital metastasis, whereas early orbital metastasis occurs in patients with more aggressive primaries. Orbital metastasis represents the presenting sign of systemic cancer in about 42 % of cases of systemic malignancy affecting the orbit [6].

Average survival after orbital metastasis detection is approximately 9 months and even shorter for more aggressive primary malignancies, especially lung cancer [6, 7]. Patients with orbital metastases frequently complain of diplopia, ptosis, proptosis, eyelid swelling, pain, and vision loss. Metastatic breast carcinoma may produce enophthalmos due to its scirrhous histological nature [8].

2.3.14.2 Metastatic Lesions in Children

In children, orbital metastases are more likely to arise from embryonal neural tumors, such as neuroblastoma and sarcomas. Metastatic neuroblastoma is second only to primary rhabdomyosarcoma as the most frequent orbital malignancy of childhood [9]. Patients develop rapidly progressive exophthalmos and eyelid ecchymosis. Isolated primary orbital neuroblastoma is exceedingly rare [10]. Other childhood tumors that metastasize to the orbit include Wilms' tumor, Ewing's tumor, and medulloblastoma [9].

2.3.15 Secondary Orbital Tumors

Secondary orbital tumors invade the orbital tissues from adjacent sites, including the eyelids (e.g., squamous cell carcinoma), conjunctiva (e.g., melanoma), lacrimal sac (e.g., adenoid cystic carcinoma), globe (e.g., retinoblastoma), paranasal sinuses (e.g., squamous cell carcinoma, sinonasal undifferentiated carcinoma), nasopharynx (e.g., esthesioneuroblastoma), and brain (e.g., glioblastoma) [11, 12].

2.4 Imaging Classification of Orbital Tumors

Orbital tumors can be differentiated based on imaging characteristics in order to determine their etiology and behavior. In general, benign orbital tumors present as well-circumscribed lesions, such as cavernous hemangioma, fibrous histiocytoma, hemangiopericytoma, lipoma, neurilemmoma, and pleomorphic adenoma. Diffuse (plexiform) neurofibroma represents a notable exception to this generalization, as this benign tumor presents as a poorly circumscribed, diffuse lesion.

Malignant orbital tumors can present as well-circumscribed or poorly circumscribed lesions. Examples of the former include mesenchymal chondrosarcoma, optic nerve glioma, optic nerve meningioma, and rhabdomyosarcoma. Examples of the latter include adenoid cystic carcinoma, fibrosarcoma, lymphoma, pleomorphic adenocarcinoma, primary orbital melanoma, and most metastatic lesions. Some metastatic lesions, such as melanoma and renal cell carcinoma, represent exceptions to this generalization and may present as well-circumscribed lesions.

2.5 Summary

Orbital tumors represent a heterogeneous group of neoplasms with varying classification schemes to provide a framework for clinical evaluation. A combination of imaging, clinical, and demographic data may be used to narrow the differential diagnosis and to determine the appropriate evaluation and treatment.

References

1. Shields JA, Bakewell B, Augsburger JJ, Donoso LA, Bernardino V. Space-occupying orbital masses in children. A review of 250 consecutive biopsies. Ophthalmology. 1986;93:379–84.
2. Jakobiec FA, Ellsworth R, Tannenbaum M. Primary orbital melanoma. Am J Ophthalmol. 1974;78: 24–39.
3. Stefanyszyn MA, Hidayat AA, Pe'er JJ, Flanagan JC. Lacrimal sac tumors. Ophthal Plast Reconstr Surg. 1994;10:169–84.
4. Jakobiec FA, Font RL, Zimmerman LE. Malignant peripheral nerve sheath tumors of the orbit: a clinicopathologic study of eight cases. Trans Am Ophthalmol Soc. 1985;83:332–66.
5. Jaeger MJ, Green WR, Miller NR, Harris GJ. Granular cell tumor of the orbit and ocular adnexa. Surv Ophthalmol. 1987;31:417–23.
6. Goldberg RA, Rootman J, Cline RA. Tumors metastatic to the orbit: a changing picture. Surv Ophthalmol. 1990;35:1–24.
7. Freedman MI, Folk JC. Metastatic tumors to the eye and orbit. Patient survival and clinical characteristics. Arch Ophthalmol. 1987;105:1215–9.
8. Cline RA, Rootman J. Enophthalmos: a clinical review. Ophthalmology. 1984;91:229–37.
9. Albert DM, Rubenstein RA, Scheie HG. Tumor metastasis to the eye. II. Clinical study in infants and children. Am J Ophthalmol. 1967;63:727–32.
10. Jakobiec FA, Klepach GL, Crissman JD, Spoor TC. Primary differentiated neuroblastoma of the orbit. Ophthalmology. 1987;94:255–66.
11. Reifler DM, Hornblass A. Squamous cell carcinoma of the eyelid. Surv Ophthalmol. 1986;30:349–65.
12. Howard GR, Nerad JA, Carter KD, Whitaker DC. Clinical characteristics associated with orbital invasion of cutaneous basal cell and squamous cell tumors of the eyelid. Am J Ophthalmol. 1992;113:123–33.

Differential Diagnosis in Children

3

Sandy X. Zhang-Nunes, Jill A. Foster, Julian D. Perry, and Paul L. Proffer

Contents

S.X. Zhang-Nunes, MD • J.A. Foster, MD (✉)
P.L. Proffer, MD
The Ohio State University Wexner Medical Center, Columbus, OH, USA

Eye Center of Columbus, Columbus, OH, USA
e-mail: sandyxz@gmail.com; fosterj@jillfoster.com

J.D. Perry, MD
Division of Ophthalmology, Cole Eye Institute, Cleveland Clinic Foundation, 9500 Euclid Avenue I-32, Cleveland, OH 44195, USA
e-mail: perryj1@ccf.org

3.1 Introduction

There are many aspects of history, examination, and imaging that aid in the differential diagnosis of orbital lesions in children. Common etiologies of orbital tumors differ significantly between children and adults. For example, rhabdomyosarcoma, one of the most common primary pediatric orbital malignancies, rarely occurs in adults.

The potential morbidity – and in some cases mortality – of pediatric orbital neoplasia requires an understanding of common findings and presentations to direct the evaluation. The history, physical examination, and diagnostic studies will limit the differential diagnosis, which then determines the need for biopsy and initial therapy (Table 3.1).

3.2 History

As with adults, the history begins with a description of the symptoms, severity, onset, and rate of progression. However, obtaining a detailed history in the pediatric patient presents unique challenges. The direct history depends upon the age, maturity, and verbal skills of the child.

In many cases, the bulk of the history requires input from the family.

The evaluator should remember that a child may deny, forget, or embellish important historical facts that can confound the evaluation of an orbital tumor. For example, a child injured with

J.D. Perry, A.D. Singh (eds.), *Clinical Ophthalmic Oncology*,
DOI 10.1007/978-3-642-40492-4_3, © Springer-Verlag Berlin Heidelberg 2014

Table 3.1 Classification and differential diagnosis of orbital tumors in children

	Benign	Benign Subtypes	Malignant
Developmental/ congenital	Dermoid	Superficial, deep	Retinoblastoma
	Plexiform neurofibroma		
	Teratoma		
	Microphthalmos with cyst and congenital cystic eye		
	Cranial orbital cephalocele	Dural meningocele, encephalic encephalocele	
	Rathke pouch cyst		
Acquired cystic	Mucocele		
	Lacrimal duct cyst		
Lacrimal	Pleomorphic adenoma (rare in children)		Adenoid cystic carcinoma (bimodal peak, 40s and in 1st decade)
Inflammatory	Ruptured dermoid		
	Idiopathic lacrimal gland inflammation		
	Idiopathic orbital inflammatory syndrome		
Vascular	Venolymphatic malformations	Lymphangiomas, venous malformations, AV malformations	
	Capillary malformations	Capillary hemangiomas	
Neural	Neurofibroma		
	Optic nerve glioma		
	Meningioma		
Mesenchymal	Leiomyoma		Rhabdomyosarcoma
Adipose	Lipoma		

a stick or toy may not disclose the cause, or a history of otherwise insignificant periorbital trauma may obscure the workup of true orbital neoplasia.

Preverbal children cannot clearly communicate subjective findings such as pain, hypesthesia, diplopia, or diminished visual acuity. In these cases, the evaluator uses nonverbal clues and physical findings to focus the examination and develop the differential diagnosis.

3.2.1 Presenting Symptoms and Complaints

As with adults, pediatric orbital neoplasia presents with a wide spectrum of symptoms, but many may be underreported in the nonverbal child (Table 3.2). Tumor location and histology determine the presenting symptoms and signs, which can be divided into sensory, motor, and structural or functional.

3.2.2 Rate of Onset

Pediatric orbital malignancies, such as rhabdomyosarcoma, often present with a subacute rate of onset that can be confused with orbital inflammation or trauma. Orbital lymphangioma may produce sudden findings due to intralesional bleeding and is sometimes precipitated by trauma, which confounds the physician evaluator. Benign tumors, such as dermoid cysts, fibrous dysplasia,

Table 3.2 Presenting features of common orbital tumors in children

Category	Entity	Common symptoms and signs
Inflammatory	Ruptured dermoid	Acute onset, pain, proptosis if orbital
Congenital	Plexiform neurofibroma	Pulsating proptosis (absent sphenoid wing); painless, slow progression
	Dermoid	Proptosis with orbital lesions; painless, slow progression
	Teratoma	Progressive severe proptosis
Vascular	Capillary hemangioma	Slow progression, pain, and pulsation rare; blanches with palpation; proptosis if posterior
	Lymphangioma	Painless proptosis but pain with intralesional bleed or upper respiratory infection; conjunctival involvement may aid diagnosis
Benign	Optic nerve glioma	Axial proptosis, slow progression; usually painless
Malignant	Rhabdomyosarcoma	Rapid onset, painless proptosis; discoloration of overlying skin
Metastasis	Leukemia (chloroma)	Unilateral or bilateral painless proptosis; rapid progression
	Neuroblastoma	Abrupt progressive proptosis; bilateral eyelid ecchymoses

and gliomas, often present with slowly advancing symptoms. The growth rate of capillary hemangioma is highly variable.

3.2.3 Past Medical History

The past medical history importantly relates to several pediatric orbital tumors. For example, proptosis that occurs predictably in conjunction with viral illness may indicate an underlying lymphangioma. Patients with lymphangioma may have airway or palatal lesions, and these may also increase during episodes of viral illness. Most patients with granulocytic sarcoma have a history of systemic leukemia. Large capillary hemangiomas are associated with Kasabach–Merritt syndrome and visceral lesions. Orbital neuroblastoma is most often metastatic from the thorax. Diseases that may simulate an orbital neoplasm in children may be associated with underlying medical conditions. For example, orbital cellulitis often occurs in the context of underlying sinusitis.

3.3 Examination

In addition to the systemic examination parameters detailed in Chap. 1, attention can also be paid to Krohel's 6 Ps of the orbital examination to help narrow the differential diagnosis (Box 3.1).

Box 3.1: The 6 Ps of the Orbital Examination [1]

- Proptosis
- Palpation
- Pulsation
- Periorbital changes
- Pain
- Progression

Modified from Krohel et al. [1].

Complete eye examination aids in the differential diagnosis as detailed in Chap. 1.

Orbital tumors frequently cause globe displacement in children. Proptosis may be quantified by using the Luedde method of exophthalmometry. Hyperglobus and hypoglobus should be noted (Chap. 1).

Palpation yields information regarding tumor location, size, and shape. A dermoid cyst may feel firm, smooth, and rubbery; an orbital and eyelid neurofibroma may have a "bag of worms" consistency; and capillary hemangiomas are soft, spongy, and often blanch with palpation. Solid tissue malignancies may produce a high degree of resistance to globe retropulsion.

3.3.1 Pulsation

Although rare, pulsations may occur with certain tumors in children, such as absence or hypoplasia of the sphenoid wing in the setting of neurofibromatosis.

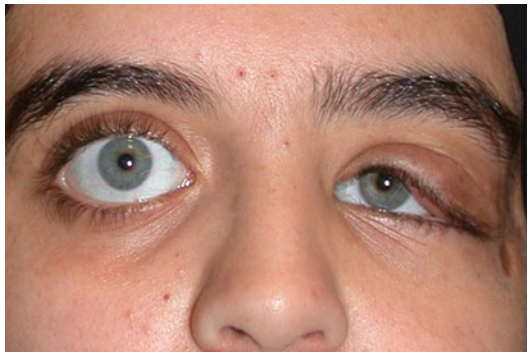

Fig. 3.1 Plexiform neurofibroma with characteristic S-shaped upper eyelid deformity

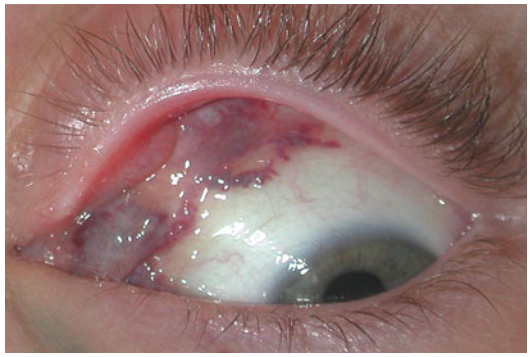

Fig. 3.2 Orbital lymphangioma visible through the conjunctiva

3.3.2 Periorbital Changes

The overlying tissues may show visible signs to suggest the etiology of an orbital neoplastic process. Neuroblastoma often presents with periorbital ecchymoses. Plexiform neurofibroma often presents with an S-shaped upper eyelid deformity with characteristic skin changes (Fig. 3.1). Lymphangioma and capillary hemangioma can be visible through the conjunctiva or in the eyelid (Fig. 3.2). Rhabdomyosarcoma often presents with periorbital discoloration similar to inflammatory signs (Fig. 3.3).

3.3.3 Head and Neck Examination

Examination of the sinuses, nasopharynx, and adjacent lymphatic drainage areas also helps to limit the differential diagnosis. Lymphangioma sometimes involves the roof of the mouth.

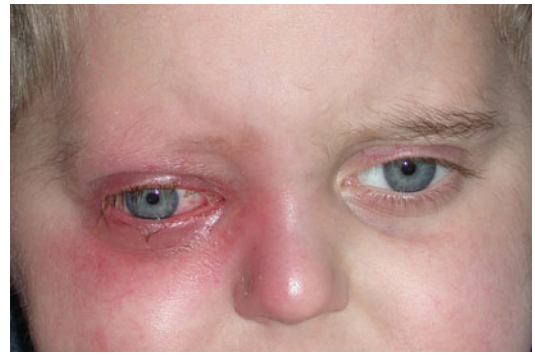

Fig. 3.3 Rhabdomyosarcoma presenting with periorbital discoloration similar to inflammatory signs

3.4 Laboratory Evaluation

Laboratory analysis can augment the information gained from the history and physical examination and further narrow the differential diagnosis. Metastatic neuroblastoma often results in high levels of urine homovanillic acid (HVA) and vanillylmandelic acid (VMA). Peripheral blood smears may be useful in the evaluation of suspected granulocytic carcinoma with orbital presentation.

3.5 Diagnostic Imaging

The evaluation of some pediatric orbital tumors, such as dermoid cyst and capillary hemangioma, may not require orbital imaging. In many cases, however, imaging is essential to solidify the diagnosis, clarify the extent of the disease, and determine the surgical approach.

CT and MR imaging studies represent the mainstay of current techniques. Orbital ultrasound may be of value in determining the size of an orbital lesion or to assess the homogeneity or flow characteristics of a lesion. CT provides the best views of bone (Fig. 3.4), and MRI is better for evaluating soft tissue pathology and blood flow (Fig. 3.5).

Orbital ultrasonography may be helpful to evaluate an orbital vascular process. A capillary hemangioma with medium to high internal reflectivity may be differentiated from a solid tumor with low reflectivity [2]. Ultrasonography may

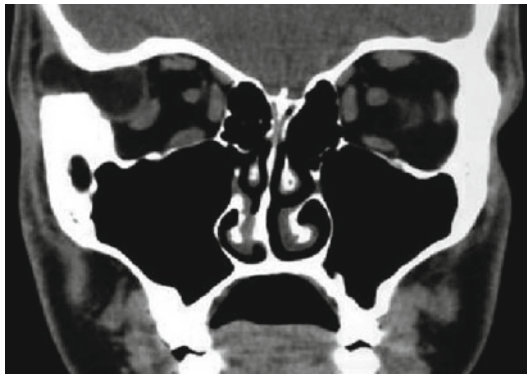

Fig. 3.4 CT scan shows bony changes associated with an orbital dermoid

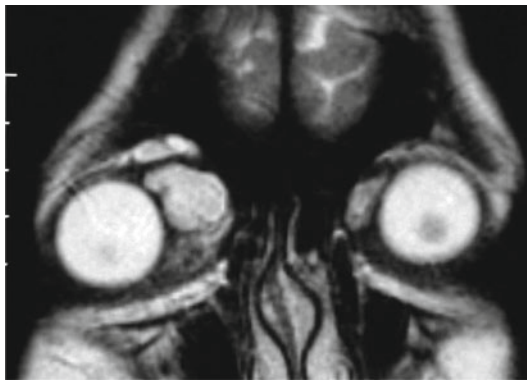

Fig. 3.5 MRI of an orbital lymphangioma

also help guide fine-needle aspiration biopsy and can be used in conjunction with interventional radiology for sclerotherapy of orbital venolymphatic malformations [3].

3.6 Biopsy

Confirmation of the diagnosis may require surgery. Surgical goals and planning are determined prior to surgery. Equipment and personnel are secured preoperatively for frozen section microscopy, microbiological studies, permanent biopsy specimens, ancillary testing, or other concomitant procedures that may be performed while the child is under anesthesia, such as bone marrow biopsy or venous port placement.

Suspected rhabdomyosarcoma often requires biopsy to establish the diagnosis (Fig. 3.6). Further chapters discuss specific surgical approaches, goals, and treatments. The differential diagnosis determines the possible outcomes of frozen section results and the anticipated appropriate extent of surgical excision. An adequate specimen should, when possible, provide tissue for frozen section and then additional tissue for further testing, including microbiological testing, cell marker studies, or electron microscopy. For evaluation of the tumor margins, marking sutures aid in specimen orientation.

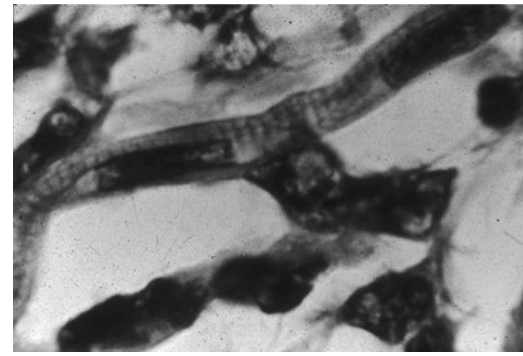

Fig. 3.6 Spindle-shaped cells containing striations in an embryonal rhabdomyosarcoma (hematoxylin and eosin)

3.7 Summary

A detailed knowledge of specific pediatric orbital disorders and their common presentations provides the framework for developing an appropriate differential diagnosis that in turn leads to appropriate workup and then management of orbital tumors in children. However, signs and symptoms of each tumor are not entirely specific, and the surgeon must be prepared to consider atypical presentations.

References

1. Krohel GB, Stewart WB, Chavis RM. Orbital disease. A practical approach. New York: Grune & Stratton; 1981. p. 9–20.
2. Byrne SF, Green RL. Ultrasound of the eye and orbit. 2nd ed. St. Louis: Mosby; 2002. p. 350–1.
3. Hill 3rd RH, Shiels 2nd WE, Foster JA, Czyz CN, Stacey A, Everman KR, Cahill KV. Percutaneous drainage and ablation as first line therapy for macrocystic and microcystic orbital lymphatic malformations. Ophthal Plast Reconstr Surg. 2012;28(2):119–25.

Differential Diagnosis in Adults

4

Bryan R. Costin, Julian D. Perry, and Jill A. Foster

Contents

B.R. Costin, MD • J.D. Perry, MD (✉)
Division of Ophthalmology, Cole Eye Institute, Cleveland Clinic Foundation, 9500 Euclid Avenue I-32, Cleveland, OH 44195, USA
e-mail: perryj1@ccf.org

J.A. Foster, MD
The Ohio State University Wexner Medical Center, Columbus, OH, USA

Eye Center of Columbus, Columbus, OH, USA
e-mail: fosterj@jillfoster.com

4.1 Introduction

The different tissue types within the orbit and the variety of diseases leading to similar external signs can confound the diagnosis of an orbital neoplasm. The orbit contains all of the vital anterior visual pathway structures and the supporting elements that move and nurture the globe. Vital structures surround the orbit, such as the anterior and middle cranial fossae, the paranasal sinuses, and high-flow vessels, including branches of the internal and external carotid arteries and the internal carotid artery itself. This astonishing variety and density of important tissues within and around the orbit can challenge even the experienced surgeon to determine the appropriate diagnostic and surgical plan. In order to treat orbital neoplasia, the surgeon must first understand orbital anatomy and then understand the spectrum of diseases that may affect the structures within the orbit.

Even when a presentation strongly suggests a specific diagnosis, the results of biopsy may reveal a surprising tissue diagnosis. Although specific lesions often present in certain locations within the orbit, significant variation occurs. Similarly, while some neoplasms occur in certain age groups, age cannot be used to rule out any diagnosis. Even the histology of a particular lesion does not necessarily predict its benign or malignant clinical behavior. However, a focused differential diagnosis minimizes the morbidity and cost of the diagnostic workup and helps establish the diagnosis effectively and efficiently.

J.D. Perry, A.D. Singh (eds.), *Clinical Ophthalmic Oncology*,
DOI 10.1007/978-3-642-40492-4_4,

A strong knowledge of the typical clinical and imaging features of orbital neoplasms as well as the spectra of possible presentations will allow the surgeon to create an effective differential diagnosis to begin the diagnostic algorithm (Table 4.1).

Table 4.1 Common orbital lesions in adults. Anatomic location and appearance on imaging studies

Location	Lesion	Appearance
Optic nerve	Glioma	Fusiform ± nerve kinking
	Meningioma	Circumferential enlargement
		"Tram-track" appearance
Intraconal space	Cavernous hemangioma	Well-defined
		Round or oval
		May remodel bone
		Does not destroy bone
	Orbital cellulitis	Varies
		Well-defined, focal disease
		Diffuse inflammation
		May cause orbital abscess
	Idiopathic orbital inflammation	Varies
		Focal inflammation
		Diffuse inflammation
		Does not destroy bone
	Lymphoproliferative disease	Varies
		Focal involvement
		Diffuse involvement
		May mimic other orbital neoplasms, infections, and inflammatory conditions
	Metastasis	Varies
		Well-defined lesion
		Diffuse lesion
		May destroy bone
Extraocular muscles	Thyroid eye disease	Diffuse enlargement of the EOM
		Spares the muscle tendon
		Bilateral but may be asymmetric
	Myositis due to idiopathic orbital inflammation	Focal or diffuse enlargement of the EOM
		Involves the muscle tendon
		May be unilateral or bilateral
	Metastasis	Focal or diffuse enlargement of one or more EOMs
		May be unilateral or bilateral
Extraconal space	Infection	Focal or diffuse
	Inflammation	Focal or diffuse
	Lymphoproliferative	Focal or diffuse
Lacrimal gland	Dacryoadenitis	Enlargement of the lacrimal gland
		May be viral, bacterial, or rheumatologic
		Bacterial infections may cause abscess formation
	Pleomorphic adenoma	Well-defined
		Round or oval mass
		May remodel bone
		Does not destroy bone
	Adenoid cystic carcinoma	Varies
		May be well- or poorly-defined
		Often destroys bone

Table 4.1 (continued)

Location	Lesion	Appearance
Lacrimal sac Orbital apex	Dacryocystitis	
Orbital bones	Osteoma	
	Sphenoid wing meningioma	Well-defined lesion May contain calcifications Hyperostosis of the associated bone
	Fibrous dysplasia	
Extrinsic lesions	Mucocele	
Diffuse	Infection	
	Inflammatory	

Although the etiologies of common orbital tumors differ significantly between children and adults, similar principles apply in developing a differential diagnosis. Similar to pediatric orbital tumors, specific elements of the history and the physical examination help establish a differential diagnosis, and the possible etiologies are further refined through appropriate imaging studies.

The advent of reliable and available imaging techniques over the past two decades has revolutionized the diagnostic algorithms employed for the workup of adult orbital neoplasia. This chapter will complement the chapter on differential diagnosis in children by focusing on technological modalities to arrive at a focused differential diagnosis in adults.

4.2 History

While orbital imaging often represents a final common pathway for the workup of adult orbital tumors prior to obtaining a tissue diagnosis, several elements of the history may help to point toward a differential diagnosis and determine the proper imaging study to obtain (Table 4.2).

Table 4.2 Important history features

Appearance and anatomic site
Rate of onset
Nature of proptosis and dystopia
Presence of pain, hypesthesia
Changes in vision
Restriction of gaze

4.2.1 Rate of Onset

Rate of onset and progression may shed light on the pathology, albeit broadly (Table 4.3). In adults, most orbital tumors produce chronic signs and symptoms, while acute orbital signs typically result from causes other than neoplasia, such as infection, inflammation, trauma, and hemorrhage. However, an underlying neoplasm may also result in inflammation, trauma, or hemorrhage. For example, an underlying vascular tumor may hemorrhage to produce an acute orbital compartment syndrome, a tumor within the lacrimal sac or lacrimal gland may result in secondary infection, mild trauma may rupture an underlying dermoid cyst to produce acute orbital signs, and metastatic and lymphoproliferative lesions may contain a significant inflammatory component.

4.3 Examination

4.3.1 Nature of Proptosis and Dystopia

Because the orbital bones limit orbital volume in each dimension except anteriorly, exophthalmometry helps determine the presence of a space-occupying lesion. The pattern of the proptosis points to the lesion's location and aides in the formation of a differential diagnosis. Axial proptosis usually signifies an intraconal lesion, while non-axial anterior globe displacement typically suggests an extraconal process. However, posterior extraconal mass lesions may also cause axial proptosis.

Table 4.3 Rate of onset of common orbital lesions

Hours	Days	Weeks	Months	Years
Trauma	Inflammatory	Inflammatory	Neoplastic	Neoplastic
Hemorrhage	Infection	Neoplastic	Lymphoid	Degenerative
Infection	Trauma	Trauma	Vascular	Lymphoid
Foreign body	Hemorrhage	Lymphoid	Inflammatory	Vascular
	Vascular	Vascular	Degenerative	Inflammatory

Dystopia, or displacement of the globe in the coronal plane, results from extraconal lesions. The direction of globe displacement is typically opposite the neoplasm. For example, inferonasal displacement of the globe is often due to a condition such as a lacrimal gland tumor in the superotemporal quadrant. Similarly, a process occurring in the superonasal quadrant of the orbit, such as a mucocele, will produce inferotemporal globe dystopia.

Sclerosing conditions, such as metastatic breast carcinoma, produce retrodisplacement of the globe resulting in enophthalmos.

4.3.2 Presence of Pain

Pain in the absence of inflammation often signifies malignancy or other more serious processes. Slowly growing benign lesions may grow quite large without producing pain, unless from exposure keratopathy. On the other hand, malignancies, such as adenoid cystic carcinoma and squamous cell carcinoma, may display tendencies toward perineural invasion to produce pain.

4.3.3 Changes in Vision

Changes in vision as a result of orbital neoplasia may occur from exposure keratopathy, induced astigmatism, choroidal folds, or optic nerve infiltration or compression. These changes may occur in the setting of a benign or a malignant neoplasm and may occur acutely or chronically. Because of the protean causes and presentations of vision loss, vision loss alone does not often point to a particular diagnosis or group of diagnoses. Tumors residing in the orbital apex produce optic neuropathy more commonly than tumors occurring more anteriorly within the orbit. Compressive optic neuropathy often produces a central scotoma with breakout to the periphery, while infiltrative or vascular optic neuropathy may produce an altitudinal-type defect. Static perimetry may occasionally be of value in determining a differential diagnosis, although characterization of optic nerve function is often more valuable as a way to follow tumor progression or treatment.

4.3.4 Gaze Restriction

Orbital tumors may occasionally present with diplopia as the first symptom. The motility disturbance may be due to direct involvement of one or more extraocular muscles by the tumor, motor neuron dysfunction, or displacement of the orbital contents. Examination can often determine the type of motility disturbance, which may assist in developing the differential diagnosis. Schwannomas or neurofibromas may involve CN III, IV, or VI. Malignant orbital neoplasms may infiltrate these nerves to produce dysfunction, or benign neoplasms may compress these motor nerves. Profound ophthalmoplegia and loss of vision may be caused by lesions at the orbital apex [1].

4.4 Diagnostic Imaging

Imaging studies show the location and tissue characteristics that ultimately determine the differential diagnosis in most cases. The history and physical examination point to the choice of imaging modality. Magnetic resonance (MR) imaging demonstrates soft tissue characteristics better and is often the study of choice for evaluation of orbital lesions. However, computed tomographic (CT) imaging studies may show subtle bony changes better, take less time, and are less costly.

Given the ubiquity of these imaging techniques, techniques with less resolution, such as B-scan ultrasonography, have assumed less importance in the workup to determine the differential diagnosis of orbital neoplasms. Doppler imaging, however, may provide useful information regarding flow characteristics of vascular lesions.

With respect to appearance on imaging, lesions may be broadly categorized as well circumscribed (i.e., round or oval) or diffuse (infiltrative). In general, well-circumscribed lesions are more likely to be benign such as a cavernous hemangioma, fibrous histiocytoma, lipoma, neurofibroma, schwannoma or neurilemmoma, and pleomorphic adenoma. Conversely, malignancy more commonly presents with a diffuse infiltrative pattern such as adenoid cystic carcinoma, fibrosarcoma, lymphoma, pleomorphic adenocarcinoma, and most metastases among others.

However, important exceptions to this trend apply as well-circumscribed lesions may be malignant, as with mesenchymal chondrosarcoma, optic nerve glioma, and some metastases (breast, renal cell, melanoma, and others). Lymphoma may also appear well circumscribed on imaging, as may a benign mixed tumor with foci of malignant transformation. Conversely, benign tumors, such as lymphangioma and plexiform neurofibroma, may demonstrate a poorly circumscribed appearance. Nonneoplastic processes such as orbital cellulitis, idiopathic orbital inflammation, sarcoidosis, and Wegener granulomatosis may also appear poorly circumscribed on imaging and can be confused with malignancy. Finally, some entities such as orbital inflammatory disease can be either focal or diffuse.

In addition to demonstrating the boundaries of an orbital lesion, imaging can distinguish which orbital structures are involved to further refine the differential diagnosis. The locations within the orbit may also aid in creating the differential diagnosis. Specific neoplasms often localize to a particular structure or location within the orbit, such as the optic nerve, the intraconal space, the extraocular muscles, the extraconal space, the lacrimal gland or lacrimal gland fossa, the nasolacrimal sac, the orbital apex, the orbital bones, areas extrinsic to the orbit, and multifocal orbital locations.

4.4.1 Optic Nerve and Nerve Sheath

Lesions located in or around the optic nerve can represent glioma, meningioma, metastasis, lymphoma or a leukemic infiltrate, as well as inflammatory conditions or infection. Optic nerve gliomas often have a fusiform appearance on imaging and may cause kinking or bending of the nerve if the tumor outgrows its space. The optic canal limits the growth of intracanalicular gliomas, but expansion of the canal may be seen on imaging in this case. Optic nerve meningiomas appear circumferentially enlarged on imaging and may exhibit a “tram-track” pattern of enhancement on CT and MR imaging studies when the tumor circumferentially surrounds the nerve without affecting the nerve itself, due to a lower central density and higher peripheral density. Orbital meningiomas may occur unrelated to the optic nerve and arise from the meninges near the orbital apex and superior orbital fissure. Less common lesions of the optic nerve include ganglioneuromas, gangliogliomas, medulloepithelioma, subarachnoid carcinomatosis, hemangioblastoma, hemangiopericytoma, and others [2].

4.4.2 Intraconal Space

In the adult patient, lesions located within the muscle cone may represent infection (orbital cellulitis with or without abscess), inflammatory disease (idiopathic, sarcoidosis, Wegener granulomatosis), venous-lymphatic malformations, hamartomas (cavernous hemangioma), hemangiopericytoma, schwannoma, lymphoproliferative disease, angiosarcoma, metastases, and other conditions. Cavernous hemangiomas appear as well-defined, oval, or round masses on CT imaging studies and typically reside within the intraconal space; however, larger lesions may extend extraconally. Bone remodeling may occur with long-standing cavernous hemangiomas, but bony destruction should raise suspicion for malignancy.

Metastatic lesions, protean in appearance and location on imaging studies, occur commonly and factor into many differential diagnoses.

Infectious processes within the orbit range from diffuse inflammation of the orbital tissues to frank abscess formation, which can occur at any location within the orbit. In the immunocompromised patient with a history of cancer, diffuse orbital disease may signal metastasis, but invasive fungal disease from organisms such as Mucor, Aspergillus, and Rhizopus should be kept in mind. Most orbital infection occurs in the context of underlying sinus disease, the presence of which helps determine the appropriate diagnostic technique.

Orbital inflammation represents a broad spectrum of disease, and the condition may appear focal or diffuse on imaging. Focal inflammation commonly involves the lacrimal gland or the extraocular muscles and may masquerade as malignancy. Diffuse inflammation may involve the intraconal or extraconal compartments and mimic lymphoproliferative disorders, lymphoma, or metastasis. Inflammatory disease rarely causes signs of bone destruction or globe indentation, and these imaging features should raise suspicion for a neoplastic etiology.

Retrobulbar hemorrhage may appear as a well-defined, hyperintense lesion on CT. Orbital varices have a variety of appearances on imaging but are typically well defined. A varix may be round, oval, tubular, cone shaped, or have a tangled, "bag-of-worms" appearance, but they often enhance with IV contrast although filling can be partial due to thrombosis or phlebolith and a sedimentation level can be seen.

4.4.3 Extraocular Muscles

Lesions of the extraocular muscles can appear focal or diffuse and may be caused by nonneoplastic conditions such as thyroid eye disease or other inflammatory diseases, trauma (intramuscular hematoma), and infection (extraocular muscle abscess). Neoplastic processes, such as lymphoproliferative disease, metastases, dermatolipoma, and schwannomas, may appear to arise from an extraocular muscle on imaging studies. Myositis due to idiopathic inflammation may mimic extraocular muscle inflammation due to thyroid eye disease. However, in thyroid, orbitopathy imaging typically demonstrates sparing of the muscle tendon, whereas in other inflammatory disorders, imaging shows tendon involvement. Metastasis and amyloidosis should also be considered in cases of bilateral enlargement of one or more extraocular muscles.

4.4.4 Extraconal Space

Neoplastic lesions that may arise outside the muscle cone include metastasis, infection, lymphoproliferative disease, meningioma, and schwannoma orbital. Inflammatory diseases and hamartomas such as cavernous hemangioma may involve the extraconal space as well. Lymphoproliferative disorders, which range from benign reactive hyperplasia to lymphoma, may be focal or diffuse on imaging studies and may mimic other neoplasms, inflammatory, and infectious conditions.

Schwannomas can arise either within or around the muscle cone and appear as well-defined ovoid or fusiform masses. They are typically located in the superior orbit and run along the course of the effected nerve. Due to this tendency, these lesions often display elongation along the anterior-posterior axis on imaging studies. Schwannomas may contain cystic cavities, probably due to degeneration, and should be included in the differential diagnosis of cystic orbital lesions.

As with schwannoma, a solitary neurofibroma may occur in the superior orbit and appear as well-defined ovoid mass with elongation along and anterior-posterior axis along the course of the effected nerve. The term "solitary" neurofibroma is used to differentiate this entity from multiple neurofibroma in which two or more neurofibromas occur in the same orbit.

Less common extraconal lesions include fibrous histiocytoma and solitary fibrous tumors, leiomyosarcoma, liposarcoma, epithelial cyst, conjunctival dermoid cyst, parasitic cysts, malignant peripheral nerve sheath tumor, and others.

4.4.5 Lacrimal Gland and Lacrimal Gland Fossa

Nonneoplastic lesions of the lacrimal gland occur much more commonly than tumors but can mimic a tumor on imaging studies. These nonneoplastic lesions of the lacrimal gland and lacrimal gland fossa include infectious and inflammatory dacryoadenitis. While most cases of inflammatory dacryoadenitis remain idiopathic, IgG4-related orbital inflammation may be responsible in approximately one-quarter of cases [3]. Infiltrative etiologies include the spectrum of lymphoproliferative disorders – from benign reactive lymphoid hyperplasia to lymphoma, as well as amyloidosis, Wegener granulomatosis, Sjögren syndrome, and sarcoidosis [4].

Neoplasms of the lacrimal gland in the adult include benign lesions such as benign mixed tumor or pleomorphic adenoma, monomorphic adenoma, and oncocytomas. Malignant tumors include adenoid cystic carcinoma, pleomorphic adenocarcinoma, squamous cell carcinoma, mucoepidermoid carcinoma, and lymphoma [5]. Schwannomas of the lacrimal gland fossa may also occur and may be mistaken for an epithelial tumor on imaging.

Adenoid cystic carcinoma may vary in appearance on CT from a poorly defined entity to a well-defined round or oval mass, but bone destruction is often present. Imaging studies of lacrimal gland tumors can help point to an epithelial malignancy when bone erosion is present. Indenting of the globe, with bone remodeling, is more commonly seen in benign epithelial neoplasms.

4.4.6 Lacrimal Sac

Lesions of the lacrimal sac include infectious dacryocystitis, papillomas, granulomatous conditions such as Wegener granulomatosis and sarcoidosis, lymphoproliferative disorders, and epithelial neoplasms. In this location, benign lesions far outnumber malignant lesions [6].

4.4.7 Orbital Apex

Lesions located at the orbital apex may be challenging to distinguish based on imaging studies. Both neoplastic and nonneoplastic conditions may affect this region and include metastases, inflammation, granulomatous inflammation (Tolosa-Hunt syndrome), hamartomas, venous and venous-lymphatic malformations, arteriovenous malformations, fibrous dysplasia, and sphenoid wing meningioma [1]. Disease processes involving the bones of the orbital apex include fibrous dysplasia, which may be monostotic or polyostotic, and Paget's disease, which can rarely involve the greater and lesser wings of the sphenoid as well as the clinoid process.

4.4.8 Orbital Bones

Evaluation of the orbital bones on imaging studies provides important information regarding the behavior and extent of an orbital neoplasm. The bone itself may give rise to a tumor, or it may be involved secondarily with indentation, bone molding, erosion, infiltration, or hyperostosis.

Primary orbital bone tumors include benign conditions such as osteoma, osteoblastoma, ossifying fibroma, aneurysmal bone cyst, brown tumor, cholesterol granulomas, and fibrous dysplasia fibrous histiocytoma as well as malignancies, such as osteosarcoma, chondrosarcoma, Ewing sarcoma, Paget's disease, multiple myeloma, and plasmacytoma. Cavernous hemangiomas may be arise within the sphenoid bone of the orbit or other orbital bones, giving a distinct appearance on imaging studies.

Fibrous dysplasia appears as an amorphous hyperdense type of bone that has a "ground-glass" appearance. On computed tomographic imaging studies, orbital bone osteomas appear as well-defined, round, or lobulated masses arising from bone, and the fibrous subtype of the tumor may have a ground-glass appearance reminiscent of fibrous dysplasia. Bone destruction is not typical. A long-standing mucocele can also present with similar bony changes.

Osteosarcoma, on the other hand, appears irregular in appearance with bone destruction along with increased areas of calcium representing deposition of new albeit neoplastic bone. Osteosarcomas vary widely in amount of osseous, cartilaginous, and fibrous tissues present, and the appearance of the tumor on imaging studies will vary accordingly.

Sphenoid wing meningiomas appear as relatively well-defined lesions, which may contain areas of calcification. While computed tomographic imaging studies may show thickened, hyperostotic sphenoid bone, MR imaging better shows cavernous sinus and intracranial involvement for evaluation of this tumor. Ewing sarcoma, which rarely occurs past the age of 30, appears as an irregular cystic mass with bone destruction on CT imaging studies. Fibrosarcomas of the orbit appear as lytic bone lesions on CT imaging studies and may erode through the paranasal sinuses and orbital walls.

Orbital bones may also be secondarily involved in certain inflammatory conditions such as Wegener granulomatosis. Orbital intraosseous hemangioma and malignant vascular tumors of the orbital bones exist but are rare. Orbital tumors of cartilaginous origin include chondromas, osteochondromas, enchondroma, and fibrochondroma. Orbital dermoids that occur deeper in the orbit usually present later in life and may produce significant bony changes, especially in the trigone region of the greater wing of the sphenoid.

4.4.9 Eyelid, Globe, Sinus, and Brain

Invasion of the orbit by neighboring periorbital pathologies is less common than intraorbital metastasis and primary orbital lesions. Neoplasms of the cranial vault, the paranasal sinuses, eyelids, and globe may all secondarily extend into the orbit.

In adults, ocular tumor extension into the orbit is uncommon due to the conspicuous effects on visual function and cosmesis, as well as the time course required for such lesions to extend into the orbit. Malignant melanoma may grow through the emissary vessels or into the optic nerve to produce microscopic or limited orbital disease, but significant orbital extension in ocular melanoma typically only occurs in neglected cases.

Cutaneous and conjunctival neoplasia around the eye can invade the orbit in neglected cases, but also in cases where appropriate patient and physician vigilance has occurred. Tumors arising in the medial canthus are more likely to result in orbital extension due to the less robust orbital septum in this region. Certain aggressive tumors, such as sebaceous cell carcinoma, dermatofibrosarcoma protuberans, and undifferentiated squamous cell carcinoma, have a higher predilection for orbital invasion. Recurrent basal cell carcinoma or basal cell carcinoma occurring in the medial canthus or in the setting of Gorlin's syndrome may also grow to involve the orbit.

Orbital invasion from tumors of the paranasal sinuses occurs relatively commonly [7]. Tumors in this region often produce few symptoms, so both benign and malignant tumors may achieve significant size prior to presentation. It is not uncommon for such tumors to grow unnoticed until they produce orbital signs and symptoms. Mucoceles and mucopyoceles may occupy an entire sinus cavity with intracranial extension prior to presentation. Mucoceles appear as relatively well-defined cystic masses within an opacified paranasal sinus, often with adjacent bone erosion and remolding. Sinonasal carcinomas, including squamous cell carcinoma, nonkeratinizing carcinoma, and sinonasal undifferentiated carcinoma, may erode into the orbit and through the medial canthal skin prior to presentation. Imaging studies reveal significant bone destruction. Inverted papillomas of the paranasal sinuses, and even the lacrimal sac, may behave aggressively to produce orbital signs and bone destruction on imaging studies. Less commonly, ossifying fibroma, sinonasal fibrosarcoma, and schwannoma may arise primarily from a paranasal sinus and erode into the orbit.

Neoplasms arising within the nasopharynx, such as esthesioneuroblastoma and nasopharyngeal carcinoma, can also extend into the orbit, as can lesions from the cranial cavity, including meningocele, encephalocele, trigeminal schwannoma, and glioblastomas.

Table 4.4 Well-circumscribed lesions vs. diffuse lesions in the adult

Well-defined appearance	Poorly-defined appearance
Cavernous hemangioma	Orbital inflammation
Fibrous histiocytoma	Metastatic lesions
Lipoma	Primary malignant tumor
Neurofibroma	Lymphoproliferative disorders
Schwannoma	
Pleomorphic adenoma	

4.4.10 Diffuse Lesions

Several entities can involve contiguous orbital structures and may arise from any location within the orbit (Table 4.4). The more common conditions that can present with this multifocal or diffuse pattern include lymphoproliferative disease, idiopathic orbital inflammation, amyloidosis, and IgG4-related orbital disease. Imaging studies may not differentiate these entities, but each has a typical anatomic predilection and constellation of imaging findings.

Conclusion

Specific elements of the history and the physical examination begin the process of formulating a differential diagnosis. These elements also determine appropriate imaging studies to further refine the list of possible etiologies. The imaging studies help guide the surgical plan for diagnosis and treatment.

References

1. Vohra ST, Escott EJ, Stevens D, et al. Categorization and characterization of lesions of the orbital apex. Neuroradiology. 2011;53(2):89–107.
2. Kralik SF, Kersten R, Glastonbury CM. Evaluation of orbital disorders and cranial nerve innervation of the extraocular muscles. Magn Reson Imaging Clin N Am. 2012;20(3):413–34.
3. Okazaki K, Umehara H. Are classification criteria for IgG4-RD now possible? The concept of IgG4-related disease and proposal of comprehensive diagnostic criteria in Japan. Int J Rheumatol. 2012;2012:357071.
4. Soheilian M, Bagheri A, Aletaha M. Dacryoadenitis as the earliest presenting manifestation of systemic Wegener granulomatosis. Eur J Ophthalmol. 2002;12(3):241–3.
5. Wang XN, Qian J, Yuan YF, et al. Space-occupying lesions of the lacrimal gland at one tertiary eye center in China: a retrospective clinical study of 95 patients. Int J Ophthalmol. 2012;5(2):208–11.
6. Demirci H, Christianson MD. Orbital and adnexal involvement in sarcoidosis: analysis of clinical features and systemic disease in 30 cases. Am J Ophthalmol. 2011;151(6):1074–80.
7. Chu Y, Liu HG, Yu ZK. Patterns and incidence of sinonasal malignancy with orbital invasion. Chin Med J (Engl). 2012;125(9):1638–42.

Imaging Techniques

5

Patrick De Potter

Contents

P. De Potter, MD, PhD
Ocular Oncology Unit, Cliniques Universitaires St-Luc, Université Catholique de Louvain, Brussels, Belgium
e-mail: patrick.depotter@uclouvain.be

5.1 Introduction

Ultrasonography, color Doppler imaging, CT, and MR imaging are the most important imaging tools for the clinician in the field of orbital oncology. Catheter diagnostic angiography has a limited role in the diagnostic approach of orbit lesions except for evaluating vascular abnormalities suggesting the diagnosis of carotid-cavernous fistula. The role of positron emission tomography with [2–18F] fluoro-2-deoxy-D-glucose (FDG) in evaluation of orbital tumors is limited because FDG accumulates in extraocular muscles in proportion to their contractile activities and decreases lesion conspicuity in regions with high physiological tracer uptake.

5.2 Techniques of Orbital Imaging

5.2.1 Ultrasonography

Ultrasonography is a noninvasive simple, fast, and economical imaging technique allowing easy detection of an orbital lesion before any decision can be made if further evaluation with CT or MR imaging is necessary. However, it is limited by the requirement of skilled operators and because penetration of the deeper regions of the orbit at energy levels acceptable for the retina cannot be achieved (Table 5.1).

Although A- and B-mode orbital ultrasonography may provide good information about

J.D. Perry, A.D. Singh (eds.), *Clinical Ophthalmic Oncology*,
DOI 10.1007/978-3-642-40492-4_5, © Springer-Verlag Berlin Heidelberg 2014

Table 5.1 Acoustic tissue properties in various orbital diseases [1, 2]

	Acoustic properties		
Tissue/disease	Reflectivity at tissue sensitivity	Attenuation	Associated features
Normal orbital fat	Very high (95–100 %)	Medium	Multiple interfaces
Orbital inflammation	High (60–95 %)	High	
Neurofibroma		Medium to high	Low reflectivity areas indicate mucoid spaces
Schwannoma			
Cavernous hemangioma			Phleboliths
Hemangiopericytoma			
Hematoma – abscess (acute)	Medium (40–60 %)	Low	
Lymphangioma		Low	Cystic spaces
Optic nerve glioma		High or medium	
Optic nerve sheath meningioma		High or medium	
Mucocele	Low (5–40 %)	Low	
Dermoid			High and low reflectivity areas (fine hair, cartilaginous remnants)
Hematoma – abscess (chronic)			
Lymphoma			Homogeneous at high sensitivity
Malignant tumor	Variable	Variable	

acoustic inner texture of an orbital lesion, it is difficult to differentiate normal from abnormal tissues and it remains a semiquantitative approach for tissue characterization (reflectivity and sound attenuation). Dynamic or real-time information represents one of the advantages of ultrasonography over CT and MRI. The relationships of a pathologic process to the normal anatomic structures can be easily shown by evaluating the same section with different gaze directions, particularly in cases of intraconal lesions. Extension to the orbital walls, especially when associated with erosion or destruction of bone, however, is better appreciated by CT. There are no studies of the relationship between reflectivity and histopathology in the orbit but most orbital lesions display less coarse and heterogeneous structures with lower reflectivity than the normal orbital tissues (Fig. 5.1) [1, 2].

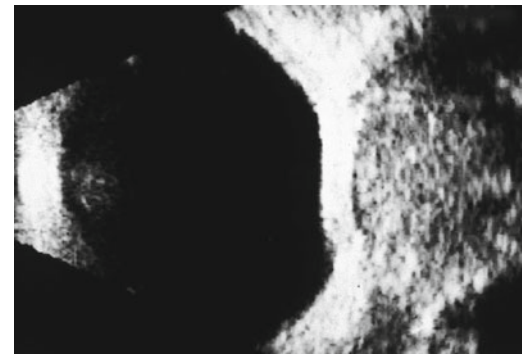

Fig. 5.1 B-scan ultrasound of cavernous hemangioma displays a well-defined oval echogenic lesion deforming the globe

5.2.2 Color Doppler Imaging (CDI)

CDI has proved to be effective in the display of the normal orbital and intraocular vasculature, tumor vascularization, and echographic differentiation of tumors from subretinal hemorrhage [3]. In patients with carotid-cavernous fistula or dural cavernous arteriovenous malformations, CDI clearly demonstrates the dilated, arterialized superior ophthalmic vein with high-velocity blood flow toward the transducer [4]. In addition, CDI may be able to differentiate meningioma from glioma of the optic nerve. It may also be effective in confirming the diagnosis of orbital varices by showing the dynamic changes throughout inspiration and expiration [5].

5.2.3 Computed Tomography

The basis of computed tomography (CT) is the measurement of different tissue absorption values (Hounsfield units) of a given tissue to neighboring structures, following exposure to x-rays.

5.2.3.1 Conventional Computed Tomography

Conventional CT provides excellent detail of the eye, orbital soft tissues, and bony orbit and has an established role in the evaluation of orbital trauma and orbital diseases (Box 5.1). However, there are several drawbacks, including relatively long exposures times and increased radiation exposure (approximately 75 mGy of radiation). Although reconstructions in the sagittal and coronal planes can be obtained from conventional CT data, these images are of poor quality under practical conditions (Table 5.2).

Box 5.1: Indications of Orbital CT as a First Imaging Step

- Evaluation of patient with proptosis with suspicion of osseous, fibro-osseous, and fibrous lesions
- Evaluation of patient with clinical diagnosis of lacrimal gland lesion
- Evaluation of orbital trauma
- Detection of calcification
- Contraindication for MRI (claustrophobia, metallic implants, allergy to contrast agent)

5.2.3.2 Helical Computed Tomography

CT studies have evolved to a spiral (helical) technique with multiple detectors or a rotating detector system. Helical CT, also known as spiral or volume acquisition CT, acquires data in a continuous fashion. With the use of image-reconstruction algorithms, multiple very thin sectioned and multiplanar computer-reformatted images can be produced that are superior to those obtained from standard incremental axial CT images. By producing planar and three-dimensional reformations with less motion artifact than conventional CT, helical CT provides useful information in almost any plane. If bony involvement is clinically suspected, bone

Table 5.2 Comparison of various imaging techniques

Technique	Comparison	
Ultrasonography	Advantages	Disadvantages
	Inexpensive Tissue characterization Dynamic information Evaluation of anterior orbital lesions	Requirement for skilled operator
Computerized tomography	Availability Short examination time	Ionizing radiation Allergic reaction with contrast agents Artifacts: High-density foreign body Positioning Partial voluming Beam hardening
Magnetic resonance imaging	High soft tissue contrast Large imaging depth No ionizing radiation Paramagnetic effects by: Methemoglobin Protein Melanin Gadopentetate dimeglumine	Slow acquisition Claustrophobia Obesity Missile and thermal injuries Artifacts: Motion Wrap around Bioinhomogeneity Chemical shifts Partial volume Flow or pulsation

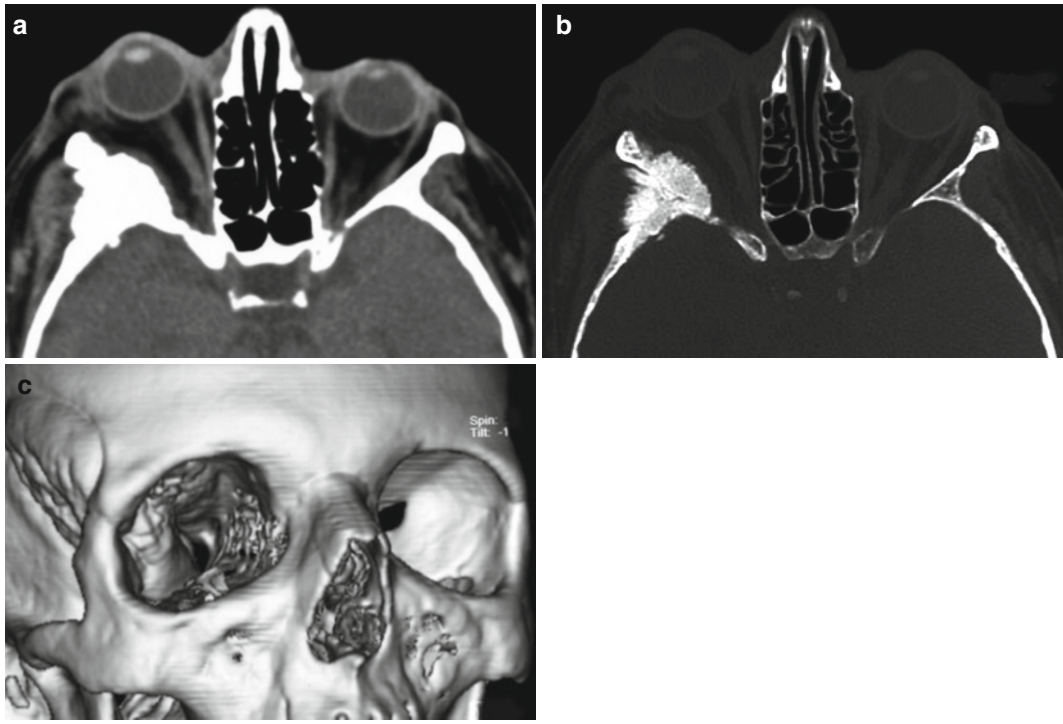

Fig. 5.2 Axial CT images of a right sphenoid wing meningioma. Helical CT showing a right hyperostotic sphenoid wing (**a**), bone windows (**b**), and three-dimensional scan (**c**)

algorithm reconstruction (bone window) should be used (Fig. 5.2) [6–8]. In addition, acquisition time is reduced, a great advantage with children and unstable patients [6–8].

5.2.3.3 Three-Dimensional (3D) Computed Tomography

Three-dimensional imaging, a computerized post-processing technique, allows unique topographic overview of selected anatomic or pathologic structures that have been isolated (a process called segmentation) from the image tissue volume [9]. For 3D CT imaging of the head and orbits, scanning technique with either 1.5-mm contiguous slices or 1-mm slices at 1.5-mm slice incrementation is recommended. Due to partial volume averaging, the thin medial wall, the orbital floor, and the anterior wall of the maxillary sinuses are not visualized, causing artificial holes often referred as pseudoforamina. Special processing techniques and sophisticated edge detection algorithms may be used to avoid these imaging artifacts. Low-contrast tissue segmentation like in tumor-muscle or tumor-neural tissue interfaces requires visual identification and manual separation [9]. Three-dimensional imaging of the orbit is a perfect technique to illustrate a wide variety of teratogenic (particularly craniofacial dysplasia and synostosis), pathogenic, traumatogenic, and iatrogenic orbital abnormalities and to comprehend the extent and location of the pathology in order to plan the surgical approach and facilitate comparison between preoperative and postoperative changes (Fig. 5.2). Computed tomography, while excellent for bony detail of the lacrimal drainage system, provides a limited soft tissue detail than MRI and suffers from image degradation in out-of-plane images.

5.2.4 Magnetic Resonance Imaging

Magnetic resonance (MR) imaging is based on a physical phenomenon called nuclear magnetic resonance effect on the atomic nuclei, primarily hydrogen atoms of water molecules in human tissues. MR images of patients are obtained by inducing electromagnetic signals from the magnetic

Box 5.2: Indications of Orbital MRI as a First Imaging Step

- Location and extent of orbital lesion
- Evaluation of orbital, intracanalicular, and prechiasmal optic pathways
- Evaluation of patient with proptosis (hemorrhagic, neoplastic, fibrosclerotic, mucinoid/cystic degeneration)
- Evaluation of patient with progressive bluish lid swelling (capillary hemangioma versus lymphangioma)
- Evaluation of tumor response after radiotherapy or chemotherapy
- Evaluation of anophthalmic socket when orbital tumor recurrence is suspected
- Orbital trauma when ferromagnetic material is excluded
- Identification of fibrovascular ingrowth within biocompatible implant

dipole movements of ^{1}H nuclei and then converting these signals into cross-sectional images.

Although CT and MR studies are complementary, MR imaging provides superior soft tissue contrast. Its multiplanar capability with outstanding tissue contrast and the absence of ionizing radiation make MR imaging an especially suitable technique for imaging orbital structures (Box 5.2) [7, 10, 11]. Moreover, the superficial location of the eye and eyelids permits the use of surface coils which improve the display of anatomic details. Current MRI is often performed using 1.5 T units of magnetic strength. The overall scan time can be shortened by fast spin-echo sequences. Fat suppression techniques are used to eliminate the extremely strong bright signal intensity from orbital fat which may overwhelm high signal intensities of enhancing surrounding lesions.

5.3 Interpretation of Imaging Studies

Interpretation of imaging studies is facilitated by evaluating radiological characteristics such as anatomic location, appearance, content, post-contrast enhancement features, and bone characteristics [7, 10–15].

5.3.1 Location

CT provides similar information to MR imaging on the location and extent of a lesion in the anterior orbital space, the globe, the intraconal-extraconal space, orbital fat, extraocular muscles, cavernous sinus, and temporal fossa. CT remains the imaging modality of choice in the evaluation of lesions located in the lacrimal gland fossa, the paranasal sinuses, and adjacent bony orbit. Due to superior soft tissue contrast resolution by MR imaging, it is the study of choice for lesions infiltrating the optic nerve, optic nerve sheath, and orbital apex.

5.3.2 Appearance

An orbital lesion may be described as having a regular (round or oval) or irregular (infiltrative) configuration. Its margin characteristics may be well circumscribed or diffuse.

5.3.3 Content

Information on the content of the lesion (cystic or solid; homogeneous or heterogeneous) could be obtained by both CT and MR imaging techniques. Both imaging techniques also detect presence of fluid/fluid or fluid/air levels. When lesion density is higher than that of the vitreous, CT images identify a lesion as solid. As wide range of tissue densities on CT scans or signal intensities on MR images relate to the internal architecture and the presence of proteinaceous or blood products, it is not always possible to differentiate a solid from a cystic orbital lesion. MR images identify tissue compounds such as melanin, methemoglobin, deoxyhemoglobin, ferritin, and proteinaceous material. Punctate or conglomerate increased densities on CT scans or foci of signal void on MR scans may be seen in trauma, vascular tumors, optic nerve sheath tumors (meningioma), epithelial lacrimal gland tumor, and malignant osseous tumors (osteosarcoma). In general, MR images provide more information about the content of the lesion than the CT images. However, CT is best suited for the detection of calcification.

5.3.4 Contrast Enhancement

The pattern of contrast enhancement (present or absent; homogeneous or heterogeneous) of orbital lesions guides in forming a differential diagnosis. Enhancement characteristics of an orbital lesion are best identified on post-contrast fat-suppressed T1-weighted images. No enhancement is documented in hemorrhagic process, dense scar tissue, collection of fluid, or necrotic portion of tumors. Minimal contrast enhancement suggests a chronic or sclerosing orbital inflammation, tissue fibrosis, or post-therapeutic scar tissue. Moderate to marked contrast enhancement is usually noticed in solid tumors as well as in acute inflammatory orbital lesions. Linear enhancement surrounding a non-enhancing well-delineated lesion suggests the cystic nature of the lesion. Well-defined linear or void of signal within an enhancing lesion may suggest air, high blood flow vessels (artery or vein), fragments of cortical bone, or foreign body. Gadolinium-enhanced MR imaging has proven as the best-suited imaging modality for assessing the fibrovascularization tissue progression into porous orbital implants (hydroxyapatite and porous polyethylene).

5.3.5 Bone Characteristics

Bone changes induced by an orbital lesion include cortical bony indentation and molding, bone erosion, bone lysis, bone infiltration, and hyperostosis. The destruction of cortical bone is seen on CT as a loss of the highly dense cortical bone and on MR scans as a discontinuity of the linear signal void produced by the normal cortical bone. CT with bone windows or 3D CT is almost always preferred to assess orbital disorder suspected to affect the bony orbit.

5.3.5.1 Bone Molding

Molding of the bone by a well-circumscribed orbital mass highly suggests a congenital lesion (dermoid cyst, lymphangioma) or a slowly growing benign tumor (cavernous hemangioma, neurofibroma, neurilemoma, and benign lacrimal gland tumor).

5.3.5.2 Bone Erosion

Bone erosion is usually seen with more aggressive inflammatory lesions, primary tumors, and secondary tumors.

5.3.5.3 Bone Lysis

Bone destruction or lysis is observed in very aggressive primary tumors, secondary malignant tumors, and inflammatory lesions (idiopathic orbital inflammation, eosinophilic granuloma).

5.3.5.4 Bone Infiltration

Tumor infiltration of the bony orbit is best seen on CT with bone algorithm reconstruction and identified on MR imaging as a discontinuity of cortical signal void and loss of high signal intensity of the fat in the bone marrow.

5.3.5.5 Hyperostosis

Hyperostosis is observed with benign osseous tumors (meningioma), malignant bone tumors (osteosarcoma), and metastatic tumors such as from prostate carcinoma. In general, osseous spiculation and inhomogeneous density are findings suggestive of a malignant tumor.

5.4 Radiological Differential Diagnosis

Orbital tumors can be classified into one of seven radiological patterns (well-circumscribed solid, ill-defined solid, circumscribed cystic, enlarged optic nerve, enlarged lacrimal gland, enlarged extraocular muscles, and anomalies of the bony orbit) to obtain reliable differential diagnosis (Box 5.3).

Box 5.3: Six Radiological Patterns of Orbital Tumors

- Well-circumscribed solid tumor
- Ill-defined solid tumor
- Circumscribed cystic tumor
- Enlarged optic nerve
- Enlarged lacrimal gland
- Enlarged extraocular muscles
- Anomalies of the bony orbit

Table 5.3 Magnetic resonance imaging features of well-circumscribed orbital tumors on spin-echo sequences

Tumor	Lesion appearance		Degree of enhancement with Gd-DTPA
	Signal intensity[a]		
	T1-WI	T2-WI	
Cavernous hemangioma	Homo	Hetero/homo (late)	Homo
	Iso/hyper	Iso/hypo	+++
Neurilemoma	Hetero	Hetero	Hetero
	Iso/hyper	Iso/hypo	+/+++
Neurofibroma	Hetero	Hetero	Hetero
	Iso/hyper	Iso/hypo	+/+++
Fibrous histiocytoma	Hetero	Hetero	Hetero
	Hyper/hypo	Hyper/hypo	++++
Hemangiopericytoma	Homo	Homo	Hetero
	Iso/hyper	Iso/hypo	++++
Orbital varix	Homo/hetero	Homo/hetero	Homo/hetero
	Iso/hyper	Iso/hypo	++++
Thrombosed varix	Hetero	Hetero	Hetero
	Iso/hyper	Iso/hypo	–/+
Orbital metastasis (skin melanoma, carcinoid)	Homo	Homo	Homo
	Iso/hyper	Iso/hypo	+/+++

[a]With respect to vitreous
Iso isointense, *Hyper* hyperintense, *Hypo* hypointense, *Homo* homogeneous, *Hetero* heterogeneous

5.4.1 Well-Circumscribed Solid Orbital Lesions

The most frequent well-circumscribed orbital tumors are cavernous hemangioma, neurilemoma, neurofibroma, fibrous histiocytoma, and hemangiopericytoma [10–15]. These tumors usually present as a well-defined, oval-to-round intraconal orbital mass on MR imaging (Table 5.3).

Cavernous hemangioma shows increasing homogeneous enhancement on delayed images owing to the pooling of the contrast material within the tumor. Tumor enhancement and delineation are best evaluated on Gd-DTPA-enhanced T1-weighted images using fat suppression techniques (frequency-selective presaturation techniques). Heterogenicity in tumor signal may be related to the presence of calcified phleboliths which produce signal void on T1- and T2-weighted images. Neurilemoma (schwannoma), neurofibroma, fibrous histiocytoma, and hemangiopericytoma may conceivably have identical non-enhancing MR characteristics of less common well-circumscribed orbital lesions such as lymphoproliferative disorder, metastasis from skin melanoma or carcinoid tumor, capillary hemangioma, orbital varix, and rhabdomyosarcoma (Fig. 5.3).

5.4.2 Ill-Defined Solid Orbital Lesions

The radiological differential diagnosis of common solid ill-defined orbital lesions in children includes capillary hemangioma, lymphangioma, plexiform neurofibroma, idiopathic orbital inflammation, and metastasis [10–16]. In adults idiopathic orbital inflammation, metastasis, primary orbital tumor, and lymphoproliferative disorder are more frequent causes.

There are no specific CT features of ill-defined orbital lesions but CT provides clues regarding the malignant nature or chronic behavior of an orbital mass if bone changes (molding, erosion, lysis, and hyperostosis) are identified on bone windows scans. Radiolucency areas within the tumor may suggest necrotic changes.

The increased signal of an inflammatory process is related to its acute stage and its high concentration of free water (Table 5.4).

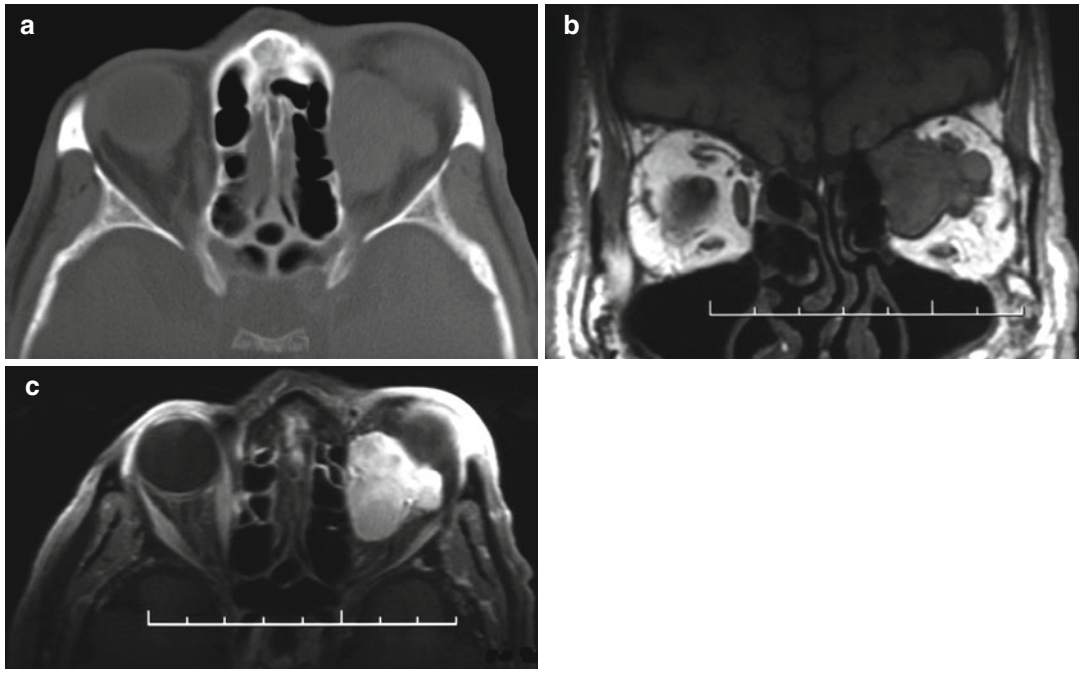

Fig. 5.3 Left orbital schwannoma. Axial CT image showing a well-circumscribed orbital mass (**a**). Coronal pre-contrast T1-weighted image. The lesion shows slight heterogeneous appearance (**b**). Axial post-contrast T1-weighted image displaying heterogeneous enhancement (**c**)

Table 5.4 Magnetic resonance imaging features of ill-defined orbital tumors on spin-echo sequences

Tumor	Lesion appearance Signal intensity[a] T1-WI	 T2-WI	Degree of enhancement with Gd-DTPA
Orbital metastasis	Homo/hetero Hyper Hypo +/+++	Homo/hetero Iso/hypo	Homo/hetero +/+++
Capillary hemangioma	Homo/hetero Iso/hyper	Homo/hetero Iso/hypo	Homo/hetero +++
Lymphoid proliferative disorder	Homo Hyper	Homo Hypo	Homo +++
Primary orbital tumor	Homo/hetero Hyper	Homo/hetero Hypo	Homo/hetero +/+++
Acute idiopathic inflammation	Homo Iso/hyper	Homo Iso/hypo	Homo +++
Chronic idiopathic inflammation (sclerosing type)	Homo Iso/hyper	Homo Hypo	Homo/hetero –/+

[a]With respect to vitreous
Iso isointense, *Hyper* hyperintense, *Hypo* hypointense, *Homo* homogeneous, *Hetero* heterogeneous

By studying T2 relaxation times, it may be possible to differentiate muscle enlargement caused by inflammatory edema from infiltrative process. Malignant tumors and occasionally inflammatory lesions may produce bone changes which appear as disruption of the regular signal void of the adjacent cortical bone or as a loss of the high signal of the marrow fat.

Table 5.5 Magnetic resonance imaging features of cystic orbital tumors on spin-echo sequences

Tumor	Lesion appearance		Degree of enhancement with Gd-DTPA
	Signal intensity[a]		
	T1-WI	T2-WI	
Dermoid cyst	Hetero	Hetero	Lumen –
	Iso/hyper	Iso/hypo	Capsule, septa +
Epithelial cyst	Homo	Homo	Lumen –
	Iso/hyper	Iso/hypo	Capsule, septa +
Mucocele	Homo	Homo	Lumen –
	Iso/hyper	Iso/hypo/hyper	Capsule, septa +
Hemorrhagic cyst/ lymphangioma	Hetero	Hetero	Lumen –
	Iso/hyper	Iso/hypo/hyper	Capsule, septa +

[a]With respect to vitreous
Iso isointense, *Hyper* hyperintense, *Hypo* hypointense, *Homo* homogeneous, *Hetero* heterogeneous

Minimal and heterogeneous enhancement is usually observed in the sclerosing type of orbital inflammation, and marked enhancement is observed in the acute type making their radiological differentiation easier. However, MRI does not provide sufficient histologic tissue specificity to allow reliable differentiation between idiopathic orbital pseudotumor, benign reactive lymphoid hyperplasia, atypical lymphoid hyperplasia, and lymphoma.

5.4.3 Well-Circumscribed Cystic Lesions

The differential diagnosis of cystic orbital lesions includes dermoid cyst, colobomatous cyst, teratoma, meningoencephalocele, lymphangioma, acquired inclusion cyst, chronic hematic cyst (cholesterol granuloma), mucocele, subperiosteal hematoma, and parasitic cyst [10–15, 17].

Orbital CT offers excellent information regarding the cystic features of the lesion as its density is similar to that of the vitreous. However, cystic lesions with higher density (high content of protein, keratinaceous material, blood products) may simulate solid well-circumscribed orbital tumor. MR studies are more specific than CT in identifying tissue component within the cystic mass as well as the linear enhancement of the capsule surrounding the non-enhancing lumen of the cyst. On MR imaging the cystic lesions appear as well-defined, round-to-oval lesions with variable signal intensities depending upon the composition of their content (Table 5.5). Dermoid cyst may have a characteristic dumbbell configuration. Fat-fluid level is characteristically seen in dermoid cyst. A fluid-fluid level is suggestive of subacute hemorrhagic lymphangioma or hemorrhagic cyst with the superior aspect of the cyst containing the methemoglobin released from the lyzed erythrocytes and the dependent portion containing the settled cellular elements of the hemorrhage with intracellular methemoglobin. The increasing concentration of proteinaceous secretions in a mucocele produces a higher signal intensity of the lesion (Fig. 5.4).

5.4.4 Enlarged Optic Nerve

The differential diagnosis of an enlarged optic nerve includes juvenile pilocytic astrocytoma, malignant glioma, secondary tumor from intraocular tumor (retinoblastoma, uveal melanoma, melanocytoma), CNS lymphoma or systemic metastatic disease, and optic neuritis [10–15, 18]. In all these diseases, the optic nerve may assume a tubular, fusiform, and lobular configuration. The differential diagnosis of an enlarged optic nerve sheath includes meningioma, meningeal spread of tumor, meningitis, arachnoidal cyst, hemorrhage, and CSF expansion as seen with pseudotumor cerebri or orbital apex compression.

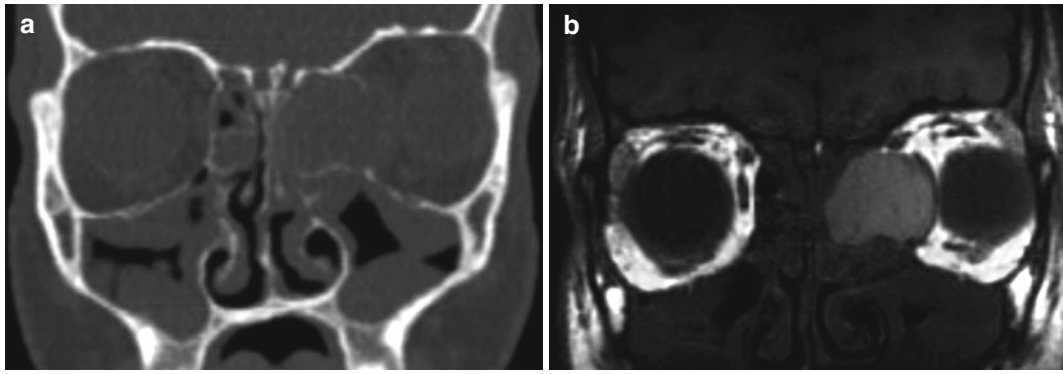

Fig. 5.4 Left ethmoidal mucocele with bilateral pansinusitis. Coronal CT with bone window suggesting the rupture of the medial orbital wall (**a**). Coronal pre-contrast T1-weighted image. The cystic lumen shows high signal intensity due to the high proteinaceous content (**b**)

The pattern of enhancement of enlarged optic nerve allows differentiation between an optic nerve lesion and an optic nerve sheath lesion. In optic nerve lesions the enhancement is within the optic nerve, whereas the enhancement is eccentric surrounding a hypointense optic nerve. The characteristic kinking and buckling of the enlarged optic nerve is highly suggestive of juvenile pilocytic astrocytoma (optic nerve glioma). On pre-contrast T1-weighted images, juvenile pilocytic astrocytoma (JPA) appears isointense with respect to the cerebral gray matter (Fig. 5.5). The tumor may be surrounded by reactive arachnoid hyperplasia which shows a slightly hypointense signal. On T2-weighted images, fusiform JPA demonstrates relatively high signal intensity, whereas large lobulated tumors tend to show a more heterogeneous signal. The peripheral hyperintense portion (perineural arachnoid gliomatosis or arachnoidal hyperplasia or CSF accumulation) surrounds a central linear core of lower signal intensity (compact proliferation of glial cells). On post-contrast studies, JPA shows variable enhancement which can be traced through the optic canal to the chiasm and optic tracts when it involves the intracranial portion of the optic nerve. The non-enhancing peripheral portion of the tumor, which is hyperintense on T2-weighted images, probably represents arachnoidal hyperplasia or an ectatic subarachnoid space around the optic nerve. The perineural arachnoid gliomatosis shows enhancement.

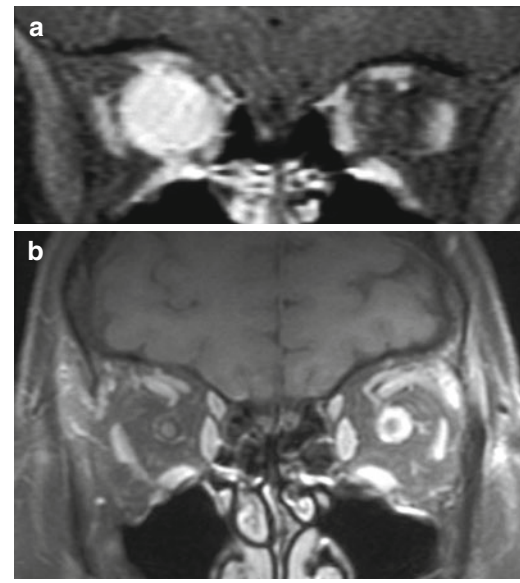

Fig. 5.5 Enlarged optic nerve on coronal post-contrast T1-weighted images. Enhancing pattern of juvenile pilocytic astrocytoma within the right optic nerve (**a**). Rim-like enhancing left optic nerve sheath meningioma (**b**)

Involvement of the optic nerve with retinoblastoma or melanoma cells, lymphoproliferative tissue, and metastatic process are best detected on post-contrast MR studies. In these cases, the pattern of enhancement within the optic nerve may be localized or diffuse.

The intensity pattern of optic nerve sheath meningioma on pre-contrast MR studies is variable and the tumor may appear isointense,

Table 5.6 Magnetic resonance imaging features of lacrimal gland lesions on spin-echo sequences

Tumor	Lesion appearance		Degree of enhancement with Gd-DTPA
	Signal intensity[a]		
	T1-WI	T2-WI	
Dacryops	Homo Iso/hyper	Homo Iso/hypo	–
Lymphoid proliferative disorder	Homo Hyper	Homo Hypo	Homo +/+++
Acute idiopathic inflammation (dacryoadenitis)	Homo Iso/hyper	Homo Iso/hypo	Homo +++
Chronic idiopathic inflammation (sclerosing type)	Homo Iso/hyper	Homo Hypo	Homo/hetero –/+
Pleomorphic adenoma (Benign mixed tumor)	Homo Iso/hyper	Homo Iso/hypo	Homo +++
Adenoid cystic carcinoma	Homo/hetero Hyper	Homo/hetero Hypo	Homo/hetero +/+++

[a]With respect to vitreous
Iso isointense, *Hyper* hyperintense, *Hypo* hypointense, *Homo* homogeneous, *Hetero* heterogeneous

hypointense, or hyperintense with respect to the optic nerve on T1- and T2-weighted images. On post-contrast films, the tumor shows marked enhancement which characteristically take a rim or eccentric pattern surrounding the non-enhancing optic nerve. A small intracanalicular or intracranial extension of the tumor is best identified on post-contrast T1-weighted images with fat suppression techniques. Calcification shows a low signal intensity on T1- and T2-weighted images without enhancement with Gd-DTPA.

On CT, the tubular or globular enlargement seen with an optic nerve sheath meningioma is nonspecific. Tram tracking, sign in which the denser and thicker optic nerve sheath outlines a central lucency representing the residual optic nerve, is characteristic but is not specific to optic nerve sheath meningioma.

5.4.5 Enlarged Lacrimal Gland

Lacrimal gland lesions may be classified as non-epithelial and epithelial. The non-epithelial lacrimal gland lesions include inflammation and lymphoid tumors, whereas the epithelial lesions included dacryops, pleomorphic adenoma, and malignant epithelial tumors (adenoid cystic carcinoma) [10–15].

Orbital CT is more specific than MRI in the detection of calcification within the enlarged lacrimal gland and in the evaluation of bone destruction in the lacrimal gland fossa. On MRI, among the non-epithelial lesion of the lacrimal gland, the inflammatory process (dacryoadenitis) usually appears more ill-defined than a lymphoid infiltrate which can mold to the globe (Table 5.6). The epithelial tumor of the lacrimal gland usually presents as a well-circumscribed mass in the lacrimal gland fossa and produces bone scalloping of the frontal bone. Adenoid cystic carcinoma may have an irregular, relatively well-defined, or infiltrative pattern with possible evidence of bone destruction.

Calcification within the enlarged lacrimal gland is highly suggestive of adenoid cystic carcinoma and appears as hypointense areas on T1- and T2-weighted images without enhancement on post-contrast scans.

5.4.6 Enlarged Extraocular Muscles

The extraocular muscles can be enlarged by infectious, inflammatory, neoplastic, vascular,

Table 5.7 Magnetic resonance imaging features of enlarged extraocular muscles on spin-echo sequences

Entity/tumor	Extent of involvement	Lesion appearance		Degree of enhancement with Gd-DTPA
		Signal intensity[a]		
		T1-WI	T2-WI	
Thyroid orbitopathy	Uni/bilateral Single/multiple Tendon (+)	Homo Hyper	Homo Iso/hypo	Homo +/+++
Idiopathic myositis	Uni/bilateral Single/multiple Tendon (+)	Homo Hyper	Homo Iso/hypo	Homo +/+++
Rhabdomyosarcoma	Unilateral Single/multiple Tendon (+/–)	Homo/hetero Iso/hyper	Homo/hetero Iso/hypo	Homo/hetero
Metastasis	Uni/bilateral Single/multiple Tendon (+/–)	Homo/hyper Hyper	Homo/hetero Hypo	Homo/hetero –/+++
Lymphoma	Uni/bilateral Single/multiple Tendon (+/–)	Homo Hyper	Homo Hypo	Homo +++
Carotid-cavernous fistula	Unilateral Multiple Tendon (–)	Homo Hyper	Homo Hypo	Homo +++

[a]With respect to vitreous
Iso isointense, *Hyper* hyperintense, *Hypo* hypointense, *Homo* homogeneous, *Hetero* heterogeneous

and degenerative processes (Table 5.7). Such involvement is usually best seen on post-contrast coronal CT and MR images [13–16]. In thyroid-associated orbitopathy, the belly of the extraocular muscles is expanded, and unlike idiopathic myositis, the tendinous attachment to the globe is usually spared [19]. Neoplastic infiltration (rhabdomyosarcoma, metastasis, lymphoma) may involve the extraocular muscle focally or diffusely with occasional sparing of the inserting tendon. Tumor necrosis may produce heterogeneous signal intensities. Focal or multifocal nodularity of the extraocular muscle(s) is highly suggestive of metastatic disease (Fig. 5.6) [13–16].

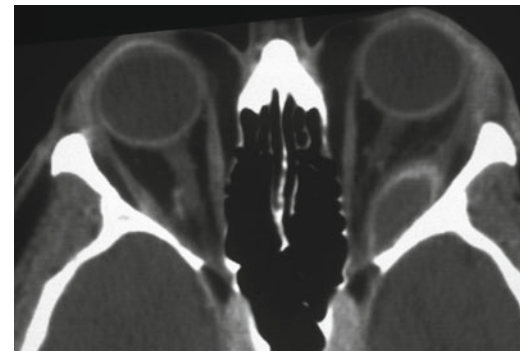

Fig. 5.6 Focal enlargement of the left lateral rectus muscle by metastatic carcinoid from the lung. The necrotic tumor does not enhance

5.4.7 Anomalies of Bony Orbit

CT remains the imaging modality of choice for the evaluation of bone abnormalities (scalloping, deformity, hyperostosis, expansion, and bone marrow invasion) as well as osseous, fibro-osseous, and fibrous tumors [10–15, 20].

The fact that cortical bone has a signal void permits bone to be demarcated from adjacent tissues on MR imaging. Good contrast is therefore available between bone and orbital fat, muscle, and brain. However, cortical bone may not be clearly defined when it lies adjacent to structures in which signal is not generated such as air, rapidly flowing blood, dura, or calcification.

Osteosarcoma appears as an ill-defined mass with a heterogeneous, hyperintense signal with respect to the vitreous and gray matter on T1-weighted scans. On T2-weighted images, the tumor has a heterogeneous lower signal intensity. After Gd-DTPA injection, osteogenic sarcoma demonstrates heterogeneous enhancement. Replacement of the cortical bone and fat marrow and orbital and cranial extension are best identified on post-contrast fat-suppressed T1-weighted images. CT scans demonstrate an irregular, invasive, and destructive tumor with lytic and sclerotic changes associated with focal areas of calcification.

Fibrous dysplasia displays sclerotic, homogeneous, dense, and ground-glass appearance on CT but alternate areas of lucency and increased density can also be identified. On MR imaging fibrous dysplasia shows very low signal intensity on T1- and T2-weighted images.

Aneurysmal bone cysts of the orbit appear as multicystic, loculated masses associated with bone destruction and possible extension to the adjacent sinuses. These tumors have heterogeneous signal intensities and fluid-fluid levels reflecting the various stages of evolution of the hemorrhagic content. Orbital CT scans show irregular expansion and destruction of bone associated with a mildly enhancing loculated cystic mass.

The major role of MR in evaluation of secondary orbital tumors from the paranasal sinuses is to delineate the extent of the infiltrative tumor process within the orbit, the sinuses, and the brain. These malignant tumors are fairly cellular and usually show a low signal intensity on T1-weighted images and increased signal on T2-weighted images with respect to orbital fat.

5.5 Summary

Ultrasonography, color Doppler imaging, CT, and MR imaging are the most important imaging tools for the clinician in the field of orbital oncology. Although orbital ultrasonography may provide good information about acoustic inner texture of an orbital lesion, it is difficult to differentiate normal from abnormal tissues. CT provides excellent detail of the eye, orbital soft tissues, and bony orbit and has an established role in the evaluation of orbital trauma and orbital diseases. Although CT and MR studies are complementary, MR imaging provides superior soft tissue contrast. Interpretation of imaging studies is facilitated by evaluating radiological characteristics such as anatomic location, appearance, content, post-contrast enhancement features, and bone characteristics. Moreover, orbital tumors can be classified into one of seven radiological patterns (well-circumscribed solid, ill-defined solid, circumscribed cystic, enlarged optic nerve, enlarged lacrimal gland, enlarged extraocular muscles, and anomalies of the bony orbit) to obtain reliable differential diagnosis.

References

1. Berges O, Bilaniuk LT. Orbital ultrasonography: ocular and orbital pathology. In: Newton TH, Bilaniuk LT, editors. Radiology of the eye and orbit. New York: Raven; 1990; chap 7.
2. Nasr AM, Abou Chacra G. Ultrasonography in orbital differential diagnosis. In: Karcioglu ZA, editor. Orbital tumors, diagnosis and treatment. New York: Springer; 2005. p. 73–83.
3. Lieb WE. Color Doppler imaging of the eye and orbit. Radiol Clin North Am. 1998;36:1059–71.
4. Karam EZ, Destarac L, Hedges TR, Heggerick PA. Abnormal ophthalmic veins: differential diagnosis and management using color Doppler imaging. Neuro-Ophthalmology. 1999;22:87–96.
5. Jacquemin C, Bosley T, Mullaney P. Orbital color Doppler imaging of optic nerve tumors. Int Ophthalmol. 1999;23:11–5.
6. Rhea JT, Rao PM, Novelline RA. Helical CT and three-dimensional CT of facial and orbital injury. Radiol Clin North Am. 1999;37:489–513.
7. Rosel P. The basics of orbital imaging. In: Karcioglu ZA, editor. Orbital tumors, diagnosis and treatment. New York: Springer; 2005. p. 84–93.
8. Klevansky A. The efficacy of multiplanar reconstructions of helical CT of the paranasal sinuses. AJR Am J Roentgenol. 1999;173:493–5.
9. Zonneveld FW, Vaandrager JM, van der Meulen JHC, Koornneef L. Three-dimensional imaging of congenital disorders involving the orbit. Radiol Clin North Am. 1998;36:1261–79.
10. De Potter P, Shields JA, Shields CL. MRI of the eye and orbit. Philadelphia: Lippincott; 1995.
11. Wichmann W. Magnetic resonance imaging (MRI). In: Muller-Forell S, editor. Imaging of orbital and

visual pathway pathology. Berlin: Springer; 2002. p. 18–23.
12. De Potter P. Imaging in orbital differential diagnosis. In: Karcioglu ZA, editor. Orbital tumors, diagnosis and treatment. New York: Springer; 2005. p. 94–103.
13. Ben Simon GJ, Annunziata CC, Fink J, Villablanca P, McCann JD, Goldberg RA. Rethinking orbital imaging. Establishing guidelines for interpreting orbital imaging studies and evaluating their predictive value in patients with orbital tumors. Ophthalmology. 2005;112:2196–207.
14. Bilaniuk LT, Zimmerman RA, Newton TH. Magnetic resonance imaging: orbital pathology. In: Newton TH, Bilaniuk LT, editors. Radiology of the eye and orbit. New York: Raven Press; 1990; chap 5.
15. Char DH, Unsöld R, Sobel DF, Salvolini U, Newton TH. Computed tomography: ocular and orbital pathology. In: Newton TH, Bilaniuk LT, editors. Radiology of the eye and orbit. New York: Raven Press; 1990; chap 9.
16. Lacey B, Chang W, Rootman J. Nonthyroid causes of extraocular muscle disease. Surv Ophthalmol. 1999; 44:187–213.
17. Bond JB, Haik BG, Taveras JL, et al. Magnetic resonance imaging of orbital lymphangioma with and without gadolinium contrast enhancement. Ophthalmology. 1992;99:1318–24.
18. Saeed P, Rootman J, Nugent R, White VA, Mackenzie IR, Koornneef L. Optic nerve sheath meningiomas. Ophthalmology. 2003;110:2019–30.
19. Ben Simon GJ, Syed HM, Douglas R, McCann JD, Goldberg RA. Extraocular muscle enlargement with tendon involvement in thyroid-associated orbitopathy. Am J Ophthalmol. 2004;137:1145–7.
20. Weinig BM, Mafee MF, Ghosh L. Fibro-osseous, osseous, and cartilaginous lesions of the orbit and paraorbital region. Correlative clinicopathologic and radiographic features, including the diagnostic role of CT and MR imaging. Radiol Clin North Am. 1998;36:1241–59.

Nonspecific Orbital Inflammation

6

Roberta E. Gausas, M.R. Damani,
and Kimberly P. Cockerham

Contents

R.E. Gausas, MD (✉) • M.R. Damani
Department of Ophthalmology, Perelman School of Medicine, University of Pennsylvania,
51 North 39th Street, Philadelphia, PA 19104, USA
e-mail: roberta.gausas@uphs.upenn.edu

K.P. Cockerham, MD, FACS
Department of Ophthalmology,
Stanford University, 2452 Watson Court, MC 5353,
Palo Alto, CA 94303, USA

6.1 Introduction

Nonspecific orbital inflammation (NSOI) is a term used to describe nonmalignant inflammation of the orbit characterized by a polymorphous lymphoid infiltrate with varying degrees of fibrosis, without a known local or systemic cause [1]. The emphasis is on lack of finding a known cause. Orbital inflammation itself is not a diagnosis, but rather a description of a tissue response to some underlying problem, such as infection, irritation, or injury, which has triggered the immune system. The injured cells release chemical factors stimulating the inflammatory response which is characterized by symptoms of pain, redness, swelling, warmth, and possible dysfunction of the tissues involved. In the case of the orbit, it is infiltration of orbital soft tissues by chronic inflammatory cells that causes findings such as proptosis, eyelid swelling, chemosis, pain, diplopia, or visual loss. Every effort must first be made to identify a specific cause of the inflammation. Navigating through the differential diagnosis of diseases that can cause or simulate orbital inflammation is challenging; however, adhering to a methodical history and exam will help facilitate the process (Table 6.1). Only once all other specific etiologies have been eliminated can one conclude with the diagnosis of nonspecific orbital inflammation, which only means that the causative pathogen or trigger could not be identified.

J.D. Perry, A.D. Singh (eds.), *Clinical Ophthalmic Oncology*,
DOI 10.1007/978-3-642-40492-4_6,

Table 6.1 Differential diagnosis of orbital inflammation

Specific etiology	
Thyroid-associated	Thyroid-associated orbitopathy (TAO)
Infectious	Bacterial: tuberculosis, syphilis Fungal: mucormycosis, aspergillosis Parasitic: echinococcosis, cysticercosis
Vasculitic	Wegener's granulomatosis Polyarteritis nodosa Hypersensitivity angiitis Systemic lupus erythematosus Giant cell arteritis
Granulomatous	Sarcoidosis Xanthogranulomatous Foreign body granuloma Erdheim–Chester disease
Sjögren's syndrome	
Noninflammatory disorders with secondary inflammation	
Neoplasia	Lymphoproliferative disorders
Vascular disorders	Dural fistula Cavernous sinus arteriovenous fistula Cavernous sinus thrombosis
Nonspecific etiology	
Other diagnoses excluded	Nonspecific orbital inflammation (NSOI)

6.2 Historical Perspective

Recognition of this entity dates to the late 1800s and early 1900s, when several authors reported patients with all the findings consistent with a presumed tumor of the orbit, but either who were subsequently noted to experience unexpected, spontaneous improvement or who, upon surgical exploration and biopsy of the orbit, were found to have benign inflammation rather than malignancy. Hence, the term "orbital pseudotumor" was coined [2]. The clinical description of a benign process masquerading as a malignant one was appropriate for that era, but, unfortunately, the term has become entrenched in medical literature despite modern breakthroughs in imaging, immunopathology, and molecular techniques that allow for ever-increasing diagnostic specificity. The modern term nonspecific orbital inflammation (NSOI), or alternatively idiopathic orbital inflammation, more accurately reflects both our current understanding of this disease process and the acknowledgement that known causes were otherwise excluded [3].

6.3 Pathogenesis

Although the exact pathogenesis of NSOI remains unknown, it is generally believed to be an immune-mediated process. Wladis documented the molecular differences between normal orbits and those of patients affected by NSOI, showing that six cytokines are upregulated in NSOI, in particular IL-12, TNF-alpha, and IFN-gamma [4]. Furthermore, in comparing orbital biopsy specimens from patients with suspected NSOI to control orbital adipose specimens from those with noninflamed orbits, Wladis identified toll-like receptors (TLRs), a class of proteins that play a key role in the innate immune system [5]. The presence of TLRs has been associated with other inflammatory diseases, such as rheumatoid arthritis and multiple sclerosis. NSOI has been associated with a number of systemic immunologic disorders including Crohn's disease, systemic lupus erythematosus, rheumatoid arthritis, diabetes mellitus, myasthenia gravis, and ankylosing spondylitis. Some authors have proposed a post-infectious etiology since NSOI has been reported following viral illness in both adult and pediatric studies [6].

6.4 Clinical Features

Rapid onset of pain associated with periorbital swelling and chemosis is the most common clinical presentation. However, recognizing that there is high variability in the symptoms and clinical findings of NSOI, which are very much dictated by the degree and anatomic location of the inflammation present, is important in the clinician's ability to recognize this disease [7]. If acute in nature, NSOI may mimic infectious orbital cellulitis. Anterior orbital inflammation

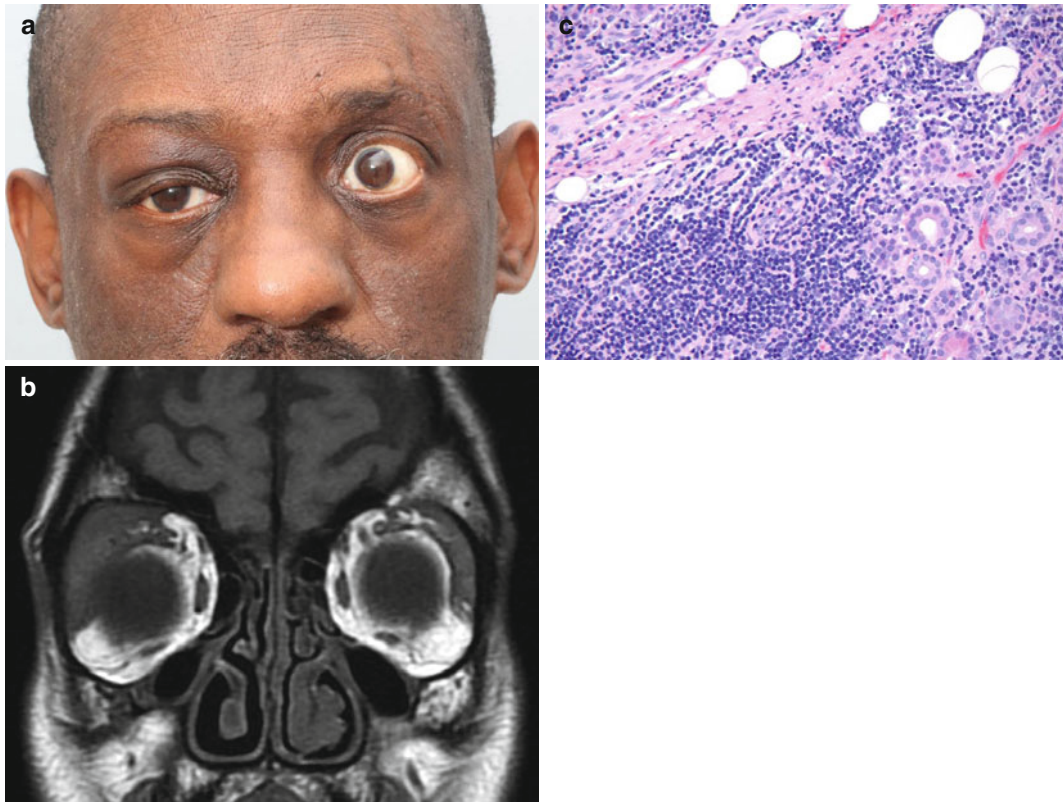

Fig. 6.1 Anterior orbital inflammation with S-shaped lid deformity (**a**). MRI reveals marked enlargement of lacrimal gland (**b**). Orbital biopsy shows lacrimal gland with focally dense chronic inflammatory cells, both lymphocytes and plasma cells, and with focal periductal fibrosis (**c**). Note absence of giant cells or lymphoepithelial lesions. No overt evidence of lymphoproliferative disorder was shown by flow cytometry

localized to the lacrimal gland may present with an S-shaped lid deformity and chemosis (Fig. 6.1). The swelling in anterior orbital inflammation may be dramatic, but vision is often spared. Conversely, inflammation localized to the orbital apex may present more insidiously with optic neuropathy and motility deficits despite a quiet anterior orbit, mimicking a neoplasm or cranial nerve palsy (Fig. 6.2). Widespread orbital inflammation may also manifest as uveitis or papillitis (Fig. 6.3). While pain or discomfort is commonly thought to be the hallmark feature of this disease, atypical cases may occur in which pain is absent.

Nonspecific orbital inflammation may be subclassified by onset: acute (within hours or days), subacute (days to weeks), chronic (weeks to months), relapsing, or recurrent.

Nonspecific orbital inflammation may be subclassified by anatomic location, with any number or amount of orbital tissues affected. The most common anatomic patterns may involve (1) one or more extraocular muscles, (2) one or both lacrimal glands, (3) anterior orbit, (4) apical orbital and perineural involvement, or (5) diffuse orbital inflammation. Inflammation localized to a specific anatomical site may acquire its own name, such as *dacryoadenitis* (inflammation localized to the lacrimal gland) or *orbital myositis* (inflammation localized to one or more extraocular muscles).

Compared to the adult population, NSOI in the pediatric population tends to manifest bilaterally more commonly and with elevated ESR, eosinophilia, and uveitis. The latter of which appears to portend a poor outcome [8].

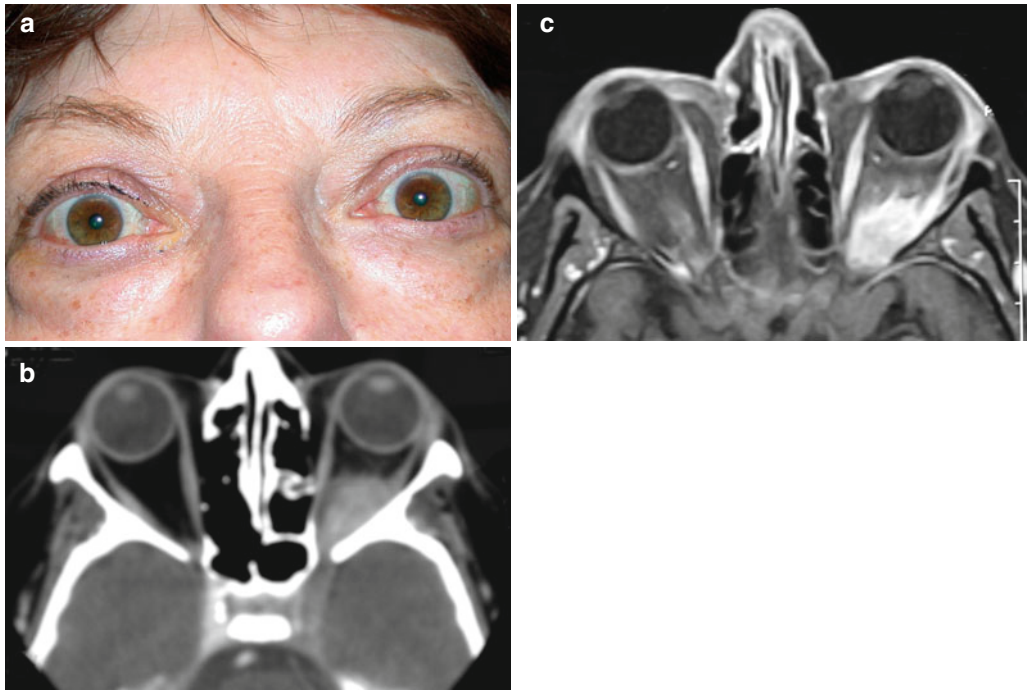

Fig. 6.2 Apical orbital inflammation. Patient with painful proptosis and optic neuropathy. Although the periorbital area and anterior segment are quiet (**a**), neuroimaging reveals an infiltrating lesion involving the orbital apex on a CT scan (**b**) and MRI (**c**)

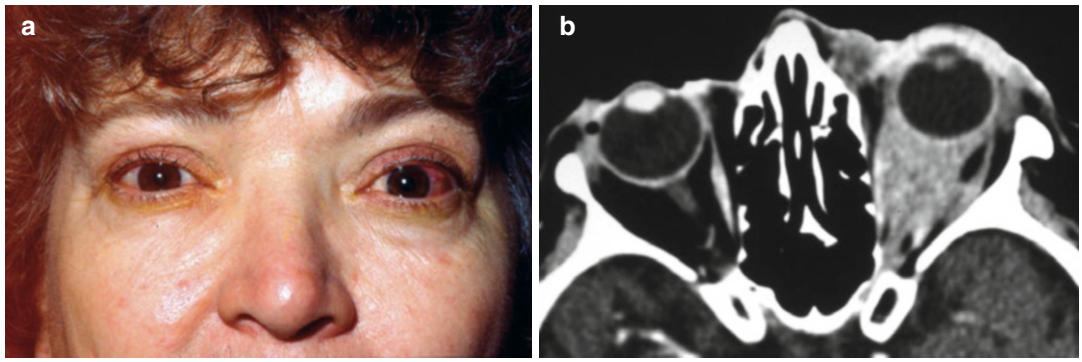

Fig. 6.3 Diffuse orbital inflammation. Patient with painful proptosis and limited motility of left eye (**a**). Orbital CT reveals periocular and retrobulbar involvement of multiple tissues (**b**)

6.5 Clinical Subtypes

6.5.1 Orbital Myositis

Orbital myositis consists of inflammation involving one or more extraocular muscles in one or both orbits. Diplopia and pain exacerbated by eye movement are the presenting signs. Examination may reveal restriction of motility and positive forced ductions. Recurrence of orbital myositis is not uncommon and may involve the same or different extraocular muscles in the same orbit or in the contralateral orbit [9].

6.5.2 Orbital Apex Syndrome

Inflammation centered in the posterior orbit may appear as an orbital apex syndrome, with ophthalmoplegia, optic neuropathy, and proptosis. The patient may present with visual loss and cranial nerve deficits, while the anterior orbit may or may not be involved. Imaging reveals a diffuse, infiltrative lesion in the apex surrounding the optic nerve (Fig. 6.2). It is crucial to eliminate other causes in such cases, because the differential diagnosis includes neoplasm, such as lymphoma, or infection, such as aspergillosis or mucormycosis.

6.5.3 Sclerosing Orbital Inflammation

A distinct sclerosing form of orbital inflammation has been identified which is characterized by dense fibrous replacement. Long believed to represent the chronic end stage of the disease, it is now thought to represent a distinct clinicopathologic entity. This sclerosing form has been shown to be histologically similar to other fibroproliferative disorders such as multifocal fibrosclerosis, a systemic disseminated fibrosing process that includes Riedel's thyroiditis, mediastinal fibrosis, sclerosing cholangitis, and fibrosis of the parotid gland, lacrimal gland, and lung [10]. Kovacs suggests that fibrosis formation in these disorders is mediated by the aberrant production of fibrogenic cytokines such as platelet-derived growth factor (PDGF) and transforming growth factor-B (TGF-B), which ultimately results in permanent alteration in tissue structure [11].

6.5.4 Nonsarcoid Granulomatous Inflammation

Another distinct form of NSOI is one which displays granulomatous inflammation similar to sarcoidosis but is not associated with systemic sarcoidosis [12].

6.5.5 Immunoglobulin G4-Related Disease and Orbital Inflammation

Since 2003, IgG4-related disease (IgG4-RD) has been recognized as a systemic fibroinflammatory condition characterized by mass-forming inflammatory reactions involving almost any organ system, in which the tissues are infiltrated by IgG4-positive plasma cells. It is usually, but not always, associated with elevated serum IgG4 concentrations. In the orbit, chronic sclerosing dacryoadenitis, characterized by bilateral lacrimal gland involvement and a dense lymphoplasmacytic infiltration, has been suggested to be an IgG4-related disease [13, 14].

Stone explains that although IgG4 is traditionally thought of as an anti-inflammatory immunoglobulin, it appears to actually play a significant role in certain immune-mediated conditions and that the identification of IgG4-RD has unified a large number of medical conditions previously thought to be limited to specific and single organ systems into a cohesive picture of systemic inflammation, linked by similar histopathologic characteristics [15].

6.6 Diagnostic Evaluation

6.6.1 Imaging

Neuroimaging plays a critical role in evaluating presumed NSOI. Although high-resolution orbital computerized tomography (CT) may demonstrate variable enhancement after administration of iodinated contrast material, contrast-enhanced magnetic resonance imaging (MRI) with fat saturation is the imaging study with the highest yield and should be performed when available. Subtle edema of the retrobulbar fat is often one of the earliest changes seen in NSOI. Orbital MRI typically shows a reticular pattern of orbital fat that is isointense to muscle in both T1- and T2-weighted images. In contrast, orbital cellulitis will be hyperintense to muscle in T2 [16]. Kapur has suggested diffusion-weighted

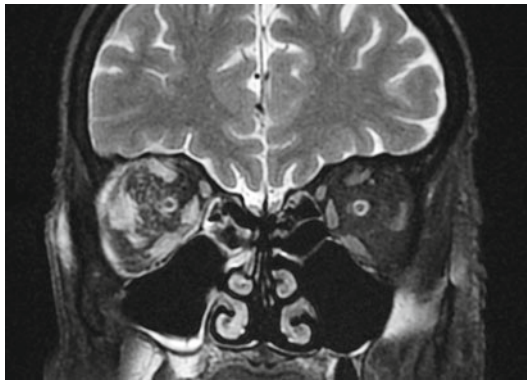

Fig. 6.4 Orbital myositis. MRI, coronal view, shows diffuse retrobulbar fat edema and thickening of all extraocular muscles in right orbit

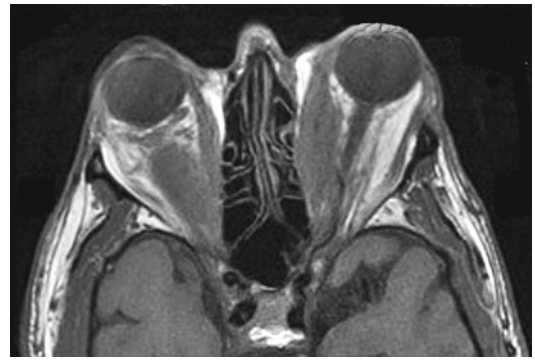

Fig. 6.5 Thyroid-associated orbitopathy. Although tendon spring is expected, in this case, muscle belly enlargement and tendon involvement of the left medial rectus muscle are evident

imaging as a method to distinguish NSOI from cellulitis and lymphoproliferative disease [17] (Fig. 6.4).

Classically, orbital myositis, a specific orbital inflammation and the most common cause of muscle enlargement, demonstrates tendon thickening in addition to extraocular muscle belly enlargement. Inflammation in TAO is generally tendon sparing. However, cases of orbital myositis *without* tendon involvement have been reported [18], and 8 cases of thyroid-associated orbitopathy *with* tendon involvement in a series of 125 patients were reported by Simon [19]. Therefore, extraocular muscle and tendon morphology may be highly suggestive but not pathognomonic in differentiating orbital inflammation as either NSOI or TAO (Fig. 6.5).

6.6.2 Laboratory Testing

Since there is an association between NSOI and other systemic conditions such as rheumatologic disease and IgG4-related disease, the typical laboratory workup for suspected NSOI should include complete blood count (CBC), electrolytes, sedimentation rate (ESR), antinuclear antibody (ANA), anti-ds DNA, antineutrophil cytoplasmic antibody (ANCA), angiotensin-converting enzyme (ACE) level, rapid plasma reagin (RPR), thyroid function tests (TFTs), and serum IgG4.

6.6.3 Biopsy

Orbital biopsy can play a powerful role in the diagnosis of NSOI. Although many authors have advocated empiric steroid treatment while reserving orbital biopsy for atypical, nonsteroid-responsive, or recalcitrant cases of presumed orbital inflammation, such an approach may lead to delay in diagnosis of other causes of inflammation because even malignancy can respond favorably to steroids initially [20]. Biopsy, on the other hand, allows definition of specific disease, identification of systemic implications, and more directed therapeutic treatment plans. Rootman found 50 % of biopsied inflammatory lacrimal gland lesions were associated with systemic disease, including Wegener's granulomatosis, sclerosing inflammation, Sjögren's syndrome, sarcoidal reactions, and autoimmune disease [21]. Except for two classic clinical scenarios, orbital biopsy should be considered whenever medically feasible. These two clinical scenarios are orbital myositis and orbital apex syndrome, as described above. In these cases, characteristic clinical and radiographic findings may strongly support the presumed diagnosis, and the risk of biopsy must be weighed against the risk of a missed diagnosis. However, recurrent orbital myositis or orbital apex syndrome, or those unresponsive to treatment, may warrant orbital biopsy.

6.6.4 Histopathology

Histopathology in the acute phase of NSOI typically reveals a diffuse polymorphous infiltrate composed of mature lymphocytes, plasma cells, macrophages, eosinophils, and polymorphonuclear leukocytes. Vasculitis of small arteries may occasionally be found [1]. In the subacute and chronic phases, an increasing amount of fibrovascular stroma is seen.

6.7 Treatment

6.7.1 Corticosteroids

As the specific pathogenesis of NSOI remains unknown, management is directed toward the common consequences of the inflammatory cascade: tissue inflammation and destruction. High-dose systemic corticosteroids, therefore, are considered the first line of therapy for NSOI, at starting doses of 60–80 mg prednisone per day. The response to steroids is typically rapid, over 1–2 days, although it may not be sustained, and requires a slow taper over weeks to months to avoid recurrence. A slow taper consists of reducing prednisone by 10 mg/day every 1–2 weeks.

However, failure to respond to steroids, dependence on steroids, and steroid intolerance are not uncommon [22, 23]. In addition, the side effects of weight gain, mood swings, insomnia, and gastric distress are common even with short-term therapy.

6.7.2 Steroid-Sparing Agents

Avoiding steroid-associated complications via alternative therapies may be desirable, and a multidisciplinary approach that utilizes the expertise of rheumatologists and/or oncologists is beneficial in organizing such treatment plans. Alternative therapeutic options include antimetabolites, such as azathioprine (Imuran), methotrexate (Rheumatrex), mycophenolate mofetil (CellCept), and leflunomide (Arava); T-cell inhibitors, cyclosporine and tacrolimus; and alkylating agents, cyclophosphamide and chlorambucil.

Recently, several reports have shown promise for biologic agents that have more targeted actions than steroids and are associated with fewer systemic side effects, although some of which are potentially life threatening and require careful monitoring. In particular, Garrity and Miguel found symptomatic and clinical improvement in patients treated with infliximab after failure to respond to conventional treatment or experiencing recurrent orbital inflammation [24, 25].

6.7.3 External Beam Radiation

NSOI is moderately radiosensitive. External beam radiation is often reserved for steroid failure, relapse, or contraindication, in doses ranging from 10 to 30 Gy. In a series of 26 orbits referred for relapse after steroid treatment, steroid resistance, or steroid contraindication, Lanciano reported complete response in 87 % of patients with soft tissue swelling, 82 % with proptosis, 78 % with extraocular muscle dysfunction, and 75 % with pain [26].

Careful patient selection, coordination with an experienced radiation therapist, and treatment planning are essential to maximize efficacy and minimize side effects. Some patients receiving radiation experience increased orbital inflammation, which may be relieved by a short course of oral corticosteroids.

6.7.4 Surgery

Incisional biopsy plays an important role in establishing a correct diagnosis in presumed NSOI, but the treatment afterwards is generally medical. Only occasionally may surgical debulking be an effective alternative to medical and radiation therapy for localized lesions. For the most severe cases of orbital inflammation in which there is irretrievable loss of vision and

uncontrollable pain, the surgical option of exenteration may be considered.

6.8 Prognosis

Although rapid resolution of pain and recovery of vision with steroid treatment is the common clinical course, the risk of recurrence is high. In a series of 24 patients, Maalouf reported a recurrence rate of 55 % [27], and in a series of 21 patients, Mombaerts reported a recurrence rate of 52 % [23]. Yuen reported a treatment failure rate of 37 % in a series of 65 patients [22].

6.9 Future

In the future, the ever-changing, often vague nomenclature used to describe noninfectious, nonmalignant orbital inflammation used presently and in the past will be replaced by designations that describe a key pathological or molecular feature. As this evolution of eliminating the "nonspecific" from this disease proceeds, it will likely bring more insight into the exact pathophysiology of orbital inflammation and provide an opening for the use of targeted biologic immunomodulatory therapy, expanding and improving our current arsenal of treatment beyond steroids.

References

1. Kennerdell JS, Dresner SC. The nonspecific orbital inflammatory syndromes. Surv Ophthalmol. 1984; 29(2):93–103.
2. Birch-Hirschfeld A. Handbuch der Gesamten Augenheilkunde. Berlin: Julius Springer; 1930. p. 251.
3. Rootman J. Why "orbital pseudotumour" is no longer a useful concept. Br J Ophthalmol. 1998;82(4): 339–40.
4. Wladis EJ, Iglesias BV, Gosselin EJ. Characterization of the molecular biologic milieu of idiopathic orbital inflammation. Ophthal Plast Reconstr Surg. 2011; 27(4):251–4.
5. Wladis EJ, Iglesias BV, Adam AP, Nazeer T, Gosselin EJ. Toll-like receptors in idiopathic orbital inflammation. Ophthal Plast Reconstr Surg. 2012; 28(4):273–6.
6. Cockerham KP, Hong SH, Browne EE. Orbital inflammation. Curr Neurol Neurosci Rep. 2003;3(5): 401–9.
7. Mombaerts I, et al. What is orbital pseudotumor? Surv Ophthalmol. 1996;41(1):66–78.
8. Bloom JN, Graviss ER, Byrne BJ. Orbital pseudotumor in the differential diagnosis of pediatric uveitis. J Pediatr Ophthalmol Strabismus. 1992;29(1):59–63.
9. Avni-Zauberman N, Tripathy D, Rosen N, Ben Simon GJ. Relapsing migratory idiopathic orbital inflammation: six new cases and review of the literature. Br J Ophthalmol. 2012;96(2):276–80.
10. McCarthy JM, et al. Idiopathic sclerosing inflammation of the orbit: immunohistologic analysis and comparison with retroperitoneal fibrosis. Mod Pathol. 1993;6(5):581–7.
11. Kovacs EJ, DiPietro LA. Fibrogenic cytokines and connective tissue production. Faseb J. 1994;8(11): 854–61.
12. Raskin EM, et al. Granulomatous idiopathic orbital inflammation. Ophthal Plast Reconstr Surg. 1995; 11(2):131–5.
13. Andrew N, Kearney D, Selva D. IgG4-related orbital disease: a meta-analysis and review. Acta Ophthalmol. 2013;91(8):694–700.
14. Cheuk W, Yuen HK, Chan JK. Chronic sclerosing dacryoadenitis: part of the spectrum of IgG4-related Sclerosing disease? Am J Surg Pathol. 2007;31(4): 643–5.
15. Stone JH M.D., M.P.H., Yoh Zen M.D., Ph.D., Deshpande V M.D. IgG4-related disease. N Engl J Med. 2012;366:539–51.
16. Uehara F, Ohba N. Diagnostic imaging in patients with orbital cellulitis and inflammatory pseudotumor. Int Ophthalmol Clin. 2002;42(1):133–42.
17. Kapur R, Sepahdari AR, Mafee MF, Putterman AM, Aakalu V, Wendel LJ, Setabutr P. MR imaging of orbital inflammatory syndrome, orbital cellulitis, and orbital lymphoid lesions: the role of diffusion-weighted imaging. AJNR Am J Neuroradiol. 2009; 30(1):64–70.
18. Patrinely JR, et al. Computed tomographic features of nonthyroid extraocular muscle enlargement. Ophthalmology. 1989;96(7):1038–47.
19. Ben Simon GJ, Syed HM, Douglas R, McCann JD, Goldberg RA. Extraocular muscle enlargement with tendon involvement in thyroid-associated orbitopathy. Am J Ophthalmol. 2004;137(6):1145–7.
20. Papalkar D, et al. A rapidly fatal case of T-cell lymphoma presenting as idiopathic orbital inflammation. Orbit. 2005;24(2):131–3.
21. Rootman J, editor. Orbital disease: present status and future challenge. Boca Raton: Taylor & Francis Group, LLC; 2005. p. 1–13.
22. Yuen SJ, Rubin PA. Idiopathic orbital inflammation: distribution, clinical features, and treatment outcome. Arch Ophthalmol. 2003;121(4):491–9.
23. Mombaerts I, et al. Are systemic corticosteroids useful in the management of orbital pseudotumors? Ophthalmology. 1996;103(3):521–8.

24. Garrity JA, Coleman AW, Matteson EL, et al. Treatment of recalcitrant idiopathic orbital inflammation (chronic orbital myositis) with infliximab. Am J Ophthalmol. 2004;138:925–30.
25. Miguel T, Abad S, Badelon I, Vignal C, et al. Successful treatment of idiopathic orbital inflammation with infliximab: an alternative to conventional steroid-sparing agents. Ophthal Plast Reconstr Surg. 2008;24(5):415–7.
26. Lanciano R, Fowble B, Sergott RC, Atlas S, Savino PJ, Bosley TM, Rubenstein J. The results of radiotherapy for orbital pseudotumor. Int J Radiat Oncol Biol Phys. 1990;18(2):407–11.
27. Maalouf T, et al. What has become of our idiopathic inflammatory pseudo-tumors of the orbit? Orbit. 1999;18(3):157–66.

Orbital Vascular Tumors

7

Bryan R. Costin and Julian D. Perry

Contents

B.R. Costin, MD • J.D. Perry, MD (✉)
Division of Ophthalmology, Cole Eye Institute,
Cleveland Clinic Foundation,
9500 Euclid Avenue I-32,
Cleveland, OH 44195, USA
e-mail: perryj1@ccf.org

7.1 Introduction

Orbital vascular lesions may be neoplastic such as capillary and cavernous hemangioma, which expand by cellular proliferation, or anomalies representing varying types and degrees of vascular dysgenesis, or *malformations*. Until recently, no consensus existed among ophthalmologists to classify the types of lesions falling under the malformation category. In response, The Orbital Society created a classification system for orbital vascular malformations in 1999 to establish a standardized classification system and to reduce clinical confusion surrounding the management of these entities (Table 7.1) [1]. This system classifies malformations based on hemodynamic behavior as opposed to their morphologic characteristics emphasizing the features most important to their management. Clinical and imaging findings are used to assign orbital vascular malformations as *no flow*, *venous flow*, or *arterial flow*, and the term "lymphangioma" was identified as inaccurate as these lesions both lack a true neoplastic origin. Under the new classification system, they are "no-flow" malformations, which are hemodynamically isolated.

Exciting treatments have been developed for both orbital vascular neoplasms and malformations. The use of beta-blockers for orbital and

J.D. Perry, A.D. Singh (eds.), *Clinical Ophthalmic Oncology*,
DOI 10.1007/978-3-642-40492-4_7, © Springer-Verlag Berlin Heidelberg 2014

Table 7.1 Diagnostic features of orbital vascular lesions

Type	Flow	Imaging		Treatment
		Doppler US angiography	CT MRI	
Lymphangioma (type I)	No flow	No flow	No enhancement Fluid levels	Debulking
Varix (type II)	Venous flow	Venous flow	Contrast enhancement Flow voids	Sclerotherapy, ligation, and excision
AV malformation (type III)	Arterial flow	Arterial flow	Contrast enhancement Flow voids	Embolization then debulking

periocular capillary hemangiomas and the treatment of cystic malformations with sclerosing agents represent alternatives to surgical excision [2–4]. These treatments are encouraging as they may mean a less invasive future in the treatment of orbital vascular lesions and a shift away from surgical excision.

7.2 Orbital Vascular Malformations

7.2.1 Introduction

Vascular development occurs during the retiform stage of embryogenesis, at approximately day 48 of development, and orbital vascular malformations result from errors during this stage. Examples include isolated lesions as well as numerous congenital syndromes, including Sturge-Weber, Osler-Weber-Rendu, Wyburn-Mason, Klippel-Trénaunay, and Blue-rubber-bleb-nevus (BLEB) syndrome. Vascular malformations grow with age, never spontaneously involute, and are comprised of ectatic venous, arteriovenous, or lymphatic vessels, lined with flat endothelial cells. The Orbital Society's hemodynamic classification divides vascular malformations into three categories by flow characteristics: no flow (type 1), venous flow (type 2), and arterial flow (type 3).

7.2.2 No-Flow (Type 1) Vascular Malformations

No-flow (type 1) malformations consist of lymphatic or combined lymphatic and venous channels, which are hemodynamically isolated from systemic circulation. Lymphatic and venolymphatic malformations typify type 1 no-flow lesions. Lymphatic malformations are thin-walled, ectatic channels lined with flat endothelium without evidence of smooth muscle. These lesions contain serous fluid, lymphocytes, cholesterol clefts, and evidence of old hemorrhage. Spontaneous hemorrhage frequently occurs into these channels creating blood-filled "chocolate" cysts.

7.2.2.1 Clinical Features

No-flow malformations occur as 3 % of all orbital tumors and over half of these lesions are diagnosed at birth (59 %) with the rest usually presenting within the first few years of life. Unilateral proptosis or swelling is the primary symptom in 76 % of patients [5]. Proptosis classically worsens with respiratory infections and prolonged head-down positioning. Other presentations include spontaneous hemorrhage, orbital infection, ptosis, and strabismus. The spontaneous hemorrhage typical of type 1 no-flow malformations has a high rate of complications, including permanent loss of vision.

7.2.2.2 Diagnostic Evaluation

Imaging studies of type 1 lesions show no venous or arterial flow (Fig. 7.1). Gadolinium-contrasted MRI optimally enhances the cystic compartments of these lesions, which can be located intraconally, extraconally, or both. Old and new hemorrhages appear as fluid levels. Angiography reveals displacement of normal veins around the lesion without filling. Direct injection of contrast material into a no-flow lesion using image

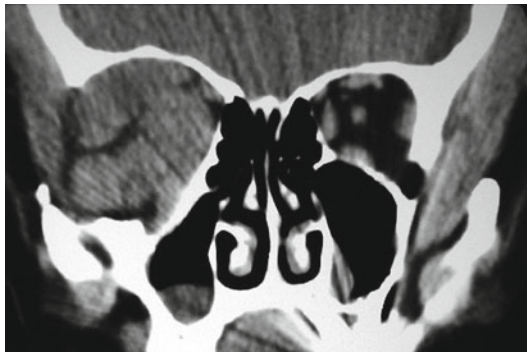

Fig. 7.1 Coronal CT imaging study shows lobulated appearance of lymphangioma (type 1 vascular lesion). Note surgical absence of lateral wall

guidance techniques and fluoroscopy confirm hemodynamic isolation without evidence of venous outflow channels.

7.2.2.3 Differential Diagnosis

The differential diagnosis of type 1 no flow includes capillary hemangioma, venous malformations, rhabdomyosarcoma, fibrosarcoma, and lymphoma. Spontaneous hemorrhage into type 1 lesions can mimic other types of retrobulbar hemorrhages.

7.2.2.4 Treatment

Management often involves a multidisciplinary approach, including an interventional radiologist and orbital surgeon. Treatment options include surgical debulking and sclerotherapy, with the latter modality becoming more and more appealing for first-line treatment [3]. Direct sclerotherapy uses stereotactic image-guided needle placement into the targeted cystic malformation. After contrast fluoroscopy confirms correct needle placement and lack of venous drainage channels, the sclerosing agent is injected. Aspiration of the sclerosing agent collapses the cysts, and subsequent fibrosis seals the malformation. Effective agents include hypertonic saline, ethyl alcohol, sodium tetradecyl sulfate, ethanolamine oleate, and OK-432, but no comparisons exist [6]. Treatments appear successful in maintaining long-term closure.

If corneal exposure is present, tarsorrhaphy may be beneficial, but persistent proptosis or compromised vision may require surgical excision or even orbital decompression. Acute hemorrhage causing compressive optic neuropathy requires emergent surgical decompression or surgical debulking. The surgical approach to extraconal lesions depends primarily on lesion location. Resection of intraconal lesions carries significant risk due to neurovascular adhesions, and these lesions should be debulked only when absolutely necessary. Complete excision of type 1 lesions is rare as these malformations frequently extend through the orbital soft tissue planes. Intraoperative visibility is often hindered when these thin-walled lesions rupture and collapse during surgery. Injection of intraluminal fibrin sealant prior to excision may improve visibility and hemostasis [7]. After the cysts are debulked, remaining tissue can be vaporized with CO_2 laser, which may also improve hemostasis and reduce recurrences.

7.2.3 Venous-Flow (Type 2) Malformations

Type 2 venous-flow vascular malformations consist of venous and mixed venolymphatic channels. Unlike type 1 lesions, which are isolated from systemic circulation, type 2 lesions are in communication with the venous system. Increased venous pressure may or may not cause the malformation to distend depending on the extent of the communication. Histopathology of type 2 malformations reveals large, thin-walled vessels within fibrous stroma. These channels are endothelial lined and contain smooth muscle.

7.2.3.1 Clinical Features

The Orbital Society distinguishes type 2 venous-flow malformations into three subclasses: non-distensible venous, distensible venous, and distensible combined venous and lymphatic malformations. Clinically, type 2 non-distensible venous malformations behave similar to type 1 lymphatic malformations with frequent episodes of spontaneous hemorrhage and thrombosis. Doppler and contrast imaging show evidence of venous flow and lesions with significant venous communication require greater caution due to the higher risk of venous thrombosis and bleeding.

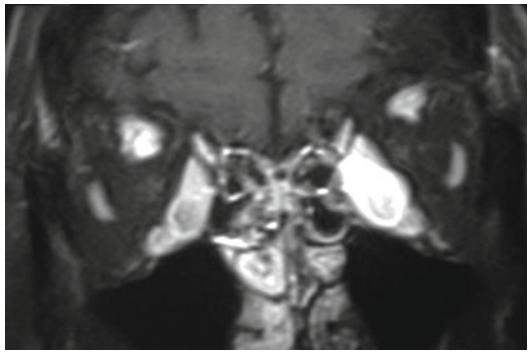

Fig. 7.2 Coronal Gd-DTPA-enhanced MRI shows bilateral contrast-enhancing lesions consistent with type 2 vascular lesions

Type 2 distensible venous malformations have a more direct communication with the venous system and typically exhibit higher flow. As such, these lesions exhibit spontaneous hemorrhage and thrombosis less frequently than malformations with lower flow. Type 2 distensible venolymphatic malformations exhibit both types 1 and 2 flow characteristics, and the impact of any venous-flow characteristics on the clinical management of this subtype emphasizes the type 2 classification.

7.2.3.2 Diagnostic Evaluation

Color Doppler and directional ultrasound detect venous flow within type 2 lesions and CT and MRI reveal diffuse contrast enhancement (Fig. 7.2). CT scan may show distensibility, bony hypertrophy, and even intraosseous extension. MR imaging best delineates these lesions and may reveal fluid levels within combined malformations. MR angiography detects the venous flow through distensible lesions but is less successful detecting low-speed flow in the non-distensible subtype, and low-speed venous flow occasionally requires direct invasive fluoroscopy or CT angiography.

7.2.3.3 Treatment

Surgical management for type 2 venous-flow malformations in the orbit is notoriously difficult. Intralesional Nd:YAG laser, delivered by optical fiber, has been recommended as a less invasive technique [8]. Other treatment options include irradiation, electrocoagulation, cryotherapy, and compression. These techniques may be used alone or preoperatively in order to reduce hemorrhagic complications. Recent advances in guidance technology have reduced the risks of sclerotherapy, which provides a less invasive treatment for symptomatic venous malformations. Sclerotherapy for venous malformations requires a detailed preprocedural evaluation by the interventional radiologist. Unlike sclerotherapy for cystic type 1 lymphoid malformation, type 2 lesions in communication with the venous system are at significantly greater risk for complications from severe bleeding. Inadvertent sclerosis of the ophthalmic vein and cavernous sinus results in immediate thrombosis, orbital compartment syndrome, and vision loss. Percutaneous image guidance methods can be used alone or in combination. X-ray fluoroscopy is often combined with duplex ultrasound. New methods include CT image fusion and frameless stereotactic guidance in combination with x-ray fluoroscopic monitoring of the injection. Introducing sclerosing agent into the normal venous drainage system should be avoided [9, 10].

Sclerosing agents induce immediate thrombosis of these channels by destroying the lesion's endothelial lining, and inciting an inflammatory reaction and fibrosis occurs within several weeks. The process works best with smaller-caliber vessels and early treatment may offer greater success. Patients receive post-procedural IV steroids to prevent excessive inflammatory edema and an orbital compartment syndrome. Larger lesions often recanalize and require multiple sessions every 3–6 weeks. Resistant lesions may ultimately require surgical treatment [11].

7.2.3.4 Surgery

Surgical excision of venous malformations carries a high risk of severe complications, including nerve damage, bleeding, inadvertent ophthalmic vein and cavernous sinus thrombosis, orbital compartment syndrome, and vision loss. Complete excision is difficult because these lesions often encase critical neuromuscular structures.

Certain precautions can minimize the risk of severe intraoperative bleeding. In addition to sclerotherapy, fibrin sealant embolization prior to excision may significantly reduce flow. Maintaining normothermia, hypotension, and elevation of the surgical field above the level of

the heart further reduces risk. Matched blood and platelet donor products should be available for higher flow lesions.

7.2.4 Arterial-Flow (Type 3) Vascular Malformations

Orbital arteriovenous malformations (AVM, type 3) display arterial-flow hemodynamics characterized by anterograde shunting of blood into the venous system. This congenital malformation begins as a slowly enlarging communication between carotid artery branches and orbital veins. Without intervening capillary beds, this low-resistance nidus recruits multiple arteries and drains through multiple dilated veins. Often, both internal and external carotid branches act as feeder vessels. Histologically, the muscularis layer of the involved arteries and veins appears abnormal.

7.2.4.1 Clinical Features

AVMs typically present in children with progressive swelling, proptosis, redness, and pain. A bruit may be audible and pulsatile proptosis is characteristic. Painful swelling occurs on Valsalva maneuver and symptoms may be worse in the morning and improve during the day. Prolonged ocular ischemia may cause glaucoma and vision loss via progressive venous hypertension or diminished peak retinal arterial pressure from shunting. Venous hypertension may cause arterialization of conjunctival vessels reminiscent of changes seen with carotid-cavernous fistula (Fig. 7.3).

Although these malformations typically display slow growth, acute aggravation of symptoms may occur after spontaneous orbital hemorrhage, and this presentation may mimic an acquired AV shunt. The older demographic and certain angiographic characteristics may help to distinguish acquired shunts from congenital malformations.

7.2.4.2 Diagnostic Evaluation

Directional ultrasound and color Doppler imaging show anterograde arterialized flow through dilated venous drainage channels. Angiography remains the standard for diagnosis and evaluates the internal and external carotid arterial systems, as well as the orbital venous system (Fig. 7.4).

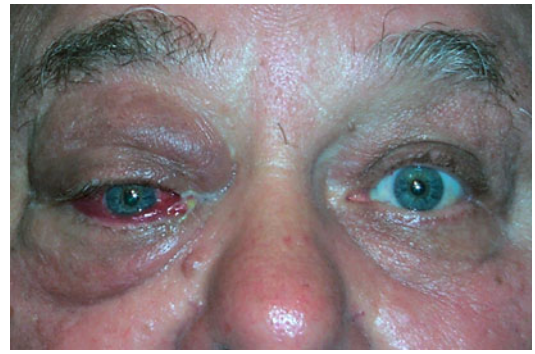

Fig. 7.3 External photograph demonstrates severe arterialization and proptosis of the right eye in a patient with type 3 orbital vascular lesion

7.2.4.3 Treatment

Surgical excision of type 3 arterial-flow lesions risks bleeding and potentially exsanguination. Preoperative endovascular embolization and gluing of the lesion significantly reduces the risks of ligation and surgical debulking. This technique employs a venous approach to avoid inadvertent embolization of critical ocular vessels. Provocative lidocaine testing can confirm radiologic positioning of the catheter distal to central retinal artery (CRA) and posterior ciliary arteries. Due to the rapid development of collateral circulation and inflammation, excision generally takes place within 24–48 h after embolization. Incomplete excision may result in rapid recurrence through recruitment of collateral vessels [12–14].

7.3 Infantile Capillary Hemangioma

7.3.1 Introduction

In 1982, Mulliken and Glowacki proposed a classification of vascular anomalies by cellular activity, separating actively proliferating hemangiomas from inactive congenital vascular malformations [15]. Infantile capillary hemangiomas represent the most common vascular lesion in children. Lined by plump propagating endothelial cells, capillary hemangiomas consist

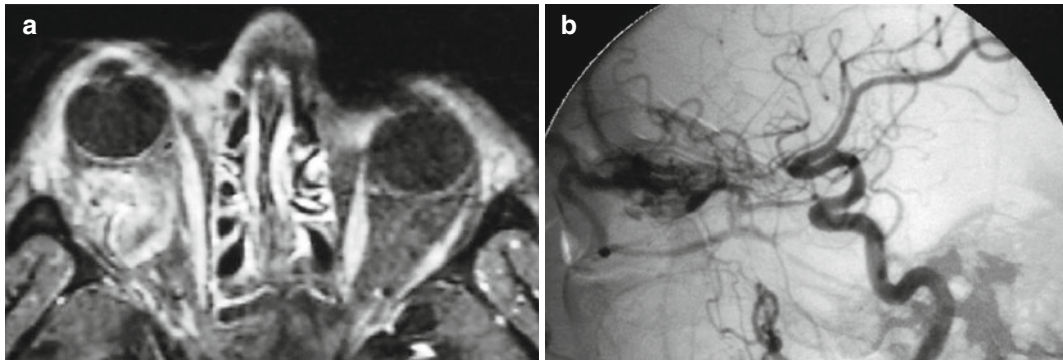

Fig. 7.4 MRI of orbital AVM shows enhancing lesion with flow voids (**a**). Angiography of orbital AVM demonstrates communication to the internal and external carotid arteries (**b**)

Table 7.2 Salient diagnostic findings of infantile capillary hemangioma

	Imaging			
			CT	
Clinical	US	Angiography	MRI	Treatment
Presentation (<age 1) Spontaneous involution (age 4–7) Superficial component red Deep component blue Expansion with crying	Irregular lesion with low internal reflectivity	Early blush with late staining	No bone involvement Contrast enhancement with late staining	Observation, laser, steroids

of hamartomatous capillaries in communication with normal vascular channels. Increased incidence in females, hormonal growth patterns, and immunohistochemical markers suggest placental origins of these benign growths.

7.3.2 Clinical Features

Orbital infantile capillary hemangiomas typically present within the first few months of life with progressive unilateral swelling and proptosis, often with a visible dark-blue anterior orbital component. Superficial extensions of lesions typically blanch on compression and the patient's parents may report expansion of the lesions upon crying. Large lesions may affect vision by causing astigmatism, corneal exposure, optic neuropathy, or amblyopia and may require therapy. Although considered a sporadic condition, a familial form may be underreported and family history should be obtained. Multiple hemangiomas should alert the clinician to systemic syndromes involving anomalies of the heart and intracranial posterior fossa. Hemangiomas associated with the Kasabach-Merritt syndrome carry high mortality due to platelet sequestration coagulopathy and high-output heart failure. Hemangiomas involving the nasopharynx may cause airway obstruction [16–19].

7.3.3 Diagnostic Evaluation

These lesions are characterized hemodynamically by dilated inflow and outflow channels on imaging (Table 7.2). Ultrasound reveals an irregular

lesion with low internal reflectivity. In the proliferative phase, CT and MR imaging reveal a lobulated, well-circumscribed, enhancing lesion without orbital bone involvement. MR imaging shows hypointensity to fat on T1-weighted images and hyperintensity to fat on T2-weighted images. Angiography shows early blushing with late lobular parenchymal staining. Urine analysis may detect elevated levels of basic fibroblast growth factor (bFGF) and matrix metalloproteinase (MMP) during active enlargement of infantile capillary hemangioma. These markers can monitor for involution or treatment progress [20].

7.3.4 Differential Diagnosis

The differential diagnosis of infantile capillary hemangioma includes lymphatic or venous malformations, which never involute. Other entities include orbital cellulitis, orbital dermoid, rhabdomyosarcoma, hemangiopericytoma, and metastatic neuroblastoma.

7.3.5 Treatment

Most infantile capillary hemangiomas benefit from conservative observation due to a high rate of spontaneous involution. Life-threatening, visually impairing, and disfiguring lesions require treatment. Although laser treatments, immunomodulating topical creams, steroid injection, and surgical management were used in the past, topical and systemic beta-blockers have come to the clinical forefront in the treatment of capillary hemangioma [2, 21, 22].

Localized intralesional steroid injection often induces the involutional phase and hastens regression. Molecular studies revealing similarities to wound healing may help explain the responsiveness to steroids [23]. Although a variety of steroid formulations have been effective, no conclusive comparisons rate their success. Many surgeons use a mixture of triamcinolone and betamethasone with good success [24]. However, injection into orbital lesions carries the serious risk of retinal arterial embolization and blindness. Slow injection under low pressure may prevent retrograde arterial flow and minimize this complication [25]. Simultaneous dilated funduscopy during injection may detect emboli to allow for immediate discontinuation of the infusion. Ultrasound needle guidance can help monitor for retrograde flow [24, 26]. Other complications include adrenal suppression, skin depigmentation, orbital fat necrosis, and localized calcification [27]. Posterior sub-Tenon's steroid infusion may reduce such systemic risks [28]. Systemic steroids (3 mg/kg/day for at least 6 weeks) can induce regression in life-threatening lesions causing glottic compression or high-output heart failure. Unresponsive lesions may benefit from alpha-2a interferon [29]. In recent years several centers have reported the use of systemic β-blockers for the treatment of infantile hemangioma, with very promising results (Volume 2 Chapter 9).

7.3.6 Prognosis

These lesions exhibit a rapid growth phase over the first few months followed by a gradual involutional phase and regression over 4–7 years.

7.4 Cavernous Hemangioma

7.4.1 Introduction

Cavernous hemangioma, the most common benign orbital tumor in adults, is characterized as a hamartoma, but these lesions may behave as low-flow arterial-side vascular malformations. Recent cases showing coexistence of cavernous hemangioma with venous malformations have raised the possibility that these hamartomas share the same pathogenesis with vascular malformation [30, 31].

Cavernous hemangioma consists of an encapsulated network of large-lumen channels connected to the normal arterial and venous system by small inflow and outflow channels. The endothelium appears flattened and stains positively for factor

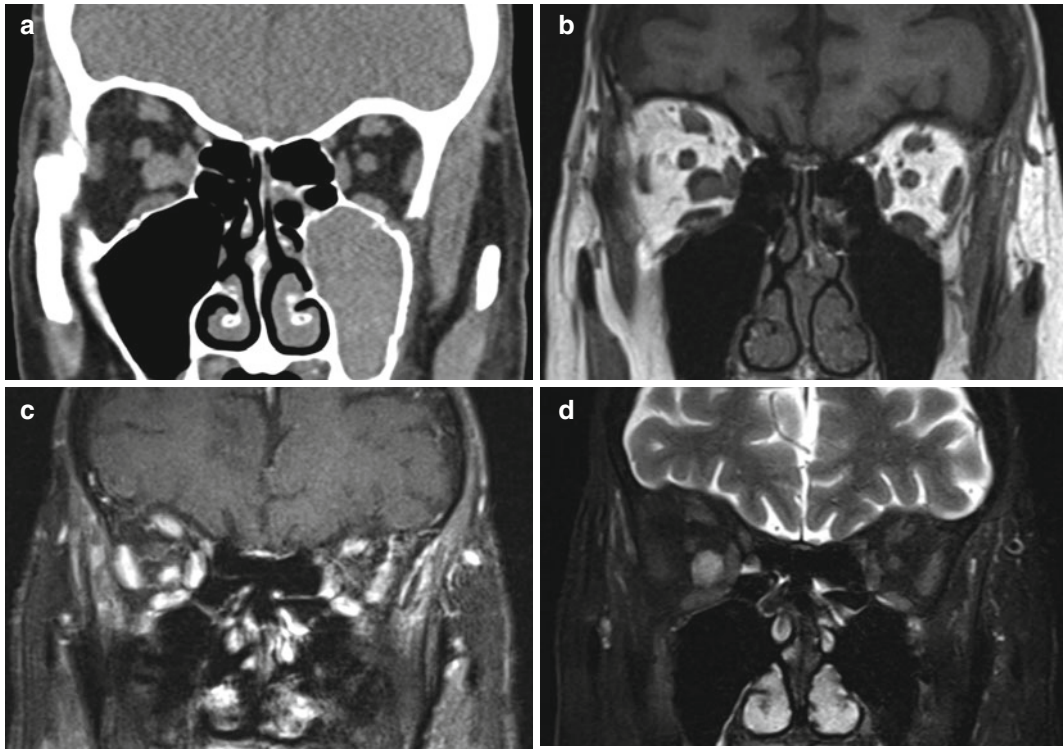

Fig. 7.5 Cavernous hemangioma. A 69-year-old woman underwent CT of the head following a bicycle accident. Incidental intraconal orbital mass was identified (**a**) in addition to opacified left maxillary sinus. Patient had no orbital signs on examination with visual acuity of 20/20. MRI revealed an intraconal circumscribed mass inferonasal to the optic nerve without signs of compression (**b**, T1). The lesion enhanced following administration of contrast (**c**, T1 fat suppressed and **d**, T2 fast suppressed)

VIII-related antigen. The channel walls contain multiple layers of spindle cells staining positive for smooth muscle actin. Recent evidence of progesterone receptors within these spindle cells may help explain the increased incidence in women and aggravation of symptoms during pregnancy [32].

7.4.2 Clinical Features

7.4.2.1 Symptoms

Patients typically present as middle-aged adults with slowly progressing, painless proptosis.

Often they are detected incidentally when imaging studies are performed for unrelated headache or trauma (Fig. 7.5). Vision may be diminished due to compressive optic neuropathy or an induced hyperopic shift. Some patients complain of diplopia.

7.4.2.2 Signs

Examination may reveal signs of compressive optic neuropathy, axial proptosis, strabismus, choroidal folds, or disc edema.

7.4.3 Diagnostic Evaluation

CT scanning typically reveals a well-circumscribed, multiloculated, intraconal mass. Lesions appear hypo- or isointense on T1-weighted images and hyperintense on T2-weighted images. Early images on angiography may show slow patchy enhancement, while later stages typically show more homogeneous pooling. Imaging may detect intracranial or cavernous sinus extension. Technetium-99m-labeled red blood cell scintigraphy can confirm the diagnosis, showing the combination of large blood volume with low flow [33].

7.4.4 Differential Diagnosis

The differential diagnosis of cavernous hemangiomas includes all etiologies for slowly progressing axial proptosis: meningiomas, lymphangioma, hemangiopericytoma, and schwannoma.

7.4.5 Treatment

Patients without significant symptoms should be followed to detect evidence of progression. Many lesions stabilize and never require surgery, but patients must understand the urgency for immediate evaluation with symptoms of progression.

Surgical indications for symptomatic patients include proptosis, diplopia, compressive optic neuropathy, and gaze-evoked amaurosis.

Lateral orbitotomy remains the standard approach to most intraconal cavernous hemangioma, which typically lie lateral to the optic nerve [34]. Intraconal lesions located adjacent to the globe can be accessed using a transconjunctival approach. Hemangiomas may be decompressed prior to excision or removed en bloc with temporary muscle disinsertion and use of a cryoprobe [12, 35]. Apical tumors or larger lesions located superior to the optic nerve may require better exposure from a transcranial approach.

7.4.6 Prognosis

Excisional surgery should result in a cure for symptomatic lesions.

7.5 Hemangiopericytoma

7.5.1 Introduction

Hemangiopericytomas are characterized by a spectrum of pericyte proliferation. Histopathology often shows a mixed pattern of ovoid cells and sinusoidal space formations creating the classic "staghorn" vascular pattern (Fig. 7.6). Varying levels of cellular atypia underlie the less benign nature of this lesion, which may malignantly transform or metastasize.

7.5.2 Clinical Features

Hemangiopericytoma typically presents in middle-aged adults as slowly progressing unilateral proptosis, often with pain and vision loss. Other signs and symptoms depend on tumor location. Frequent intracranial extension and invasion into sinus cavities may produce additional associated symptoms.

7.5.3 Diagnostic Evaluation

Ultrasound reveals an encapsulated and well-defined solid mass with low internal reflectivity. Orbital hemangiopericytoma has been reported to undergo cystic changes within necrotic zones and may resemble the echographic appearance of lymphangiomas. On MRI, T1-weighted images reveal a well-defined hypointense mass to fat. T2-weighted studies show less lesion definition. CT imaging often detects bony changes around these contrast-enhancing lesions. Angiography typically reveals early tumor blush with rapid washout of contrast. Diagnosis of this lesion requires histologic confirmation.

7.5.4 Differential Diagnosis

The differential diagnosis for hemangiopericytoma includes meningiomas, lymphangioma, cavernous hemangioma, and schwannoma.

7.5.5 Treatment

Although the majority of these lesions are benign, the high rate of malignant transformation and recurrent disease mandates aggressive en bloc excision with wide margins. Adjunctive radiation therapy may be of benefit although conclusive studies are difficult due to the rarity of this tumor [36, 37].

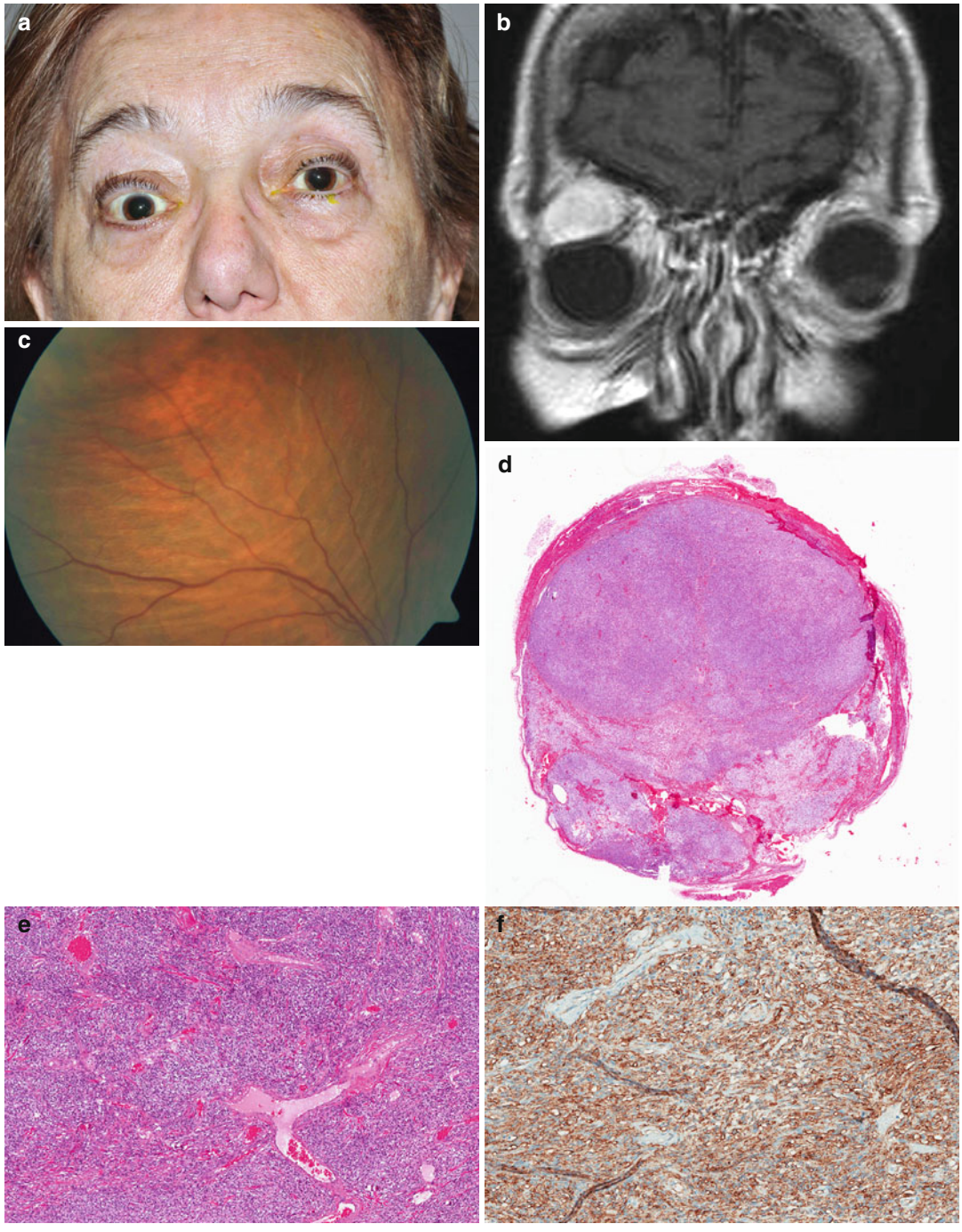

Fig. 7.6 Hemangiopericytoma. Clinical appearance of proptosis and hypoglobus (**a**). Coronal (**b**) MRI showing a circumscribed enhancing mass. Funduscopic examination revealed choroidal folds (**c**). Low-power photomicrograph demonstrating a well-circumscribed cellular lesion (**d**). Medium-power photomicrograph revealing relatively uniform spindle cells without a recognizable growth pattern. Small areas of densely pink "ropey" collagen are seen, as is a branched "staghorn" blood vessel (**e**). CD34 stain is diffusely and strongly positive in the spindle cells (**f**) (**d**, **e**, **f** Courtesy of Thomas Plesec, MD, Cleveland, Ohio, USA)

7.5.6 Prognosis

The spectrum of aggressiveness of a particular lesion is difficult to predict as even more histologically benign lesions may result in clinically invasive disease or malignant transformation. The elusive nature of this entity warrants aggressive surgery and often adjuvant therapy.

Conclusion

Classifying orbital vascular malformations by hemodynamic categories permits proper treatment. Overlap with hamartoma creates further confusion regarding classification but the clinical and radiologic features assist in establishing the diagnosis and directing treatment.

References

1. Harris GJ. Orbital vascular malformations: a consensus statement on terminology and its clinical implications. Am J Ophthalmol. 1999;127(4):453–5.
2. Aletaha M, Salour H, Bagheri A, et al. Successful treatment of orbital hemangioma with propranolol in a 5-year-old girl. Orbit. 2012;31(1):18–20.
3. Taban M, Goldberg RA. Propranolol for orbital hemangioma. Ophthalmology. 2010;117(1):195–5.e4.
4. Hill RH, Shiels WE, Foster JA, et al. Percutaneous drainage and ablation as first line therapy for macrocystic and microcystic orbital lymphatic malformations. Ophthal Plast Reconstr Surg. 2012;28(2):119–25.
5. Greene AK, Burrows PE, Smith L, Mulliken JB. Periorbital lymphatic malformation: clinical course and management in 42 patients. Plast Reconstr Surg. 2005;115(1):22–30.
6. Hall N, Ade-Ajai N, Pierro A, et al. Is intralesional injection of OK-432 effective in the treatment of lymphangioma in children? Surgery. 2003;133:238–42.
7. Boulos PR, Harissi-Dagher M, Kavalec C, Hardy I, Codere F. Intralesional injection of Tisseel fibrin glue for resection of lymphangiomas and other thin-walled orbital cysts. Ophthal Plast Reconstr Surg. 2005;21(3):171–6.
8. Werner JA, Dunne AA, Folz BJ, Rochels R, Bien S, Ramaswamy A, Lippert BM. Current concepts in the classification, diagnosis and treatment of hemangiomas and vascular malformations of the head and neck. Eur Arch Otorhinolaryngol. 2001;258(3):141–9.
9. Ernemann U, Westendorff C, Troitzsch D, et al. Navigation-assisted sclerotherapy of orbital venolymphatic malformation: a new guidance technique for percutaneous treatment of low-flow vascular malformations. AJNR Am J Neuroradiol. 2004;25(10):1792–5.
10. Hayashi N, Masumoto T, Okubo T, et al. Hemangiomas in the face and extremities. De Lorimier AA. Sclerotherapy for venous malformations. J Pediatr Surg. 1995;30:188–93.
11. Lee CH, Chen SG. Direct percutaneous ethanol sclerotherapy for treatment of a recurrent venous malformation in the periorbital region. ANZ J Surg. 2004;74(12):1126–7.
12. Goldberg RA, Garcia GH, Duckwiler GR. Combined embolization and surgical treatment of arteriovenous malformation of the orbit. Am J Ophthalmol. 1993;116:17–25.
13. Hayes BH, Shore JW, Westfall CT, Harris GJ. Management of orbital and periorbital arteriovenous malformations. Ophthalmic Surg. 1995;26(2):145–52.
14. Lee BB, Do YS, Yakes W, et al. Management of arteriovenous malformations: a multidisciplinary approach. J Vasc Surg. 2004;39:590–600.
15. Mulliken JB, Glowacki J. Hemangiomas and vascular malformations in infants and children: a classification based on endothelial characteristics. Plast Reconstr Surg. 1982;69(3):412–22.
16. Coats DK, Paysse EA, Levy ML. PHACE: a neurocutaneous syndrome with important ophthalmologic implications: case report and literature review. Ophthalmology. 1999;106:1739–41.
17. Walter JW, Blei F, Anderson JL, Orlow SJ, Speer MC, Marchuk DA. Genetic mapping of a novel familial form of infantile hemangioma. Am J Med Genet. 1999;82:77–83.
18. Shields CL, Shields JA, Minzter R, et al. Cutaneous capillary hemangiomas of the eyelid, scalp, and digits in premature triplets. Am J Ophthalmol. 2000;129(4):528–31.
19. Drolet BA, Esterly NB, Frieden IJ. Hemangiomas in children. N Engl J Med. 1999;341:173–81.
20. Marler JJ, Fishman SJ, Kilroy SM, Fang J, Upton J, Mulliken JB, Burrows PE, Zurakowski D, Folkman J, Moses MA. Increased expression of urinary matrix metalloproteinases parallels the extent and activity of vascular anomalies. Pediatrics. 2005;116(1):38–45.
21. Berman B, Poochareon VN, Villa AM. Novel dermatologic uses of the immune response modifier imiquimod 5 % cream. Skin Therapy Lett. 2002;7:1–10.
22. Clymer MA, Fortune DS, Reinisch L, Toriumi DM, Werkhaven JA, Ries WR. Interstitial Nd:YAG photocoagulation for vascular malformations and hemangiomas in childhood. Arch Otolaryngol Head Neck Surg. 1998;124(4):431–6.
23. North PE, Waner M, Mizeraki A, Mihm MC. GLUT 1: a newly discovered immunohistochemical marker for juvenile hemangiomas. Hum Pathol. 2000;31:11–22.
24. Neumann D, Isenberg SJ, Rosenbaum AL, Goldberg RA, Jotterand VH. Ultrasonographically guided injection of corticosteroids for the treatment of retroseptal capillary hemangiomas in infants. J AAPOS. 1997;1(1):34–40.

25. Egbert JE, Paul S, Engel WK, Summers CG. High injection pressure during intralesional injection of corticosteroids into capillary hemangiomas. Arch Ophthalmol. 2001;119(5):677–83.
26. Egbert JE, Schwartz GS, Walsh AW. Diagnosis and treatment of an ophthalmic artery occlusion during an intralesional injection of corticosteroid into an eyelid capillary hemangioma. Am J Ophthalmol. 1996;121(6):638–42.
27. Goyal R, Watts P, Lane CM, Beck L, Gregory JW. Adrenal suppression and failure to thrive after steroid injections for periocular hemangioma. Ophthalmology. 2004;111(2):389–95.
28. Coats DK, O'Neil JW, Paysse EA, et al. SubTenon's infusion of steroids for treatment of orbital hemangiomas. Ophthalmology. 2003;110:1255–9.
29. Ezekowitz RA, Mulliken JB, Folkman J. Interferon alfa-2a therapy for life-threatening hemangiomas of infancy. N Engl J Med. 1992;326:1456–63.
30. Kodama T, Tane N, Ohira A, Matsuoka Y, Maruyama R. Concomitant cavernous hemangioma and venous angioma of the orbit. Jpn J Ophthalmol. 2004;48(4):415–7.
31. Gelal F, Feran H, Rezanko T, Vidinli BD. Giant cavernous angioma of the temporal lobe: a case report and review of the literature. Acta Radiol. 2005;46(3):310–3.
32. Di Tommaso L, Scarpellini F, Salvi F, Ragazzini T, Foschini MP. Progesterone receptor expression in orbital cavernous hemangiomas. Virchows Arch. 2000;436(3):284–8.
33. Gdal-On M, Israel O. Cryoextraction of orbital hemangiomas diagnosed by Tc-99M-labeled red blood cells. Vision Res. 1995;35:169.
34. McNab AA, Wright JE. Cavernous haemangiomas of the orbit. Aust N Z J Ophthalmol. 1989;17:337–45.
35. Kiratli H, Bulur B, Bilgic S. Transconjunctival approach for retrobulbar intraconal orbital cavernous hemangiomas. Orbital surgeon's perspective. Surg Neurol. 2005;64(1):71–4.
36. Karcioglu ZA, Nasr AM, Haik BG. Orbital hemangiopericytoma: clinical and morphologic features. Am J Ophthalmol. 1997;124(5):661–72.
37. Croxatto JO, Font RL. Hemangiopericytoma of the orbit: a clinicopathologic study of 30 cases. Hum Pathol. 1982;13:210–8.

Benign Orbital Tumors

8

Bhupendra C.K. Patel

Contents

B.C.K. Patel, MD, FRCS
Division of Oculoplastic and Orbital Service,
John A. Moran Eye Center, University of Utah,
50 North Medical Drive, Salt Lake City,
UT, 84132, USA
e-mail: bhupendra.patel@hsc.utah.edu

J.D. Perry, A.D. Singh (eds.), *Clinical Ophthalmic Oncology*,
DOI 10.1007/978-3-642-40492-4_8, © Springer-Verlag Berlin Heidelberg 2014

8.1 Introduction

Benign orbital tumors represent a broad spectrum of tumors (Chap. 2). In addition, orbital inflammation and infection may clinically simulate an orbital neoplasm (Chap. 6). In a recent survey of 1,264 consecutive patients with suspected orbital tumor referred to an ophthalmic oncology center, 64 % of the lesions were benign [1].

Benign orbital tumors may be congenital or more frequently acquired. Benign tumors more commonly are of vascular (Chap. 7), neural (Chap. 9), meningeal, fibrolytic, and osseous origin. Benign tumors may also arise from the lacrimal gland (Chap. 10) and lacrimal sac (Chap. 11). The details of clinical examination (Chap. 1) and imaging techniques (Chap. 5) supplement contents of this review. Benign orbital tumors not covered under other chapters are reviewed herein.

8.2 Conjunctival Epithelial Cysts

8.2.1 Introduction

Conjunctival orbital cysts are usually secondary to previous trauma or surgery and are generally observed in adults, even when they are primary in nature. Rarely, they may present in neonates [1].

8.2.2 Clinical Features

Non-pulsatile proptosis is the usual manifestation in adults and in children, although worsening of the proptosis on crying has been noted in a neonate with an orbital cyst [1].

8.2.3 Differential Diagnosis

In adults, the differential diagnosis includes dermoids and lymphangiomas. In neonates and children, the differential diagnosis includes orbital teratoma, colobomatous cyst, lymphatic malformations, dacryoceles, and meningocele/encephalocele.

8.2.4 Diagnostic Evaluation

With improvement in image resolution of routine prenatal ultrasonography and ultrafast fetal magnetic resonance imaging, it is possible to detect a wide range of fetal ocular abnormalities such as cataract, microphthalmos, dacryocele, and retinoblastoma. Orbital cysts have similarly been detected during routine prenatal ultrasonography (Figs. 8.1 and 8.2). MRI will show no solid component or calcification within the lesion.

8.2.5 Treatment

Surgical removal of the whole of the cyst or partial removal is usually curative.

8.3 Dermoid and Epidermoid Cysts

8.3.1 Introduction

Dermoid cysts are the most common orbital cysts, representing up to 5 % of all orbital tumors [2]. Epidermoid cysts have a single layer of keratinized or nonkeratinized epithelium without evidence of adnexal structures. Most epidermoid

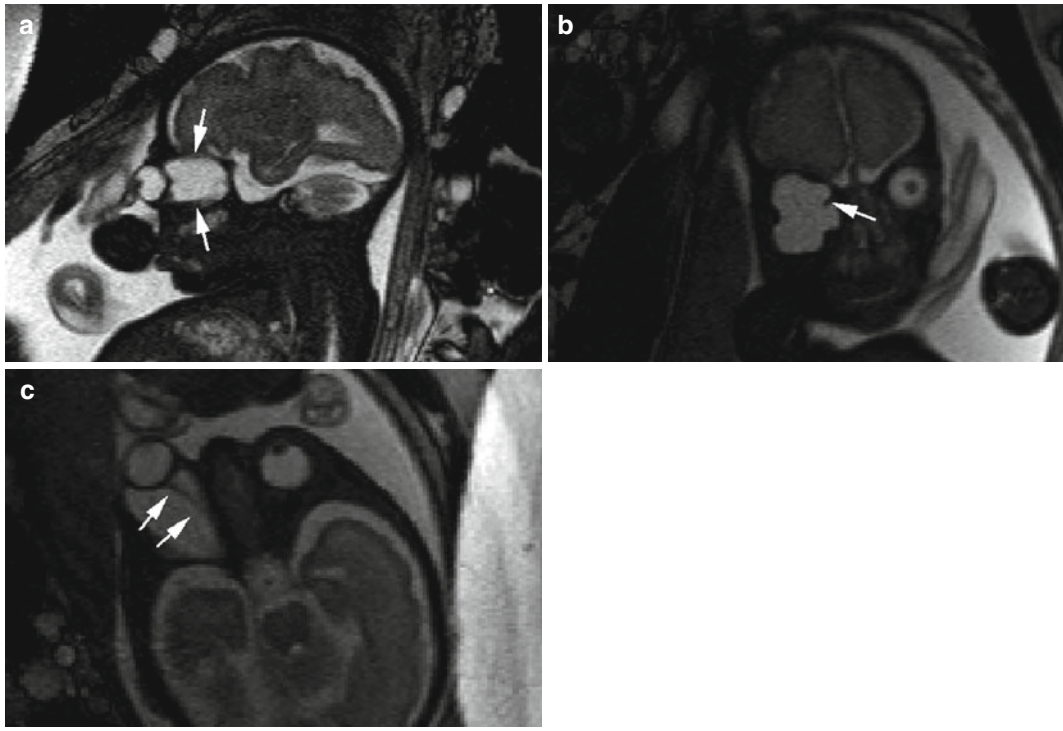

Fig. 8.1 Ultrafast magnetic resonance imaging image of the fetus. Right parasagittal view shows an orbital cyst (*arrows*) resulting in marked proptosis (**a**). Coronal (**b**) and axial (**c**) views show an orbital cyst resulting in attenuation of the optic nerve. Note absence of any solid component. The globe is of normal size and shape (Reproduced with permission from Singh et al. [1])

cysts are traumatic in origin [3]. Dermoids, on the other hand, are choristomas with adnexal structures such as hair, sebaceous glands, and lipid. They arise from ectodermal nests pinched off at suture lines. Clinically, dermoid and epidermoid cysts may present very similarly and so are now usually differentiated by location: superficial or deep. Histopathology of dermoids may show hair, keratin, sebaceous glands, macrophages, lipid globules, multinucleated giant cells, and calcium.

8.3.2 Clinical Features

Most dermoid cysts are present in infancy with a well-defined, round periorbital mass. Approximately 60 % of all dermoids arise superotemporally from the frontozygomatic suture; 25 % arise superomedially from the frontolacrimal suture (Fig. 8.3) [4]. Others may arise from frontoethmoidal sutures and in the deep temporalis fossa [5]. A few may arise from the sphenozygomatic suture.

The cysts are usually less than 2 cm in diameter and cause little ocular displacement. They are smooth, firm, nontender, and nonfluctuant. Many are not intraorbital but sit on the frontozygomatic suture or just behind the orbital rim. Mild lateral upper eyelid ptosis is often seen. Deeper dermoids may be seen along the medial and lateral orbital walls. These deeper dermoids remodel bone over many years. They may cause extraorbital expansion of the cyst into the temporal fossa or into the intracranial cavity [6]. Such patients may present with proptosis on mastication [7]. Deeper cysts often present later, in the third or fourth decade. Other presentations of

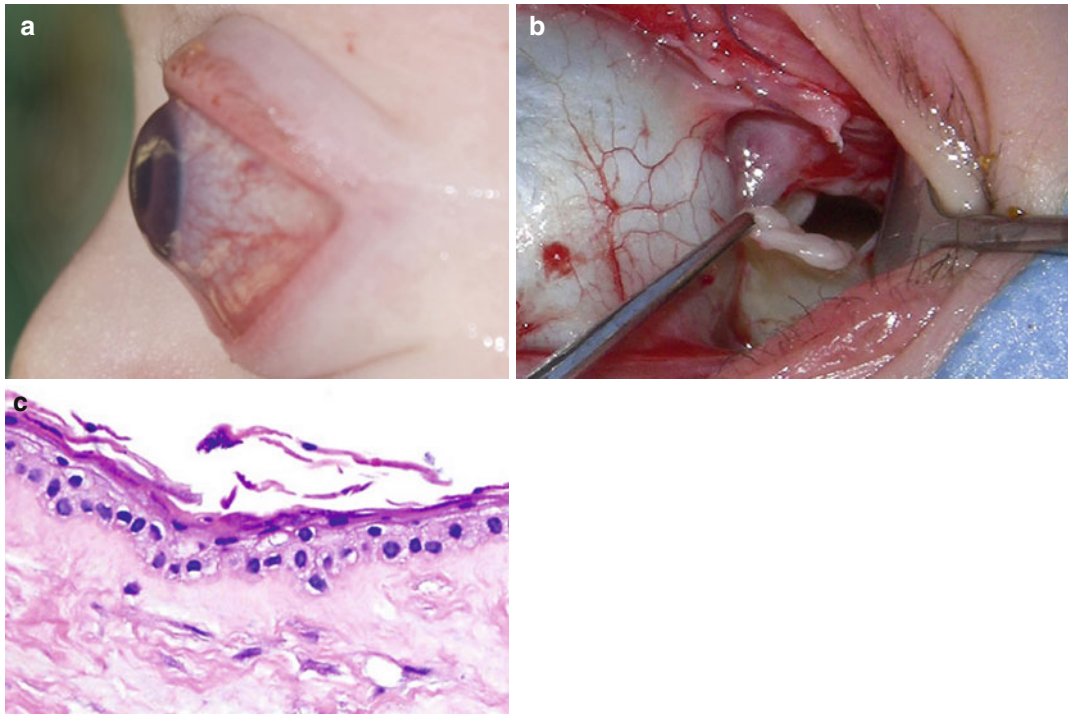

Fig. 8.2 Marked proptosis of the right globe at birth (**a**). A 5 × 4 mm rectangular piece of the cyst wall was removed via anterior transconjunctival orbitotomy (**b**). Histopathologic examination revealed cyst wall lined by squamous epithelium with mild focal keratinization (**c**, hematoxylin and eosin, original magnification ×40). Subsequent orbital excision and biopsy of the orbital cyst/mass revealed teratoma (Reproduced with permission from Singh et al. [1])

deep cysts include proptosis and displacement of the eye opposite to the site of the cyst. Most patients will not have diplopia or visual problems as the cysts are of long duration [8].

Patients may present with discomfort because of leakage. Asymptomatic leakage of lipid and keratin may lead to inflammation and adherence of the dermoid cyst to neighboring structures. Intermittent lid swelling with localized redness and pain may be seen. Chronic inflammation may be seen even in asymptomatic patients. Ruptured dermoids may present with a fistula to the skin [9].

8.3.3 Differential Diagnosis

Superomedial lesions may be confused with retention cysts and orbitofrontal mucoceles. Medial dermoids must be differentiated from encephaloceles. Deep midline intranasal dermoid cysts may present like discharging lacrimal sac mucoceles in children. Unlike mucoceles, the dermoids present with a central cutaneous dimple.

Deep superotemporal dermoids should be differentiated from lacrimal gland tumors radiographically, as dermoids often are isodense to fat and produce bony changes only in proximity to the frontozygomatic suture. Ultrasound may help confirm the cystic nature of the dermoid, although debris within the cyst may make the distinction difficult.

8.3.4 Diagnostic Evaluation

On CT scans, the majority of orbital dermoids have some adjacent bony changes, which are rounded and well defined (Fig. 8.3). A well-defined

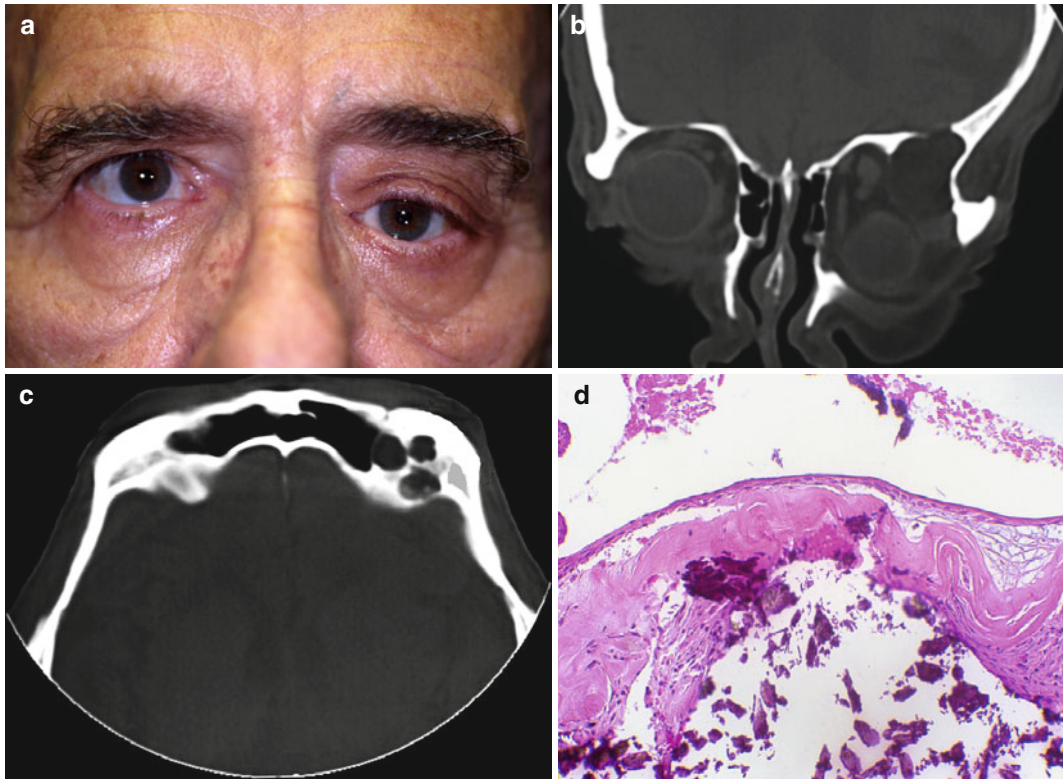

Fig. 8.3 Dermoid cyst. A 75-year-old male presented with left proptosis and hypoglobus with double vision of several months duration (**a**). CT scan demonstrated thinning of the superotemporal orbital wall (**b**, coronal view) and a cystic lesion (**c**, axial view). The cyst wall is lined with stratified epithelium and there is keratin within the lumen (**d**)

wall is seen with a center of fat density. Some will show calcification and fluid levels. In the presence of previous rupture, the margins may be irregular. The presence of a tunnel, channel, or cleft through the adjacent wall is noted in as many as a third of cases [10]. Many patients have a blind pit or cleft in the bone. Irregular bony margins suggest rupture with granulomatous distribution of the adjacent bone. Posterior masses may show bony pressure effects. Ultrasonography may be used for an anterior cyst.

8.3.5 Treatment

Surgical aim is to completely remove the dermoid. Dermoids presenting in childhood are removed soon after presentation to avoid traumatic rupture. Most can be safely removed via an anterior or anterolateral orbitotomy. An upper eyelid skin crease approach with appropriate distraction of the incision can be used for removal of most superolateral dermoids. The cryoprobe may be used to provide traction during the dissection around the wall. While the plane of dissection is easier to follow if the cyst is intact, sometimes, especially for large cysts, decompression of the cyst is necessary to allow complete excision. If an inadvertent rupture of the cyst should occur, the area should be irrigated with an antibiotic solution, and the contents and lining should be meticulously removed.

Deeper superotemporal and inferotemporal cysts can be accessed via a lateral orbitotomy with removal of the lateral orbital wall [11]. A transfrontal craniotomy approach is used when cysts extend intracranially and for cysts at the apex of the orbit. Dumbbell tumors with extension into the temporal fossa are removed

first from the orbit. The temporal component and the bony canal are subsequently removed. The bony tunnel should be cored out to remove the connecting stalk in dumbbell tumors.

8.4 Intradiploic Arachnoid Cyst

8.4.1 Introduction

Arachnoid cysts are congenital outpouchings within the arachnoid membrane filled with cerebrospinal fluid (CSF). Occasionally, these cysts occur in the intracranial intradiploic space, the majority of which have been reported following head trauma and associated with posttraumatic skull fractures in children. While the majority of intradiploic arachnoid cysts described in the literature have been traumatic in origin, there have been several reported nontraumatic cases. These nontraumatic cystic lesions are presumed to be congenital, with CSF pulsating through a dural defect into the intradiploic space and leading to gradual enlargement with thinning of the inner and outer tables of bone. Given the low pressure of CSF pulsations, Thomas and Rout have speculated that the lesions must be initiated before ossification of the cranium since normal CSF pressure would not likely cause intradiploic expansion in otherwise intact bone. Although these nontraumatic cases are presumed to be congenital, these cysts are generally identified in older patients.

8.4.2 Clinical Features

Patients may present with local pain or diffuse headache or proptosis. Sometimes, these lesions are identified as incidental findings when imaging is performed for non-associated symptoms. The majority of these lesions have been identified in the occipital bone and the frontotemporal region. Figure 8.4 illustrates a case in a child where the sphenoid bone was involved.

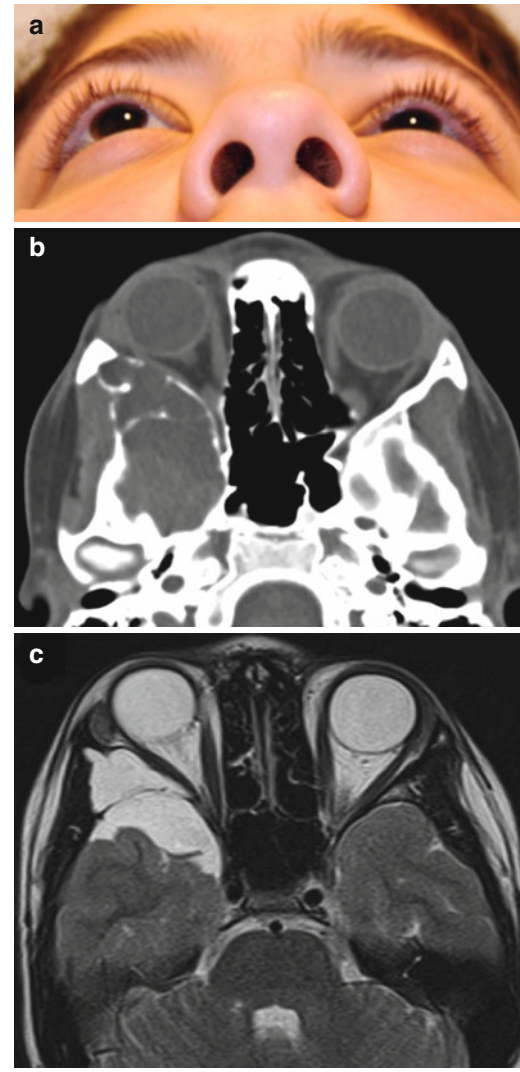

Fig. 8.4 Intradiploic cyst. External chin-up photograph demonstrates gross axial proptosis of the right eye (**a**). The eye otherwise appears normal. Axial non-contrast CT image demonstrates marked expansion and remodeling centered in the greater wing of the sphenoid. There is also an immediately adjacent arachnoid cyst overlying the right temporal lobe (**b**). Axial T2-weighted image confirms the presence of a middle cranial fossa arachnoid cyst and demonstrates fluid signal intensity in the cyst similar to that within the remodeled and expanded greater wing of sphenoid (**c**). External photographs show progressive right orbital fullness, most evident superior to the lateral brow, dating 2006 (**d-A**), 2008 (**d-B**), 2010 (**d-C**), and current 2011 (**d-D**)

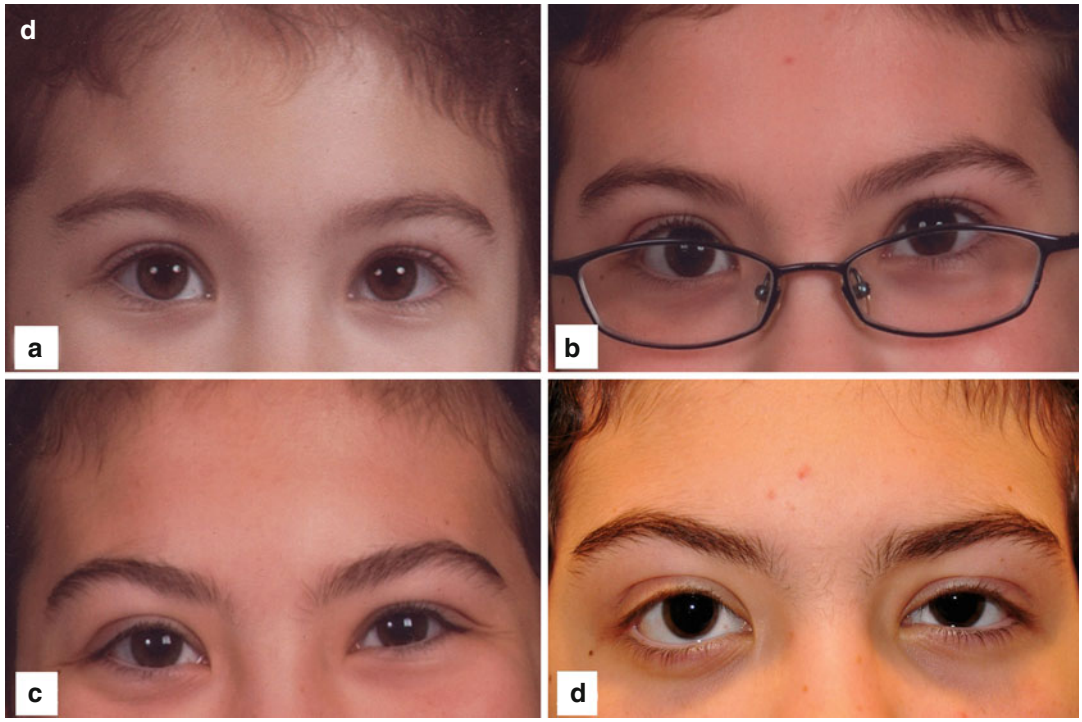

Fig. 8.4 (continued)

8.4.3 Differential Diagnosis

In the pediatric population the differential for calvarial lesions includes epidermoid or dermoid cyst, eosinophilic granuloma, aneurysmal bone cyst, lymphatic or vascular malformations, cystic fibrous dysplasia, multiple myeloma, giant cell tumor, metastatic disease, rhabdomyosarcoma, Ewing sarcoma, osteogenic carcinoma, and osteogenic sarcoma.

8.4.4 Diagnostic Evaluation

On CT scans, osseous expansion and remodeling is seen. MRI scans show no enhancement and no solid component of the mass and will follow CSF signal intensity on all pulse sequences [12].

8.4.5 Treatment

Surgical treatment of these lesions consists of craniectomy or craniotomy with fenestration of the cyst, excision of its pedicle, and repair of the dural defect, sometimes combined with implants to replace bony defects.

8.5 Mucocele

8.5.1 Introduction

Mucoceles occur mostly in adults; 60 % affect the frontal sinus, while 30 % occur in the ethmoid sinus, and 10 % occur in the maxillary sinus. They result secondary to an obstruction of the ostium of the affected sinus. Mucoceles may result from facial fractures, nasal or sinus sur-

gery, paranasal osteomas, chronic polyposis, or congenital abnormalities [13]. Mucoceles in childhood suggest underlying cystic fibrosis.

8.5.2 Clinical Features

Obstruction of the normal sinus ostia will create entrapment of the secretory epithelium, accumulation of mucous, pressure on the surrounding bony structures, thinning of the bony walls, and extension through the wall into the adjacent orbit, nasopharynx, or cranial cavity [14]. Mucocele may develop slowly with subacute exacerbations mimicking orbital cellulitis. Extension of the mucocele into the orbit will result in proptosis or other globe displacement, ptosis, a palpable superonasal mass, diplopia, headache, orbital pain, or visual impairment (Fig. 8.5). Orbital apex involvement may lead to orbital apex syndrome with deep orbital pain, headache, and visual impairment.

8.5.2.1 Frontoethmoid Mucocele

Clinical features are dependent upon the location of the sinus involved. Frontoethmoid mucocele may present with superomedial fullness, inferolateral displacement, epiphora, hypertelorism, or fistula [15]. Hypertelorism, seen more often in bilateral mucoceles, may be associated with cystic fibrosis.

8.5.2.2 Sphenoid and Posterior Ethmoid Sinus Mucocele

Sphenoid and posterior ethmoid sinus mucocele may cause visual changes and proptosis.

8.5.2.3 Maxillary Mucocele

A maxillary mucocele usually causes proptosis but may cause enophthalmos secondary to erosion of the floor of the orbit [16].

8.5.3 Diagnostic Evaluation

CT scans show a well-defined homogenous mass isodense with brain. Cystic contents completely fill the enlarged sinus and displace, rather than destroy, the bony margins (Fig. 8.5). The bone thins and the mucocele becomes part of the orbit.

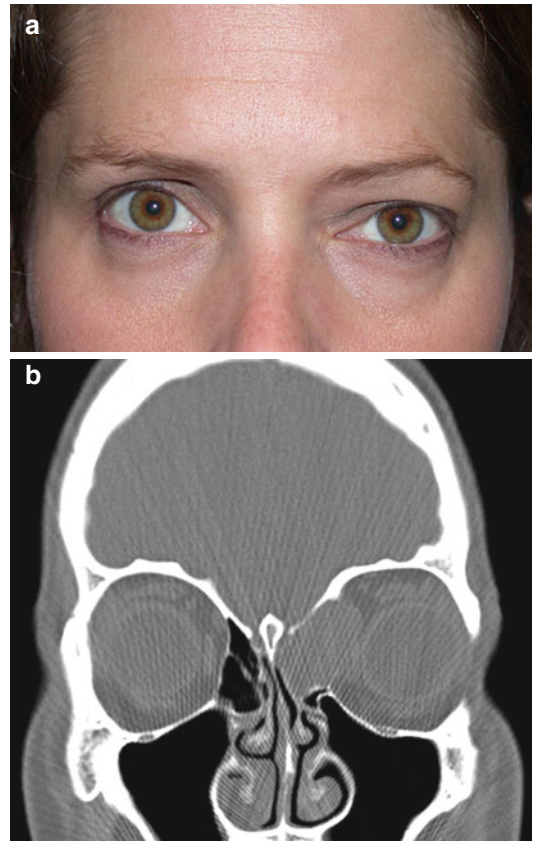

Fig. 8.5 Frontal mucocele. A 38-year-old female with a 2-week history of left periorbital pain and diplopia on upgaze (**a**). CT scan demonstrating left frontal mucocele with opacification of the frontal sinus and erosion of the superomedial orbital wall (**b**). The orbital component is well defined and rounded. The orbital structures are displaced inferiorly and laterally

8.5.4 Treatment

Management involves complete surgical removal of the lining and reestablishment of normal drainage or obliteration of the sinus. The optimal obliteration technique remains controversial. Methods include use of muscle, fat, and alloplastic materials. Repair of the bony defect is rarely required.

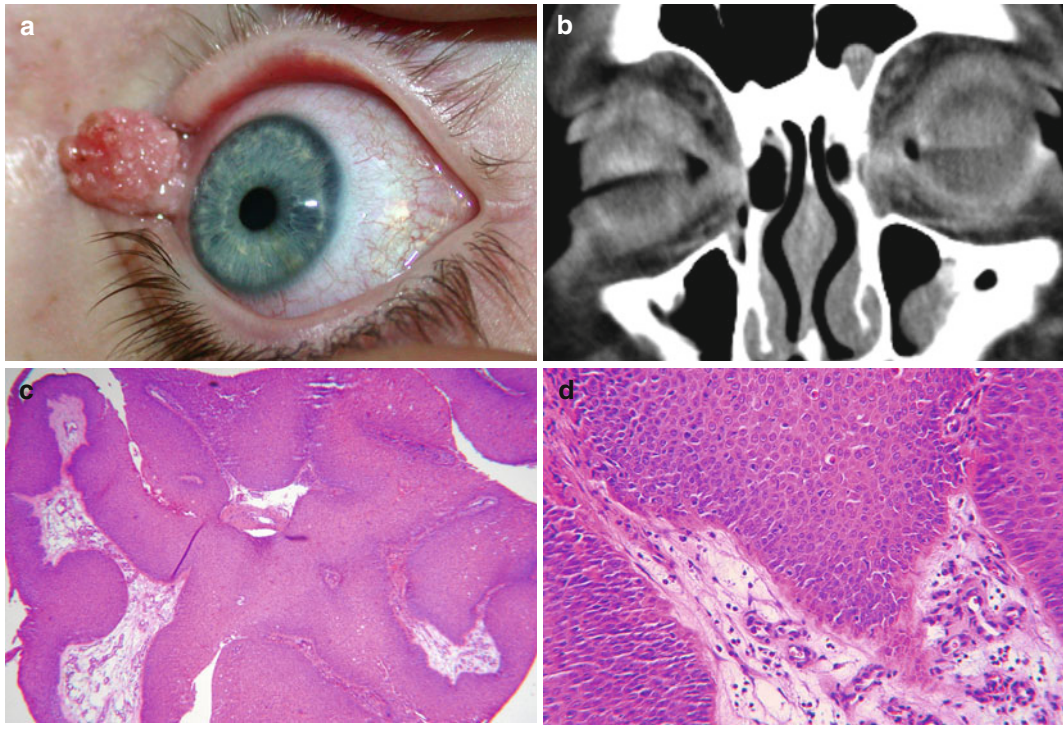

Fig. 8.6 Inverted papilloma. A large exophytic tumor at the caruncle (**a**). CT scan showing a diffuse mass in the caruncular region and the nasolacrimal duct (**b**). Ribbons of respiratory epithelium enclosed by basement membrane which grows into the subjacent stroma with micromucous cysts (**c**, **d**)

Displacement of the globe often improves after effective treatment [17].

Orbital extension of inverted papilloma occurs in 2–3 % of cases.

8.6 Sinonasal Inverted Papilloma

8.6.1 Introduction

Primary inverted papilloma of the lacrimal system is unusual; most inverted papillomas arise from the lateral nasal wall and the maxillary and ethmoid sinuses and rarely from the frontal and sphenoid sinuses.

8.6.2 Clinical Features

Primary nasolacrimal system papillomas and secondarily invading sinonasal inverted papillomas present with epiphora and a medial canthal mass.

8.6.3 Diagnostic Evaluation

CT scans reveal soft tissue attenuation in the lacrimal sac and nasolacrimal duct with bone remodeling and thinning and expansion of the nasolacrimal duct (Fig. 8.6). Associated changes will be seen in the adjoining sinuses when the primary origin is from the sinus. The lesion is a benign polypoid proliferation of the sinonasal mucosa, but the behavior is locally aggressive. Bony destruction with intraorbital and intracranial extension may be seen [18].

8.6.4 Treatment

The etiology of inverted papilloma is not well characterized: DNA viruses such as human

papilloma virus (HPV) types 6 and 11 and the Epstein-Barr virus have been identified in the lesions. HPV presence indicates a higher likelihood of both malignancy and recurrence. Traditionally, these lesions have been approached via a medial maxillectomy through a lateral rhinotomy incision or midface degloving. Total resection with adequate margins has been the standard of care. Many cases are now effectively treated using endoscopic approaches, avoiding external incisions [19]. Recurrence of the tumor has been reported to range from 27 to 71 %. Malignant transformation into carcinoma occurs in about 10 % of cases.

8.7 Cholesterol Granuloma

8.7.1 Introduction

Nomenclature for cholesterol granuloma has changed from previous terms, including hematic cyst, hematoma, hematocele, chocolate cyst, blood cyst, subperiosteal hemorrhage, and orbital cholesteatoma. A cholesterol granuloma is not a true cyst, as it lacks an epithelial lining.

Cholesterol granulomas are seen mostly in men in their fourth or fifth decade in the superotemporal orbital wall and sometimes in the zygoma. Although factors causing elevated venous pressure, blood clotting diseases, and other causes have been invoked, it is now recognized that most cholesterol granulomas are caused by previous trauma [20]. Hematogenous debris accumulation creates an osmotic gradient with resultant absorption of fluid and increased volume. An anticoagulant effect caused by high concentrations of fibrinogen degradation products may also result in recurrent hemorrhage.

8.7.2 Clinical Features

The patient usually presents with a superolateral mass developing over weeks to years, causing inferior globe displacement, proptosis, and limited upgaze with diplopia in upgaze (Fig. 8.7). The patient may rarely have blurred vision. Headache or pain in the region of the mass may also occur.

8.7.3 Diagnostic Evaluation

CT scans reveal a well-defined, nonenhancing osteolytic lesion with bone erosion and sometimes intralesional bone fragments. The mass is usually homogenous and isodense with the brain [21]. The smooth margins contrast with the moth-eaten appearance seen with malignant tumors such as plasma cell myeloma. These lesions do not transgress the frontozygomatic suture. The differential diagnosis includes dermoid cyst and lacrimal gland carcinoma.

8.7.4 Treatment

Surgical evacuation of the lesion via a percutaneous approach is usually curative. There is usually a yellow-brown viscous material within the cavity containing friable tissue and loose bone. The bone itself may be yellow. The fluid is altered blood in various stages of degeneration and organization. Bone wax may be used to control oozing that occurs from the bony lining. Occasionally, a drain may be necessary at the end of the procedure. It is not necessary to pack the cavity. Recurrence is rare and when seen usually indicates subtotal curettage [22].

8.8 Orbital Cephalocele

8.8.1 Introduction

Cephaloceles are protrusions of brain tissue through bony defects. An encephalocele is a protrusion of the parenchymal brain. A meningocele has protrusion of dura, while a mixture of brain and meninges is a meningoencephalocele. All

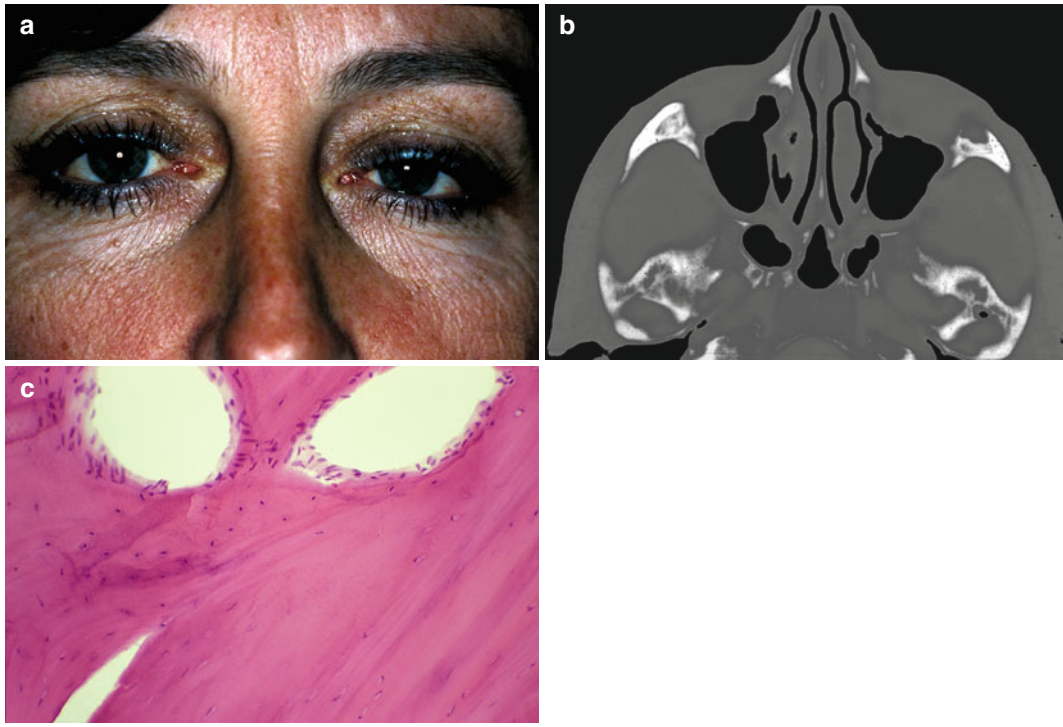

Fig. 8.7 Cholesterol granuloma. A 42-year-old female presents with left hypoglobus and a tender mass over the superolateral left orbital rim. History of trauma to the left orbit 6 months previously (**a**). Expansion of the diploic space of the left frontal bone is seen (**b**). Osteoid material with vascular channels (**c**). Older cholesterol granulomas would show frank cholesterol granulomas and lipid-laden histiocytes

cephaloceles retain some attachment to the brain by a cord or stalk of tissue. These are often associated with other congenital facial anomalies involving the midline structures.

8.8.2 Clinical Features

Cephaloceles may be anterior, basal, or posterior.

8.8.2.1 Anterior Cephalocele

Anterior cephalocele is the commonest, presenting as a paranasal mass located at the nasofrontal-orbital junction. The lesion may be soft or firm and is usually painless.

8.8.2.2 Basal Cephalocele

Basal cephalocele is associated with a defect in the cribriform plate and present with a midline mass. The patient may have a broad nasal root, hypertelorism, and inferolateral globe displacement. The basal cephalocele may be confused with a mucocele and may also present as bilateral nasolacrimal duct obstructions [23].

8.8.2.3 Posterior Cephalocele

Posterior orbital cephalocele is less common; they herniate through a foramen or a dehiscence in the sphenoid bone and may present with pulsatile proptosis, optic nerve atrophy, and strabismus [24].

8.8.3 Diagnostic Evaluation

CT scans show a homogenous lesion, isodense with the brain. Dermoid and teratoma show more fluid content. Mucocele is usually present below

the medial canthal tendon, while cephalocele is located above the tendon.

8.8.4 Treatment

Management involves excision of the extracranial extension and stalk and repair of the dural and bony defect. Surgical repair involves a combined craniofacial and neurosurgical approach with correction of other facial deformities [25].

8.9 Neurofibroma and Neurilemmoma (Schwannoma)

8.9.1 Introduction

Neurofibromas are twice as common as schwannomas in the orbit and, together, constitute 4 % of all orbital tumors. Isolated, solitary neurofibromas usually present in middle age and are in 90 % of instances unassociated with neurofibromatosis. Plexiform neurofibromas may involve any of the cranial, sympathetic, and parasympathetic nerves in the orbit. Schwannomas are well-defined, encapsulated, slowly growing tumors that develop as eccentric growths from peripheral nerves. They are usually solitary and may also be associated with neurofibromatosis.

8.9.2 Clinical Features

Most neurofibroma and neurilemmoma manifest as a solitary mass, frequently in the upper quadrants. They are solid, isolated, circumscribed, slow-growing masses leading to displacement and local expansion of the orbit with associated anesthesia, paresthesia, and hypesthesia [26, 27]. In more superficial locations, the tortuous enlarged nerves produce a characteristic "bag of worms" feel, and the overlying skin may be thickened (elephantiasis neuromatosa). When intraconal, the tumor presents with proptosis, lid swelling, posterior indentation of the globe, and diplopia in extremes of gaze (Fig. 8.8). Apical tumors may extend through the superior and inferior orbital fissure. Defects in the greater wing of sphenoid may be seen.

8.9.3 Diagnostic Evaluation

Neurofibroma and neurilemmoma are homogenous, well-circumscribed tumors with a density similar to brain on CT scans with contrast enhancement. CT scans demonstrate bony expansion and may show superior orbital fissure expansion [28]. MRI shows isointensity to vitreous on T1-accentuated images and hypointensity to vitreous on T2-weighted sequences (Fig. 8.8).

8.9.4 Differential Diagnosis

The differential diagnosis of neurofibroma includes all causes for slowly progressing axial proptosis: meningioma, lymphangioma, fibrous histiocytoma, hemangiopericytoma, and cavernous hemangioma. On MR imaging, the lesion is indistinguishable from cavernous hemangioma, fibrous histiocytoma, and hemangiopericytoma.

8.9.5 Treatment

Although solitary orbital neurofibroma and neurilemmoma may be easily excised, the involved nerve is, by necessity, sacrificed. Therefore, care should be taken to identify the involved nerve as a sensory nerve rather than a motor nerve. Solitary neurofibroma and neurilemmoma are seen during surgery as well-defined, firm, circumscribed, rubbery, gray masses with little vascularity. Plexiform neurofibroma is vascular and diffusely intertwined with normal tissues. Complete surgical resection is rarely possible. When indicated, resection of plexiform neurofibroma is best approached through transfrontal craniotomy. Bleeding is always a problem. Repair of bony defects is necessary in the presence of pulsating proptosis. Complications can include bleeding, hematoma, cerebral edema, recurrence of pulsating proptosis and secondary socket, and orbital deformities.

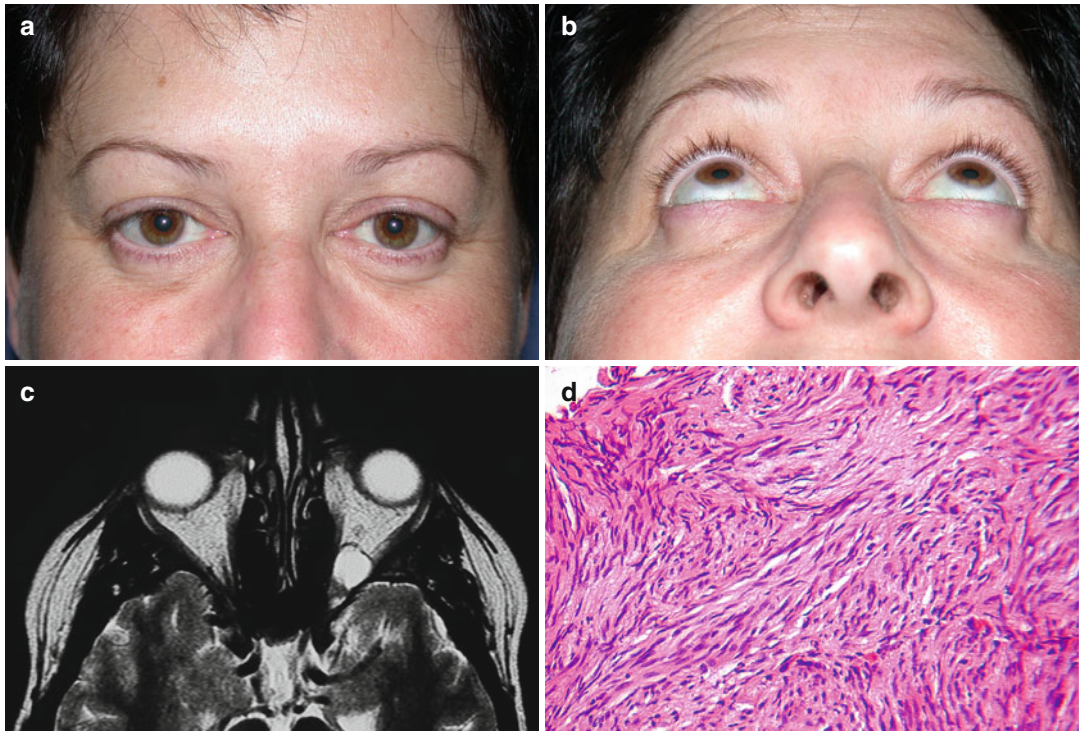

Fig. 8.8 Schwannoma. A 51-year-old female presents with left blurred vision, hypoglobus (**a**), and proptosis (**b**). MRI (T2-weighted image) shows a well-circumscribed apical superior orbital mass hyperintense to fat (**c**). Note spindle-shaped nuclei in whirling or fascicular pattern within eosinophilic glassy cytoplasm (**d**, H&E original magnification ×200)

8.10 Solitary Fibrous Tumor

8.10.1 Introduction

Solitary fibrous tumor (SFT) is a spindle cell tumor which arises most commonly from the pleura. The first case of SFT was described as recently as 1994 [29].

8.10.2 Clinical Features

Clinical presentation is like that of a hemangioma or hemangiopericytoma with proptosis, globe displacement, double vision, and vision changes (Fig. 8.9). Although orbital SFT typically follows a benign course, evidence of local invasion and malignancy may be seen. Although usually confined to the orbit, extraorbital extension has been described [30].

8.10.3 Diagnostic Evaluation

On imaging, the lesions usually appear well defined and may appear encapsulated with mild to moderate enhancement. Clinically, they are difficult to distinguish from hemangiopericytomas. Generally, there is no bony erosion although a few cases of bony erosion and extension of the tumors have been described. T2-weighted MRI images may reveal a hypointense or a hyperintense mass, depending upon the density of the fibrous matrix. Ultrasonically, SFTs have low reflectivity with moderate sound attenuation. There has been controversy regarding the classification of SFT and orbital hemangiopericytoma as discrete entities due to overlapping histologic characteristics. Immunohistochemical studies help to distinguish SFT from other tumors, as it generally displays positivity for CD34, CD99, and bcl-2. Although hemangiopericytomas may

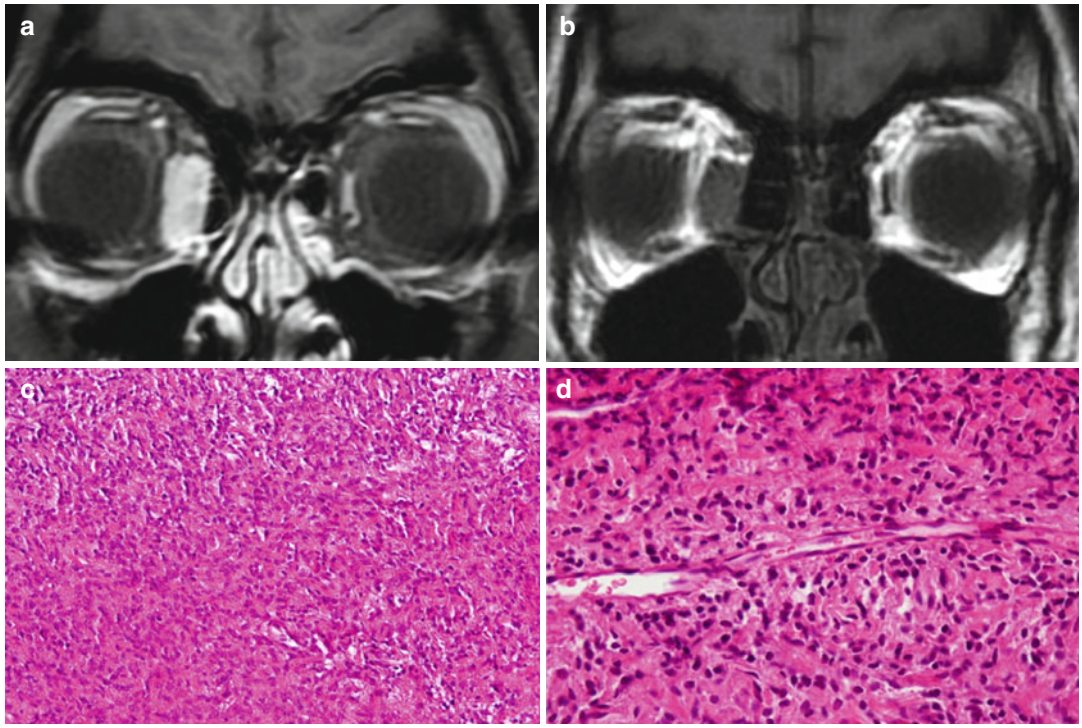

Fig. 8.9 Solitary fibrous tumor. A 37-year-old male who presents with a 3-week history of pressure behind the right eye with right proptosis and a headache. MRI showing an enhanced right medial orbital tumor (**a**, **b**). Tumor marked by cellularity and multiple small slit-like staghorn spaces (**c**). Benign-appearing vascular endothelial cells with some oval to spindle-shaped cells consistent with pericytes. No dysplastic features noted (**d**)

also be positive for CD34, CD99, and bcl-2, hemangiopericytomas are usually focally or less intensely immunopositive. Staghorn vascular patterns are often seen in SFT and in hemangiopericytoma. Epithelial membrane antigen and smooth muscle actin may occasionally be expressed, while SFT is usually negative for S100 and cytokeratins [31]. Histologic features suggestive of aggressive behavior include a high mitotic rate of more than 4 mitoses per 10 high-powered fields, necrosis, hypercellularity, nuclear pleomorphism, and high MIB-1 labelling.

8.10.4 Treatment

Definitive management of SFT of the orbit is complete removal. In the presence of subtotal excision, close follow-up is indicated. Recurrence is usually seen in the presence of subtotal resection.

8.11 Meningioma

8.11.1 Introduction

Meningiomas constitute 20 % of adult and 2 % of childhood intracranial tumors. Primary meningioma, which affects a younger age group, arises within the orbit and may arise from the optic nerve sheath or the orbital surface of the sphenoid bone. The secondary type extends into the orbit from an intracranial source. These secondary tumors arise from the sphenoid ridge, the basofrontal region, the suprasellar area, the olfactory groove, and the paranasal sinuses [32]. Most

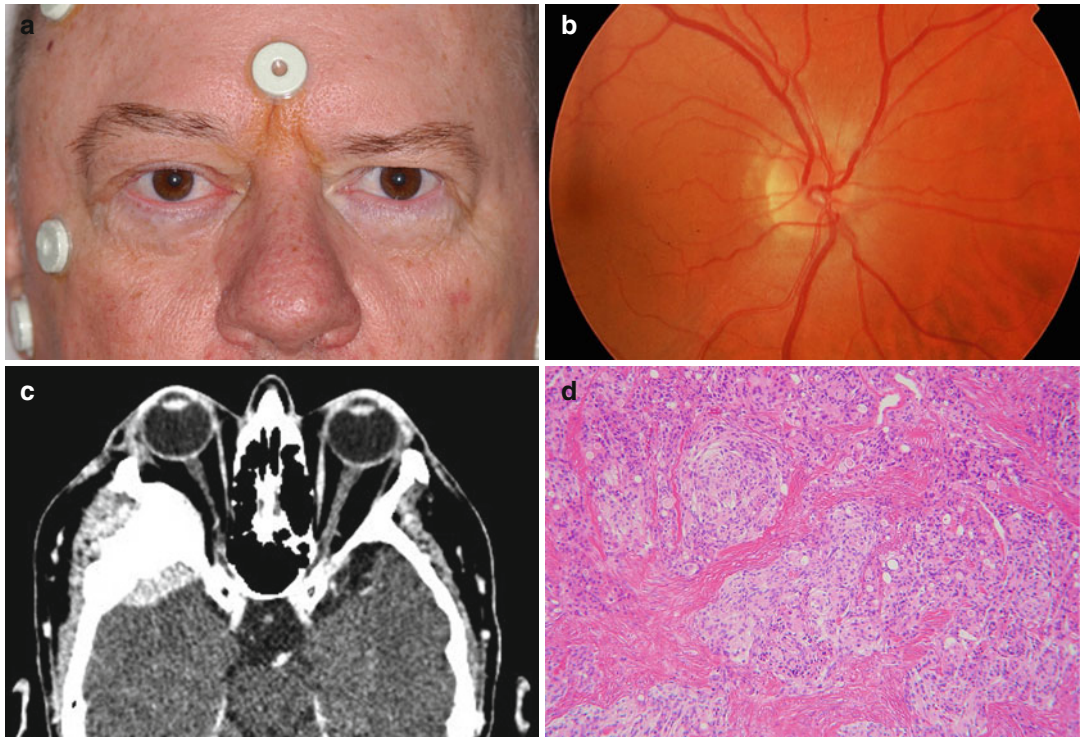

Fig. 8.10 Sphenoidal wing meningioma invading orbit. A 58-year-old male presented with bump on temple, decreased vision, and right-sided headaches (**a**). Right optic disc was edematous (**b**). CT scan demonstrated a right sphenoidal wing hyperostosis with a well-defined and homogenous soft tissue mass extending into the orbit (**c**). Histopathology shows parallel interlacing bundles of elongated cells. Whorled meningothelial cells are also present (**d**)

adult meningiomas are seen in the fifth decade with females being affected 75 % of the time. Previous ionizing radiation and neurofibromatosis type 2 are predisposing factors. Only primary optic nerve sheath meningioma is discussed in this chapter.

8.11.2 Clinical Features

Patients may present with proptosis, decreased visual acuity, disc pallor, eyelid edema, disturbance of ocular motility, headaches or orbital pain, and seizures (Fig. 8.10). Chemosis is often seen. Some patients will have "boggy edema" of the eyelids. The more medial sphenoidal ridge tumors cause cranial nerve palsies, visual deficits, and venous obstructive signs. Proptosis is less prevalent in secondary meningiomas. A mass may be palpable in the temporal fossa when lateral expansion of meningiomas of the greater wing of the sphenoid bone occurs. Occasional bilateral meningiomas have been reported. Visual field testing as well as CT or MR imaging may help to judge progression of the tumor.

8.11.3 Diagnostic Evaluation

CT and MRI are both useful imaging modalities [33]. CT imaging often shows hyperostosis, and calcification is seen in 25 % of the cases (Fig. 8.10). MRI shows a hyperintensity lesion against the isointense brain on T1-weighted sequences allowing delineation of intracranial meningiomas, especially when gadolinium enhancement is used.

8.11.4 Treatment

It is believed that meningioma in patients younger than 20 years are more aggressive and require earlier surgical intervention. Observation is warranted in older patients and where vision is not at risk. Observation is particularly warranted in meningiomas of the optic nerve where surgical resection is associated with high morbidity due to injury to the vascular supply of the optic nerve with 94 % of patients reporting worsened vision postoperatively [34]. When the tumor is close to or abuts the globe, local radiation delivery may be difficult. In such cases, observation is also indicated (Fig. 8.11).

Major indications for surgery are disfiguring or severe proptosis, temporal fullness, orbital

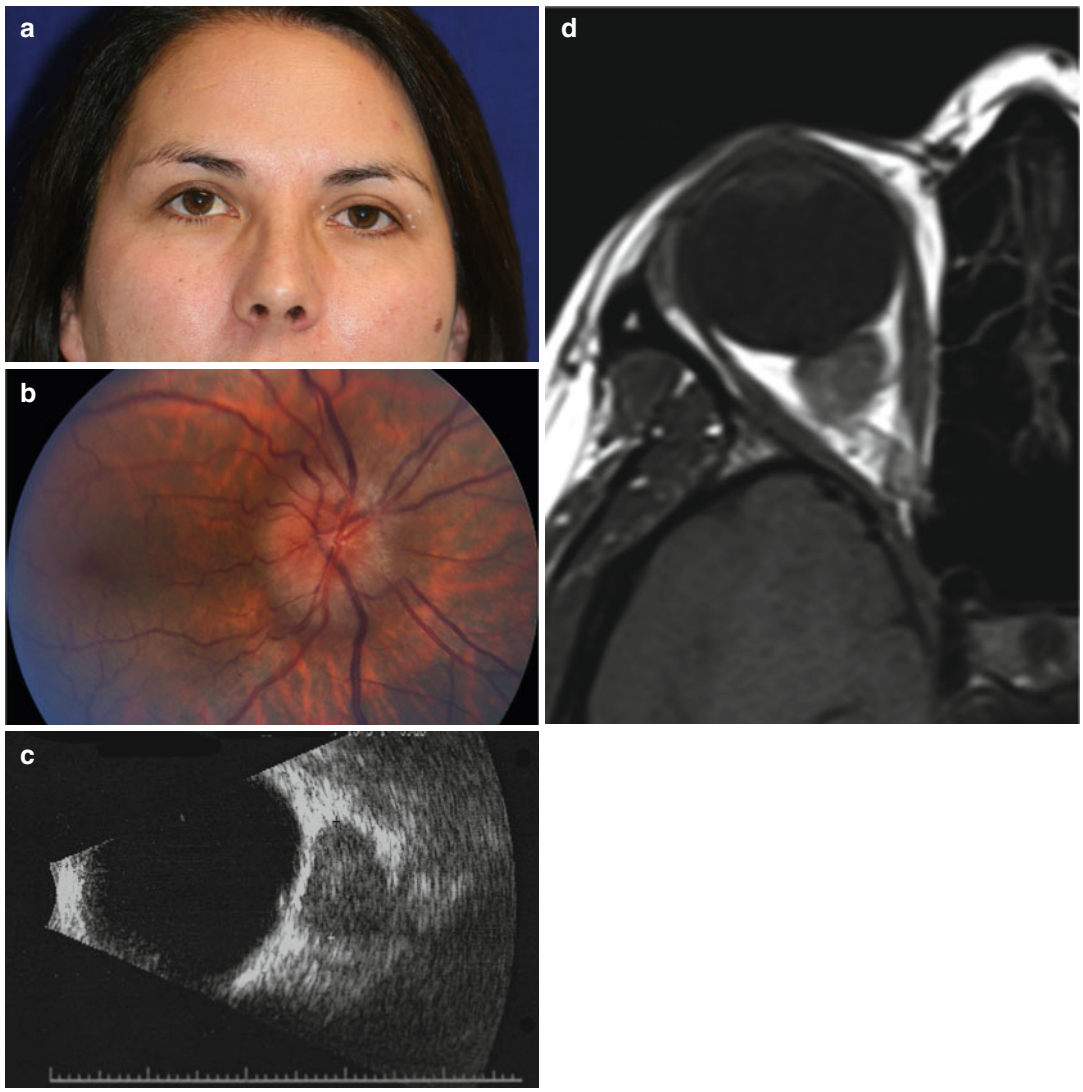

Fig. 8.11 Optic nerve sheath meningioma. A 38-year-old female presents with left proptosis and left hypoglobus (**a**). Fundus shows disc swelling (**b**). Ultrasonography shows an orbital mass abutting the globe (**c**). MRI shows mass involving the optic nerve, but the optic nerve cannot be made out distinctly from the mass (**d**, T1 and **e**, T2). CT scan shows absence of calcification in the mass (**f**). Histopathology shows a characteristic pattern of meningothelial meningioma. Note the whorls and nests of tumor cells (**g**, H&E 100×). Meningothelial cells have round to oval nuclei with intranuclear vacuoles. Mitotic activity is low (**h**, H&E 400×)

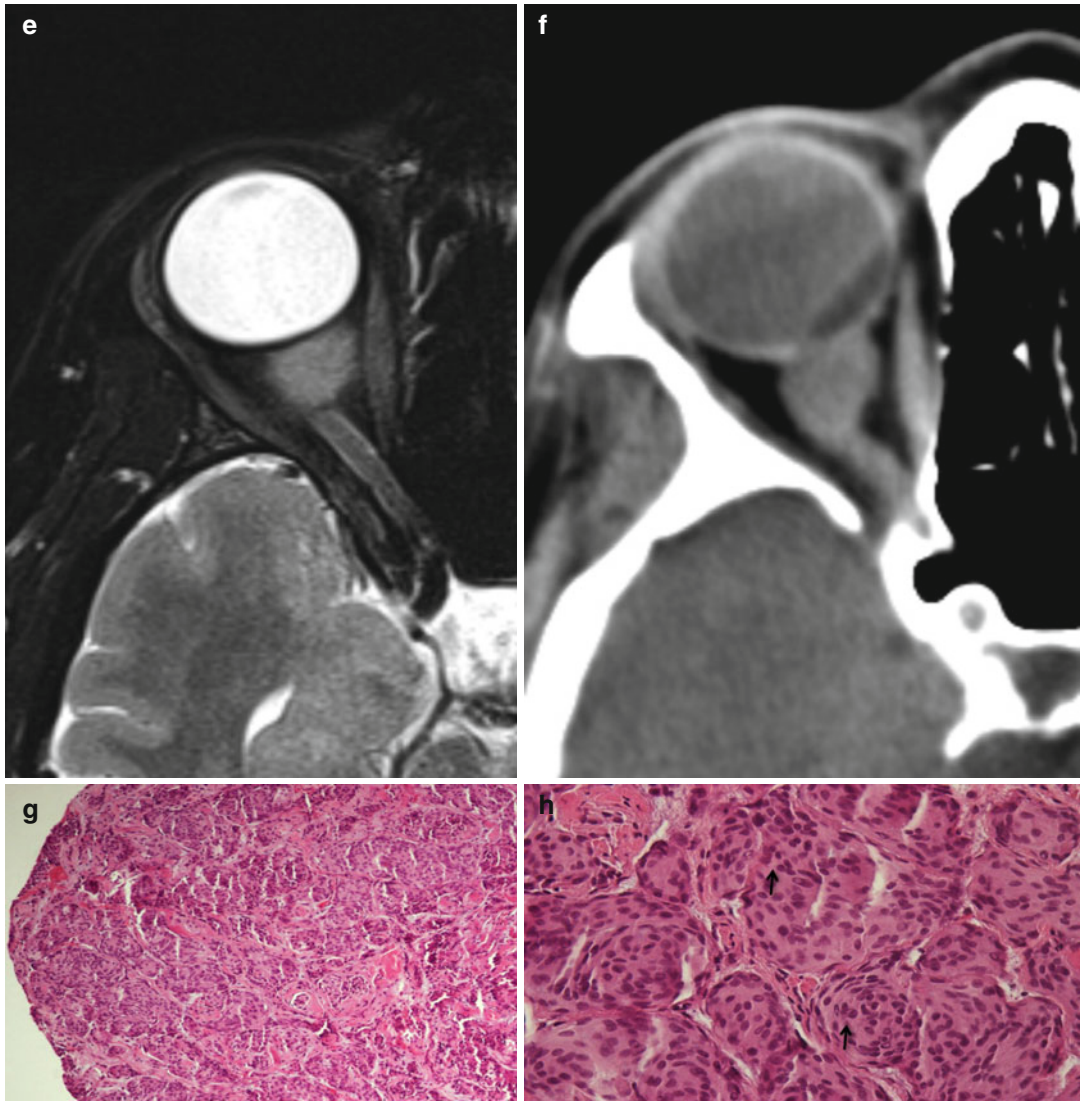

Fig. 8.11 (continued)

congestion, and impaired vision [35]. Aggressive excision or debulking of sphenoid wing tumors may allow improvement in cosmesis, alleviate compressive symptoms, and postpone visual loss [36]. Most patients undergoing surgical resection of sphenoidal ridge meningioma develop recurrences over several years requiring further surgery. Recurrence, residual, and cavernous sinus disease may be treated with radiotherapy [37]. Stereotactic radiosurgical techniques allow more accurate delivery of radiation.

8.12 Teratoma

8.12.1 Introduction

Teratoma, formerly called teratoid cysts or teratoid tumors, is a tumor composed of tissues derived from more than one germ layer and usually from all three. They are rare tumors, usually seen at birth or in the neonatal period. Rarely, they may be seen in adolescents and adults [38].

Table 8.1 The differential diagnosis of orbital teratoma

Category	Subcategory	Diagnosis
Congenital anomaly of the globe		Congenital cystic eyeball Microphthalmos with cyst Congenital glaucoma
Congenital anomaly of the orbit		Cephalocele
Orbital tumor	Primary	Hemangioma Lymphangioma Rhabdomyosarcoma Plexiform neurofibroma
	Secondary	Retinoblastoma
	Metastatic	Neuroblastoma Leukemia

8.12.2 Clinical Features

A typical teratoma presents as a rapidly bulging eye with marked orbital distortion in an infant. The mass may be soft or solid. The tumor enlarges rapidly and may present with marked orbital and facial changes. The persistent enlargement of this neoplasm is attributed to mucus secretion from the embryonic intestinal tissue. While malignant teratomas are seen, most teratomas are benign [39, 40].

8.12.3 Diagnostic Evaluation

The differential diagnosis includes orbital hemangioma, lymphangioma, rhabdomyosarcoma, retinoblastoma, metastatic tumors (neuroblastoma and leukemia), microphthalmos with cyst, congenital cystic eyeball, unilateral congenital glaucoma, cephalocele, and plexiform neurofibroma (Table 8.1). CT imaging shows orbital enlargement with focal calcification in the lumen of the tumor. Erosion of the greater wing of sphenoid bone may be seen. The definitive diagnosis of an orbital teratoma is made by histopathology which shows gut-like structures, the sine qua non for diagnosis of a teratoma.

8.12.4 Treatment

Although vision preservation is rare, surgery should remove the tumor but retain the eye if possible to encourage orbitofacial development. In more severe tumors, enucleation is necessary. Recurrent teratomas may undergo malignant degeneration. Therefore, close follow-up is necessary.

8.13 Fibrous Histiocytoma

8.13.1 Introduction

Fibrous histiocytoma is the most common mesenchymal orbital tumor in adults, seen most commonly in middle-aged adults. They may be benign, locally aggressive, or malignant. Fibrous histiocytoma is defined as a proliferating, complex admixture of fibroblasts and histiocytic-like cells of biphasic nature in a fibrous or collagenous matrix of varying proportion, associated with minor contents of lymphocytes, macrophages, capillaries, lipid, and reticulin [41].

8.13.2 Clinical Features

These tumors, presenting most commonly with an upper nasal quadrant mass, are seen mostly in middle adult life. They are slow-growing, relatively firm masses. Patients present with proptosis, a mass effect, decreased vision, double vision, pain, eyelid swelling, and ptosis.

8.13.3 Diagnostic Evaluation

CT scans show a well-defined, irregular mass of uniform density. Bony erosion and enlargement of the orbit are seen with recurrent or malignant tumors. Ultrasound shows a well-defined mass with a smooth round or oval contour. Cystic cavities may be identified within the tumor.

8.13.4 Differential Diagnosis

Superotemporal tumors may mimic a lacrimal gland tumor. CT scan appearance of the tumor may resemble neurofibromas, schwannomas, or

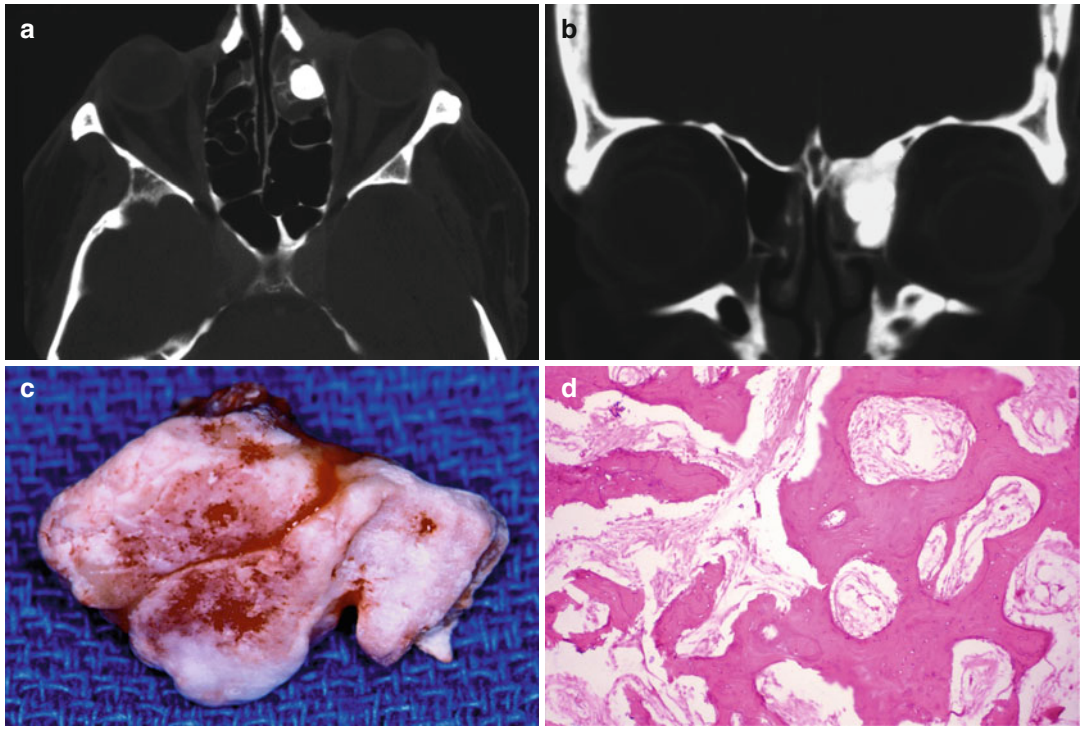

Fig. 8.12 Osteoma. CT scan showing a well-circumscribed radiodense mass in the medial wall of the left orbit (**a**, axial view) (**b**, coronal view). Typical appearance of the resected osteoma (**c**). Osteoma is composed of compact bone devoid of fibrovascular stroma (**d**)

cavernous hemangiomas. Histopathologically, benign fibrous histiocytoma must be differentiated from locally aggressive and malignant variant [42].

8.13.5 Treatment

Surgical excision via an orbitotomy is indicated. Complete excision is recommended as complete resection of the tumor results in a high rate of recurrence. Grossly, the tumor appears as a lobulated, well-circumscribed, firm, grayish white to yellow tan mass. Histopathology shows cartwheel bundles of elongated fibroblasts with spindle-shaped uniformly staining nuclei set in a dense fibrous stroma. The majority of tumors fall in the benign or intermediate group. However, aggressive tumors may spread locally some years after initial diagnosis. Malignant change may occur (Chap. 13).

8.14 Osteoma

8.14.1 Introduction

Primary osteomas of the orbit, although rare, are the most common bony tumor of the orbit. They are well-defined benign tumors of bone. Most are seen in the superonasal orbit and arise secondarily from the frontal sinus, ethmoidal sinus, and junctions [43].

8.14.2 Clinical Features

Osteoma is essentially an overgrowth of bone and present as rock hard mass without pain. Most are solitary and asymptomatic (Fig. 8.12). However, larger lesions may cause proptosis and globe displacement. The patient may present with headaches. Chronic sinusitis or mucocele may result in frontal or frontoethmoid lesions. Frontal sinus

osteoma present with proptosis and downward displacement of the eye; ethmoidal osteomas produce a more lateral shift of the eye. Gardner syndrome is an autosomal dominant familial polyposis of the large bowel associated with osteoma of the skull or jaws and epidermal and sebaceous cysts of the subcutaneous tissues [44]. Some osteoma present with gaze-induced visual loss.

8.14.3 Diagnostic Evaluation

CT scans show a sharply circumscribed, very dense, rounded, or lobulated mass arising from bone (Fig. 8.12). Fibrous osteoma has a low-density, ground-glass appearance similar to fibrous dysplasia or ossifying fibroma. The adjacent paranasal sinus may be opacified from secondary drainage obstruction.

8.14.4 Treatment

If osteoma is symptomless, it may be followed [45]. Resection is indicated when secondary complications arise. Sphenoidal mass is resected endoscopically to prevent encroachment of the optic canal [46]. Recurrence is rare. Histologically, osteoma may be classified as compact, cancellous, and fibrous.

8.15 Fibrous Dysplasia

8.15.1 Introduction

Fibrous dysplasia is a benign, developmental disorder characterized by proliferation of fibrous tissue. It is a hamartomatous malformation thought to be an arrest of bone maturation at the woven bone stage. The fibrous tissue replaces and distorts medullary bones. Three forms have been described: monostotic, polyostotic, and McCune-Albright syndrome.

8.15.1.1 Monostotic Fibrous Dysplasia

Monostotic fibrous dysplasia usually involves one bone around the orbit. The monostotic type accounts for 80 % of cases. The frontal bone is most frequently affected, followed by the sphenoid and ethmoid [47].

8.15.1.2 Polyostotic Fibrous Dysplasia

Polyostotic fibrous dysplasia involves multiple bones.

8.15.1.3 McCune-Albright Syndrome

McCune-Albright syndrome is a constellation of polyostotic fibrous dysplasia, sexual precocity, and cutaneous pigmentation [48].

8.15.2 Clinical Features

Although fibrous dysplasia progresses slowly, sudden exacerbation of disfigurement may be seen over weeks. Symptoms depend upon the anatomic site of the affected bone, the number of bones affected, the rate and duration of tumor growth, and the soft tissues compressed or displaced or distorted. Anterior tumors affecting the frontal, ethmoid, or maxillary bones displace the globe in the direction opposite to the involved bone. Unilateral progressive proptosis and globe displacement sometimes occur with limitation of ocular movement and diplopia (Fig. 8.13). Nasolacrimal duct obstruction may be seen. Patients may also present with persistent headaches or discomfort and compression at the orbital apex with involvement of III, IV, and VI and visual loss [49]. The optic chiasm may also be affected.

Secondary sphenoid sinus mucoceles may occur with sudden loss of vision because of compression of the optic nerve. Patients may develop an intralesional hemorrhage or a secondary aneurysmal bone cyst, both of which can cause compression of the optic nerve. Slow compression of the optic canal or at the chiasm may also

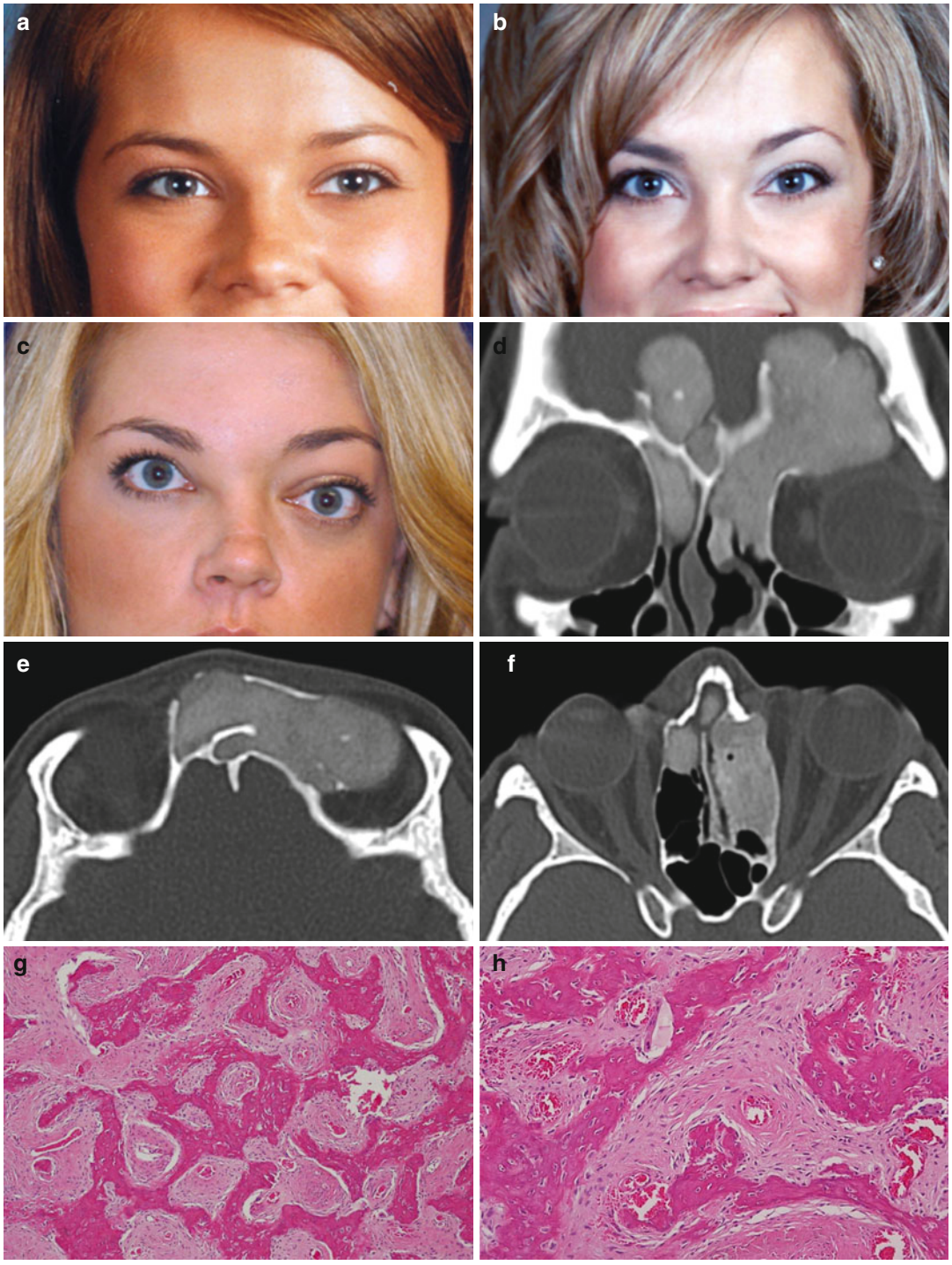

Fig. 8.13 Fibrous dysplasia. Clinical appearance at age 14 years (**a**), 18 years (**b**), and 21 years (**c**). Bone-window CT showing typical ground-glass appearance of fibrous dysplasia (**d**, **e**, **f**). Pattern of dense fibrous connective tissue in between spicules of woven bone (**g**, H&E 40×). The *light pink* is the fibrous connective tissue – it contains immature osteoprogenitor cells. The *dark pink* is immature woven bone. At higher magnification you can easily make out chondrocytes in the immature osseous structure. Of note, there are no osteoblasts (**h**, H&E 200×)

result in chronic visual loss. Malignant transformation (in less than 1 % of cases) to osteogenic sarcoma, fibrosarcoma, or chondrosarcoma may occur if prior radiotherapy has been administered [50].

8.15.3 Diagnostic Evaluation

CT scans show increased bone thickness. Increased fibrous content makes the bone look more lucent in appearance and may show a cystic appearance; a more prominent osseous component gives a ground-glass or sclerotic character. Mixed pattern of alternating sclerosis and radiolucency is often seen. The orbital contour is narrowed and adjacent sinuses are replaced with dense bone.

8.15.4 Differential Diagnosis

Differential diagnosis includes hyperostotic meningioma which will show an associated enhancing soft tissue component (best visualized on MRI). Other conditions to be considered include Paget's disease and cystic bone lesions, such as Langerhans cell histiocytosis. Although juvenile ossifying fibromas have been distinguished from fibrous dysplasia, such fibromas may occur in the presence of fibrous dysplasia (Fig. 8.14) [51].

8.15.5 Treatment

There has been much debate about whether surgical intervention before the patient is symptomatic is useful. As the complications of major craniofacial surgical intervention are significant, surgery is only indicated for gross deformity, functional deficits, pain, or sarcomatous transformation. In the presence of optic canal compression, resection and reconstruction are indicated. However, as most patients with fibrous dysplasia will remain asymptomatic during long-term follow-up, expectant management has been recommended in asymptomatic patients even in the presence of radiological evidence of apical compression of the optic nerve [52].

8.16 Aneurysmal Bone Cyst

8.16.1 Introduction

Aneurysmal bone cyst is a reactive lesion of bone. Aneurysmal bone cyst may arise in the orbit secondary to trauma or as a result of local vascular disturbance. In 30 % of cases, the cyst is associated with an underlying bone lesion, such as fibrous dysplasia, non-ossifying fibroma, or giant cell tumor [53]. The orbital roof is most commonly involved.

8.16.2 Clinical Features

Patients present with proptosis, displacement of the globe, and diplopia secondary to cranial nerve palsy (Fig. 8.15). There may be pain and local swelling. The patient may present with refractive changes. Compressive optic neuropathy and visual loss are rare.

8.16.3 Diagnostic Evaluation

CT scans show an irregular lytic bone lesion with cortical destruction (Fig. 8.15). A fluid level may be seen within the cavities due to hemorrhage with settled blood products. The margins of the tumor may show calcification. MRI scans show a multicystic mass with

associated bone destruction. Fluid-filled levels may be seen with varying levels of signal intensity, depending upon the state of the blood within the cyst [54].

8.16.4 Treatment

Complete surgical curettage is usually curative. The prognosis is usually excellent. Visual

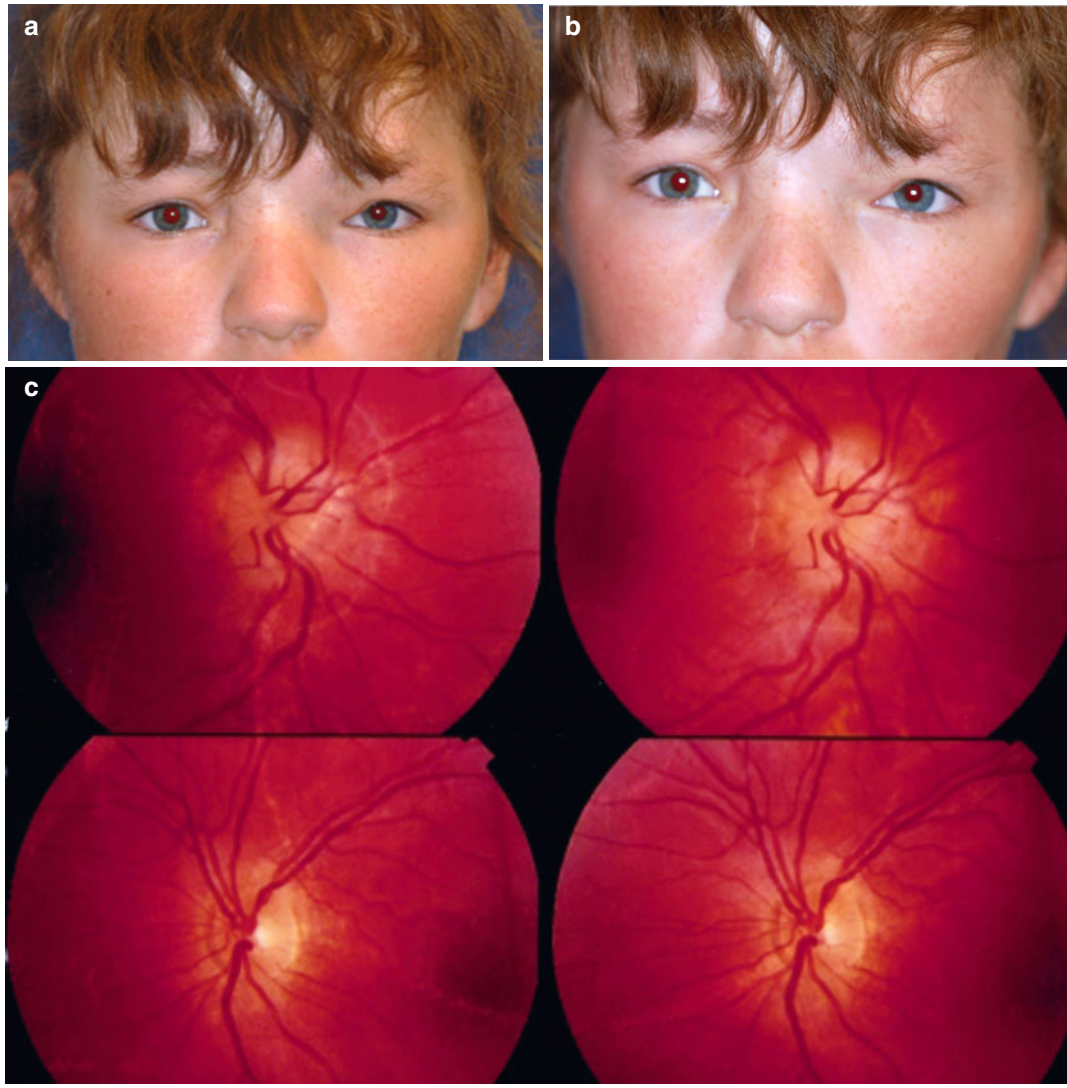

Fig. 8.14 Fibroma arising from fibrous dysplasia. Left hypoglobus and proptosis with superonasal mass at age 15 years (**a** and **b**). Right optic nerve swelling with evidence of compression of the right optic nerve (**c**). T1-weighted MRI scan shows typical low signal in the ethmoid and sphenoid sinus, typical of fibrous dysplasia (**d**). At low magnification you can see fascicles of dense irregular fibrous connective tissue (**e**, 40× and **f** 200×). These findings are consistent with a dense fibroma. Normal bone is seen on the far left with marrow space, osteoblasts, and vessels. Fibrous dysplastic bone is on the right (**g**, 40×)

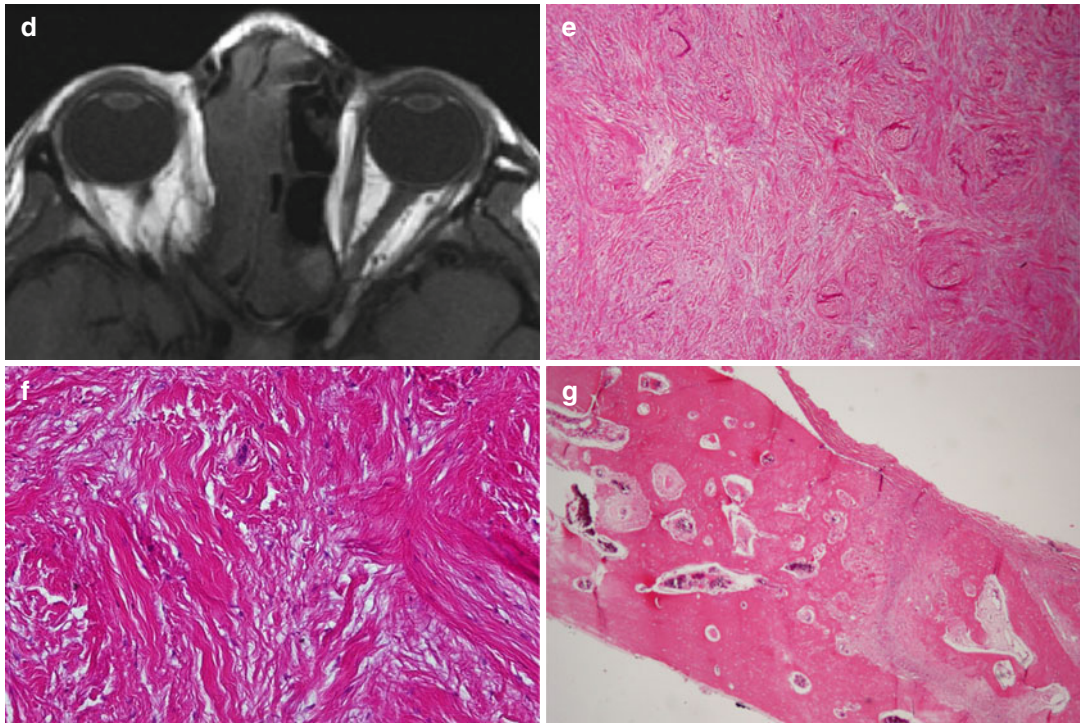

Fig. 8.14 (continued)

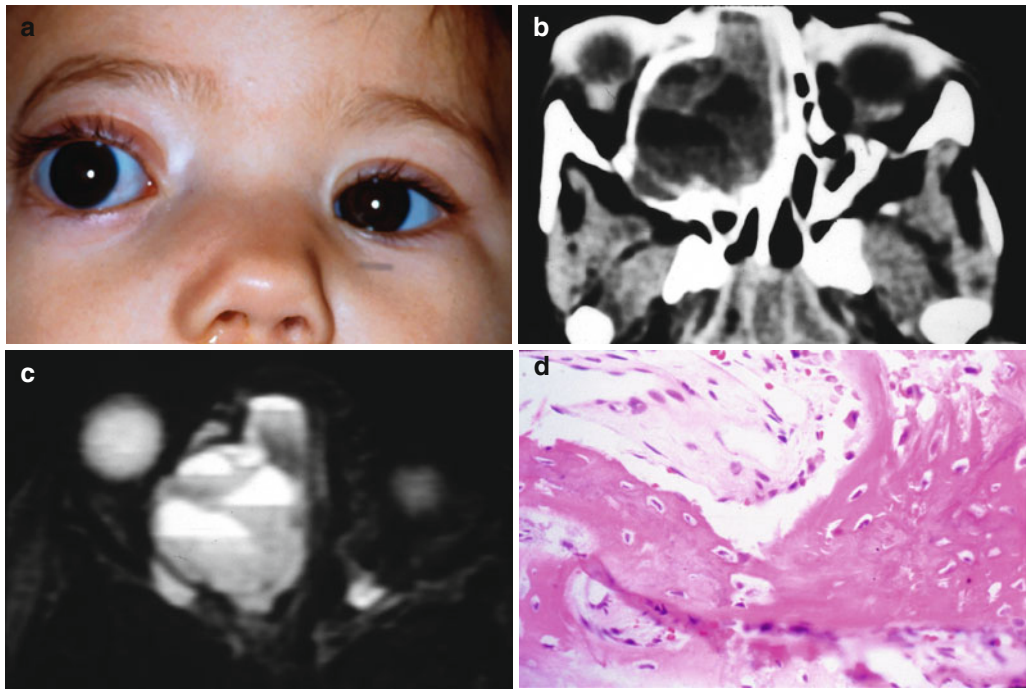

Fig. 8.15 Aneurysmal bone cyst. Eleven-month-old child with 3-week history of right proptosis and nasal obstruction (**a**). CT scan shows expansile lytic mass (**b**). MRI with contrast shows fluid levels with heterogenous signal intensity. Fresh blood is hyperintense on T2-weighted images (**c**). Trabeculated bone with cavernous spaces filled with thick fibrous septa, blood, and cellular areas (**d**)

compromise is very rare. Radiation, used in the past, is inadvisable because of potential risk of radiation-induced sarcoma.

References

1. Singh AD, Traboulsi EI, Reid J, Patno D, Chapa J, Rodriguez R, Iben S, Schoenfield L. Orbital cyst: prenatal diagnosis. Ophthalmology. 2009;116(10):2042–42.e2.
2. Shields JA, Shields CL, Scartozzi R. Survey of 1264 patients with orbital tumors and simulating lesions: the 2002 Montgomery Lecture, part 1. Ophthalmology. 2004;111(5):997–1008.
3. Shields JA, Kaden IH, Eagle Jr RC, Shields CL. Orbital dermoid cysts: clinicopathologic correlations, classification and management. Ophthal Plast Reconstr Surg. 1997;13:265–76.
4. Bonavolonta G, Tranfa G, de Conciliis C, Strianese D. Dermoid cysts: 16-year survey. Ophthal Plast Reconstr Surg. 1995;11:187–92.
5. Meyer DR, Lessner AM, Yeatts RP, Linberg JV. Primary temporal fossa dermoid cysts. Characterization and surgical management. Ophthalmology. 1999;106(2):342–9.
6. Perry JD, Tuthill R. Simultaneous ipsilateral temporal fossa and orbital dermoid cysts. Am J Ophthalmol. 2003;135(3):413–5.
7. Emerick GT, Shields CL, Shields JA, et al. Chewing-induced visual impairment from a dumbbell dermoid cyst. Ophthal Plast Reconstr Surg. 1997;13:57–61.
8. Sherman RP, Rootman J, Lapointe JS. Orbital dermoids: clinical presentation and management. Br J Ophthalmol. 1984;68:642–52.
9. Wells TS, Harris GJ. Orbital dermoid cyst and sinus tract presenting with acute infection. Ophthal Plast Reconstr Surg. 2004;20(6):465–7.
10. Sathananthan N, Moseley IF, Rose GE, Wright JE. The frequency and clinical significance of bone involvement in outer canthus dermoid cysts. Br J Ophthalmol. 1993;77(12):789–94.
11. Yuen HK, Chong YH, Chan SK, Tse KK, Chan N, Lam DS. Modified lateral orbitotomy for intact removal of orbital dumbbell dermoid cyst. Ophthal Plast Reconstr Surg. 2004;20(4):327–9.
12. Thomas TA, Rout D. Non-traumatic intraosseous cerebrospinal fluid cyst with associated craniovertebral anomalies: a case report and suggested mechanism of formation. Neurol India. 2010;58:122–4.
13. Illiff CE. Mucoceles in the orbit. Arch Ophthalmol. 1973;89:392–5.
14. Delfini R, Missori P, Iannetti G, et al. Mucoceles of the paranasal sinuses with intracranial and intraorbital extension: report of 28 cases. Neurosurgery. 1993;32:901–6.
15. Lund VJ, Rolfe ME. Ophthalmic considerations in fronto-ethmoidal mucoceles. J Laryngol Otol. 1989;103:667–9.
16. Garber PF, Abramson AL, Stallman PT, Wasserman PG. Globe Ptosis secondary to maxillary sinus mucocele. Ophthal Plast Reconstr Surg. 1995;11:254–60.
17. Benninger MS, Marks S. The endoscopic management of sphenoid and ethmoid mucoceles with orbital and intranasal extension. Rhinology. 1995;33:157–61.
18. Golub JS, Parikh SL, Budnick SD, Bernardino CR, DelGaudio JM. Inverted papilloma of the nasolacrimal system invading the orbit. Ophthal Plast Reconstr Surg. 2007;23(2):151–3.
19. Nakamaru Y, Furuta Y, Takagi D, Oridate N, Fukuda S. Preservation of the nasolacrimal duct during endoscopic medial maxillectomy for sinonasal inverted papilloma. Rhinology. 2010;48(4):452–6.
20. McNab AA, Wright GE. Orbitofrontal cholesterol granuloma. Ophthalmology. 1990;97:28–32.
21. Hill CA, Moseley IF. Imaging of orbitofrontal cholesterol granuloma. Clin Radiol. 1992;46:237–42.
22. Sia DI, Davis G, Selva D. Recurrent orbitofrontal cholesterol granuloma: a case report. Orbit. 2012;31(3):184–6.
23. Bagheri A, Naghibozakerin J, Yazdani S. Cerebrospinal fluid leakage during dacryocystorhinostomy in a patient with meningoencephalocele. Eur J Ophthalmol. 2005;15(4):500–3.
24. Strandberg B. Cephalocele of posterior part of orbit. General survey, with report of case. Arch Ophthal. 1949;42:254–65.
25. Songur E, Mutluer S, Gurler T, et al. Management of frontoethmoidal (sincipital) encephalocele. J Craniofac Surg. 1999;10:135–9.
26. Rose GE, Wright JE. Isolated peripheral nerve sheath tumours of the orbit. Eye. 1991;5:668–73.
27. Rootman J, Goldberg C, Robertson W. Primary orbital schwannomas. Br J Ophthalmol. 1982;66:194–204.
28. Dervin JE, Beaconsfield M, Wright JE, Moseley IF. CT findings in orbital tumors of nerve sheath origin. Clin Radiol. 1989;40:475–9.
29. Tam ES, Chen EC, Nijhawan N, Harvey JT, Howarth D, Oestreicher JH. Solitary fibrous tumor of the orbit: a case series. Orbit. 2008;27(6):426–31.
30. Young TK, Hardy TG. Solitary fibrous tumor of the orbit with intracranial involvement. Ophthal Plast Reconstr Surg. 2011;27(3):e74–6.
31. Gengler C, Guillou L. Solitary fibrous tumour and haemangiopericytoma: evolution of a concept. Histopathology. 2006;48:63–74.
32. Honeybul S, Neil-Dwyer G, Lang DA, Evans BT, Ellison DW. Sphenoid wing meningioma en plaque: a clinical review. Acta Neurochir (Wien). 2001;143(8):749–57.
33. Ehlers N, Malmros R. The suprasellar meningioma. A review of the literature and presentation of a series of 31 cases. Acta Ophthalmol Suppl. 1973;121:1–74.
34. Bloch O, Matthew S, Gurvinder K, Barani IJ, Parsa AT. Fractionated radiotherapy for optic nerve sheath meningiomas. J Clin Neurosci. 2012;19:1210–5.
35. Shrivastava RK, Sen C, Costantino PD, Della Rocca R. Sphenoorbital meningiomas: surgical limitations and lessons learned in their long-term management. J Neurosurg. 2005;103(3):491–7.

36. Sandalcioglu IE, Gasser T, Mohr C, Stolke D, Wiedemayer H. Spheno-orbital meningiomas: interdisciplinary surgical approach, resectability and long-term results. J Craniomaxillofac Surg. 2005;33(4):260–6.
37. Peele KA, Kennerdell JS, Maroon JC, et al. The role of postoperative irradiation in the management of sphenoid wing meningiomas. A preliminary report. Ophthalmology. 1996;103:1761–7.
38. Mamalis N, Garland PE, Argyle JC, Apple DJ. Congenital orbital teratoma: a review and report of two cases. Surv Ophthalmol. 1985;30:41–6.
39. Gnanaraj L, Skibell BC, Coret-Simon J, Halliday W, Forrest C, DeAngelis DD. Massive congenital orbital teratoma. Ophthal Plast Reconstr Surg. 2005;21(6):445–7.
40. Mahesh L, Krishnakumar S, Subramanian N, Babu K, Biswas J. Malignant teratoma of the orbit: a clinicopathological study of a case. Orbit. 2003;22(4):305–9.
41. Jacobiec FA, Howard GM, Jones IS, Tannenbaum M. Fibrous histiocytomas of the orbit. Am J Ophthalmol. 1974;77:333–45.
42. Font RL, Hidayat AA. Fibrous histiocytoma of the orbit. A clinicopathologic study of 150 cases. Hum Pathol. 1982;13:199–209.
43. Grove Jr AS. Osteoma of the orbit. Ophthalmic Surg. 1978;9:23–39.
44. McNab AA. Orbital osteoma in Gardner's syndrome. Aust N Z J Ophthalmol. 1998;26:169–70.
45. Ciappetta P, Delfini R, Iannetti G, et al. Surgical strategies in the treatment of symptomatic osteomas of the orbital walls. Neurosurgery. 1992;31:628–35.
46. Naraghi M, Kashfi A. Endonasal endoscopic resection of ethmoido-orbital osteoma compressing the optic nerve. Am J Otolaryngol. 2003;24(6):408–12.
47. Bibby K, McFadzean R. Fibrous dysplasia of the orbit. Br J Ophthalmol. 1994;78:266–70.
48. Albright F, Butler AM, Hampton AO, Smith P. Syndrome characterized by osteitis fibrosa disseminata, areas of pigmentation and endocrine dysfunction with precocious puberty in females. N Engl J Med. 1937;216:727–46.
49. Osguthorpe JD, Gudeman SK. Orbital complications of fibrous dysplasia. Otolaryngol Head Neck Surg. 1987;97:403–5.
50. Yabut SM, Kenan S, Sissons HA. Malignant transformation of fibrous dysplasia. A case report and review of the literature. Clin Orthop. 1988;228:281–9.
51. Linhares P, Pires E, Carvalho B, Vaz R. Juvenile psammomatoid ossifying fibroma of the orbit and paranasal sinuses. A case report. Acta Neurochir (Wien). 2011;153(10):1983–8.
52. Amit M, Collins MT, FitzGibbon EJ, Butman JA, Fliss DM, Gil Z. Surgery versus watchful waiting in patients with craniofacial fibrous dysplasia–a meta-analysis. PLoS One. 2011;6(9):e25179.
53. Lucarelli MJ, Bilyk JR, Shore JW, et al. Aneurysmal bone cyst of the orbit associated with fibrous dysplasia. Plast Reconstr Surg. 1995;96:440–5.
54. Patel BC, Sabir DI, Flaharty PM, Anderson RL. Aneurysmal bone cyst of the orbit and ethmoid sinus. Arch Ophthalmol. 1993;111:586–7.

Optic Nerve Tumors

9

Jonathan J. Dutton

Contents

9.1 Introduction

Primary tumors of the optic nerve include anterior visual pathway gliomas and optic nerve sheath meningiomas. Both are relatively rare lesions that result in significant visual morbidity. Together they account for less than 4 % of all orbital tumors. There has been controversy about the natural history and appropriate management of these lesions, resulting from small sample sizes and short follow-up periods. Other tumors, such as gangliogliomas and primary lymphomas, have also been described but are extremely rare (Table 9.1).

9.2 Anterior Visual Pathway Glioma

Optic pathway gliomas (OPG) are uncommon benign lesions classified as pilocytic astrocytomas. They represent 1.5–4 % of all orbital tumors and 50–55 % of all primary optic nerve tumors [1, 2].

9.2.1 Clinical Features

9.2.1.1 Age Distribution

Gliomas have been described in patients from birth to 79 years of age. However, 71 % of cases occur in children in the first decade of life and 90 % within the first two decades. The overall

J.J. Dutton
Department of Ophthalmology,
University of North Carolina, Chapel Hill, NC, USA
e-mail: jonathan_dutton@med.unc.edu

J.D. Perry, A.D. Singh (eds.), *Clinical Ophthalmic Oncology*,
DOI 10.1007/978-3-642-40492-4_9, © Springer-Verlag Berlin Heidelberg 2014

Table 9.1 Diagnostic features of optic nerve tumors

Lesion	Mean age	Sex	Location	Prognosis
Optic nerve glioma	8.8 years	F = M	ON, OC, MB	Vision = fair to good Life = 36 % mortality
Malignant optic glioma	48 years	65 % M	OC +/– ON	Vision = blindness Life = 100 % mortality
Optic sheath meningioma	41 years	60 % F	ON	Vision = poor Life = 0 % mortality

ON optic nerve, *OC* optic chiasm, *MB* midbrain

mean age at presentation is 8.8 years for all optic gliomas.

9.2.1.2 Sex Distribution

The sexual distribution for all optic pathway gliomas shows approximately equal numbers of males and females. For gliomas confined to the optic nerve, 65 % occur in females, compared to 35 % for males. For tumors involving the optic chiasm, there is no sex predilection.

9.2.1.3 Location

About 20–25 % of optic gliomas are confined to the optic nerve alone, but in three-quarters of cases the chiasm is involved [3, 4]. Of the tumors that involve the chiasm, 40 % eventually extend into the adjacent hypothalamus or third ventricle. Several studies have shown that the orbital optic nerve is involved more frequently in patients with NF1 (21.5 %) than in those without NF1 (5.5 %) [5].

9.2.1.4 Association with Neurofibromatosis Type 1

Optic pathway gliomas may be sporadical or syndromic, the latter mostly associated with neurofibromatosis type 1. The reported incidence of neurofibromatosis type 1 (NF1) among patients with optic gliomas varies from 10 to 70 %, with an overall incidence of 29 % [1]. Although some reports have shown no difference in the course and prognosis of optic pathway gliomas with and without NF1, others have suggested a more indolent course and a better prognosis in patients with OPG and NF1 [6–8].

When associated with NF1 the glioma may present at a somewhat later age and show progression for a long time, justifying regular ophthalmological monitoring of this population over a long period [9, 10].

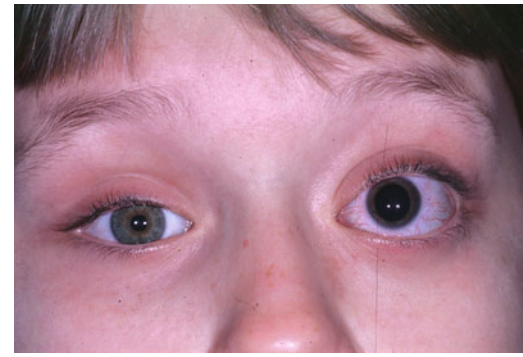

Fig. 9.1 External photograph of a child with a left orbital optic nerve glioma showing axial proptosis

9.2.1.5 Signs and Symptoms

The specific findings of optic pathway gliomas depend principally on the location of the tumor. Regardless of location, 85 % of patients lose some vision, with about 25 % retaining good vision between 20/20 and 20/40. About 60 % of patients show vision of 20/300 or worse.

Proptosis is a presenting sign in 95 % of patients with an optic nerve glioma (Fig. 9.1). With gliomas of the optic chiasm, proptosis is much less common, seen in fewer than 20 % of patients, and all with concomitant intraorbital involvement. Limitation of ocular motility is seen infrequently with optic gliomas. It is reported in 30 % of intraorbital lesions and 20 % of gliomas involving the chiasm. Pain and headache are present in up to 30 % of patients with chiasmal tumors. Other rare symptoms seen with CNS invasion include nystagmus, spasmus nutans, seizures, hypothalamic signs, and hydrocephalus. On funduscopic examination 60 % of patients demonstrate some degree of optic atrophy. Disc edema, primarily associated with intraorbital gliomas, is seen in half of such cases. Disc edema occurs in

Box 9.1: Optic Pathway Glioma

- Early visual loss 88 %
- Optic disc swelling 35 %
- Optic disc atrophy 59 %
- Proptosis, orbital tumors 94 %; chiasmal tumors 22 %
- Nystagmus 24 %
- Hypothalamic signs 26 %
- Increased intracranial pressure 27 %

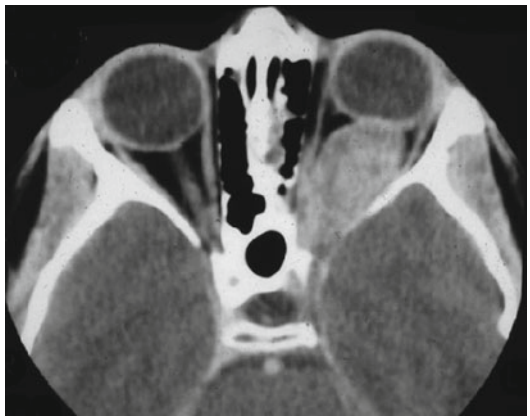

Fig. 9.2 Axial CT scan shows a fusiform glioma of the left optic nerve

only 20 % of patients with chiasmal tumors, and in these cases the tumor is usually contiguous with the intraorbital optic nerve (Box 9.1).

9.2.2 Diagnostic Evaluation

Imaging studies reveal enlargement of the optic canal in up to 80 % of patients with a glioma involving the optic nerves. Enlargement and J-shaped excavation of the sella turcica may be associated with chiasmal gliomas but are reported in only 25 % of patients.

9.2.2.1 Computed Tomography

Computed tomography (CT) imaging typically demonstrates enlargement of the optic nerve and/or chiasm. Contrast enhancement ranges from imperceptible to moderate but generally is less than with sheath meningiomas. Typical optic gliomas show a well-outlined fusiform swelling of the optic nerve (Fig. 9.2), but occasionally they may be more rounded or even tubular. Calcification occurs only occasionally.

9.2.2.2 Magnetic Resonance Imaging

Magnetic resonance imaging (MRI) has proved superior to CT for evaluation of chiasmal, hypothalamic, and optic tract lesions. Gliomas demonstrate normal to slightly prolonged T1 relaxation times, which image isointense to slightly hypointense compared to normal optic nerve. The T2 relaxation time is prolonged, giving a hyperintense image on T2-weighted sequences.

9.2.3 Histopathology

Although optic gliomas were formerly considered congenital nonneoplastic hamartomas with self-limiting growth, their histologic features, rates of growth, rare malignant potential, and a clear tendency to invade the leptomeninges show that these tumors are true neoplasms that have the ability to invade locally.

Optic gliomas arise from supporting astrocytes of the optic nerve and along the visual pathway. Most are classified as benign pilocytic astrocytomas in which proliferating neoplastic astrocytic cells predominate. Proliferating astrocytes may extend through the pia mater into the arachnoid and subarachnoid space, where they provoke an exuberant reactive proliferation of fibrovascular tissue and meningothelial cells. This so-called arachnoidal hyperplasia may extend beyond the limits of the tumor itself, simulating tumor extension. Enlargement of optic gliomas may occur as a result of proliferation of neoplastic cells, reactive arachnoidal proliferation, or an accumulation of extracellular, PAS-positive mucosubstance secreted by the astrocytes.

9.2.4 Treatment Options

Anterior visual pathway gliomas are neoplasms with the potential to spread into contiguous areas of the optic nerve, chiasm, and adjacent brain.

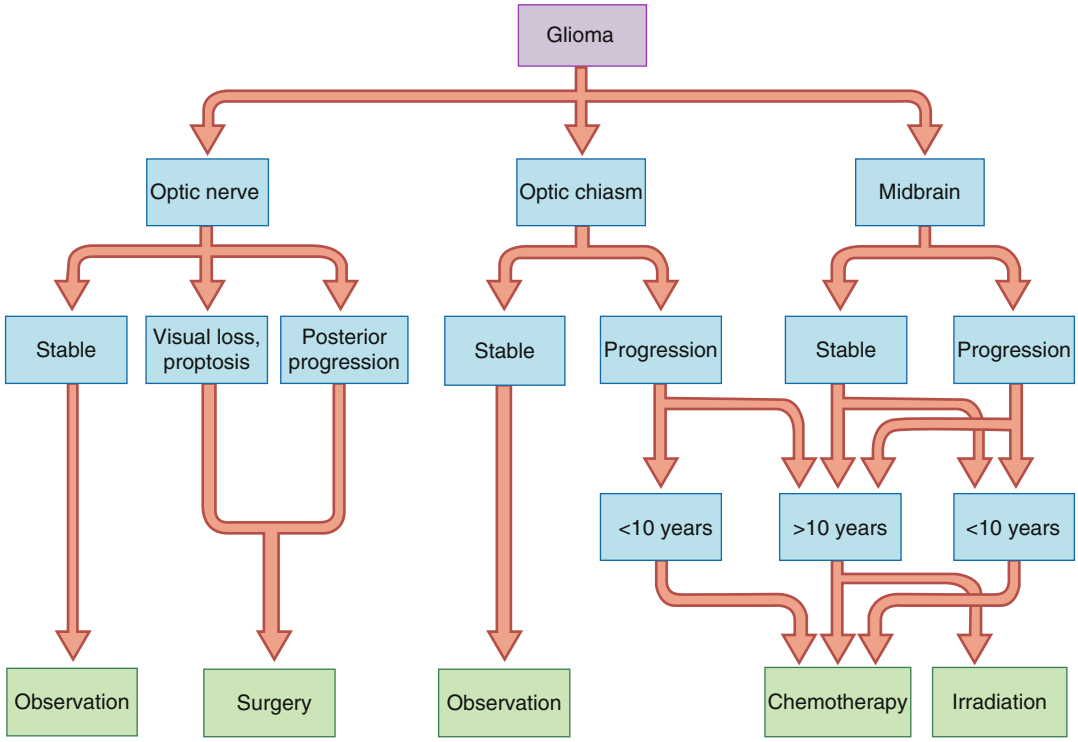

Fig. 9.3 Proposed management algorithm for treatment of anterior visual pathway glioma

They appear at an early age, grow slowly for a few years, and vision generally stabilizes in most cases. However, indolent growth can be seen in up to 40 % of cases. Although the best treatment options are still evolving, an algorithm for the management of patients with optic pathway gliomas is suggested (Fig. 9.3). As with most medical decisions, treatment must be individualized based on patient symptoms, findings, and clinical course [11].

9.2.4.1 Observation

Long-term survival shows a good prognosis even in patients followed conservatively without intervention [12–15]. After an initial period of deterioration, vision tends to stabilize in nearly 80 % of cases. There is little difference in visual outcome or survival in patients undergoing treatment versus observation alone [1]. However, significant progression of tumor can occur in some patients despite clinically stable visual acuity for many years.

9.2.4.2 Surgery

Until recently, surgery was considered the treatment of choice for optic nerve gliomas. Today most authorities limit the indications for surgery to resectable tumors involving the orbital or intracranial optic nerves or for direct inspection or biopsy of the chiasm. Once vision is lost, surgery can be beneficial for severe proptosis or orbital pain. Where vision is present, surgical intervention carries a very significant risk of visual morbidity and mortality.

9.2.4.3 Radiotherapy

The role of radiotherapy has been a subject of debate for decades. Some studies have failed to show any benefit of radiotherapy on long-term survival, visual acuity, or both [1]. However, other studies showed improvement or stability in visual acuity after treatment and better progression-free survival interval [16, 17]. Overall, the data suggest a possible benefit. Any potential benefit must also be tempered by the

adverse effects of radiotherapy on the central nervous system in younger children. Several cases of malignant transformation have been reported following radiotherapy.

9.2.4.4 Chemotherapy

Several reports have suggested a role for chemotherapy in the management of optic pathway gliomas. Most studies show stabilization of vision and/or tumor regression in 50–65 % of treated patients [18–21]. Although this is not much better than for tumors observed conservatively, chemotherapy may be useful for young children with progressive lesions in order to delay the potential complications of radiotherapy.

9.2.5 Prognosis

A review of the literature shows that for all patients with optic pathway gliomas in all locations and with all forms of treatment, including observation, tumor recurrence or progression occurs in 38 % of cases [1]. The overall tumor-related mortality is 36 % with a mean follow-up of 11 years. However, with longer follow-up intervals of 25–30 years, the prognosis for survival may be considerably worse. The outlook for vision is actually rather good. About 55 % of patients retain stable vision or show some improvement. Only 45 % show progressive loss of vision. One case has been reported of spontaneous malignant transformation [22]. Spontaneous regression has been reported [23].

9.2.5.1 Glioma Confined to the Optic Nerve

For gliomas initially confined to the optic nerve and treated conservatively or incompletely excised, recurrence or progression is seen in 17 %. The mortality rate is 12 %, typically from intracranial extension. The prognosis for vision, however, is good, with over 90 % remaining stable over many years. With optic nerve tumors treated by complete surgical excision or partial excision plus radiotherapy, the mortality rate drops to zero. The same is true for tumors that progress but remain confined to the optic nerve. Obviously, the prognosis for vision in such cases is poor after surgery.

9.2.5.2 Gliomas with Extension to the Chiasm

Gliomas that extend to the chiasm but that do not invade the adjacent hypothalamus or third ventricle show results similar to those for untreated optic nerve tumors. Chiasmal gliomas left untreated or that are partially excised show a mortality rate of 17 % over a mean follow-up period of 10 years. As with optic nerve tumors, death results from extension into the hypothalamus or third ventricle. Recurrence or progression of tumor after partial excision is seen in 64 % of cases. Visual prognosis in this group is good, with 80 % remaining stable. In patients with chiasmal tumors radiotherapy may delay progression to some extent. Mortality in this group is 22 %, and recurrence or progression of tumor is seen in 43 % of cases. Prognosis for vision is similar to that of untreated patients, with 68 % remaining stable or demonstrating a slight improvement.

9.2.5.3 Gliomas with Extension to the Chiasm and Hypothalamus

In patients with chiasmal tumors plus hypothalamic or third ventricle involvement at the time of presentation, the prognosis for life is markedly reduced. The mortality rate is 50 % or more over 15 years. For patients who received radiotherapy, recurrence or progression is noted in 52 %, but the mortality rate is somewhat better, at 43 %.

9.3 Malignant Optic Nerve Glioma

In 1973 Hoyt et al. [24] described five cases of optic pathway glioma in adults which had an aggressive behavior and a uniformly fatal outcome. To date less than 50 additional cases have been reported in the literature, all confirming the original concept of the disease.

9.3.1 Clinical Features

9.3.1.1 Age Distribution

Malignant optic pathway gliomas have been seen in patients from 6 to 79 years old but occur most commonly in middle age. The mean age at presentation is 48 years.

9.3.1.2 Sex Distribution

This disease has a distinct sexual predilection, with 65 % occurring in males and 35 % in females.

9.3.1.3 Location

In all described cases, the optic chiasm is the major site of origin. In all cases except one [25]. the disease is bilateral with both optic nerves also involved. In only 23 % of cases does the tumor extend to the intraorbital portion of the nerve. In nearly half of patients, the tumor extends posterior to the optic tracts, hypothalamus, or temporal lobe [1].

9.3.1.4 Signs and Symptoms

All patients present with rapidly progressive loss of vision, first in one and then in the second eye. In 63 % of cases, both eyes may be affected at presentation. Initially the condition may be misdiagnosed as optic neuritis. Bilateral blindness typically results within a matter of months. Optic disc edema is seen in most patients, and, if they survive long enough, optic atrophy results. Orbital signs are uncommon, as most tumors are confined to the intracranial compartment. Proptosis and ophthalmoplegia are seen in only 20–25 % of cases (Box 9.2).

Box 9.2: Malignant Optic Glioma

- Very rapid loss of vision to blindness over weeks to months
- Optic disc swelling 43 %
- Optic disc atrophy 31 %
- Proptosis 23 %
- Ophthalmoplegia 19 %
- Other neurologic signs 35 %

9.3.2 Diagnostic Evaluation

Enlargement and enhancement of the optic chiasm on CT or MRI is the most common finding, seen in 80 % of cases. One or both optic nerves may also be involved along their intracranial portions. The final diagnosis is usually made only after tissue biopsy.

9.3.3 Histopathology

Histopathology shows malignant astrocytes with pleomorphic nuclei and areas of vascular proliferation and necrosis. Subpial extension along the optic pathways is seen. There is invasion into the optic chiasm and nerve and into adjacent areas of the brain.

9.3.4 Treatment

To date no treatment has proved effective in slowing the progression of this disease. Neither surgery nor radiotherapy up to 60 Gy has significantly altered the prognosis [26].

9.3.5 Prognosis

Prognosis for vision is dismal, with all patients progressing to profound visual loss within months of initial presentation. The prognosis for life is equally dismal, with a nearly 100 % mortality rate. The mean survival rate is typically less than 1 year.

9.4 Optic Nerve Sheath Meningioma

Meningiomas are the second most common brain neoplasms after gliomas. They represent 15–20 % of all intracranial tumors in adults and 2 % of intracranial tumors in children [27]. Although most orbital meningiomas are extensions from intracranial sites, primary orbital meningiomas have been documented and account for 1.3 % of all meningiomas.

9.4.1 Clinical Features

9.4.1.1 Age Distribution

Despite several reports of orbital meningiomas occurring with high frequency in young individuals, most series confirm that this is a disease primarily of middle age. On imaging studies, meningiomas may be confused with arachnoid proliferation associated with optic gliomas in young patients. The mean age for presentation of optic sheath meningioma is 41 years, and only 4 % of patients are under 20 [27, 28].

9.4.1.2 Sex Distribution

It has long been recognized that meningiomas occur more frequently in females. When large series are examined the ratio has tended to equalize, but there does appear to be a slight female preponderance of approximately 60 %.

9.4.1.3 Laterality

A slight predilection for the right optic nerve has been reported in several studies. Others have not confirmed these findings. However, when larger series are examined 52 % of sheath meningiomas occurred in the right optic nerve, 42 % in the left, and 6 % were bilateral [27]. Interestingly, among bilateral cases 60 % are canalicular meningiomas, compared to all sheath meningiomas together, where canalicular tumors account for only 8 %.

9.4.1.4 Sites of Origin

For optic sheath meningiomas 94 % are unilateral and 6 % bilateral. In about 8 % of cases the meningioma is confined to the optic canal. Among these canalicular tumors there is a significant propensity toward bilaterality, 65 % being unilateral and 35 % bilateral. About 4 % of optic sheath meningiomas show focal tumor invasion of the optic disc, sclera, choroid, and retina. Tumor may enter the globe along penetrating vascular channels. Dutton [27] noted that 18 of 475 cases of primary orbital meningioma arose ectopic to the optic nerve sheath. The exact etiology of such lesions remains uncertain, and it is possible that in some cases they represent other lesions mistaken for meningiomas.

9.4.1.5 Association with Neurofibromatosis Type 1

The incidence of NF1 in patients with sheath meningiomas is unclear because most studies in the past failed to mention the occurrence. Of the studies that specifically examined for NF, 9 % of patients were affected. This is considerably lower than the 29 % association with optic gliomas but still significantly higher than the 0.3–0.5 % incidence of NF in the general population.

9.4.1.6 Signs and Symptoms

The most frequent presenting symptom of optic sheath meningioma is loss of vision, seen in 97 % of cases. In about 45 % visual acuity is 20/20–20/40, and in only 25 % is it counting fingers or worse. Visual loss usually takes place over several years. In bilateral cases, visual loss in the two eyes may be separated in time by 2–30 years. Visual field defects are noted in 83 % of patients. Most commonly these include peripheral constriction; central, centrocecal, and paracentral scotomas; altitudinal defects; and increased size of the blind spot. Proptosis is found on initial examination in 65 % of patients (Fig. 9.4, Box 9.3). It is seen less frequently in patients with canalicular lesions, as they typically have significant visual loss while the tumor is still very small. Limitation of ocular motility is variable but may be seen in more than half of patients. Upgaze is commonly severely impaired, possibly because of stiffening of the optic nerve from the relatively firm tumor.

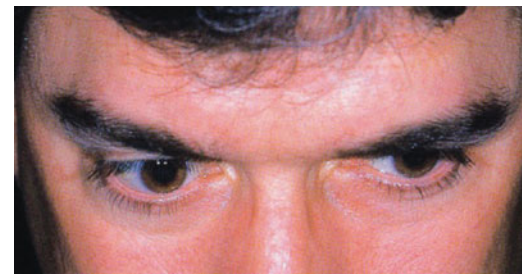

Fig. 9.4 External photograph of a patient with a right orbital optic nerve sheath meningioma demonstrating proptosis

Box 9.3: Optic Nerve Sheath Meningioma
- Slowly progressive visual loss 96 %
- Optic disc swelling 48 %
- Optic disc atrophy 66 %
- Proptosis 65 %
- Decreased ocular motility 47 %
- Optociliary shunt vessels 30 %
- Increased intracranial pressure 27 %

Chronic disc edema is an early finding in 48 % of patients. Optic atrophy, which may be subtle, is a somewhat later finding, noted in two-thirds of cases at presentation. Both edema and atrophy may be seen together, and overall 98 % of patients will show one or the other of these two findings. The association between optic sheath meningiomas and optociliary shunt vessels has long been considered a key finding suggestive of optic sheath meningiomas. However, chronic disc edema and congestion of the central retinal vein usually precede the first appearance of shunts by several years, and the shunts usually disappear as optic atrophy becomes complete. In fact, optociliary shunt vessels are relatively infrequent with sheath meningiomas, being seen in only 30 % of reported cases. Because shunts tend to appear some years after symptoms begin and involute as optic atrophy is complete, this probably does not indicate their true incidence.

9.4.2 Diagnostic Evaluation

9.4.2.1 Computed Tomography

Plain orbital radiographs and tomography through the optic canals demonstrate enlargement of the optic foramen in less than 30 % of cases. CT scanning demonstrates enlargement of the optic nerve in 97 % of examinations. The most common pattern is diffuse tubular enlargement, but a globular or fusiform shape may be seen also. Tram-tracking, a radiographic sign in which the denser and thickened optic nerve sheath outlines a central lucency representing the residual optic nerve, is a characteristic of sheath meningioma (Fig. 9.5). Contrast studies generally show moderate to marked enhancement. Calcification, an important finding, may help differentiate meningiomas from optic gliomas. It is seen in 20–50 % of patients.

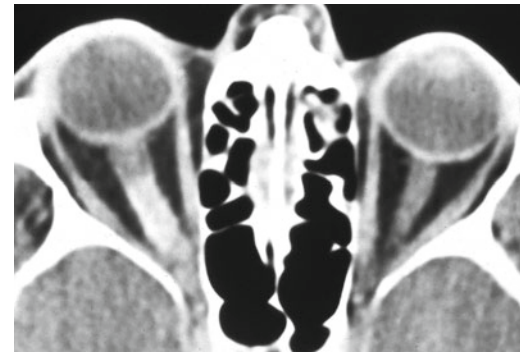

Fig. 9.5 Axial CT scan shows a tubular optic nerve sheath meningioma with tram-tracking. The involved sheath enhances brightly, with the uninvolved optic nerve centrally

9.4.2.2 Magnetic Resonance Imaging

Magnetic resonance imaging shows a thickening of the nerve and sheath contrasted against orbital fat, and there is increased signal intensity compared to normal nerve on both the T1- and T2-weighted sequences.

9.4.3 Histopathology

Optic meningiomas arise from meningothelial cap cells of the arachnoid villi that lie along the intraorbital optic nerve. Two histologic patterns are seen. In the meningothelial or syncytial pattern, polygonal cells are arranged in sheets separated by vascular trabeculae. In the transitional pattern, spindle-shaped or oval cells are arranged in a concentric whorl formation. Psammoma bodies are seen more commonly in the transitional pattern and contain the calcifications noted on radiologic studies. Meningioma typically remains indolent over many years. As the tumor grows within the subarachnoid space, it commonly encircles the optic nerve. Compression results in obstruction to axoplasmic flow, disc edema, dilatation of optociliary shunt channels, and eventually demyelinization and optic atrophy. Tumor cells may also invade through the dura and into surrounding orbital tissues. Although they do invade along the intracranial optic nerve to the chiasm, meningiomas do not invade the brain.

9.4.4 Treatment

The most appropriate therapy for optic sheath meningiomas has been a matter of some controversy. For sheath meningiomas that extend to the intracanalicular or intracranial portions of the optic nerve, the decision regarding treatment becomes less complex. The major rationale for treatment is the perceived risk of spread to the contralateral optic nerve. The actual risk of tumor spread from one optic nerve to the other remains unknown, but based on the high incidence of bilaterality with canalicular tumors and on documented unilateral tumors with progressive posterior extension, it may be very real. Because vision in such cases will eventually be lost, treatment to prevent possible extension to the contralateral side is justified. In most cases radiotherapy may slow or halt tumor progression. However, in cases of treatment failure, surgical excision should be considered. Newer treatment options have gained considerable support over the past decade, and these are changing the approach to management. A proposed treatment algorithm is shown in Fig. 9.6.

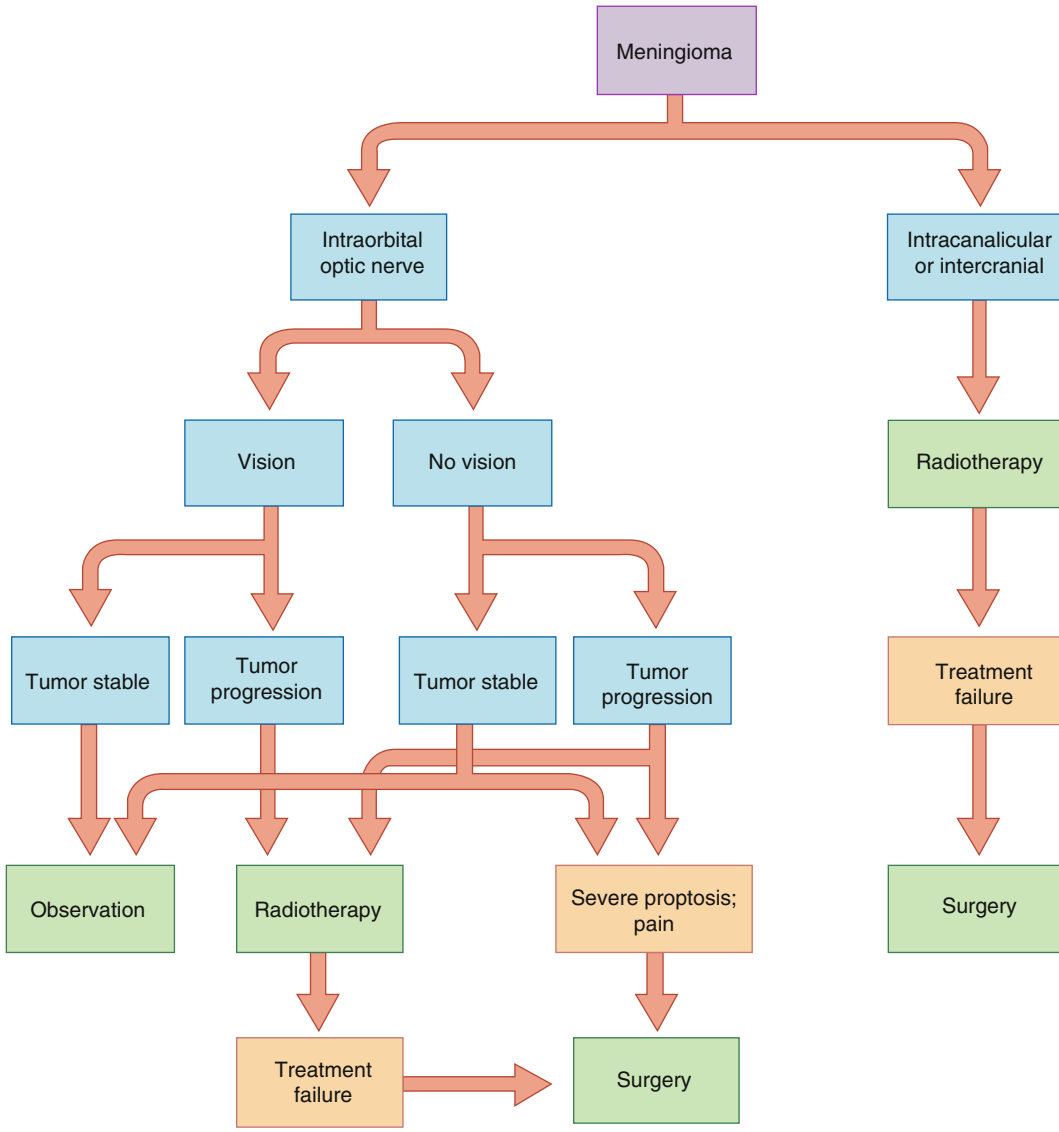

Fig. 9.6 Proposed management algorithm for treatment of optic nerve uninvolved optic nerve centrally, sheath meningioma

9.4.4.1 Observation

For meningiomas confined to the intraorbital optic nerve, when vision remains and symptoms and radiographic findings are stable, observation without treatment is appropriate [28]. The only possible exceptions that justify surgery are small anterior tumors and cases in young children, where biopsy for diagnosis may be indicated. Progressive visual loss is expected in most cases, but some patients may remain stable for many years. The prognosis for life is excellent, and there have been no tumor-related deaths reported for this disease.

9.4.4.2 Surgery

Some have considered surgical excision necessary to prevent intracranial extension. This may be possible for some small anterior orbital lesions [29] or even with some posterior tumors [30], but in general the morbidity is high and loss of vision is a very common sequela due to disruption of vascular supply to the optic nerve. Once blindness results, surgical extirpation may be necessary for relief of disfiguring proptosis, orbital pain, or intraocular complications. Incomplete excision has been associated with diffuse orbital invasion and intracranial spread to the chiasm. The risk of such spread outweighs the potential benefit of attempted resection. Attempts to decompress the optic nerve by opening the dural sheath have proved disappointing and have resulted in massive orbital invasion requiring exenteration following surgical decompression. For lesions in the optic canal, canal decompression with dural sheath release may preserve sight in some cases [31].

9.4.4.3 Radiotherapy

For lesions that show progression by worsening symptoms or radiographic findings, radiotherapy would be an appropriate option. In the past radiotherapy was considered ineffective; however, more recent reports using newer techniques suggest that in appropriate doses radiotherapy can be effective [32]. Fractionated stereotactic radiotherapy may offer a promising refinement with fewer complications [33]. The optimum total dose appears to be in the range of 50–55 Gy. Stability or improvement of vision has been reported in 50–95 % of cases. Similar results are being reported with the use of three-dimensional conformal fractionated radiation [34]. Complications of radiotherapy are reported in up to 15 % of cases and include new visual field defects, central retinal artery occlusion, and encephalopathy. More recently, staged fractionated robotic CyberKnife radiosurgery with 20 Gy has given local control with visual improvement in 80 % of patients [35].

9.4.5 Prognosis

Patients with optic sheath meningiomas have an excellent prognosis for life. There are few, if any, documented cases of tumor-related death. The prognosis for vision, however, is poor. Without treatment, in most patients visual loss progresses slowly but inexorably to blindness in the affected eye. However, in some cases a spontaneous improvement in vision or visual field has been reported. Surgery offers little additional benefit and in most cases accelerates the process of visual loss. Rarely, a small anteriorly situated tumor may be excised with preservation or improvement of vision. Radiotherapy may stabilize or improve visual symptoms in some cases.

References

1. Dutton JJ. Gliomas of the anterior visual pathway. Surv Ophthalmol. 1994;38:427–52.
2. Shields JA, Shields CL, Scartozzi R. Survey of 1264 patients with orbital tumors and simulating lesions: the 2002 Montgomery Lecture, part I. Ophthalmology. 2004;111:997–1008.
3. Binning MJ, Liu JK, Kestle JR, et al. Optic pathway gliomas: a review. Neurosurg Focus. 2007;23:E2.
4. Astrup J. Natural history and clinical management of optic pathway gliomas. Br J Neurosurg. 2003;17:327–35.
5. Czyzyk E, Jozwiak S, Roszkowski M, Schwartz RA. Optic pathway gliomas in children with and without neurofibromatosis 1. J Child Neurol. 2003;18:471–8.
6. Grill J, Laithier V, Raquin MA, et al. When do children with optic pathway tumors need treatment? An oncological perspective in 106 patients treated in a single center. Eur J Pediatr. 2000;159:692–6.

7. Singhal D, Birch JM, Kerr B, et al. Neurofibromatosis type 1 and sporadic gliomas. Arch Dis Child. 2002;87:65–70.
8. Shamji MF, Benoit BG. Syndromic and sporadic pediatric optic pathway gliomas: review of clinical and histopathological differences and treatment implications. Neurosurg Focus. 2007;23:E3.
9. Thiagalingam S, Flaharty M, Billson F, North K. Neurofibromatosis type 1 and optic pathway gliomas: follow-up of 54 patients. Ophthalmology. 2004; 111:568–77.
10. Segal L, Darvish-Zargar M, Dilenge ME, et al. Optic pathway gliomas in patients with neurofibromatosis type 1: follow-up of 44 patients. J AAPOS. 2010;14: 155–8.
11. Lee AG, Dutton JJ. A practice pathway for the management of gliomas of the anterior visual pathway: an update ad an evidenced-based approach. Neuro-ophthalmology. 1999;22:139–55.
12. Glaser JS, Hoyt WF, Corbett J. Visual morbidity with chiasmal glioma. Long-term studies of visual fields in untreated and irradiated cases. Arch Ophthalmol. 1971;85:3–12.
13. Hoyt WF, Bagdassarian SA. Optic gliomas of childhood: natural history and rationale for conservative management. Br J Ophthalmol. 1969;53:793–8.
14. Tow SL, Chandela S, Miller NR, Avellino AM. Long-term outcome in children with gliomas of the anterior visual pathway. Pediatr Neurol. 2003;28:262–70.
15. Mikaeloff Y, Chaix Y, Grill J, et al. Optic pathway gliomas in neurofibromatosis type 1. Longitudinal study of 30 cases in two multidisciplinary practices. Arch Pediatr. 2002;9:797–804.
16. Khafaga Y, Hassounah M, Kandil A, et al. Optic gliomas: a retrospective analysis of 50 cases. Int J Radiat Oncol Biol Phys. 2003;56:807–12.
17. Combs SE, Schulz-Ertner D, Moschos D, et al. Fractionated stereotactic radiotherapy of optic pathway gliomas: tolerance and long-term outcome. Int J Radiat Oncol Biol Phys. 2005;62:814–9.
18. Aquno VM, Fort DW, Kamen BA. Carboplatin for the treatment of children with newly diagnosed optic chiasm gliomas: a phase II study. J Neurooncol. 1999;41: 255–9.
19. Silva MM, Goldman S, Keating G, et al. Optic pathway hypothalamic gliomas in children under three years of age: the role of chemotherapy. Pediatr Neurosurg. 2000;33:151–8.
20. Hsu TR, Wong TT, Chang FC, et al. Responsiveness of progressive optic pathway tumors to cisplatin-based chemotherapy in children. Childs Nerv Syst. 2008;24:1457–61.
21. Kelly JP, Leary S, Khanna P, Weiss AH. Longitudinal measures of visual function, tumor volume, and prediction of visual outcomes after treatment of optic pathway gliomas. Ophthalmology. 2012;119:1231–7.
22. Zoeller GK, Brathwaite CD, Sandberg DI. Malignant transformation of an optic pathway glioma without prior radiation therapy. J Neurosurg Pediatr. 2010;5:507–10.
23. Parsa CF, Hoyt CS, Lesser RL, et al. Spontaneous regression of optic gliomas: thirteen cases documented by serial neuroimaging. Arch Ophthalmol. 2001;119:516–29.
24. Hoyt WF, Meshel LG, Lessell S, et al. Malignant optic glioma of adulthood. Brain. 1973;96:121–32.
25. Wabbels B, Demmier A, Seitz J, et al. Unilateral adult malignant optic nerve glioma. Graefes Arch Clin Exp Ophthalmol. 2004;242:741–8.
26. Dario A, Iadini A, Cerati M, Marra A. Malignant optic glioma of adulthood. Case report and review of the literature. Acta Neurol Scand. 1999;100:350–3.
27. Dutton JJ. Optic nerve sheath meningiomas. Surv Ophthalmol. 1992;37:167–83.
28. Miller NR. New concepts in the diagnosis and management of optic nerve sheath meningioma. J Neuroophthalmol. 2006;26(3):200–8.
29. Yuceer N, Erdogan A, Ziya H. Primary optic nerve sheath meningiomas. Report of seven cases (clinical neuroradiological, pathological and surgical considerations in seven cases). J Neurosurg Sci. 1994;38:155–9.
30. Cristante L. Surgical treatment of meningiomas of the orbit and optic canal: a retrospective study with particular attention to the visual outcome. Acta Neurol (Wien). 1994;126:27–32.
31. Norris JH, Norris JS, Akinwunmi J, Malhotra R. Optic canal decompression with dural sheath release: a combined orbito-cranial approach to preserving sigh from tumours invading the optic canal. Orbit. 2010;31:34–43.
32. Pacelli R, Cella L, Conson M, et al. Fractionated stereotactic radiation therapy for orbital optic nerve sheath meningioma – a single institution experience and a short review of the literature. J Radiat Res. 2011;52:82–7.
33. Abouaf L, Girard N, Lefort T, et al. Standard-fractionated radiotherapy for optic nerve sheath meningioma: visual outcome is predicted by mean eye dose. Int J Radiat Oncol Biol Phys. 2012;82: 1268–77.
34. Narayan S, Cornblath WT, Sandler HM. Preliminary visual outcomes after three-dimensional conformal radiation therapy for optic nerve sheath meningioma. Int J Radiat Oncol Biol Phys. 2003;56:537–43.
35. Romanelli P, Bianchi L, Muacevic A, Beltramo G. Staged image guided robotic radiosurgery for optic nerve sheath meningiomas. Comput Aided Surg. 2011;16:257–66.

Lacrimal Gland Tumors

10

David H. Verity, Omar M. Durrani,
and Geoffrey E. Rose

Contents

D.H. Verity
G.E. Rose, DSc, MS, FRCS, FRCOphth (✉)
Oculoplastic and Orbital Service,
Moorfields Eye Hospital, City Road,
London EC1V 2PD, UK
e-mail: geoff.rose@moorfields.nhs.uk

O.M. Durrani
Oculoplastic and Orbital Service,
Birmingham and Midland Eye Centre,
City Hospital NHS Trust, Dudley Road,
Birmingham, West Midlands,
B18 7QH, UK

10.1 Introduction

While 9–15 % of orbital tumors arise in lacrimal gland, inflammatory or infiltrative diseases – such as sarcoidosis, Wegener's granulomatosis, IgG4 disease, or other (nonspecific) dacryoadenitis – comprise two-thirds of lacrimal gland masses and can present with signs and symptoms similar to tumors [1, 2]. Often a firm diagnosis can be reached only with tissue biopsy.

Inflammatory lesions typically present with acute or subacute symptoms that can include a painful, tender swelling in the lacrimal gland area, an "S-shaped" deformity of the upper eyelid, or conjunctival redness and injection (Fig. 10.1). Lymphomas tend to produce chronic, painless globe displacement, although some present with inflammatory features, which portend a worse prognosis [3].

Benign or malignant tumors can present similarly, and both enter the differential diagnosis for many lacrimal masses. Most primary tumors of the lacrimal gland, of which half are benign, are epithelial in origin; however, other very rare

J.D. Perry, A.D. Singh (eds.), *Clinical Ophthalmic Oncology*,
DOI 10.1007/978-3-642-40492-4_10,

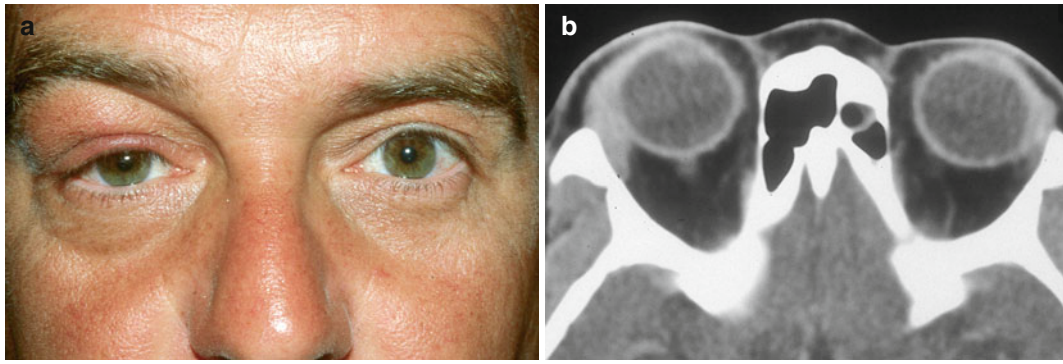

Fig. 10.1 S-shaped deformity of the right upper lid caused by subacute dacryoadenitis (**a**). CT showing right lacrimal gland enlargement with molding around the globe (**b**)

benign tumors – such as hemangiopericytoma, neurilemmoma, neurofibroma, lymphangioma, and other vascular malformations – can be centered on the gland. In addition to a thorough history and examination, high-resolution imaging plays a key role in establishing an appropriate treatment plan.

10.2 Epidemiology

Almost all benign lacrimal gland tumors are pleomorphic adenomas (Table 10.1) [4], and adenoid cystic carcinoma is the commonest malignant epithelial tumor [5]. Carcinoma arising in prior pleomorphic adenoma ("malignant mixed tumor") represents the second most common lacrimal gland malignancy [1, 5, 6], whereas mucoepidermoid carcinomas, primary adenocarcinomas, and squamous carcinomas are rare. Lymphoma, associated with systemic disease in a minority, accounts for about 10–14 % of all lacrimal gland masses [1, 2], while metastases to the lacrimal gland are very uncommon; the latter tend to mimic the primary lesion, most such masses being fast growing and associated with a poor prognosis.

10.3 Clinical Features

Pleomorphic adenomas present from childhood [7] to old age, with a peak incidence in middle age and without a significant gender bias [4].

Table 10.1 Common primary lacrimal gland tumors

Types	Nomenclature
Benign tumors	Pleomorphic adenoma
	Myoepithelioma[a]
Malignant tumors	Adenoid cystic carcinoma
	Malignant mixed tumor (carcinoma arising within pleomorphic adenoma)
	Mucoepidermoid carcinoma
	Adenocarcinoma

[a]Rare

Likewise, malignant epithelial tumors present at a similar age to pleomorphic adenomas have a peak incidence in the fourth decade and do not have a gender bias [5].

10.3.1 Symptoms

Patients with lacrimal gland tumors typically present with upper eyelid swelling or mass, but other features depend on the size, site, and nature of the lesion. Tumors in the palpebral lobe are rarer than orbital lobe tumors and, because of the anterior location, tend to present earlier with a palpable upper eyelid mass or an alteration in lid contour [8]. Patients with pleomorphic adenomas generally have a slowly progressive, uninflamed mass that has been present for over a year or have a facial asymmetry noted by others (Fig. 10.2). Larger tumors may also cause limitation of eye movements with diplopia or visual disturbances due to distortion of the globe by the firm tumor mass, with or without choroidal folds [4, 5].

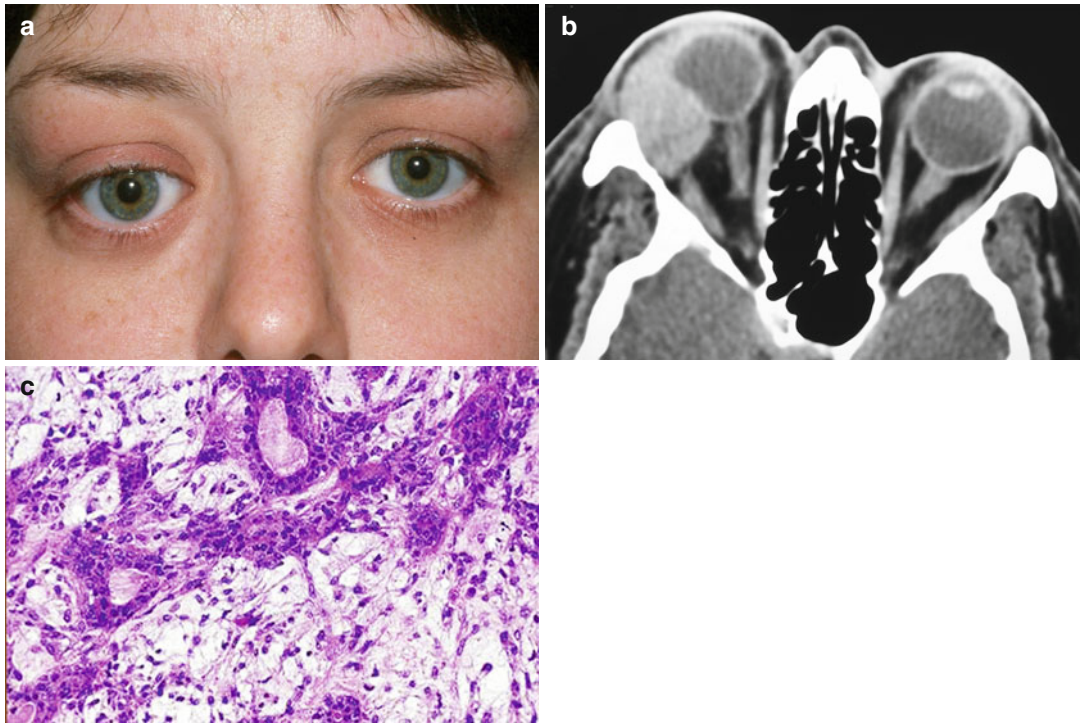

Fig. 10.2 Facial asymmetry due to pleomorphic adenoma of the right lacrimal gland (**a**). CT showing marked enlargement of the right lacrimal gland with indentation of the globe (**b**). Epithelial cells centrally with eosinophilic cytoplasm and myoepithelial cells surrounding ducts showing clear lumen (**c**, hematoxylin and eosin)

Pain occurs rarely with pleomorphic adenoma or lacrimal lymphoma, but primary malignant tumors of the lacrimal gland are characterized by a short history and persistent pain. Lacrimal gland carcinoma tends to spread posteriorly along the lateral orbital wall, displacing the lateral rectus inferomedially, with microscopic invasion of the orbital fat and a propensity for perineural spread. Later in the disease it tends to breach orbital periosteum, with spread to the bone and temporalis fossa, or extend through the superior orbital fissure into the middle cranial fossa.

10.3.2 Signs

Anterior enlargement of the gland occurs primarily with adenomas of the palpebral lobe: such adenomas are palpable in the lateral aspect of the upper lid and tend to be very hard in consistency – like a "chickpea." Occasionally palpebral lobe enlargement presents as a prominent gland in the upper fornix [8]. In contrast, orbital lobe tumors are often difficult to palpate – being set deep in the lacrimal fossa posterior to the orbital rim – and are characterized by progressive hypoglobus and relatively little proptosis, often passing unnoticed by the patient or relatives for years [4].

Malignant infiltration of cranial nerves at the superior orbital fissure or in the cavernous sinus causes episcleral congestion, ptosis, diplopia, and periorbital sensory disturbance; indeed, in the presence of a lacrimal gland mass, persistent pain and sensory disturbance are strong predictors of malignancy. The rate of growth, although faster than for benign tumors, varies amongst different malignancies: adenocarcinomas progress rapidly, well-differentiated mucoepidermoid carcinomas have a relatively slow course, and the relentless growth of adenoid cystic carcinoma varies from extremely slow to slowly progressive [5]. Lacrimal gland metastases tend to follow the

course of the parent tumors, while the generally indolent lymphomas may be primary orbital disease or part of a systemic condition [3].

10.4 Diagnostic Evaluation

Multi-slice or helical computed X-ray tomography (CT), the prime technique for providing high-resolution orbital images free of motion artifact, is invaluable in the differentiation of lacrimal gland masses. Bone changes are poorly shown on magnetic resonance imaging, and this modality is less useful than CT with lacrimal gland lesions, where an appreciation of the contour and quality of the adjacent lateral orbital wall is essential [9].

10.4.1 Benign Tumors

Pleomorphic adenomas appear as well-defined, but sometimes nodular and non-homogenous, lesions that show moderate enhancement with intravenous contrast (Fig. 10.2). Palpebral lobe tumors lie anterior to the orbital rim, whereas expansion of the lacrimal fossa with preservation of intact cortical bone is seen in many cases of orbital lobe adenomas, the latter frequently flatten the globe, and discrete flecks of calcification are distinctly rare [4].

10.4.2 Malignant Tumors

Malignant lesions are less defined, with infiltration into surrounding tissues, and "pitting" erosion of the cortical bone within the fossa is not uncommon (Fig. 10.3). Calcification occurs in about one-third of carcinomas [5] but is diffuse as compared to pleomorphic adenomas; lymphomas and metastases are only very rarely calcified. In contrast to hard adenomas that flatten the globe, rapidly growing and softer lesions (such as carcinomas and lymphomas) mold around the globe, and carcinomas also tend to displace the lateral rectus inferomedially as they extend backwards along the lateral orbital wall.

10.5 Pathology

As pleomorphic adenomas and adenoid cystic carcinomas account for most lacrimal gland tumors, only their features will be discussed; details of other tumors can be found elsewhere in the literature [6].

10.5.1 Pleomorphic Adenoma

Pleomorphic adenomas are typically solitary, lobulated, firm, grayish-white masses, and microscopic examination shows sheets, cords, or masses of epithelial cells that are of ductal origin (Fig. 10.2c). The "pleomorphic" appearance arises from epithelial metaplasia giving myxoid and pseudocartilaginous areas. Tiny tumor buds lie within the "pseudocapsule" of compressed neighboring tissues, and this probably accounts for tumor recurrence where the resection margin is insufficient.

10.5.2 Adenoid Cystic Carcinoma

Adenoid cystic carcinomas are gray-white, somewhat soft lesions that, although often showing macroscopic sparing of muscles and bone, will often have some areas of adherence to orbital fat or Tenon's fascia. Microscopic examination shows small hyperchromatic, basophilic cells with varying amount of stroma (Fig. 10.3c), and five subtypes have been described: cribriform (most common), tubular, solid (basaloid), sclerosing, and comedo-carcinomatous. The basaloid pattern is least common but associated with the most aggressive behavior [5].

10.6 Differential Diagnosis

The sudden onset of a painful, swollen, and tender lacrimal gland is likely to be of inflammatory or infectious origin (bacterial or viral), rather than a tumor. Lacrimal gland swelling persisting for more than a few weeks and poorly responding

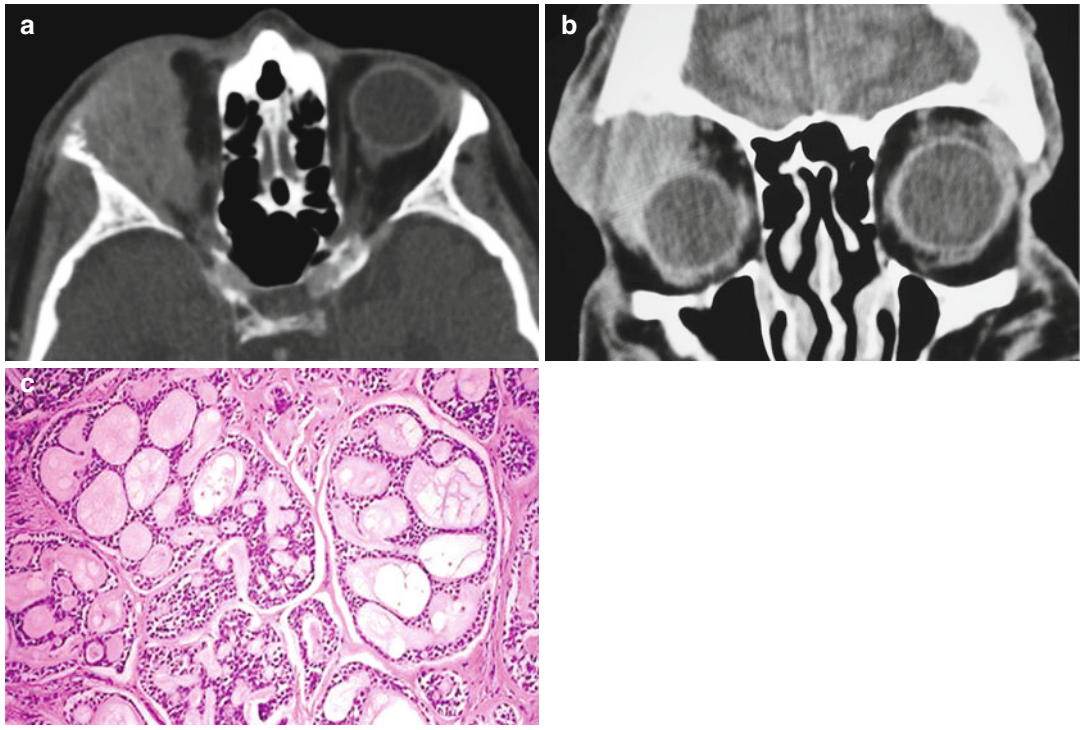

Fig. 10.3 Adenoid cystic carcinoma of the right lacrimal gland with destruction of the lateral orbital wall bone (**a**, bone window). Soft tissue invasion of the right temporalis fossa through lateral wall defect (**b**). Typical cribriform appearance (**c**, hematoxylin and eosin)

to anti-inflammatory agents might, however, suggest underlying carcinoma and should be further investigated with orbital imaging and, if appropriate, biopsy.

Differentiation of benign adenoma from primary malignancy is the key to appropriate surgical planning, as pleomorphic adenoma requires intact excision, whereas malignancy necessitates incisional biopsy [10]. Prior to high-resolution imaging, a clinical scoring was proposed to differentiate the two groups (Table 10.2) [4] – this being based on duration of symptoms and the presence of pain; painless lesions of over 10 months' duration were typically pleomorphic adenomas (although the differential diagnosis included lymphoma, sarcoidosis, and chronic mild dacryoadenitis), whereas malignant tumors had a shorter history relative to their size, as well as persistent pain and paresthesia. Although this algorithm results in a minority of glands (having been thought to be adenomas) being excised intact [11], this result – the inadvertent, but intact, excision of a nonfunctioning gland – is a mere inconvenience as compared with the problems of dealing with pervasively recurrent pleomorphic adenoma [10]. Although fine-needle aspiration biopsy, widely used for salivary tumors, can reliably diagnose pleomorphic adenoma [12], such foreknowledge has limited practical value in the final clinical management.

The advent of high-resolution CT has now become the major determinant in management of lacrimal gland masses: A well-circumscribed tumor should be treated like a pleomorphic adenoma, whereas incisional biopsy should be carried out if the mass molds to the globe or where there is radiologic evidence of bone invasion or intraorbital extension. A diagnosis of malignant transformation within a pleomorphic adenoma (malignant mixed tumor) should be

Table 10.2 Management plan for a mass within the lacrimal gland

Characteristics		Score	
		−1	+1
Clinical	Duration of acute symptoms	<10 months	>10 months
	Persistent pain	Present	Absent
	Sensory loss	Present	Absent
Radiologic (features on thin slice CT images)	Well-defined mass	Present	Absent
	Molding of mass to globe or along lateral orbital wall	Present	Absent
	Tumor calcification	Present	Absent
	Invasion of bone	Present	Absent
	Duration of symptoms in relation to tumor size	Present	Absent
Therapeutic recommendation	Total score	Probable diagnosis	Type of biopsy
	−8 to +2	Carcinoma	Incisional
	−6 to +2	Malignant mixed tumor	Incisional or excisional
	+3 to +8	Pleomorphic adenoma	Total excision *without* prior biopsy

Adapted from Rose and Wright [4]

considered when a patient with long-standing symptoms develops a dramatic acceleration of symptoms, especially if accompanied by recent pain [13].

10.7 Treatment

10.7.1 Pleomorphic Adenoma

Pleomorphic adenomas should be excised intact with a cuff of normal tissue and handling with sharp instruments should be avoided. Palpebral lobe tumors are readily resected through an upper lid skin crease incision, although some tumors may be accessible through the upper conjunctival fornix. Orbital lobe tumors can be resected through a skin crease incision, which can be extended into the lateral canthal rhytids where lateral osteotomy is required. Avoidance of capsular breach, with tumor mobilization on an island of intact periosteum and a buffer of normal tissue at the isthmus between the orbital and palpebral gland, gives an excellent chance of long-term cure [14]. If intraoperative spillage of cells occurs, the breach should be treated by surgical isolation, cautery of the capsular breach, and lavage of the operative field; cyanoacrylate glue may be applied to minor capsular breaches during surgery. Excision of the orbital lobe alone, with preservation of palpebral lobe, reduces the incidence of dry eye and secondary corneal disease [4].

If a pleomorphic adenoma has been inadvertently biopsied, which is distinctly rare with contemporary imaging, the biopsy tract and the tumor should be meticulously excised as recurrence of pleomorphic adenoma is typically infiltrative and may otherwise necessitate extensive tissue resection or even exenteration [10, 15, 16].

10.7.2 Adenoid Cystic Carcinoma

A group of patients with this tumor, selected for craniofacial resection as being "better prognosis candidates with lesser disease," fared no better than another group judged unsuitable for major surgery [5], and others have reported similar outcomes [17]. These findings might, indeed, suggest that disruption of the orbital walls actually seeds tumor into cranial bone and thereby worsens the outlook for this aggressive tumor. Current evidence therefore favors tumor debulking followed by 55–60 Gy of

fractionated external beam irradiation, this probably delaying tumor recurrence and improving survival; [5] the areas irradiated should include the superolateral soft tissues of the orbit, lacrimal fossa, lateral orbital wall, and the orbital apex to include the superior orbital fissure as well as anterior cavernous sinus. Although brachytherapy with locally implanted radioactive plaques or seeds might give local disease control, it fails to treat the superior orbital fissure and cavernous sinus where recurrences from perineural spread tend to arise and for this reason has little or no role in the management of malignant lacrimal gland disease.

Chemotherapy alongside exenteration and radiotherapy delays tumor recurrence and improves survival [18, 19], although it remains unclear which parts of the regime carry efficacy [20]. Two or three cycles of intra-arterial cisplatin (delivered via the external carotid artery) – with concomitant intravenous doxorubicin) – are given over a few weeks prior to orbital exenteration, this dual chemotherapy leading to a marked reduction in tumor size and, thereby, facilitation of surgery [18, 19]. External beam radiotherapy is administered after orbital exenteration and, where tolerated, the intravenous chemotherapy consolidated to a total of six cycles.

10.7.3 Malignant Mixed Tumor

Malignant mixed tumors – that is, malignancy (generally adenocarcinomas) arising within a preexisting pleomorphic adenoma – can be treated by local excision followed by irradiation. Primary adenocarcinomas of the lacrimal gland are very rare and progress rapidly to involve other orbital tissues, the temporalis fossa, and the cranium and are generally treated with resection followed by radiotherapy [5, 17, 21, 22].

10.7.4 Metastatic Tumors

Metastatic deposits in the lacrimal gland carry a poor prognosis, and their treatment, generally palliative, reflects that of the primary tumor and generally necessitates palliative orbital irradiation and, where appropriate, chemotherapy.

10.8 Prognosis

10.8.1 Pleomorphic Adenoma

Intact excision of lacrimal gland pleomorphic adenomas would appear curative [14] and imperative in most cases, as these benign tumors undergo malignant transformation in up to 20 % of cases after 20 years – especially after incomplete excision [23].

10.8.2 Carcinomas

The prognosis for primary epithelial carcinomas of the lacrimal gland is guarded and is determined by the cell type. Adenoid cystic carcinomas are characterized by late recurrence, often with distant metastasis, but perineural spread and direct seeding into the cranial diploe is thought to be responsible for intracranial recurrence after extensive local resections [5]. The median disease-free period is about 2–4 years after treatment [5, 17, 21], and the basaloid variant carries a particularly poor prognosis [5, 17, 24]. Although addition of chemotherapy might improve this poor prognosis [18, 19], the assessment of "cure" for this tumor is very difficult as late recurrence is common – being reported as late as 24 years after presentation [6].

10.8.3 Systemic and Metastatic Tumors

The prognosis for lacrimal gland lymphoma depends on multiple factors: systemic dissemination is more likely in patients with orbital or lacrimal gland involvement as well as patients with prior systemic disease [3]. Where ophthalmic symptoms have been present for more than a year, systemic dissemination is less likely [3]. Histologic classification of infiltrating cells is a further determinant for morbidity, the 5-year

mortality rate varying from 12 % for marginal zone lymphoma to 53 % for diffuse large B cell lymphoma [25].

10.9 Genomics

Genetic anomalies have been demonstrated in relation to adenoid cystic carcinoma of lacrimal gland [26], but more recent investigations for this tumor in other sites have demonstrated a fusion oncogene between MYB and NFIB, with a translocation between chromosome 6q22-23 and chromosome 9p23-24 [27]. This fusion oncogene possibly leads to an overexpression of MYB target proteins – these being associated with modulation of cellular apoptosis, cell cycle control, cell growth and adhesion, and angiogenesis – and future therapeutic options could be aimed at altering these responses.

Conclusion

High-resolution CT scanning has improved the ability to differentiate between pleomorphic adenoma and other lacrimal gland masses, but the prognosis for lacrimal gland carcinoma remains poor, despite advances in diagnosis and treatment of other malignancies. Orbital irradiation after debulking of lacrimal malignancies seems to give the best disease-free interval, while combined intra-arterial and intravenous chemotherapy might improve the outcome for these tumors. Cranio-orbital resection does not appear to prolong life, probably because of the propensity of adenoid cystic carcinoma to perineural spread or micrometastasis.

References

1. Shields JA, Shields CL, Epstein JA, Scartozzi R, Eagle RC. Primary epithelial malignancies of the lacrimal gland: the 2003 Ramon L. Font Lecture. Ophthalmic Plast Reconstr J. 2004;20:10–21.
2. Shields JA, Shields CL, Scartozzi R. Survey of 1264 patients with orbital tumors and simulating lesions: the 2002 Montgomery Lecture, part 1. Ophthalmology. 2004;111:997–1008.
3. Jenkins C, Rose GE, Bunce C, et al. Clinical features associated with survival of patients with lymphoma of the ocular adnexa. Eye. 2003;17:809–20.
4. Rose GE, Wright JE. Pleomorphic adenoma of the lacrimal gland. Br J Ophthalmol. 1992;76:395–400.
5. Wright JE, Rose GE, Garner A. Primary malignant neoplasms of the lacrimal gland. Br J Ophthalmol. 1992;76:401–7.
6. Rootman J, White V, Hind A. Tumors of the lacrimal gland. In: Rootman J, editor. Disease of the orbit. A multidisciplinary approach. 2nd ed. Philadelphia: Lippincott Williams & Wilkins; 2003.
7. Cates CA, Manners RM, Rose GE. Pleomorphic adenoma of the lacrimal gland in a 10 year old girl. Br J Ophthalmol. 2002;86:249–50.
8. Vangveeravong S, Katz SE, Rootman J, White V. Tumors arising in the palpebral lobe of the lacrimal gland. Ophthalmology. 1996;103:1606–12.
9. Aviv RI, Miszkiel K. Orbital imaging: part 2. Intraorbital pathology. Clin Radiol. 2005;60:288–307.
10. Rose GE. To crash or not to crash? Probability in the management of benign lacrimal gland tumours. Eye. 2009;23:1625–8.
11. Prabhakaran VC, Cannon PS, McNab A, et al. Lesions mimicking lacrimal gland pleomorphic adenoma. Br J Ophthalmol. 2010;94:1509–12.
12. Kopp ED, Sahlin S, Tani E, Skoog L, Seregard S. Fine- needle aspiration biopsy in lacrimal gland pleomorphic adenoma. Eye. 2010;24:386–9.
13. Perzin KH, Jakobiec FA, Livolsi VA, Desjardins L. Lacrimal gland malignant mixed tumors (carcinomas arising in benign mixed tumors): a clinico-pathologic study. Cancer. 1980;45:2593–606.
14. Currie ZI, Rose GE. Long-term risk of recurrence after intact excision of pleomorphic adenomas of the lacrimal gland. Arch Ophthalmol. 2007;125:1643–6.
15. Ni C, Kuo PK, Dryja TP. Histopathological classification of 272 primary epithelial tumors of the lacrimal gland. Chin Med J (Engl). 1992;105:481–5.
16. Rose GE, Wright JE. Exenteration for benign orbital disease. Br J Ophthalmol. 1994;78:14–8.
17. Skinner HD, Garden AS, Rosenthal DI, et al. Outcomes of malignant tumors of the lacrimal apparatus. Cancer. 2011;117:2801–10.
18. Meldrum ML, Tse DT, Benedetto P. Neoadjuvant intracarotid chemotherapy for treatment of advanced adenocystic carcinoma of the lacrimal gland. Arch Ophthalmol. 1998;116:315–21.
19. Tse DT, Benedetto P, Dubovy S, Schiffman JC, Feuer WJ. Clinical analysis of the effect of intraarterial cytoreductive chemotherapy in the treatment of lacrimal gland adenoid cystic carcinoma. Am J Ophthalmol. 2006;141:44–53.
20. Le Tourneau C, Razak ARA, Levy C, et al. Role of chemotherapy and molecularly targeted agents in the treatment of adenoid cystic carcinoma of the lacrimal gland. Br J Ophthalmol. 2011;95:1483–9.
21. Esmaeli B, Ahmadi MA, Youssef A, et al. Outcomes in patients with adenoid cystic carcinoma of the

lacrimal gland. Ophthal Plast Reconstr Surg. 2004;20: 22–6.
22. Heaps RS, Miller NR, Albert DM, et al. Primary adenocarcinoma of the lacrimal gland. A retrospective study. Ophthalmology. 1993;100:1856–60.
23. Font RL, Gamel JW. Epithelial tumors of the lacrimal gland: an analysis of 265 cases. In: Jakobiec FA, editor. Ocular and adnexal tumors. Birmingham: Aesculapius; 1978. p. 787–805.
24. El-Sawy T, Savar A, Williams MD, De Monte F, Esmaili B. Prognostic accuracy of the seventh edition vs sixth edition of the American Joint Committee on cancer tumor classification for adenoid cystic carcinoma of the lacrimal gland. Arch Ophthalmol. 2012;130:664–6.
25. Jenkins C, Rose GE, Bunce C, et al. Histological features of ocular adnexal lymphoma (REAL classification) and their association with patient morbidity and survival. Br J Ophthalmol. 2000;84:907–13.
26. Tse D. Clinical and microdissection genotyping analyses of the effect of intra-arterial cytoreductive chemotherapy in the treatment of lacrimal gland adenoid cystic carcinoma. Trans Am Ophthalmol Soc. 2005;103:337–67.
27. Persson M, Andren Y, Mark J, Horlings HM, Persson F, Stenman G. Recurrent fusion of MYB and NFIB transcription factor genes in carcinomas of the breast and head and neck. Proc Natl Acad Sci. 2009;106: 18740–4.

Lacrimal Sac Tumors

11

Jacob Pe'er

Contents

11.1 Introduction

Tumors of the lacrimal drainage system, especially the lacrimal sac, are rare, and since the first publications reporting such tumors by Spratt, Duke-Elder, Radnot and Gall, and others [1–7], only about 700 cases have been reported in the medical literature in the last 110 years; about five new cases are reported per year worldwide. Despite their rarity, physicians should be aware of the clinical features of lacrimal sac tumors, as many are life-threatening and early diagnosis and appropriate treatment can save lives. These tumors often masquerade as a chronic inflammatory process. Due to the rarity of lacrimal sac tumors, large clinical studies with statistically meaningful data are unavailable, and we learn about the biological behavior, management, and prognosis of these tumors only from case series and case reports.

11.2 Clinical Features

Lacrimal sac tumors are usually diagnosed in adults, with average age in the 50s and with benign tumors appearing about a decade earlier than malignant tumors [1–9]. Tumors in the lacrimal sac have also been reported in children and infants [9–11]. Although a series from China report that men are more commonly affected [8, 12], most series show no significant gender difference in the incidence of lacrimal sac tumors [1–7, 9, 13]. Various series report

J. Pe'er, MD
Department of Ophthalmology,
Hadassah University Hospital,
Jerusalem, Israel
e-mail: peer@hadassah.org.il

J.D. Perry, A.D. Singh (eds.), *Clinical Ophthalmic Oncology*,
DOI 10.1007/978-3-642-40492-4_11, © Springer-Verlag Berlin Heidelberg 2014

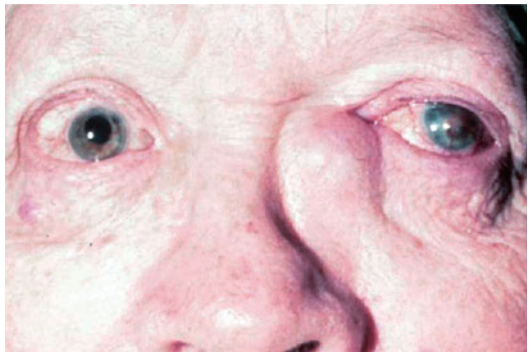

Fig. 11.1 A man with a transitional cell carcinoma of the lacrimal sac of the left eye presenting with a mass that reaches a level above the medial canthal tendon (Courtesy of Dr. Mary A. Stefanyszyn)

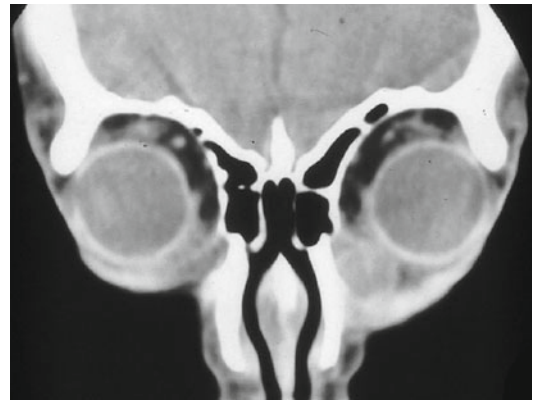

Fig. 11.2 A CT scan shows a mass over the left lacrimal sac area (Courtesy of Dr. Mary A. Stefanyszyn)

malignancy in 50–95 % of lacrimal sac tumors and an epithelial origin in about three-quarters of tumors [1–9, 12, 13].

Most lacrimal sac tumors present with symptoms of dacryostenosis and/or dacryocystitis due to obstruction or partial obstruction of the drainage [8, 9, 14]. Thus, most patients complain of epiphora as well as redness, swelling, and purulent discharge. Due to the similarity of symptoms, lacrimal sac tumors are often found inadvertently at the time of dacryocystorhinostomy (DCR) for presumed dacryostenosis. This is the reason that DCR specimens should always be submitted for pathologic evaluation [15].

The main sign of lacrimal sac tumors is the development of a mass in the area of the lacrimal sac (Fig. 11.1); the appearance of a mass above the medial canthal tendon level is most typical. In benign tumors the typical mass grows slowly and is elastic in consistency, with distinct margins, and is freely movable under the skin. On the other hand, most malignant tumors grow faster, and the mass is firm, noncompressible, and fixed to the underlying tissue. Fistulous tracts can develop. Bleeding from the puncta, either spontaneously or on applying pressure to the lacrimal sac, epistaxis, or dark bloody nasal discharge may occur in some patients, especially those with epithelial tumors [9]. Some patients with a malignant tumor complain of pain [7].

In advanced cases of malignancy, ulceration over the mass can be seen and involvement of the preauricular, submandibular, and cervical lymph nodes can be diagnosed. In some cases, regional lymph node involvement appears before discovery of the primary tumor. When a tumor grows significantly to involve the orbit, proptosis and limitation of ocular motility may develop. Local invasion of the face, nose, ethmoid and maxillary sinuses, and palate, as well as intracranial extension, can occur [2].

11.3 Diagnostic Evaluation

In one series of 377 DCR specimens [15], lacrimal sac neoplasms resulting in chronic lacrimal drainage obstruction occurred in 4.6 % of cases; in 2.1 % they were not suspected before surgery. Therefore, in every case of a mass in the lacrimal sac area that causes obstruction, lacrimal sac tumor should be suspected. Inflammatory response in this area does not rule out the diagnosis of a tumor. In such patients, history of blood-stained tears or epistaxis should increase the suspicion.

Imaging studies are important in evaluation of lacrimal sac tumors [2, 3, 8, 9, 14]. CT scan shows a solid mass over the lacrimal sac area and may display dilatation of the lacrimal fossa and/or bony erosion or destruction of the lacrimal fossa and, in advanced cases, invasion into neighboring structures (Fig. 11.2). Dacryocystography (DCG) may reveal a filling defect of the sac

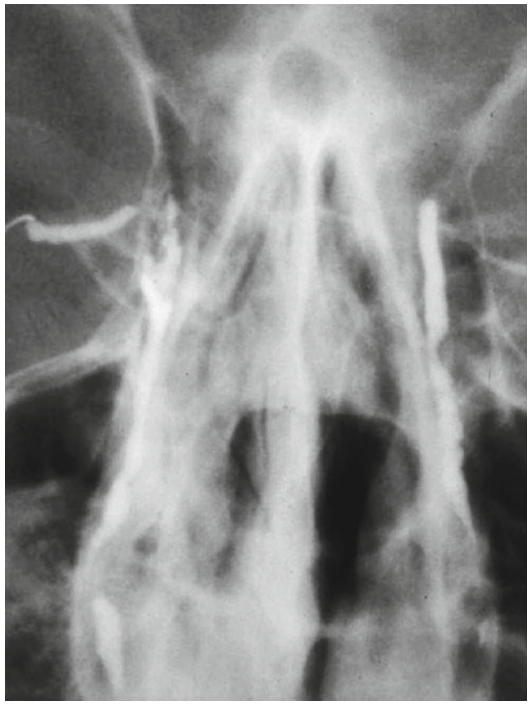

Fig. 11.3 Dacryocystogram reveals a mottled defect in the right lacrimal sac as compared to the smooth outline of the left lacrimal sac (Courtesy of Dr. Mary A. Stefanyszyn)

lumen or a distended sac with uneven or mottled contrast media or delay in draining of the contrast material (Fig. 11.3). In cases of benign tumor or early stages of tumor, the lacrimal drainage system may be patent, such that negative results do not rule out a tumor. Ultrasound of the lacrimal sac area can also be used, and some experts have found magnetic resonance imaging (MRI) to be superior to computed tomography for imaging of the lacrimal sac, as MRI provides better tumor definition and determination of the cystic or solid nature of the mass [11].

Since most patients with lacrimal sac tumors present with symptoms and signs of dacryocystitis, the main differential diagnosis includes acute or chronic dacryocystitis. Inflammatory disorders of the lacrimal sac, such as granulomas or granulation tissue, or infectious processes due to tuberculosis or fungus, should also be included in the differential diagnosis.

The final diagnosis can be ascertained only by histopathological examination, for which excisional biopsy is preferred. If the entire tumor cannot be removed, deep incisional biopsy is essential since the tumor periphery may show only inflammatory response, leading to misdiagnosis. When a patient with suspected lacrimal sac tumor has involvement of the nasal cavity, biopsy via the nasal route is possible.

Table 11.1 Histopathological classification of epithelial tumors of the lacrimal sac

Benign
Papilloma
Squamous papilloma
Transitional cell papilloma
Mixed-cell papilloma
Papilloma unspecified
Oncocytoma
Pleomorphic adenoma (mixed tumor)
Mucocele
Cysts
Cylindroma
Malignant
Papilloma with carcinoma
Carcinoma
Squamous cell carcinoma
Transitional cell carcinoma
Mixed squamous/transitional carcinoma
Oncocytic adenocarcinoma
Mucoepidermoid carcinoma
Adenoid cystic carcinoma
Adenocarcinoma
Adenocarcinoma ex-pleomorphic adenoma
Eccrine adenocarcinoma
Undifferentiated carcinoma
Secondary tumors

11.4 Histopathological Classification

Lacrimal sac tumors are divided into two major groups: epithelial tumors, which constitute the majority of the lacrimal sac tumors, accounting for about 75 % of all reported cases, and non-epithelial tumors, which account for the remaining 25 % [8, 9, 15–18]. All types of reported lacrimal sac tumors, common and rare, are listed in Tables 11.1 and 11.2.

Often it is difficult to establish whether a tumor arises primarily in the lacrimal sac, rather

Table 11.2 Histopathological classification of non-epithelial tumors of the lacrimal sac

Mesenchymal—fibrous tissue tumors
Benign
Fibrous histiocytoma
Lipoma
Juvenile xanthogranuloma
Malignant
Malignant fibrous histiocytoma
Mesenchymal—vascular tumors
Benign
Hemangiopericytoma
Cavernous hemangioma
Capillary hemangioma
Angiofibroma
Hemangioendothelioma
Glomus tumor
Malignant
Kaposi's sarcoma
Melanocytic tumors
Benign
Nevi
Malignant
Melanoma
Lymphoproliferative tumors
Benign reactive lymphoid hyperplasia
Malignant lymphoma
Leukemic infiltrate (granulocytic sarcoma)
Plasmacytoma
Neural tumors
Neurofibroma
Neurilemmoma (schwannoma)
Inflammatory pseudotumors
Secondary tumors

than from other parts of the nasolacrimal system, nose, paranasal sinuses, cutaneous adnexa, conjunctiva, or caruncle, with subsequent spread to the sac [7]. The lacrimal sac tumors, epithelial and non-epithelial, reported in the literature are believed to arise primarily in the lacrimal sac.

The lacrimal drainage system is composed of the canaliculus, which is lined by nonkeratinized stratified squamous epithelium, and the lacrimal sac and nasolacrimal duct, which are lined by stratified columnar (transitional) epithelium. The transitional epithelium contains mucous glands and is histologically similar to the epithelium lining the nasal passages and paranasal sinuses.

The origin of most benign and malignant epithelial tumors is in the epithelial lining of the lacrimal sac and therefore can be either squamous or transitional type [5, 7, 9]. The papilloma may exhibit an exophytic growth pattern, growing towards the sac lumen, or an inverted pattern, growing towards the stroma. The latter tends, more than the former, to be more invasive, to recur, and sometimes to undergo malignant change. Some of the papillomas may show foci of carcinoma, evidence that they may be the source for the development of carcinomas. Marked inflammation is often seen in the stroma of the papillomas. Human papilloma viruses (HPV) type 6 or 11 have been found in lacrimal sac papillomas and carcinomas [19].

Squamous cell carcinomas may range from well-differentiated tumors with keratin pearls and intercellular bridges to poorly differentiated tumors. Transitional cell carcinoma may show a papillary pattern and be composed of cylindrical epithelial cells (Fig. 11.4). Goblet cells may be seen. Both types of carcinomas invade the lacrimal sac wall and produce a hard mass.

Most other epithelial tumors of the lacrimal sac, benign and malignant, are of glandular origin and are similar to those found in glands such as the lacrimal and salivary glands. The most common benign tumors in this group are the oncocytoma and pleomorphic adenoma and, among the malignant tumors, oncocytic adenocarcinoma and adenoid cystic carcinoma. Epithelial tumors with a basal cell component were also reported [20]. The existing mixed glands with serous and mucous cells in the lacrimal sac as well as in the nasolacrimal duct wall are the origin of these tumors [16].

Non-epithelial tumors of the lacrimal sac constitute about one-quarter of the lacrimal sac tumors; of these, about half are mesenchymal tumors, one-quarter melanomas, and one-quarter lymphoproliferative tumors. Only a few neural tumors were reported [17]. The mesenchymal tumors appear at a relatively young age, compared to other groups of lacrimal sac tumors.

In the recent literature, fibrous histiocytoma is the most common mesenchymal tumor of the lacrimal sac, but it does not appear in the

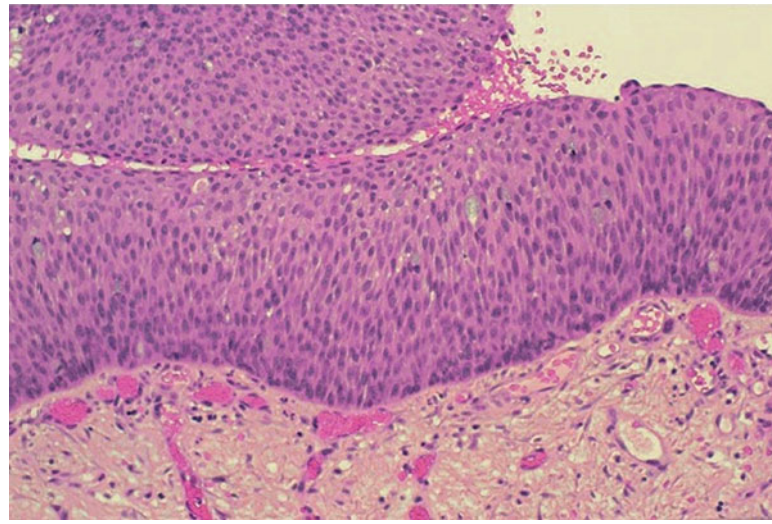

Fig. 11.4 Histological picture of transitional cell carcinoma of the lacrimal sac, showing cylindrical epithelial cells. Some goblet cells are seen among the epithelial cells (hematoxylin and eosin, original magnification ×40) (Courtesy of Dr. Mary A. Stefanyszyn)

earlier literature, probably because it was recognized only in the past 40 years. These tumors are composed of cells resembling fibroblasts and histiocytes and contain xanthomatous cells and multinucleated giant cells. Most fibrous histiocytomas that were described in the lacrimal sac are benign, and some are locally aggressive. No malignant fibrous histiocytomas of the lacrimal sac were reported.

Among the very rare vascular tumors of the lacrimal sac, the most commonly reported is hemangiopericytoma, which shows a vascular pattern of sinusoidal spaces, among which are solid areas of spindle-shaped cells. Even benign-appearing lesions have the potential to metastasize. Other types of hemangiomas are reported as individual cases and include capillary hemangioma, cavernous hemangioma, angiofibroma, hemangioendothelioma, and Kaposi's sarcoma.

It is difficult to classify the lymphoproliferative tumors of the lacrimal sac reported in the literature, due to their rarity and frequent classification system changes. In recent publications it appears that most lymphomas in this region are of the non-Hodgkin's B-cell type [10, 11, 14]. The common types are diffuse large B-cell lymphoma (DLBCL) and MALT lymphoma [21]. Leukemic infiltrates in the lacrimal drainage system are probably more frequent than reported [10]. Multiple myeloma of the lacrimal sac may also occur.

Melanoma of the lacrimal sac, like melanomas of other mucous membranes, has a poor prognosis and is probably the most malignant tumor of the lacrimal sac [17]. It originates in melanocytes in and under the epithelial lining of the lacrimal sac; most are composed of epithelioid melanoma cells.

Neural tumors of the lacrimal sac are extremely rare. They originate from adjacent neural elements and invade the lacrimal sac wall. The medical literature contains reports of two neurilemmomas and two neurofibromas.

Secondary tumors of the lacrimal sac may originate either from adjacent structures such as the nose, paranasal sinuses, orbit, conjunctiva, and skin or as metastases, although the latter are rarely confined to the lacrimal sac alone.

11.5 Treatment

The treatment of lacrimal sac tumors depends on the histological typing, malignancy, and the extent of its invasion through the lacrimal sac to adjacent tissue [2, 8–14]. The treatment of choice is complete surgical removal of the tumor. When epithelial and mesenchymal tumors are confined to the lacrimal sac, dacryocystectomy is performed, and this usually suffices for benign tumors. Intact excision of the tumor with the periosteum of the fossa and supplemental external irradiation can be

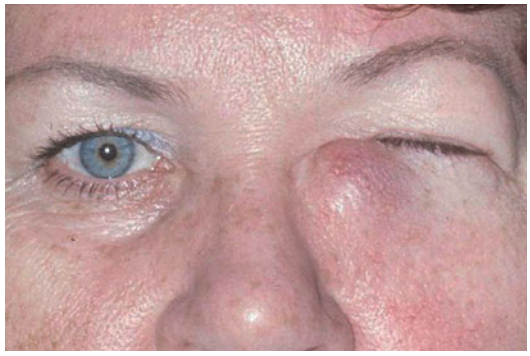

Fig. 11.5 A woman with squamous cell carcinoma of the left lacrimal SCC presenting with irreducible hard mass and a history of chronic dacryocystitis (Courtesy of Dr. Mary A. Stefanyszyn)

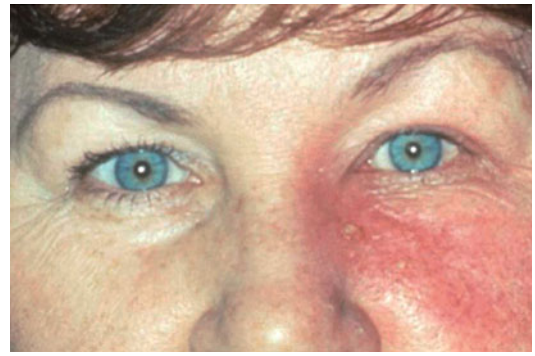

Fig. 11.6 The same woman of Fig. 11.5 following extensive surgical resection of the tumor and postoperative radiation, soon after the radiation. Tumor is not seen but redness, dryness, and scaling skin are evident (Courtesy of Dr. Mary A. Stefanyszyn)

added if the tumor is malignant. Deep incisional biopsy, with or without frozen section, is performed when the mass is found, by imaging, to extend beyond the lacrimal fossa, or when lacrimal sac malignancy is clinically obvious. The definitive therapy is determined according to the histopathological diagnosis. In some cases, biopsy can be taken through nasal endoscopy.

Extension of tumors, mainly premalignant and malignant, down the nasolacrimal duct accounts for recurrences and failure of therapy; therefore, lateral rhinotomy, which offers a greater chance of cure, should be performed. More extensive surgical excision of the canaliculi and nasolacrimal duct, together with the sac, may be needed in certain cases. When the tumor extends beyond the lacrimal drainage system to adjacent tissue, more radical surgery is needed. This may include exenteration of the orbital tissue, paranasal sinus resection, and cervical lymph node dissection. Postoperative radiotherapy is recommended for malignant epithelial tumors, with a suggested tumor dose of approximately 60 Gy. Recurrent lesions may be treated with further surgery or radiotherapy (Figs. 11.5 and 11.6).

The primary treatment of lacrimal sac lymphoma, after incisional or excisional biopsy, consists of radiotherapy with or without chemotherapy, with a favorable response in most patients. Malignant melanoma of the lacrimal sac has a poor prognosis, and various treatments such as extensive surgical resection, radiotherapy, or chemotherapy may delay recurrence but usually do not improve survival.

11.6 Clinical Course

The outcome in cases of lacrimal sac tumor depends on the stage at the time of diagnosis, the histopathological features of the tumor including its growth pattern, and the appropriateness of treatment. Ni and his colleagues [8] offered four stages for the evolution of lacrimal sac tumors: Stage 1, in which there are symptoms and signs but no definite tumor mass is seen or palpable; Stage 2, in which obvious tumor formation is confined to the sac; Stage 3, in which the tumor extends beyond the lacrimal sac to adjacent structures such as the orbit or paranasal sinuses; and Stage 4, which is marked by evident metastases.

Malignant tumors of the lacrimal sac display three types of growth [8]: along the surface of the epithelium, protruding toward the lumen as papillary growth, and infiltrating the wall of the sac as solid cell nests. There are three main modes of tumor spread [8]: direct extension is the most common, to adjacent structures such as the orbit, nasolacrimal duct, paranasal sinuses, and the skull; lymphatic metastases mainly to the submandibular, preauricular, and cervical

glands; and remote, most probably hematogenous spread—the most common site is to the lung.

Benign papillomas of the lacrimal sac often recur, especially those with an inverted pattern, which show recurrence rates of 10–40 % [14]. Most of the papillomas that recur do not reveal malignant changes [7]. Low-grade carcinomas have variable cure rates depending on the extent of the disease and the treatment. Recurrence rate of invasive squamous cell and transitional cell carcinoma appears to be about 50 % with up to 50 % of those being fatal, although some series reported a much better outcome.

Recurrence and mortality rates of non-epithelial lacrimal sac tumors vary [9, 14, 17]. Benign fibrous histiocytoma has a good prognosis if completely excised, while the malignant potential of hemangiopericytoma can be unpredictable. Lymphoid lesions respond to radiotherapy and chemotherapy and have variable prognosis depending on the extent of the disease and the type of the tumor. The most dismal prognosis is that of malignant melanoma, which is often fatal in a short period of time in spite of aggressive treatment.

References

1. Spratt CN. Primary carcinoma of the lacrimal sac. Arch Ophthalmol. 1937;18:267–73.
2. Duke-Elder S. Diseases of the lacrimal passages—tumours and pseudo-tumours. In: Duke Elder S, editor. Textbook of ophthalmology, vol. 13, pt. II. St. Louis: CV Mosby; 1974. p. 735–59.
3. Jones IS. Tumors of the lacrimal sac. Am J Ophthalmol. 1956;42:561–6.
4. Radnot M, Gall J. Tumoren des Traensackes. Ophthalmologica. 1966;151:1–22.
5. Harry J, Ashton N. The pathology of tumours of the lacrimal sac. Trans Ophthalmol Soc UK. 1968; 88:19–35.
6. Schenck NL, Ogura JH, Pratt LL. Cancer of the lacrimal sac. Ann Otol Rhinol Laryngol. 1973;82:153–61.
7. Ryan SJ, Font RL. Primary epithelial neoplasms of the lacrimal sac. Am J Ophthalmol. 1973;76:73–88.
8. Ni C, D'Amico DJ, Fan CQ, Kuo PK. Tumors of the lacrimal sac: a clinicopathological analysis of 82 cases. Int Ophthalmol Clin. 1982;22:121–40.
9. Stefanyszyn MA, Hidayat AA, Pe'er JJ, Flanagan JC. Lacrimal sac tumors. Ophthal Plast Reconstr Surg. 1994;10:169–84.
10. Yip CC, Bartley GB, Habermann JM, Garrity JA. Involvement of the lacrimal drainage system by leukemia and lymphoma. Ophthal Plast Reconstr Surg. 2002;18:242–6.
11. Schefler AC, Shields CL, Shields JA, Demirci H, Maus M, Eagle Jr RC. Lacrimal sac lymphoma in a child. Arch Ophthalmol. 2003;121:1330–3.
12. Bi YW, Chen RJ, Li XP. Clinical and pathological analysis of primary lacrimal sac tumors. Zhonghua Yan Ke Za Zhi. 2007;43:499–504 (article in Chinese).
13. Kroll J, Busse H. Tumours of the lacrimal passages. Klin Monbl Augenheilkd. 2008;225:91–5.
14. Parmar D, Rose GE. Management of lacrimal sac tumours. Eye (Lond). 2003;17:599–606.
15. Anderson NG, Wojno TH, Grossniklaus HE. Clinicopathologic findings from lacrimal sac biopsy specimens obtained during dacryocystorhinostomy. Ophthal Plast Reconstr Surg. 2003;19:173–6.
16. Pe'er J, Hidayat AA, Ilsar M, Landau L, Stefanyszyn MA. Glandular tumors of the lacrimal sac. Their histologic patterns and possible origins. Ophthalmology. 1996;103:1601–5.
17. Pe'er JJ, Stefanyszyn M, Hidayat AA. Nonepithelial tumors of the lacrimal sac. Am J Ophthalmol. 1994; 118:650–8.
18. Campbell RJ, Sobin LH. Tumours of the lacrimal drainage system. In: Histological typing of tumours of the eye and its adnexa. 2nd ed. World Health Organization international histological classification of tumors. Berlin: Springer; 1998. p. 25–6.
19. Sjo NC, von Buchwald C, Cassonnet P, Flamant P, Heegaard S, Norrild B, Prause JU, Orth G. Human papillomavirus: cause of epithelial lacrimal sac neoplasia? Acta Ophthalmol Scand. 2007;85:551–6.
20. Katircioglu YA, Yildiz EH, Kocaoglu FA, Ozer E, Ornek F, Duman S. Basal cell carcinoma in lacrimal sac. Orbit. 2006;26:303–7.
21. Sjo LD, Ralfkiaer E, Jul BR, et al. Primary lymphoma of the lacrimal sac: an ORTC ophthalmic oncology task force study. Br J Ophthalmol. 2006;90:1004–9.

Orbital and Adnexal Lymphoma

12

Mary E. Aronow, Brian T. Hill, and Arun D. Singh

Contents

M.E. Aronow, MD
Department of Ophthalmic Oncology,
Cole Eye Institute, Cleveland Clinic,
9500 Euclid Avenue, Cleveland, OH 44195, USA

B.T. Hill, MD, PhD
Taussig Cancer Institute, Cleveland Clinic,
9500 Euclid Avenue, Cleveland, OH 44195, USA

A.D. Singh, MD (✉)
Department of Ophthalmic Oncology,
Cole Eye Institute, Cleveland Clinic Foundation,
9500 Euclid Avenue, Cleveland, OH 44195, USA
e-mail: singha@ccf.org

Taussig Cancer Institute, Cleveland Clinic,
9500 Euclid Avenue, Cleveland, OH 44195, USA

12.1 Introduction

Orbital and adnexal lymphoma (OAL) includes a heterogeneous group of lymphomas, the majority of which are low-grade, indolent, B cell, non-Hodgkin's lymphomas (NHLs) [1]. By definition, OAL affects structures including the eyelids, conjunctiva, lacrimal apparatus, extraocular muscles, and the orbit. Disease may be limited to a single, localized tumor, or it may be multifocal. Overlap with ocular adnexal sites is common (10–20 % of cases), and coexisting uveal involvement has been observed [2–6]. Moreover, OAL can affect regional, central, and peripheral lymph nodes as well as other distant extranodal sites. The 10-year, disease-specific mortality is approximately 5–10 % [7]. Many of the advances in understanding OAL were initially demonstrated in systemic lymphoma (Box 12.1).

J.D. Perry, A.D. Singh (eds.), *Clinical Ophthalmic Oncology*,
DOI 10.1007/978-3-642-40492-4_12, © Springer-Verlag Berlin Heidelberg 2014

Box 12.1: Important Aspects of Ocular Adnexal Lymphoma

- OAL consists primarily of five types of lymphoma, the most common of which is the extranodal marginal zone type.
- The diagnosis depends on pathology, immunophenotypic analysis, and molecular genetic studies.
- Updated lymphoma classifications allow excellent diagnostic accuracy.
- Treatment of local disease consists of radiation and other local modalities with good local control but variable long-term prognosis.
- Low-grade tumors with systemic involvement are treated by observation or local methods.
- Chemotherapy is used for high-grade disease with systemic involvement.
- Infection and chronic inflammation may play a role in lymphomagenesis, and new treatment modalities may be directed at them.

12.2 Epidemiological Aspects

OAL is a rare disease, likely representing as many as 8 % of all extranodal NHLs [1]. Its incidence is approximately 0.2 per 100,000 [8]. There is a slight female predilection (60 % of cases in most series) [9–11]. It affects most ethnic groups although there is significant geographic variation among systemic lymphoma, with the white population in the United States showing the highest incidence. The overall incidence of systemic lymphoma is increasing, although corresponding information does not exist for OAL [12].

Among ophthalmic tumors, OAL comprises 6–8 % of orbital and 10–15 % of adnexal lesions [13–16]. Localized, ocular-only disease is present at diagnosis in 60–80 % of cases, while the remainder have systemic involvement at the time of ophthalmic presentation [17, 18]. Bilateral disease is observed in 10–15 % of individuals with ocular-only lymphoma [19]. Among affected ocular sites, the frequencies of involvement are conjunctiva 20–33 %, orbit/lacrimal gland 46–74 %, and eyelid 5–20 % [7, 20]. Distinction between these sites can be difficult, and combined involvement may be underreported [11, 21].

Many cases previously diagnosed as benign reactive lymphoid hyperplasia (BRLH) are now considered malignant lymphoma using current diagnostic techniques [22]. Retrospective studies of patients diagnosed with BRLH have revealed that up to 80 % are now classified as malignant lymphoma [22]. At present, BRLH represents a minority of cases and is a diagnosis of exclusion.

12.3 Etiology and Pathogenesis: B Cell Biology and Lymphomagenesis

The largest advances in understanding lymphoma pathogenesis and etiology as well as classification derive from the refined immunophenotypic (IPA) characterization of lymphocyte surface markers combined with concurrent advances in understanding of the molecular genetic of lymphocyte biology. This has resulted in a mechanistic hypothesis for lymphomagenesis which connects specific lymphoma types to different precursor cells and genetic events. Lymphoma classification, diagnosis, and pathogenesis are intertwined with their immunopathology and molecular biology.

The relationship between stages of lymphocyte development and their associated lymphoma types, which are based on IPA, is shown in Table 12.1 [23]. Tumors arise from germinal center cells (follicular lymphoma), cells of the mantle zone (mantle cell lymphoma), or memory B cells (extranodal marginal zone lymphoma), all of which have undergone antigen exposure. From a molecular genetic standpoint, during normal lymphocyte maturation, errors may occur in which an antigen receptor gene region is juxtaposed to an oncogene region resulting in deregulation of the oncogenic region. Less often, a

Table 12.1 Immunophenotypic expression of ocular adnexal lymphoma

Type	Precursor cell	CD3	CD5	CD10	CD20	CD23	CD43	CD79	Bcl-2	Bcl-6	Cyclin D1
EMZL	Memory B cell	–	–	–	+	–	+	+	–	–	–
FL	Centrocyte	–	–	+	+	+/–	–		+	+	–
MCL	Mantle cell	–	+	–	+				–		+
LPL	Memory B cell	–	+	–	+	+					
DLBCL	Centroblast	–	–	+	+			+			

EMZL extranodal marginal zone lymphoma, *FL* follicular lymphoma, *MCL* mantle cell lymphoma, *LPL* lymphoplasmacytic lymphoma, *DLBCL* diffuse large B cell lymphoma

novel oncogenic protein is formed by fusion of two other genes. Chromosomal translocations underlying these alterations are well described in up to 90 % of systemic lymphoma [24, 25]. Limited data suggests that these translocations are less common in OAL [26, 27].

The theory that lymphoma develops due to errors occurring during normal lymphocyte response to infection or inflammation is referred to as the infection/inflammation/mutation (IMM) model of lymphomagenesis. This has been corroborated in two ways. One is the recognized association of lymphoma with chronic antigen stimulation and infection, immune suppression, and autoimmune disease [28]. The prototypic example of the IMM model is gastric extranodal marginal zone lymphoma in which an organ the endogenous mucosal-associated lymphoid tissue (MALT) develops lymphoma in response to chronic *H. pylori* infection. With the recent understanding that most OAL are also extranodal marginal zone lymphoma/MALT lymphomas, studies have shown evidence of DNA from infectious agents including *C. psittaci* and *H. pylori* in OAL [29, 30]. Infection as an underlying etiology for OAL shows variation among geographic regions and also within different series in the same geographic location [29, 31, 32]. Treatment implications of this are discussed below.

In addition to its therapeutic implications, perhaps the most important consequence of the IMM model is that it explains why the ocular adnexa, which has little if any endogenous lymphoid tissue, has lymphoma as its most common neoplasia. Similar mechanisms may occur in RLH. Based on the relative infrequency of OAL, there may be other factors required for lymphomagenesis.

12.4 Classification

OAL represents the malignant end of the spectrum of ocular adnexal lymphoproliferative disorders. As previously noted, BRLH and reactive lymphoid hyperplasia (RLH) with atypia represent a minority of cases and together comprise benign and intermediate forms of the disease, respectively [33, 34]. OAL is a localized form of lymphoma which has been integrated into the schema of lymphoproliferative diseases described in two major classification systems, the Revised European–American Lymphoma classification in 1994 [35] and the 2008 World Health Organization (WHO) Classification of Tumors of Hematopoietic and Lymphoid Tissue [36].

OAL can be divided by the type and site(s) of tissue involvement. The vast majority of OAL are of the non-Hodgkin's B cell type. Despite the extensive numbers of systemic lymphoma subtypes, most OAL belong to one of five subtypes: extranodal marginal zone (EMZL or MALT lymphoma), follicular lymphoma (FL), diffuse large B cell lymphoma (DLBCL), mantle cell lymphoma (MCL), and lymphoplasmacytic lymphoma (LPL) (Table 12.2) [11, 17, 37–44]. The vast majority, approximately 80 %, are of the EMZL type in most series [1].

OAL is termed solitary if it is the only site involved, secondary when contiguous sites are involved, and systemic if remote sites are involved. OAL is solitary in 60–80 % of cases at the time of presentation [17, 37, 39, 44]. The rate of progression to systemic involvement can only be accurately identified using current criteria since the misclassification was so high prior to the use of the WHO classification.

Table 12.2 Distribution of various types of ocular adnexal lymphoma

Author	Year	Patients	EMZL (%)	Follicular (%)	Mantle zone (%)	Lymphoplasmacytic (%)	Diffuse large B cell (%)	Plasmacytoma (%)	T cell
White	1995	43	Not done						
Nakata	1999	44	77	–	4	2	14	–	–
Jenkins	2000	192	54	11	2	24	8		<1
McKelvie	2001	70	63	17	3		11		1
Shields	2001	117	Not done						
Mannami	2001	43	86	–	2	–	12	–	
Bhatia	2001	47	17	53			26		
Coupland	2003	230	59	12	3	4	13	4	3
Fung	2003	98	57	18	4		7		
Sharara	2003	17	47	12	18	6	18	–	
Cho	2003	57	98		2				
Sullivan	2005	69	35	22	1	4	7	3	6
Rosado	2006	62	89	–	–	–	<1	–	–
Ferry	2007	353	52	23	5	1	8	–	<1
Oh	2007	128	75	–	3	1	5	1	4
Hatef	2007	43	44	21	1	–	21	–	<1
Rootman	2011	122	60	12	1	4	4	–	–
Watkins	2011	57	28	2	5	–	4	4	5
Zanni	2012	41	63	10	5	5	17	–	–
Total		1,833	17–98	11–53	1–18	4–24	1–26	1–4	1–6

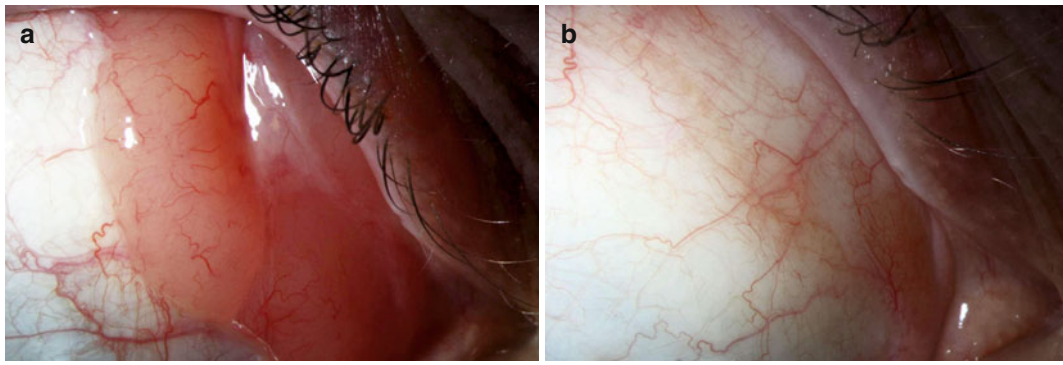

Fig. 12.1 Conjunctival lymphoma with typical salmon color and diffuse margins (**a**). After radiation treatment there is complete resolution of the mass (**b**)

12.5 Clinical Features

12.5.1 Symptoms

Subjective complaints in OAL are broad and may include lacrimal gland, orbital, and conjunctival mass or apparent eyelid mass, exophthalmos, pain, or diplopia. Many lesions are asymptomatic. If the lacrimal gland is involved, dry eye symptoms may occur.

12.5.2 Signs

OAL have site-specific presentations which affect how the diagnosis is made. In the conjunctiva, lesions present typically with salmon or flesh pink color (Fig. 12.1a). Clinical appearance does not allow distinction of benign from malignant lymphoproliferative disease. In the orbit, lacrimal gland, and eyelid, the lymphoma presents as a mass, which if palpable, is typically

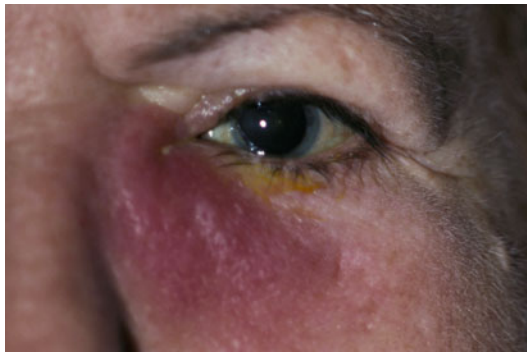

Fig. 12.2 Clinical view of lymphoma involving the nasolacrimal sac region

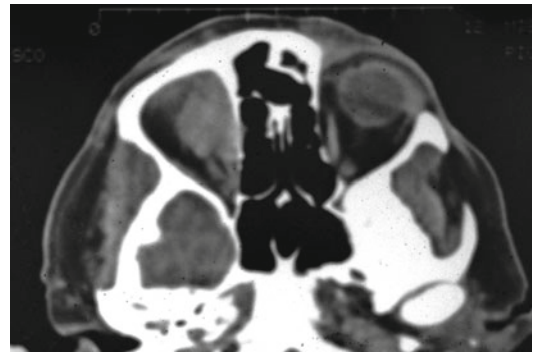

Fig. 12.3 Axial CT scan of patient in Fig. 12.2, showing superior orbital mass with irregular margins, which molds to orbital wall

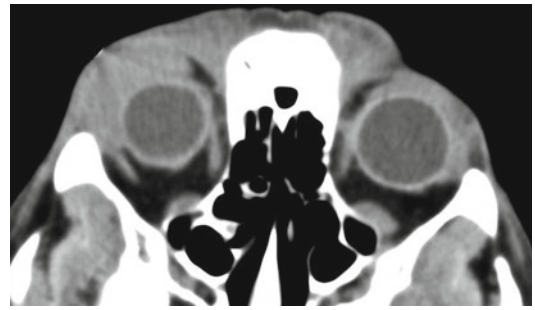

Fig. 12.4 Axial CT scan demonstrating bilateral orbital involvement. Note that the tumor is diffusely infiltrating around the orbital structures

firm. Mobility is variable depending upon attachment to other structures. Diplopia may occur upon how rapidly the mass develops. Exophthalmos and decreased retropulsion of the globe may be the only clinical signs. Secondary ptosis may also occur. Involvement of the nasolacrimal drainage system can occur (Fig. 12.2). Compression or invasion of the optic nerve can lead to vision loss. During orbital biopsy, OAL appears as a white to pink mass reflecting its leukocytic and vascular characteristics.

12.6 Diagnostic Evaluation

Evaluation of OAL involves characterization of the lesion and staging. Biopsy should be obtained by open methods to allow sufficient material for multiple special studies: pathology, lymphocyte immunophenotypical analysis, and molecular genetic studies to identify gene rearrangements indicative of clonality and/or translocations.

12.6.1 Local Imaging Studies

Imaging studies of the orbit play an important role in OAL but are performed at different times depending on the presentation. With conjunctival disease, the lesion is frequently biopsied first, and imaging of the orbit follows to assess orbital involvement. With orbital and lid disease, the orbit is usually imaged to optimize the biopsy process. Contrast-enhanced CT and MRI scans of the orbits will show enhancing lesions which can be discrete or diffuse (Figs. 12.3 and 12.4). Lymphoid lesions typically mold to structures such as the globe or bony orbit. Neuroimaging will reveal orbital lesions in up to 50 % of clinically unsuspected cases [21]. Paranasal sinus involvement is not uncommon.

It is important to emphasize the frequency of overlap that occurs between OAL and uveal lymphoma [2–6]. For this reason, ancillary imaging studies such as B-scan ultrasonography and angiography are useful in characterizing the full extent and laterality of disease. This is particularly important in cases with subtle extra-scleral extension (ESE) or occult involvement of the fellow eye. B-scan ultrasonography is a sensitive modality for detecting ESE. The pattern of ESE may be crescentic thickening, a discrete mass (often adjacent to the optic nerve), or diffuse choroidal thickening in cases where uveal lymphoma overlaps with

OAL. Fluorescein (FA) and indocyanine green angiography (ICG) are also useful in suspected cases of uveal involvement. ICG demonstrates a characteristic pattern of focal hypofluorescence corresponding to clinically observed choroidal infiltrates. These foci may represent regions of choroidal non-perfusion secondary to space-occupying choroidal infiltration by lymphoma cells. ICG is superior to FA in visualizing the choroidal circulation and is therefore a particularly useful imaging modality in confirming the diagnosis and extent of disease burden [45]. When performed, FA may show early hyperfluorescence, hypofluorescent spots corresponding clinically observed choroidal infiltrates, choroidal folds, or a normal angiogram.

12.6.2 Staging Procedures

Since OAL can coexist with lymphoma in other sites, after OAL is classified, staging is performed. This includes a thorough physical examination by an experienced medical oncologist. Invasive staging has been replaced by the use of high-resolution contrast-enhanced imaging techniques: CT of the chest, abdomen, and pelvis and MRI of the brain. Imaging of the neck is performed if cervical nodes are palpated or suspected to be enlarged. Laboratory evaluation includes complete blood count (CBC), hepatic enzymes, and serum lactate dehydrogenase (LDH). Although part of the formal staging process for lymphoma, bone marrow aspiration and biopsy has very low yield in patients with OAL in the absence of cytopenias and radiographic evidence of systemic disease.

While not typically performed by the ophthalmologist, understanding of the staging process is important for multidisciplinary management of OAL. A modified version of the Ann Arbor classification is still commonly used. Tumor types are divided into indolent or high grade based on their expected clinical behavior. Indolent tumors (EMZL, FL, LPL) are divided into two stages, while high-grade lesions (DLBCL, MZL) are divided into three stages (Table 12.3). The Ann Arbor staging system has several deficiencies for characterizing OAL, particularly as it results in a disproportionate staging distribution. Two-thirds of primary OAL cases present as a localized mass, which under the Ann Arbor system are classified as Stage 1E [9, 17, 19, 46–49]. Analysis

Table 12.3 Staging of NHL by Ann Arbor and tumor–node–metastasis systems

Ann Arbor system	
Indolent lymphomas: EMZL, FL, LPL	
Stage I	Localized disease (Ann Arbor [AA] I, IE and II, IIE)
Stage II	Disseminated disease (Ann Arbor [AA] III and IV)
Aggressive lymphomas: DLBCL, MCL	
Stage I	Localized or extranodal disease (Ann Arbor [AA] I or IE)
Stage II	2 or more nodal sites; 3 or more extranodal sites
Stage III	Stage II with additional poor prognostic features
Tumor–node–metastasis system[a]	
T classification	
	TX – Lymphoma extent not specified
	T0 – No evidence of lymphoma
	T1 – Conjunctival lymphoma alone
	T2 – Orbital lymphoma with or without conjunctival involvement
	T3 – Preseptal eyelid lymphoma in addition to conjunctival/orbital disease
	T4 – Invasion of adjacent structures, such as bone and brain
N classification	
	NX – Lymph node involvement not assessed
	N0 – No evidence of lymph node involvement
	N1 – Involvement of ipsilateral regional lymph nodes
	N2 – Involvement of contralateral or bilateral regional lymph nodes
	N3 – Involvement of peripheral lymph nodes not draining ocular adnexal region
	N4 – Involvement of central lymph nodes
M classification	
	MX – Lymphoma dissemination not assessed
	M0 – No evidence of involvement of additional extranodal sites
	M1 – Lymphoma involvement of other organs (at diagnosis or subsequently)

E Extranodal disease

[a]Modified from the American Joint Committee on Cancer (AJCC) seventh edition TNM-based staging manual for OAL

can be challenging because of the use of different criteria, but overall rates for initial staging are 60–80 % for IE, 4–25 % for IIE, and 16–18 % for Stage III and IV combined [7, 38, 39]. Studies using criteria of extraorbital disease showed Stage III and IV rates of 22–36 % at diagnosis [17, 37, 42]. This precludes the ability to differentiate the majority of OAL cases from one another based upon disease extent within the ocular adnexal structures which may have important prognostic implications [20, 50].

More recently, a tumor–node–metastasis (TNM)-based staging system for primary OAL has been developed under the guidance of the American Joint Committee on Cancer (AJCC) [51, 52]. This system addresses many of the shortcomings of the Ann Arbor system and more precisely defines disease extent. The ultimate goal of the proposed TNM-based system is to facilitate future studies aimed at identifying clinical and histomorphologic features of OAL of prognostic significance and to assess treatment outcomes. To date, the feasibility of this system has only been analyzed in a limited capacity [53].

12.7 Differential Diagnosis

The clinical and imaging differential diagnosis of OAL is extensive, due to the paucity of specific features. It includes inflammatory lesions (Fig. 12.5), benign lymphoproliferative lesions (Fig. 12.6) [34], epithelial tumors, melanocytic tumors, infectious lesions, and lacrimal gland lesions of the conjunctiva. In the orbit and lid, any mass including metastases, dacryoadenitis, inflammations, and other benign and malignant tumors must be considered.

12.8 Pathologic Features

Pathologic analysis can identify obvious lymphomas but cannot reliably differentiate lymphoma types (Fig. 12.7). Recent data has shown that using the current WHO classification, 76 % of lesions previously classified as RLH are now reclassified as lymphomas. This is due to the recognition that a small number of malignant lymphocytes, whose presence is indicative of lymphoma, can be overshadowed by surrounding normal or reactive lymphoid cells.

The common immunophenotypic expressions of the various types of OAL are shown in Table 12.1. IPA can be carried out qualitatively on tissue sections or quantitatively on dispersed cells (flow cytometry). The use of intact tissue allows localization of marker expression, which can be critical in making the correct diagnosis. For example, overexpression of cytoplasmic Bcl-2 is not seen in normal follicular structures and is consistent with follicular lymphoma (Fig. 12.8) [34]. Immunohistochemistry, however, may not detect such critically important cells when sampling effect limits their presence. Flow cytometry, in contrast, does not give

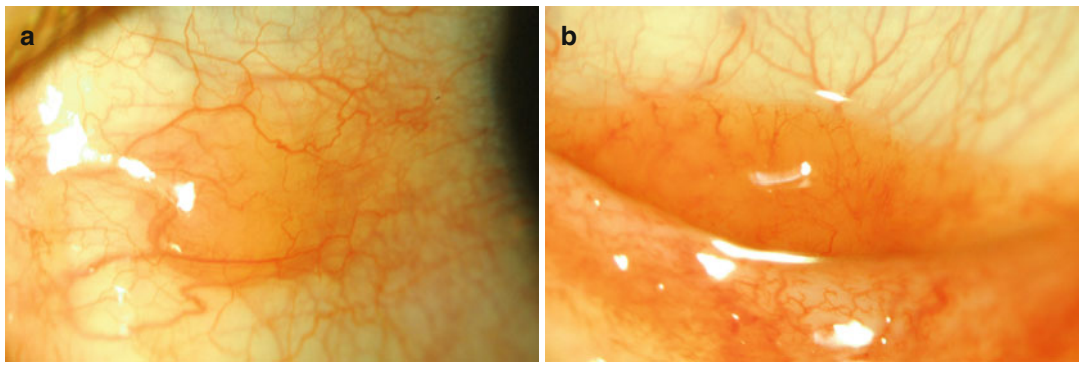

Fig. 12.5 Bulbar (**a**) and forniceal (**b**) idiopathic inflammatory conjunctival granuloma simulating ocular adnexal lymphoma

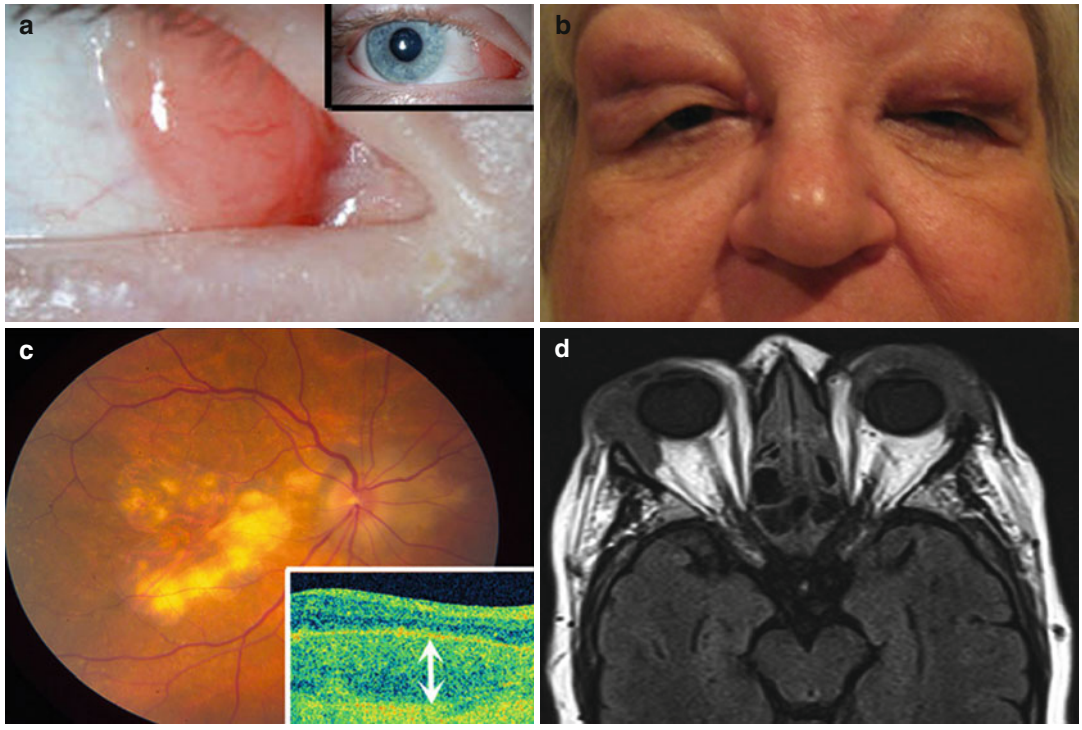

Fig. 12.6 Clinical presentations of reactive lymphoid hyperplasia. Salmon patch lesion of the right eye which was biopsy-proven RLH. *Inset* shows the lesion on the bulbar conjunctiva was limited to the medial canthal region (**a**). Facial photograph of patient with bilateral RLH of the lacrimal gland demonstrates fullness of both orbits and cheeks (**b**). Fundus photograph of the right eye of the same patient reveals creamy choroidal lesions consistent with uveal reactive hyperplasia (**c**). The *inset* demonstrates choroidal thickening observed on OCT (*arrow*). The left fundus and OCT revealed similar findings. MRI of same patient demonstrates bilateral lacrimal gland swelling (**d**). Reproduced with permission from Stacy et al. [34]

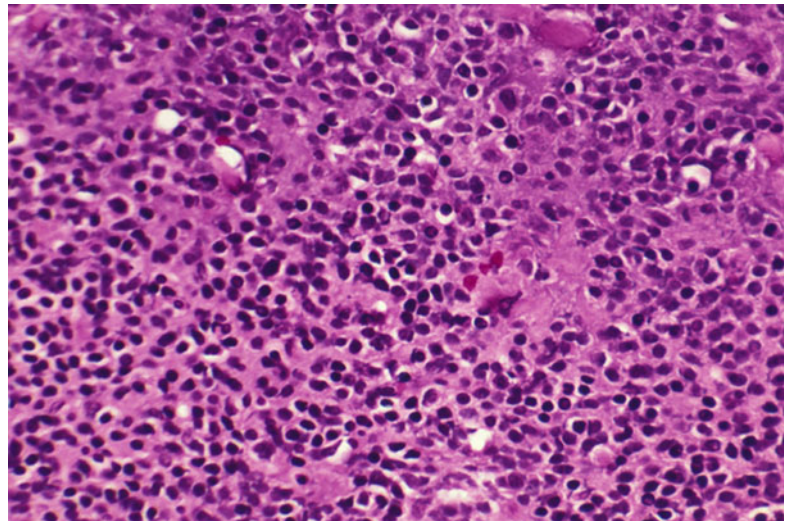

Fig. 12.7 Photomicrograph of monomorphic lymphocytes typical of EMZL-type ocular adnexal lymphoma (H&E, Original magnification ×100)

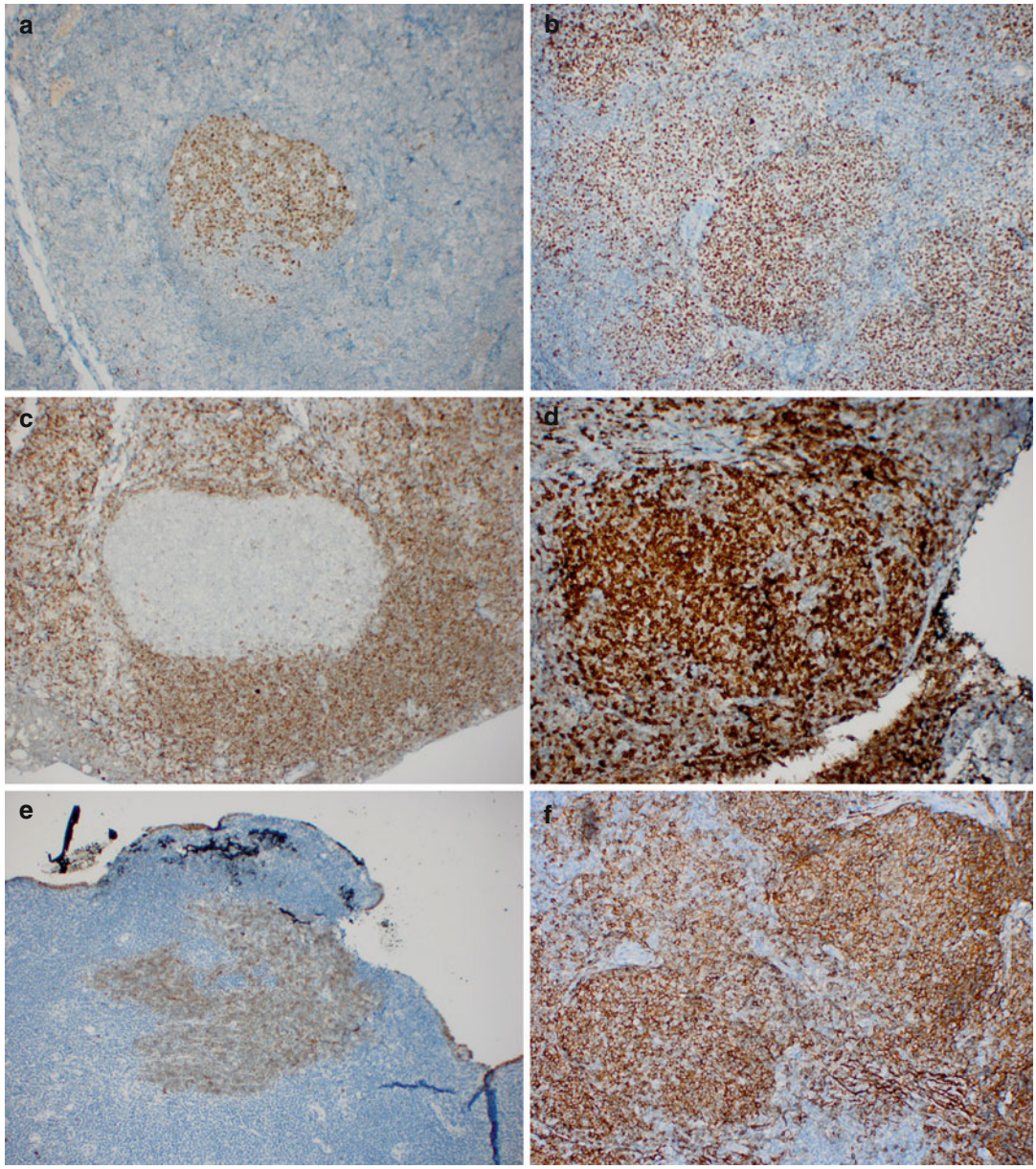

Fig. 12.8 Immunohistochemical characterization of reactive lymphoid hyperplasia and follicular lymphoma Bcl-6 stains B cells within follicles of RLH (**a**). Follicles of FL are also positive for Bcl-6 (**b**). The follicles of RLH are negative for Bcl-2 (**c**). Follicles of FL are positive for BCL-2 (**d**). Follicles in RLH are positive for CD10 (**e**). Follicles of FL are also positive for CD10 but with more interfollicular staining than RLH (**f**) (immunoperoxidase reactions, 200×) (Reproduced with permission from Stacy et al. [34])

anatomic information but can accurately assign the immunophenotype of involved cells with very small amounts of specimen.

Molecular genetic analysis of OAL is important in two ways. Identification of overexpressed heavy chain gene rearrangements is indicative of clonality and typically represents malignancy. Tumor cells can be analyzed for translocations, which may be indicative of a specific lymphoma type (Table 12.4). Translocation of the MALT

Table 12.4 Common translocations observed in ocular adnexal lymphoma

Type	Genetic change	Mechanism	Frequency	Proto-oncogene
EMZL	t(11;18)(q21;q21)	Fusion	50 %	API2/MLT
		Transcript deregulation	Rare	Bcl-10
Follicular	t(14;18)(q32;q21)	Transcript deregulation	80–90 %	Bcl-2
Mantle cell	t(11;14)	Transcript deregulation	70 %	Bcl-1 (encodes cyclin D1)
Lymphoplasmacytic	T(9;14)(p13;q32)	Transcript deregulation	50 %	PAX-5
Diffuse large B cell lymphoma	Der(3)(q27)	Transcript deregulation		Bcl-6

gene with API2 [t(11;18)(q21;q21)] is of specific interest since its presence is generally associated with more aggressive disease [54]. The expansion of the tools for lymphocyte characterization has paradoxically increased the chances for contradictory or incomplete characterizations using the new criteria. In such situations, the wisdom of an experienced hematopathologist is critical, though some lesions will remain unclassifiable.

12.9 Rare Variants

There are several rare variants and simulating conditions of OAL such as Langerhans cell histiocytosis (LCH), Rosai–Dorfman disease, T cell lymphoma, T cell/natural killer (NK)-cell lymphoma (lethal midline granuloma), and Burkitt lymphoma that we have included in this review.

12.9.1 Langerhans Cell Histiocytosis

LCH is characterized by a proliferation of Langerhans cells and inflammatory cells that generally affects children and young adults. The disease may be localized, or it may affect multiple systems including the skin, bone, lungs, and lymphatics. Ophthalmic disease is observed in 10–23 % of cases and most often manifests as a solitary lesion within the orbit; however, intraocular involvement in the form of an atrophic retinochoroidopathy has been reported [55–57]. Confirmation of diagnosis is made by biopsy, which demonstrates numerous histiocytes, giant cell formation, and eosinophilic granulocytes. Transmission electron microscopy (TEM) reveals characteristic intracytoplasmic Birbeck granules [56].

12.9.2 Rosai–Dorfman Syndrome

Also labeled as sinus histiocytosis with massive lymphadenopathy, it is a benign form of idiopathic histiocytosis that typically affects children and young adults. The majority of individuals (approximately 80 %) develop painless cervical lymphadenopathy [58]. Extranodal involvement may affect multiple systems including the respiratory tract, skin, bones, visceral organs, and the central nervous system. The disease has multiple ophthalmic manifestations including lesions within the orbit, eyelid, and lacrimal apparatus. Compressive optic neuropathy, uveitic glaucoma, serous retinal detachment, and marginal corneal infiltrates have been reported [59]. Ocular adnexal involvement occurs in approximately 10 % of patients with extranodal disease [60].

12.9.3 T Cell Lymphoma

In rare cases, OAL can be of T cell origin. In a review of 353 individuals with OAL, only a single case (0.3 %) was of T cell lineage [19]. As with B cell neoplasms, a heterogeneous group of T cell lymphomas can involve the ocular adnexal structures (Fig. 12.9). Most T cell lymphomas affecting the ocular adnexal structures are aggressive and carry a poor prognosis.

Most non-B-cell lymphomas are an extension of the malignant stage of mycosis fungoides or a secondary manifestation of systemic T cell lymphoma. In a series of seven individuals with OAL of T cell origin, three cases were peripheral T cell lymphomas (PTCL) demonstrating positivity for CD3, CD8, and βF1 and negativity for CD56. Two cases were positive for CD3 and CD30

while negative for CD56 and were classified as anaplastic large-cell lymphomas of T cell type (T-ALCL) [61]. The remaining two cases were positive for CD3 and CD56 and negative for βF1. These two cases were positive for Epstein–Barr virus (EBV) by in situ hybridization, consistent with T cell/natural killer (NK)-cell lymphoma of nasal type (also referred to as lethal midline granuloma) [61, 62].

12.9.4 Burkitt Lymphoma

Burkitt lymphoma is a rare entity associated with translocation between chromosomes 8 and 14 affecting c-myc [63]. Three forms, all of which may affect the orbit, have been described. The African type frequently involves the orbits and maxillary bones and is associated with the presence of antibodies against Epstein–Barr virus (EBV) antigens [63]. The non-African type usually affects lymph nodes, bone marrow, and viscera. The third form affects immunocompromised individuals and is associated with acquired immunodeficiency syndrome (AIDS) (Fig. 12.10) [64–66]. Recent review of 16 immunocompetent individuals with sporadic orbital Burkitt lymphoma revealed a median age at diagnosis of 12 years [67]. Presenting symptoms included proptosis, ophthalmoplegia, and eyelid edema. Fourteen (88 %) in this series had systemic involvement [67]. Biopsy of orbital lesions reveals a characteristic "starry-sky" appearance associated with Burkitt lymphoma [66]. Prognosis is guarded for this extremely aggressive lymphoma as significant mortality (54 %) is observed within 1 year of presentation [67].

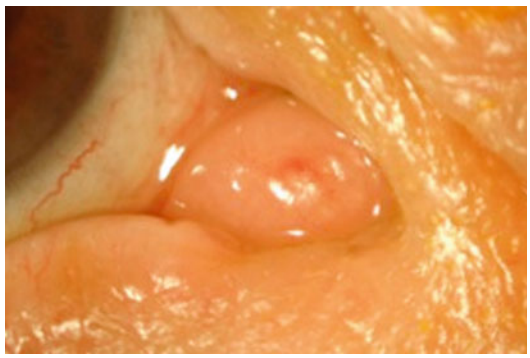

Fig. 12.9 T cell lymphoma of the caruncle in a patient with slowly progressive mycosis fungoides

12.10 Treatment

The treatment of OAL is an area of controversy, progress, and change. Currently OAL treatment depends on whether the disease is localized or systemic. Local disease can be very effectively treated with radiation alone. Systemic disease is frequently treated in a manner similar to other indolent lymphomas, typically using rituximab alone or in combination with cytotoxic

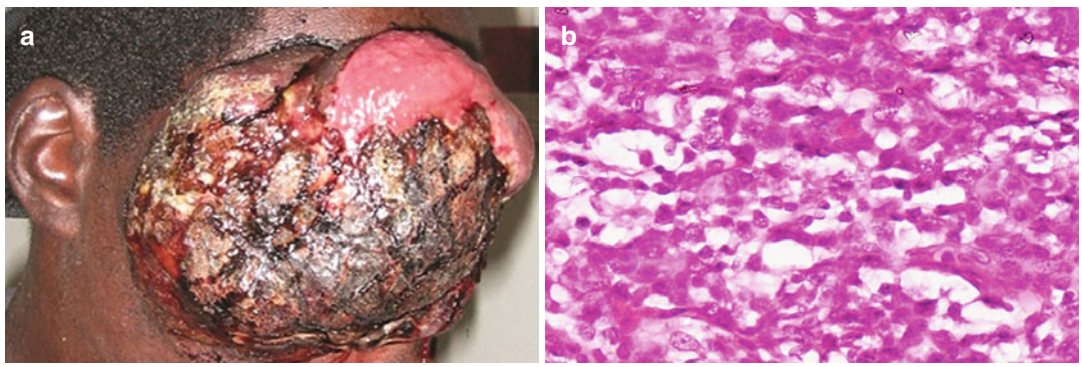

Fig. 12.10 A 24-year-old Haitian man presented with rapidly progressive right eye proptosis (**a**). An exenteration was performed and the tissue sample was sent to the pathology laboratory, which revealed the characteristic "starry-sky" appearance of a Burkitt lymphoma (**b**). The patient expired shortly after due to complications from systemic involvement. Reproduced with permission from Giuliari et al. [66]

chemotherapy. With the recognition that the vast majority of OAL are of the EMZL/MALT type and that there may be an infectious basis for this subgroup of OAL, there is possibility of deferring cytotoxic modalities. A second controversy is whether to treat indolent OAL. A survey of treatment modalities follows.

12.10.1 Surgery

Surgery has been reported to be successful in managing certain cases of highly localized OAL and has been recommended for Stage I MALT systemic lymphoma in some sites. Its applicability remains dubious for most OAL due to the diffuse nature and frequent juxtaposition of OAL to sensitive ocular tissues. Surgery should therefore be reserved for localized, isolated lesions of the conjunctiva [7, 21].

12.10.2 Cryotherapy

Cryotherapeutic ablation of OAL has limited use in the management of OAL. It has resulted in variable success due to debulking the tumor without complete elimination of malignant tissue. It may have application in a limited number of patients with conjunctival OAL who are unable to receive other treatment modalities [11].

12.10.3 Radiation

Historically, external beam radiation (EBRT) has been the most frequently used modality for treatment of OAL. Analysis of this modality is confounded by small patient numbers in most series, the use of early and inaccurate classification schemes, short follow-up times, and apparent lack of ophthalmic follow-up. Complications were detected at a rate of up to 50 % higher when close ophthalmic follow-up was performed.

Both electron and photon irradiations have been successfully employed in OAL. Dosage is based on the tumor grade or type [17, 37, 40]. Typical doses are 28–36 Gy for low-grade OAL and 30–40 Gy for high-grade OAL. The role of lens shielding to decrease cataract formation is controversial with some studies showing no effect on local recurrence and others showing recurrences occurring in patients who underwent lens-sparing radiation treatment protocols [68, 69].

Analysis of radiation dose response relationship of EMZL revealed that 5-year local tumor control rates of EMZL were 81 % with doses below 30 Gy but 100 % with doses higher than 30 Gy [37]. Variable sensitivity to radiotherapy based upon lymphoma subtype was observed as follicular lymphoma showed a 100 % response rate to both high and low doses. While radiation studies frequently emphasize the ability to obtain local control, the effect of this modality on the overall course and prognosis is less clear (Fig. 12.1b). Even Stage IV-EA disease showed good local control, though survival was significantly lower. Multiple studies revealing higher rates of delayed systemic recurrence suggest that longer follow-up is necessary for accurate assessment of treatment effect [17].

12.10.4 Chemotherapy

Since OAL frequently presents as localized disease (Stage IE), chemotherapy is rarely used, with the exception of aggressive DLBCL (Fig. 12.11) [70]. The review of chemotherapy used in lymphoma is beyond the scope of this chapter. Standard chemotherapy for OAL when it is part of more advanced disease is that of standard systemic lymphoma regimens using single-agent rituximab alone or in combination with cyclophosphamide, doxorubicin, vincristine, and prednisone (CHOP); the alkylating agent chlorambucil; and, more recently, bendamustine which has dual properties of an alkylating agent and a purine analogue. While some have used systemic corticosteroids for tumor suppression of OAL, steroids offer ineffective long-term control.

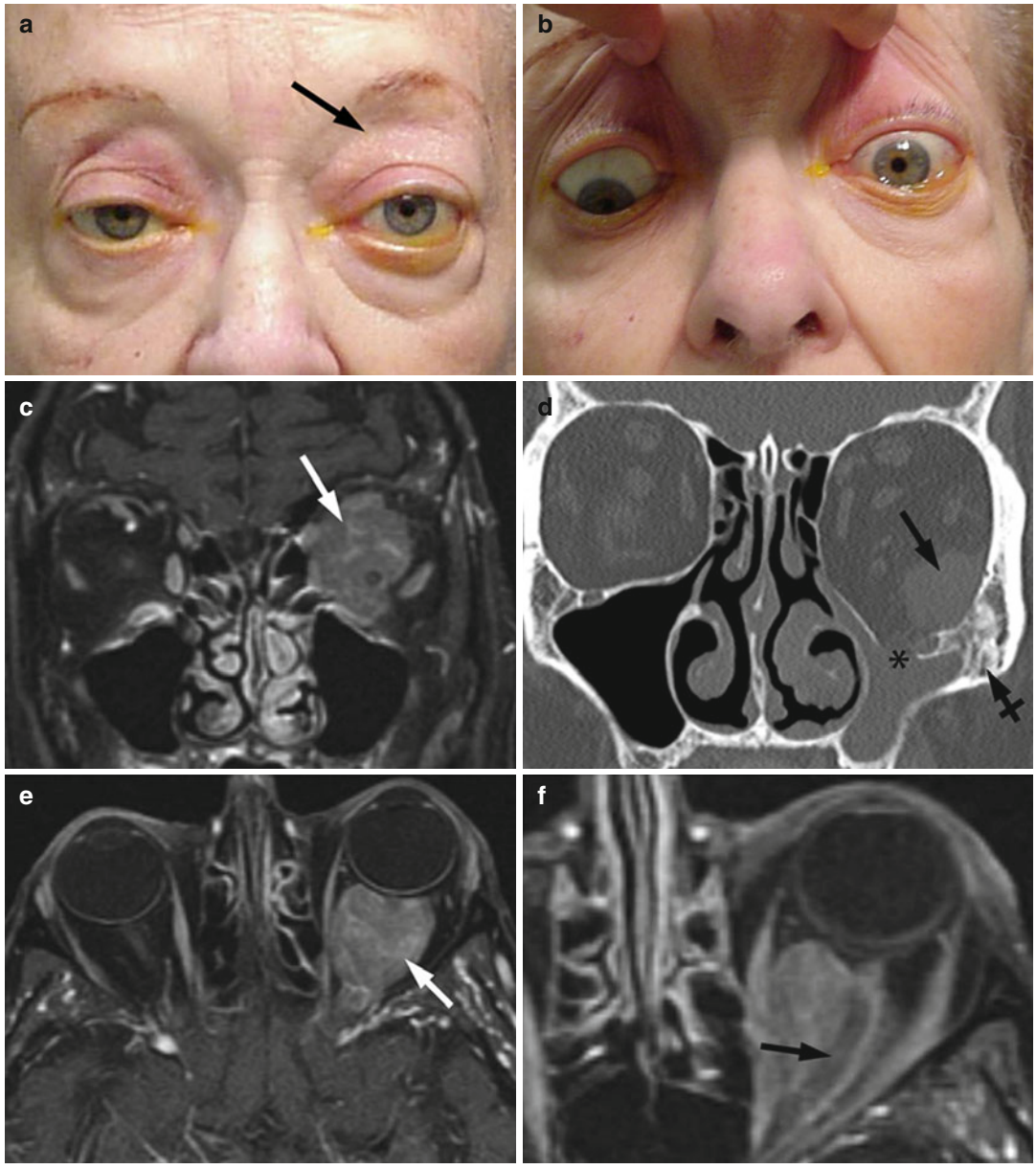

Fig. 12.11 Clinical and radiographic features of diffuse large B cell lymphoma of the orbit. (**a**) Patient with mass in the left upper orbit (*arrow*) producing mild, non-congestive proptosis. (**b**) The lesion's mass effect resulted in limited eye movements, including infraduction of the left globe. (**c**) Typical location of an orbital lymphoid tumor (*arrow*) in the superior and superonasal regions of the orbit. There is no bone erosion. (**d**) An unusual infero-temporal tumor (*arrow*) has created adjacent bone changes (*crossed arrow*). An old inferior, posttraumatic orbital floor fracture (*) explains the absence of clinical proptosis. (**e**) An intraconal, retrobulbar mass (*arrow*) is accompanied by moderate proptosis (3–4 mm). (**f**) In the same patient portrayed in (**e**), an axial CT image at the level of the optic nerve reveals that the tumor encases it (*arrow*) asymmetrically, with a more prominent component found nasally. The patient had a decline in visual acuity and an afferent pupillary defect. Reproduced with permission from Stacy et al. [70]

12.10.5 Immunotherapy

12.10.5.1 Interferon

Interferon (IFN-alpha) has been used rarely for OAL despite its long-standing use in systemic lymphoma. One report of five cases showed 80 % initial complete response with short-term follow-up [71]. One patient with Stage IIA disease died of systemic lymphoma at 1 year. More data regarding local and systemic efficacy are needed prior to acceptance of this modality.

12.10.5.2 Rituximab

Antilymphocyte antibodies are a recent form of lymphoma treatment. The most commonly used has been an antibody to CD-20, rituximab, which leads to destruction of B cells using mechanisms of complement and antibody-mediated destruction as well as induction of apoptosis. These antibodies are effective when used alone but also significantly increase the remission rates when used in combination with chemotherapy [72].

12.10.6 Antimicrobial Treatment

A recent development in OAL management is based on the IMM model of lymphomagenesis. There is increasing evidence of the role of chronic infection in OAL. Both *C. psittaci* and *H. pylori* have been implicated [29, 30]. Follow-up data from *C. psittaci* detection studies have suggested a therapeutic effect following antibiotic therapy with doxycycline, presumably by eradication of the infection which underlies lymphomagenesis. Other studies have shown an effect in small numbers of patients using anti-*H. pylori* triple therapy [73]. Overall, antibiotic treatment regimens have shown variable results by study group and geographic location [32, 74]. Larger studies are needed to clarify the role of antibiotics in treatment of OAL.

12.11 Prognosis

Prognosis of OAL is evaluated in three ways: local control, systemic involvement, and death from lymphoma. Excellent local control has been reported using external beam radiation. Among OAL, EMZL has a quantitatively better prognosis than other tumor types with regard to spread of tumor and lymphoma-related death, though the risk ratio was similar among the milder forms EMZL, LPCL, and FCL. The mortality ranges were EMZL 0–20 %, DLBCL 25–75 %, FL 20–37 %, MCL 38–100 %, and LPL 14–100 % [7, 17, 37, 38].

Extraorbital spread can occur in over 45 % of EMZL patients with mean follow-up of 63 months, suggesting that longer follow-up is needed [17]. Patients with indolent disease may survive decades without treatment.

12.12 Future Research

Future research will be focused on the mechanisms of lymphomagenesis to determine whether prelymphomatous conditions can be detected and treated with less toxic methods. One key question is whether the role of infectious agents will be as important as in gastric lymphoma where it has revolutionized care. Understanding lymphomagenesis may also allow for more targeted therapeutic agents.

References

1. Freeman C, Berg JW, Cutler SJ. Occurrence and prognosis of extranodal lymphomas. Cancer. 1972;29(1):252–60.
2. Fuller ML, Sweetenham J, Schoenfield L, Singh AD. Uveal lymphoma: a variant of ocular adnexal lymphoma. Leuk Lymphoma. 2008;49(12):2393–7.
3. Grossniklaus HE, Martin DF, Avery R, et al. Uveal lymphoid infiltration. Report of four cases and clinicopathologic review. Ophthalmology. 1998;105(7):1265–73.
4. Baryla J, Allen LH, Kwan K, et al. Choroidal lymphoma with orbital and optic nerve extension: case and review of literature. Can J Ophthalmol. 2012;47(1):79–81.
5. Sarraf D, Jain A, Dubovy S, et al. Mucosa-associated lymphoid tissue lymphoma with intraocular involvement. Retina. 2005;25(1):94–8.
6. Tagami M, Nagai T, Sekimukai D, et al. Uveal extranodal marginal zone B-cell lymphoma of the mucosa-associated lymphoid tissue type with concomitant extraocular lesions in a Japanese man. Jpn J Ophthalmol. 2011;55(5):585–7.

7. Coupland SE, Hellmich M, Auw-Haedrich C, et al. Prognostic value of cell-cycle markers in ocular adnexal lymphoma: an assessment of 230 cases. Graefes Arch Clin Exp Ophthalmol. 2004;242(2):130–45.
8. Cohen VM, Sweetenham J, Singh AD. Ocular adnexal lymphoma. What is the evidence for an infectious aetiology? Br J Ophthalmol. 2008;92(4):446–8.
9. Hatef E, Roberts D, McLaughlin P, et al. Prevalence and nature of systemic involvement and stage at initial examination in patients with orbital and ocular adnexal lymphoma. Arch Ophthalmol. 2007;125(12):1663–7.
10. Bayraktar S, Bayraktar UD, Stefanovic A, Lossos IS. Primary ocular adnexal mucosa-associated lymphoid tissue lymphoma (MALT): single institution experience in a large cohort of patients. Br J Haematol. 2011;152(1):72–80.
11. Shields CL, Shields JA, Carvalho C, et al. Conjunctival lymphoid tumors: clinical analysis of 117 cases and relationship to systemic lymphoma. Ophthalmology. 2001;108(5):979–84.
12. Fisher SG, Fisher RI. The epidemiology of non-Hodgkin's lymphoma. Oncogene. 2004;23(38): 6524–34.
13. Shields JA, Bakewell B, Augsburger JJ, Flanagan JC. Classification and incidence of space-occupying lesions of the orbit. A survey of 645 biopsies. Arch Ophthalmol. 1984;102(11):1606–11.
14. Char DH. Orbital lymphoid lesions. In: Char DH, editor. Clinical ocular oncology. Philadelphia: Lippincott-Raven; 1997.
15. Henderson JW. The individual tumors. In: Henderson JW, Farrow GM, editors. Orbital tumors. New York: Raven; 1994.
16. Spraul CW, Grossniklaus HE. Analysis of 24,444 surgical specimens accessioned over 55 years in an ophthalmic pathology laboratory. Int Ophthalmol. 1997;21(5):283–304.
17. Jenkins C, Rose GE, Bunce C, et al. Histological features of ocular adnexal lymphoma (REAL classification) and their association with patient morbidity and survival. Br J Ophthalmol. 2000;84(8):907–13.
18. Jenkins C, Rose GE, Bunce C, et al. Clinical features associated with survival of patients with lymphoma of the ocular adnexa. Eye (Lond). 2003;17(7):809–20.
19. Ferry JA, Fung CY, Zukerberg L, et al. Lymphoma of the ocular adnexa: a study of 353 cases. Am J Surg Pathol. 2007;31(2):170–84.
20. Knowles DM, Jakobiec FA, McNally L, Burke JS. Lymphoid hyperplasia and malignant lymphoma occurring in the ocular adnexa (orbit, conjunctiva, and eyelids): a prospective multiparametric analysis of 108 cases during 1977 to 1987. Hum Pathol. 1990;21(9):959–73.
21. Stafford SL, Kozelsky TF, Garrity JA, et al. Orbital lymphoma: radiotherapy outcome and complications. Radiother Oncol. 2001;59(2):139–44.
22. Cockerham GC, Hidayat AA, Bijwaard KE, Sheng ZM. Re-evaluation of "reactive lymphoid hyperplasia of the uvea": an immunohistochemical and molecular analysis of 10 cases. Ophthalmology. 2000;107(1):151–8.
23. LeBien TW, Tedder TF. B lymphocytes: how they develop and function. Blood. 2008;112(5):1570–80.
24. Ye H, Liu H, Attygalle A, et al. Variable frequencies of t(11;18)(q21;q21) in MALT lymphomas of different sites: significant association with CagA strains of H pylori in gastric MALT lymphoma. Blood. 2003;102(3):1012–8.
25. Raffeld M, Jaffe ES. bcl-1, t(11;14), and mantle cell-derived lymphomas. Blood. 1991;78(2):259–63.
26. Takada S, Yoshino T, Taniwaki M, et al. Involvement of the chromosomal translocation t(11;18) in some mucosa-associated lymphoid tissue lymphomas and diffuse large B-cell lymphomas of the ocular adnexa: evidence from multiplex reverse transcriptase-polymerase chain reaction and fluorescence in situ hybridization on using formalin-fixed, paraffin-embedded specimens. Mod Pathol. 2003;16(5): 445–52.
27. Remstein ED, James CD, Kurtin PJ. Incidence and subtype specificity of API2-MALT1 fusion translocations in extranodal, nodal, and splenic marginal zone lymphomas. Am J Pathol. 2000;156(4):1183–8.
28. Hoover RN. Lymphoma risks in populations with altered immunity – a search for mechanism. Cancer Res. 1992;52(19 Suppl):5477s–8.
29. Ferreri AJ, Guidoboni M, Ponzoni M, et al. Evidence for an association between Chlamydia psittaci and ocular adnexal lymphomas. J Natl Cancer Inst. 2004; 96(8):586–94.
30. Chan CC, Smith JA, Shen DF, et al. Helicobacter pylori (H. pylori) molecular signature in conjunctival mucosa-associated lymphoid tissue (MALT) lymphoma. Histol Histopathol. 2004;19(4):1219–26.
31. Chanudet E, Zhou Y, Bacon CM, et al. Chlamydia psittaci is variably associated with ocular adnexal MALT lymphoma in different geographical regions. J Pathol. 2006;209(3):344–51.
32. Husain A, Roberts D, Pro B, et al. Meta-analyses of the association between Chlamydia psittaci and ocular adnexal lymphoma and the response of ocular adnexal lymphoma to antibiotics. Cancer. 2007; 110(4):809–15.
33. Amin S, Ramsay A. Orbital and lacrimal gland progressive transformation of germinal centres – an underdiagnosed entity? Br J Ophthalmol. 2012;96(9): 1242–5.
34. Stacy RC, Jakobiec FA, Schoenfield L, Singh AD. Unifocal and multifocal reactive lymphoid hyperplasia vs follicular lymphoma of the ocular adnexa. Am J Ophthalmol. 2010;150(3):412–26.e1.
35. Harris NL, Jaffe ES, Stein H, et al. A revised European-American classification of lymphoid neoplasms: a proposal from the International Lymphoma Study Group. Blood. 1994;84(5):1361–92.
36. Swerdlow SH, Campo E, Harris NL, et al., editors. World Health Organization Classification of Tumours of Haematopoietic and Lymphoid Tissues. Lyon: IARC Press; 2008.
37. Fung CY, Tarbell NJ, Lucarelli MJ, et al. Ocular adnexal lymphoma: clinical behavior of distinct

World Health Organization classification subtypes. Int J Radiat Oncol Biol Phys. 2003;57(5):1382–91.
38. McKelvie PA, McNab A, Francis IC, et al. Ocular adnexal lymphoproliferative disease: a series of 73 cases. Clin Experiment Ophthalmol. 2001;29(6): 387–93.
39. Mannami T, Yoshino T, Oshima K, et al. Clinical, histopathological, and immunogenetic analysis of ocular adnexal lymphoproliferative disorders: characterization of malt lymphoma and reactive lymphoid hyperplasia. Mod Pathol. 2001;14(7):641–9.
40. Bhatia S, Paulino AC, Buatti JM, et al. Curative radiotherapy for primary orbital lymphoma. Int J Radiat Oncol Biol Phys. 2002;54(3):818–23.
41. Sharara N, Holden JT, Wojno TH, et al. Ocular adnexal lymphoid proliferations: clinical, histologic, flow cytometric, and molecular analysis of forty-three cases. Ophthalmology. 2003;110(6):1245–54.
42. Nakata M, Matsuno Y, Katsumata N, et al. Histology according to the Revised European-American Lymphoma Classification significantly predicts the prognosis of ocular adnexal lymphoma. Leuk Lymphoma. 1999;32(5–6):533–43.
43. White VA, Gascoyne RD, McNeil BK, et al. Histopathologic findings and frequency of clonality detected by the polymerase chain reaction in ocular adnexal lymphoproliferative lesions. Mod Pathol. 1996;9(11):1052–61.
44. Cho EY, Han JJ, Ree HJ, et al. Clinicopathologic analysis of ocular adnexal lymphomas: extranodal marginal zone b-cell lymphoma constitutes the vast majority of ocular lymphomas among Koreans and affects younger patients. Am J Hematol. 2003; 73(2):87–96.
45. Saatci AO, Arikan G, Ozcan MA, et al. Indocyanine green angiographic features of systemic non-Hodgkin's lymphoma and bilateral choroidal involvement. Ophthalmic Surg Lasers Imaging. 2006;37(3):236–9.
46. Coupland SE, Krause L, Delecluse HJ, et al. Lymphoproliferative lesions of the ocular adnexa. Analysis of 112 cases. Ophthalmology. 1998;105(8): 1430–41.
47. Decaudin D, de Cremoux P, Vincent-Salomon A, et al. Ocular adnexal lymphoma: a review of clinicopathologic features and treatment options. Blood. 2006;108(5):1451–60.
48. Gardiner JA, White VA, Gascoyne RD, Rootman J. Histopathologic, immunophenotypic and genotypic analyses in ocular adnexal lymphoproliferative disorders. Aust N Z J Ophthalmol. 1992;20(3):247–51.
49. Plaisier MB, Sie-Go DM, Berendschot TT, et al. Ocular adnexal lymphoma classified using the WHO classification: not only histology and stage, but also gender is a predictor of outcome. Orbit. 2007;26(2):83–8.
50. Johnson TE, Tse DT, Byrne Jr GE, et al. Ocular-adnexal lymphoid tumors: a clinicopathologic and molecular genetic study of 77 patients. Ophthal Plast Reconstr Surg. 1999;15(3):171–9.
51. Coupland SE, White VA, Rootman J, et al. A TNM-based clinical staging system of ocular adnexal lymphomas. Arch Pathol Lab Med. 2009;133(8):1262–7.
52. Edge SE, Byrd DR, Compton CC, et al. AJCC cancer staging manual. 7th ed. New York: Springer; 2009. http://www.springerlink.com. Accessed 18 Jan 2013.
53. Lee SE, Paik JS, Cho WK, et al. Feasibility of the TNM-based staging system of ocular adnexal extranodal marginal zone lymphoma of mucosa-associated lymphoid tissue (MALT lymphoma). Am J Hematol. 2011;86(3):262–6.
54. Liu H, Ye H, Dogan A, et al. T(11;18)(q21;q21) is associated with advanced mucosa-associated lymphoid tissue lymphoma that expresses nuclear BCL10. Blood. 2001;98(4):1182–7.
55. Moore AT, Pritchard J, Taylor DS. Histiocytosis X: an ophthalmological review. Br J Ophthalmol. 1985; 69(1):7–14.
56. Herwig MC, Wojno T, Zhang Q, Grossniklaus HE. Langerhans cell histiocytosis of the orbit: five clinicopathologic cases and review of the literature. Surv Ophthalmol. 2013;58(4):330–40.
57. Thanos A, Vavvas D, Young LH, Foster CS. Choroidal neovascular membrane formation and retinochoroidopathy in a patient with systemic langerhans cell histiocytosis: a case report and review of the literature. Case Rep Ophthalmol. 2012;3(1):128–35.
58. Rosai J, Dorfman RF. Sinus histiocytosis with massive lymphadenopathy: a pseudolymphomatous benign disorder. Analysis of 34 cases. Cancer. 1972;30(5):1174–88.
59. Vemuganti GK, Naik MN, Honavar SG. Rosai Dorfman disease of the orbit. J Hematol Oncol. 2008;1:7.
60. Zimmerman LE, Hidayat AA, Grantham RL, et al. Atypical cases of sinus histiocytosis (Rosai-Dorfman disease) with ophthalmological manifestations. Trans Am Ophthalmol Soc. 1988;86:113–35.
61. Coupland SE, Foss HD, Assaf C, et al. T-cell and T/natural killer-cell lymphomas involving ocular and ocular adnexal tissues: a clinicopathologic, immunohistochemical, and molecular study of seven cases. Ophthalmology. 1999;106(11):2109–20.
62. Mendenhall WM, Olivier KR, Lynch Jr JW, Mendenhall NP. Lethal midline granuloma-nasal natural killer/T-cell lymphoma. Am J Clin Oncol. 2006;29(2):202–6.
63. Ruf IK, Rhyne PW, Yang H, et al. Epstein-Barr virus regulates c-MYC, apoptosis, and tumorigenicity in Burkitt lymphoma. Mol Cell Biol. 1999;19(3):1651–60.
64. Burkitt D. A sarcoma involving the jaws in African children. Br J Surg. 1958;46(197):218–23.
65. Reifler DM, Warzynski MJ, Blount WR, et al. Orbital lymphoma associated with acquired immune deficiency syndrome (AIDS). Surv Ophthalmol. 1994; 38(4):371–80.
66. Giuliari GP, Sadaka A, Cortez MA, Paniagua A. Orbital Burkitt's lymphoma: an aggressive presentation. Case Rep Ophthalmol Med. 2012;2012:354043.

67. Baker PS, Gold KG, Lane KA, et al. Orbital Burkitt lymphoma in immunocompetent patients: a report of 3 cases and a review of the literature. Ophthal Plast Reconstr Surg. 2009;25(6):464–8.
68. Le QT, Eulau SM, George TI, et al. Primary radiotherapy for localized orbital MALT lymphoma. Int J Radiat Oncol Biol Phys. 2002;52(3):657–63.
69. Uno T, Isobe K, Shikama N, et al. Radiotherapy for extranodal, marginal zone, B-cell lymphoma of mucosa-associated lymphoid tissue originating in the ocular adnexa: a multiinstitutional, retrospective review of 50 patients. Cancer. 2003;98(4):865–71.
70. Stacy RC, Jakobiec FA, Herwig MC, et al. Diffuse large B-cell lymphoma of the orbit: clinicopathologic, immunohistochemical, and prognostic features of 20 cases. Am J Ophthalmol. 2012;154(1):87–98.
71. Blasi MA, Gherlinzoni F, Calvisi G, et al. Local chemotherapy with interferon-alpha for conjunctival mucosa-associated lymphoid tissue lymphoma: a preliminary report. Ophthalmology. 2001;108(3):559–62.
72. Sullivan TJ, Grimes D, Bunce I. Monoclonal antibody treatment of orbital lymphoma. Ophthal Plast Reconstr Surg. 2004;20(2):103–6.
73. Abramson DH, Rollins I, Coleman M. Periocular mucosa-associated lymphoid/low grade lymphomas: treatment with antibiotics. Am J Ophthalmol. 2005; 140(4):729–30.
74. Ferreri AJ, Govi S, Pasini E, et al. Chlamydophila psittaci eradication with doxycycline as first-line targeted therapy for ocular adnexae lymphoma: final results of an international phase II trial. J Clin Oncol. 2012;30(24):2988–94.

Malignant Orbital Tumors

13

Bhupendra C.K. Patel

Contents

Malignant orbital tumors represent a broad spectrum of tumors which include primary tumors, secondary tumors (extension from adjacent structures), and metastatic tumors. In addition, orbital inflammation and infection may clinically simulate an orbital neoplasm (Chapter 6). In a recent survey of 1,264 consecutive patients with suspected orbital tumor referred to an ophthalmic oncology center, 36 % were malignant tumors [1]. The percentage of malignant tumors increases with age, due to higher incidence of lymphoma and metastasis in the older age groups [1].

Malignant tumors of vascular (Chapter 7), neural (Chapter 9), fibrous, and osseous origin are rare in the orbit. Rhabdomyosarcoma is the

B.C.K. Patel, MD, FRCS
Division of Oculoplastic and Orbital Service,
John A. Moran Eye Center, 50 North Medical Drive,
Salt Lake City, UT 84132, USA
e-mail: bhupendra.patel@hsc.utah.edu

J.D. Perry, A.D. Singh (eds.), *Clinical Ophthalmic Oncology*,
DOI 10.1007/978-3-642-40492-4_13, © Springer-Verlag Berlin Heidelberg 2014

most frequent primary malignant orbital tumor in children (Chapter 14), and lymphoproliferative disorders including lymphoma are most frequent in older adults (Chapter 12). Malignant orbital tumors may also arise from the lacrimal gland (Chapter 10) and lacrimal sac (Chapter 11). The details of clinical examination (Chapter 1), clinical evaluation (Chapter 2), and imaging techniques (Chapter 5) supplement contents of this review. Malignant orbital tumors not covered under other chapters are reviewed herein.

13.1 Esthesioneuroblastoma

13.1.1 Introduction

Esthesioneuroblastoma is a tumor of neural crest origin that arises from the sensory olfactory epithelium and can invade the cribriform plate, the ethmoid sinuses, and the orbit. Most esthesioneuroblastomas seen in the orbit have invaded the orbit secondarily [2]. Approximately 25 % of newly diagnosed esthesioneuroblastomas will present with orbital extension. The peak incidence is in the second to third decades. They are frequently mistaken for other small cell tumors.

13.1.2 Clinical Features

When confined to the nasal cavity or paranasal sinus, patients will have nasal obstruction, bloody nasal discharge, and headache. Three-quarters of patients with olfactory esthesioneuroblastoma have ophthalmic symptoms such as periorbital pain, epiphora, decreased vision, and diplopia. The most common ophthalmic signs include eyelid edema and proptosis. Ptosis and cranial nerve palsies may also be present.

13.1.3 Diagnostic Evaluation

CT scans show an isodense homogenous tumor in the nasal cavity and ethmoid sinus, often with orbital extension [3]. Esthesioneuroblastomas are classified according to their location: Group A tumors are confined to the nasal cavity, group B tumors affect the nasal cavity and one or more paranasal sinuses, and group C tumors extend into the cranium or orbit.

13.1.4 Treatment

The prognosis is best for group A (75 % survival at 5 years) and worst for group C (less than 45 % survival at 5 years). Treatment consists of aggressive craniofacial resection with adjunctive radiotherapy and chemotherapy. Esthesioneuroblastoma is characterized by extended remissions and multiple recurrences.

13.2 Malignant Peripheral Nerve Sheath Tumor

13.2.1 Introduction

This rare tumor may develop de novo, following radiotherapy, or secondary to plexiform neurofibroma. About 50 % of patients with malignant peripheral nerve sheath tumors are associated with neurofibromatosis [4].

13.2.2 Clinical Features

These tumors are seen in the fourth and fifth decades, except in patients with neurofibromatosis when it occurs in the teens. Patients present with proptosis and globe displacement. Periorbital pain, hypoesthesia, ptosis, and visual loss frequently occur.

13.2.3 Diagnostic Evaluation

CT imaging shows an irregular, nodular, poorly defined mass. There may be bone destruction or enlargement of the superior orbital fissure. The supraorbital nerve is more commonly affected. T1-weighted MRI shows a heterogenous signal isointense with muscle and hypointense to fat. T2-weighted sequence shows a signal that is hyperintense to both muscle and fat [5]. Ultrasound

may show cystic spaces within the tumor. Histopathologically, the tumors can resemble fibrosarcomas with long fascicles of spindle cells forming a herringbone pattern. Immunostaining for S-100 protein, Leu-7, and myelin basic protein confirms nerve sheath differentiation.

13.2.4 Treatment

In cases of orbital involvement, exenteration is often needed. Ancillary chemotherapy and radiotherapy have been used but do not appear to improve survival. Recurrences are typical and often grow rapidly. Sometimes, recurrences are seen after many years. Most patients with orbital disease develop intracranial extension or pulmonary metastases [6].

13.3 Alveolar Soft Part Sarcoma

13.3.1 Introduction

This is a rare tumor, believed to be of myogenic origin [7]. It occurs mostly in the lower extremities and buttocks. Head and neck region is the site of primary tumor in only 10 % of cases. The mean age at presentation is 20–30 years. Females are affected three times more frequently than males.

13.3.2 Clinical Features

Proptosis and globe displacement develop rapidly over 4–6 months. Apical tumors cause visual loss, orbital congestion, and ocular motility disturbances. Sensory nerve involvement causes pain [8]. Anterior masses may present as eyelid lumps with dilated epibulbar vessels.

13.3.3 Diagnostic Evaluation

CT imaging shows a moderately well-defined mass, usually involving the superior orbit with marked contrast enhancement owing to tumor hypervascularity. Tumor necrosis results in a central area of low attenuation. Histopathology shows large, round, or polygonal cells with large nuclei and prominent nucleoli.

13.3.4 Treatment

Wide surgical resection is mandatory. For recurrences or large tumors, orbital exenteration is necessary. The role of chemotherapy and radiotherapy has not definitively been determined [9]. Tumors localized to the orbit carry a better prognosis than alveolar soft part sarcoma developing in the lower extremities and buttocks. The tumor-related mortality is about 15 % over 10 years for orbital alveolar soft part sarcoma.

13.4 Osteosarcoma

13.4.1 Introduction

Osteosarcoma, also called osteogenic sarcoma, is the most common primary malignant neoplasm of bone. Most cases arise de novo but may arise secondary to Paget's disease, fibrous dysplasia, radiation therapy, giant cell tumor, or osteoblastoma [10]. Osteosarcoma is also seen as a second tumor in patients with familial retinoblastoma, even in the absence of a history of radiotherapy [11]. Although it may affect any of the orbital bones, the maxillary bone is the most frequent orbital site of the tumor.

13.4.2 Clinical Features

Most patients present with chronic symptoms, of at least several months to a year. Presentations include proptosis, dysesthesias, and diplopia. However, patients may present with rapid onset painful proptosis and sudden decrease in vision.

13.4.3 Diagnostic Evaluation

CT imaging shows a mixed lytic and sclerotic mass with indistinct margins. The appearance

depends upon the predominance of osseous, cartilaginous, or fibrous tissue components. Bone destruction and calcification with new bone formation often occurs.

13.4.4 Treatment

Management of osteosarcoma involves preoperative chemotherapy, resection, and continuation of the chemotherapy. Radiotherapy may be used as an adjunctive treatment for residual tumor. The prognosis of osteosarcoma involving the orbital bones remains poor. It is rare for a patient to survive 5 years following treatment.

13.5 Malignant Fibrous Histiocytoma

Fibrous histiocytoma is the most common mesenchymal orbital tumor in adults, seen most commonly in middle-aged adults (Chapter 91) [12]. They may be benign, locally aggressive, or malignant (Chapter 28). Patients present with proptosis, a mass effect, decreased vision, double vision, pain, eyelid swelling, and ptosis (Fig. 13.1). Malignant fibrous histiocytoma or myxofibrosarcoma may arise de novo or follow orbital radiotherapy, especially in children with the germline mutation of retinoblastoma (Chapter 71). Malignant fibrous histiocytoma requires exenteration. Although metastases are rare, the tumor shows local infiltrative features with a tendency to local recurrence.

13.6 Leiomyosarcoma

13.6.1 Introduction

Leiomyosarcomas are usually seen as radiation-induced tumors following orbital irradiation in children. They arise from the smooth muscle in blood vessels, Muller's muscle, and smooth muscle precursor cells decades after the radiation [13, 14].

13.6.2 Clinical Features

Patients present with progressive painless proptosis. The duration of symptoms varies from 6 weeks to 18 months. Globe proptosis and displacement are seen. Patients develop motility disturbance and visual loss. Anterior lesions may be palpable as a firm mass [15].

13.6.3 Diagnostic Evaluation

A heterogeneously dense, well-defined, lobulated mass is seen within the orbit on CT scans. The borders may mold around the globe. Destruction of the adjacent bone may be seen. Histopathology may show well-differentiated or poorly differentiated tumors with multinucleated giant cells [16].

13.6.4 Treatment

Most cases require aggressive resection with extended orbital exenteration, including adjacent bones. Local or small tumors may be treated with local resection and adjunctive radiotherapy. Systemic metastases require chemotherapy. Local resection alone is associated with 60 % local recurrence within 3 years. Most patients progress to develop metastases to the lungs, liver, kidney, and brain.

13.7 Liposarcoma

13.7.1 Introduction

Liposarcoma is common soft tissue sarcoma in adults, but it rarely arises within the orbit [17]. Very rarely, liposarcoma may metastasize to the orbit [18].

13.7.2 Clinical Features

There are no specific clinical features diagnostic of liposarcoma. In a series of five cases, diplopia

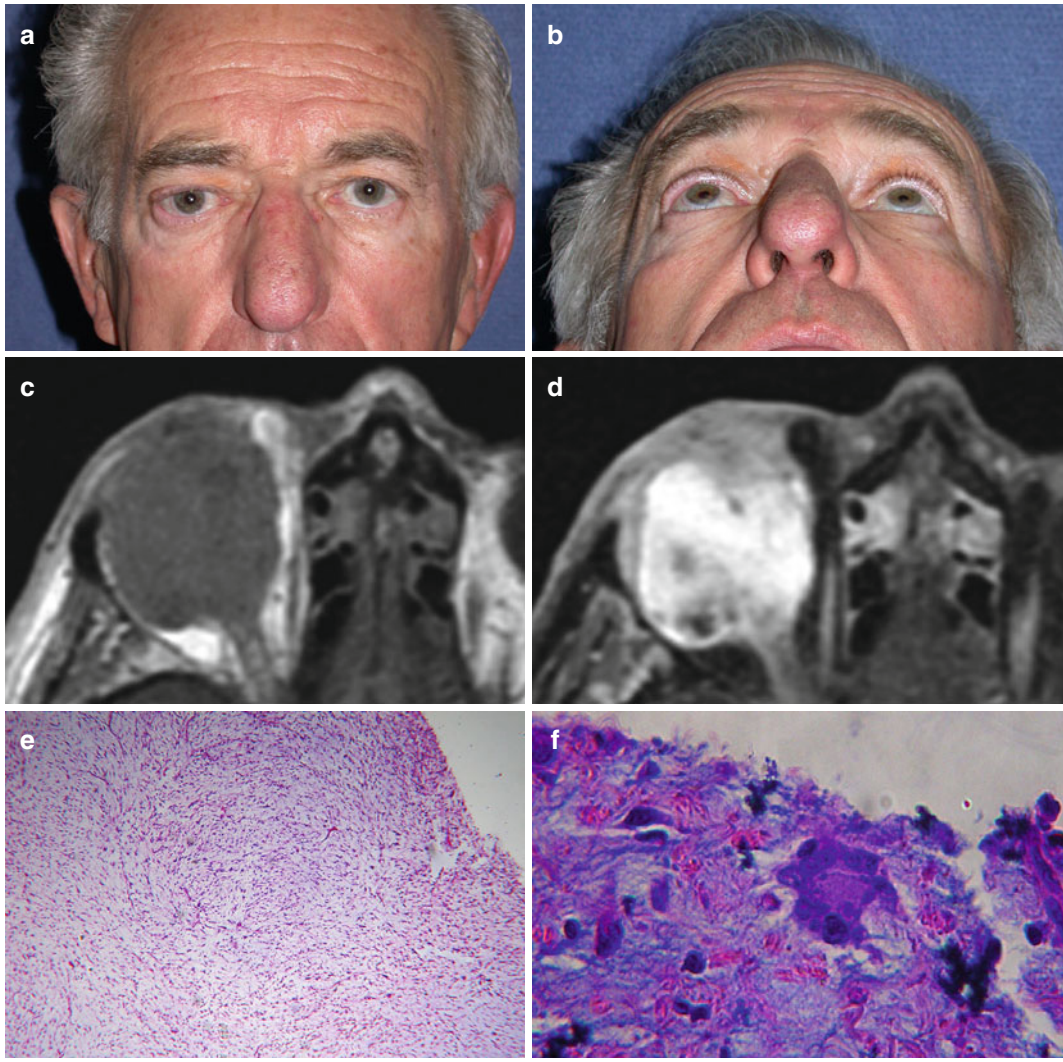

Fig. 13.1 Malignant histiocytoma or myxofibrosarcoma. A 75-year-old male with onset of double vision over 2 months and limitation of ocular movements in all fields of gaze. Note hypoglobus (**a**) and proptosis (**b**) on the right side. MRI shows a right superior orbital mass (**c**) which enhances irregularly with gadolinium (**d**). On histopathology, storiform or cartwheel-like growth pattern is seen (**e**). Note Touton giant cell (**f**). Exenteration was performed and the patient is recurrence-free at 4 years

and proptosis were most frequent clinical findings (Fig. 13.2) [19].

13.7.3 Diagnostic Evaluation

CT scan appearance of fat density enclosed by a radiodense pseudocapsule can lead to an initial impression of a cyst [19]. MRI will confirm presence of fat within the lesion (hyperintense signals in T1-weighted images) [19]. Liposarcoma should be considered in the differential diagnosis of any unusual mesenchymal tumor in the orbit [17].

13.7.4 Treatment

Limited resection followed by radiation may be adequate treatment in well-differentiated tumors

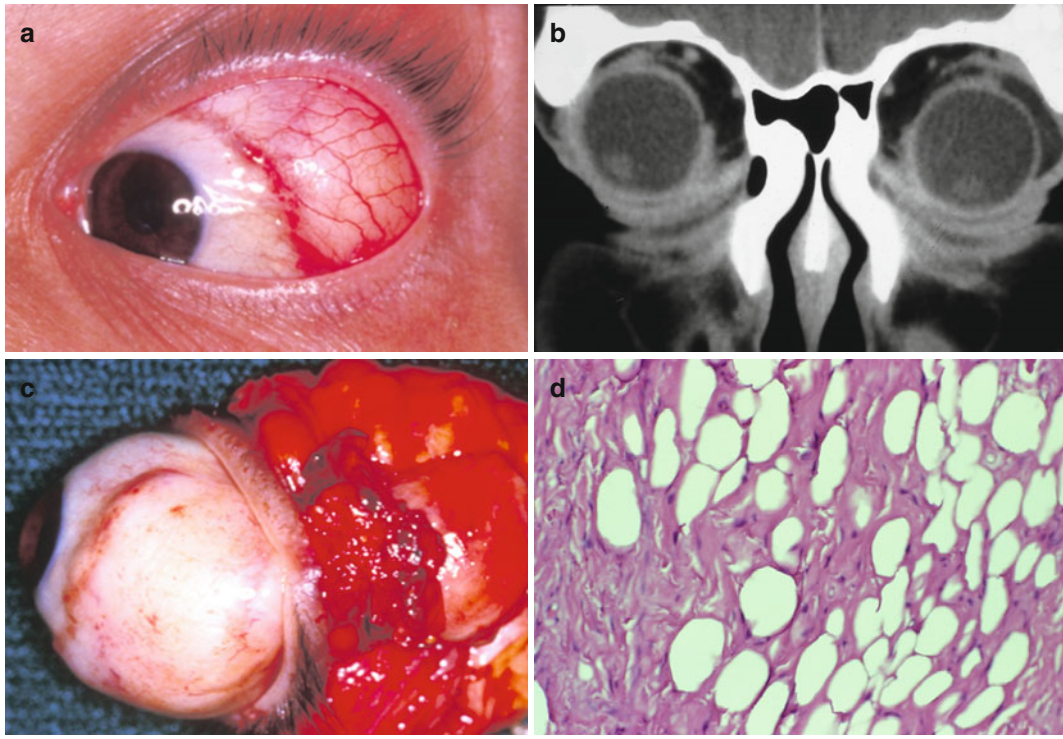

Fig. 13.2 Liposarcoma. A 45-year-old male presents with left retrobulbar pain and a mass in the superotemporal fornix (**a**). CT scan shows a superotemporal mass with the consistency of fat (**b**). Gross specimen of exenteration although some patients can be managed with local excision (**c**). Low-grade liposarcoma with vacuolated and signet ring cells (**d**)

without invasion into orbital structures [20]. In some cases, despite exenteration and radiation, delayed local recurrence has been observed [21]. Regional or distant metastases are uncommon [19].

13.8 Secondary Orbital Tumors

13.8.1 Introduction

Secondary orbital tumors represent contiguous orbital extension of a primary ocular, conjunctival, eyelid, sinus, or intracranial tumor. Basal cell carcinoma, squamous cell carcinoma, melanoma, and sebaceous cell carcinoma of the eyelid may secondarily invade the orbit because of late presentation, incomplete excision (sebaceous cell carcinoma), rapid and aggressive growth, or perineural spread (squamous cell carcinoma and melanoma).

13.8.2 Clinical Features

13.8.2.1 Basal Cell Carcinoma

Basal cell carcinoma invasion of the orbit is most often seen medially with extraocular muscle restriction and fixation of the tumor to the adjacent bone (Fig. 13.3) [22].

13.8.2.2 Squamous Cell Carcinoma

Squamous cell carcinoma tends to spread along fascia and fatty planes relatively rapidly compared to basal cell carcinoma (Fig. 13.4). Perineural invasion may occur and is associated with pain or ophthalmoplegia [23]. Squamous cell carcinoma is capable of metastasis to regional preauricular or submandibular lymph nodes. Squamous cell carcinoma of the conjunctiva may also invade the orbit.

13.8.2.3 Melanoma

Multiple recurrences of conjunctival melanoma associated with primary acquired melanosis may

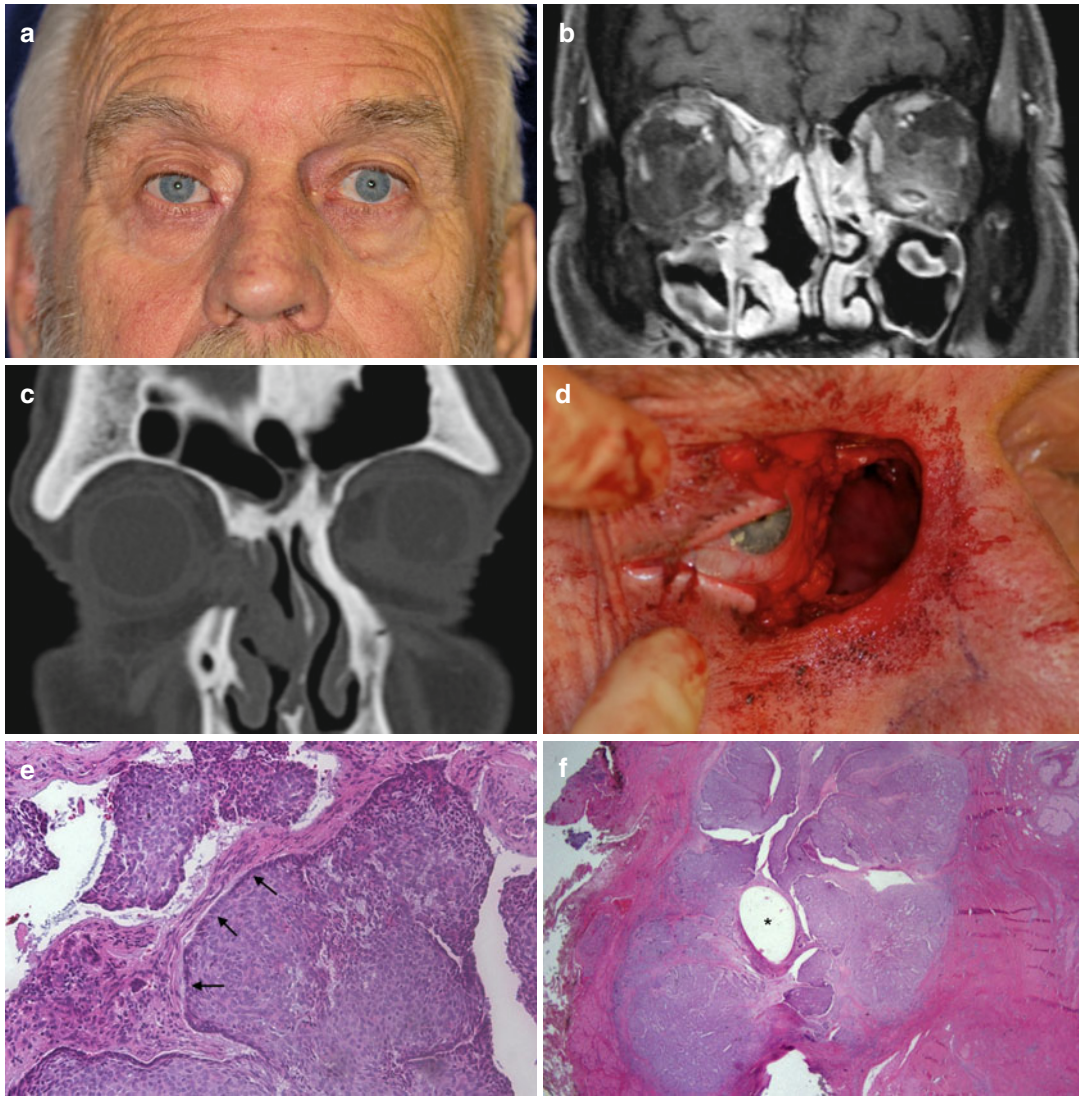

Fig. 13.3 Basal cell carcinoma invading the orbit: treated with globe preservation. A 72-year-old male presents with double vision and medial canthal scarring with dystopia, 2 years after resection of a medial canthal basal cell carcinoma (**a**). MRI scans show invasion of the tumor into the anterior third of the orbit with spread along the medial rectus muscle to the middle of the orbit (**b**). CT scans show bony invasion of tumor into the anterior ethmoids (**c**). Globe-preservation resection of tumor with frozen section controls performed (**d**). Patient is alive with no recurrence 5 years after surgery. H/E-stained frozen section, note the palisading nuclei (**e**, *arrows* 100×). The tumor surrounded the nasolacrimal duct (**f**, *asterisk* 20×)

lead to orbital extension. On rare occasions, uveal melanoma may extend into the orbit (Fig. 13.5).

13.8.2.4 Sebaceous Carcinoma

Sebaceous carcinoma is more prevalent in Asian populations. About one-third of epithelial malignancies invading the orbit are sebaceous carcinoma. This tumor tends to spread to the lymphatic system and subsequently to the lung, liver, brain, or skull.

13.8.2.5 Merkel Cell Carcinoma

Merkel cell carcinoma is an eyelid neoplasm that may arise in the eyelid or periocular region. They demonstrate rapid growth with a bulging, red appearance with overlying telangiectatic vessels

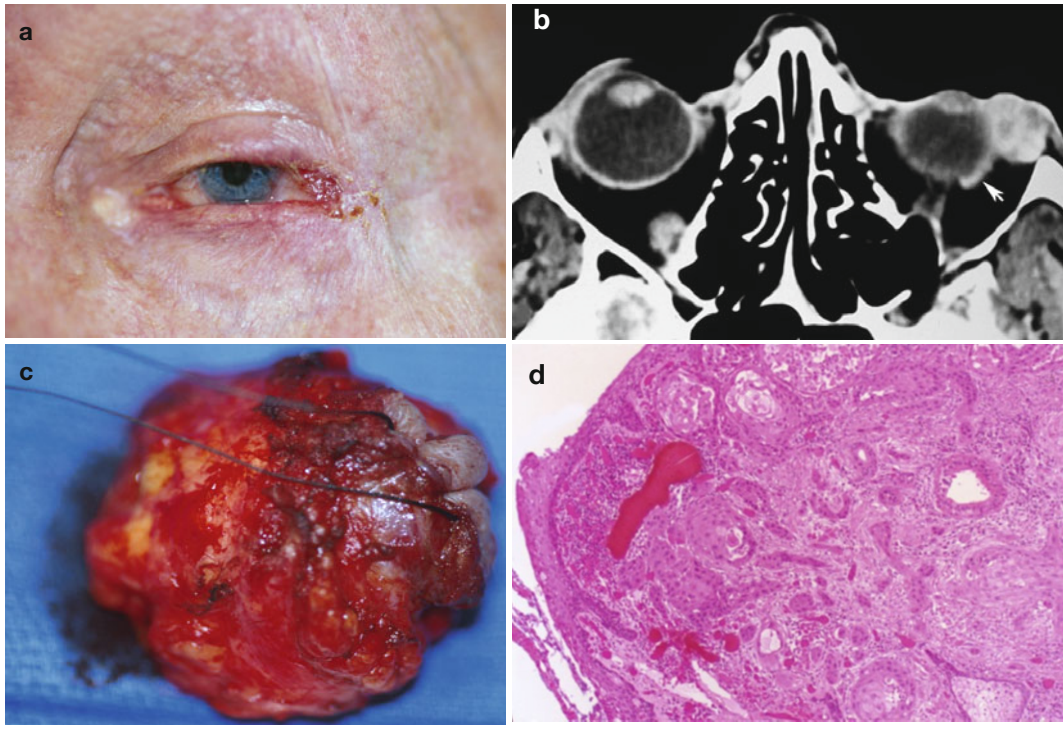

Fig. 13.4 Extension of squamous cell carcinoma into the orbit. A 71-year-old male with a 5-year history of multiple resections of left lower lid squamous cell carcinoma (**a**). CT scan shows an irregular but lobulated, well-defined density involving the tissues anterior to the orbital septum and extending into the retroseptal space (**b**, *arrow*). Mohs resection was attempted, but the deep tumor could not be removed necessitating exenteration (**c**). On histopathology, islands of squamous cells with dyskeratosis and keratin whorls were observed (**d**)

in the elderly (Fig. 13.6). The diagnosis is confirmed by the characteristic immunocytochemical and electron microscopic features. The tumor is associated with local recurrence and satellite lesions, regional nodal metastases, and distant metastases in about half of patients. Orbital invasion is associated with tumor recurrence and may lead to intracranial spread.

13.8.3 Diagnostic Evaluation

Careful assessment of extraocular muscle function is necessary in patients with periorbital malignancies. Medial spread of a tumor will often present with restriction of gaze followed by double vision. CT scans will reveal an irregular, often lobulated, well-defined mass extending from the preseptal to the postseptal space. Spread down the nasolacrimal duct and along the extraocular muscles may be seen.

13.8.4 Treatment

For orbital basal cell carcinoma, a globe-sparing resection may be attempted. However, the more aggressive basal cell carcinomas and squamous cell carcinomas may require aggressive resection with free borders and may need an exenteration.

Sebaceous carcinomas need a radical resection and lymph node dissection. Radiotherapy may control local disease if the patient is unable to undergo surgery. When conjunctival malignant melanoma spreads into the orbit, exenteration with nodal resection may be required. Treatment of Merkel cell carcinoma consists of aggressive surgical excision with wide margins and postoperative radiotherapy.

Mutation in the patched 1 gene (PTCH1) has been implicated in BCC, and overexpression of epidermal growth factor receptor (EGFR) has been shown in SCC. Vismodegib, an inhibitor of smoothened, which is activated upon binding of

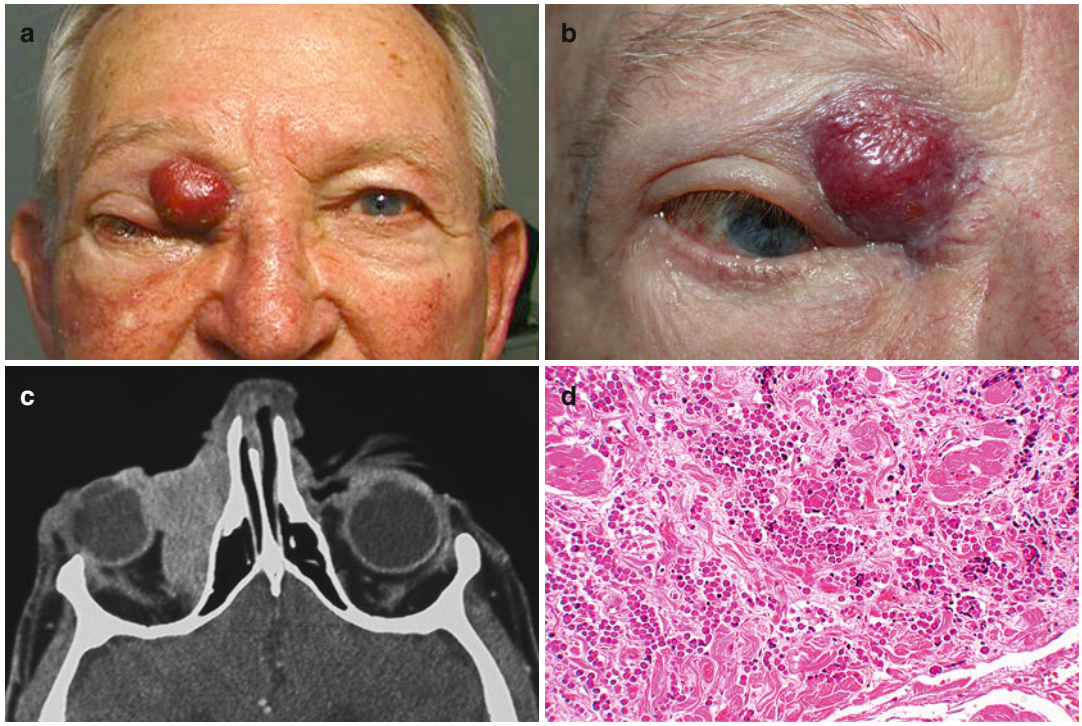

Fig. 13.5 Merkel cell carcinoma. A 78-year-old gentleman with a right medial canthal lesion initially biopsied elsewhere and diagnosed as basal cell carcinoma (**a**). He was referred after "recurrence." Note typical building reddish lesion with overlying vascularity (**b**). CT scan showed diffuse tumor with orbital invasion but without bone involvement (**c**). Note relatively large cells with uniformly staining eosinophilic cytoplasm (**d**)

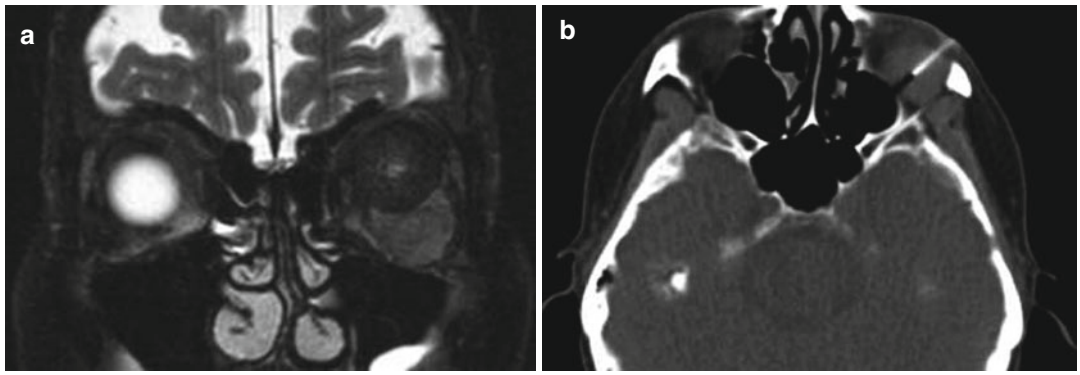

Fig. 13.6 Secondary melanoma. Orbital melanoma following enucleation for a large uveal melanoma. Histopathology of the globe was negative for extrascleral extension. MRI (T2) showing partially vascularized orbital implant with an orbital mass (**a**). The clinical diagnosis was confirmed by CT-guided fine needle aspiration biopsy (**b**)

hedgehog to Ptc, has been shown to significantly decrease BCC tumor size or even produce complete resolution, especially in cases of basal cell nevus syndrome. Similarly, EGFR inhibitors have been shown to significantly decrease SCC tumor size in cases of locally advanced and metastatic disease. Vismodegib has been used to reduce bulky eyelid and periocular basal cell carcinomas in patients with the basal cell nevus syndrome. Similarly, erlotinib (EGFR inhibitor) has been shown to be useful in patients with SCC when the patient is not a candidate for

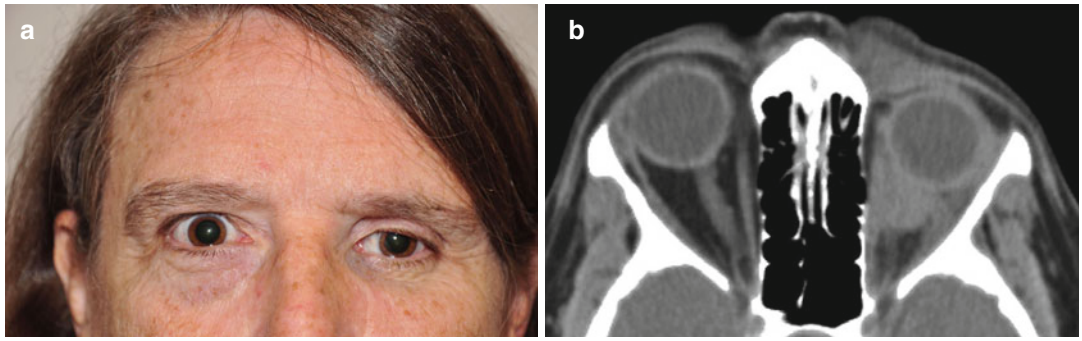

Fig. 13.7 Metastatic breast carcinoma. Orbital enophthalmos is evident on clinical examination (**a**) and CT scan (**b**). Note orbital mass in the affected left orbit

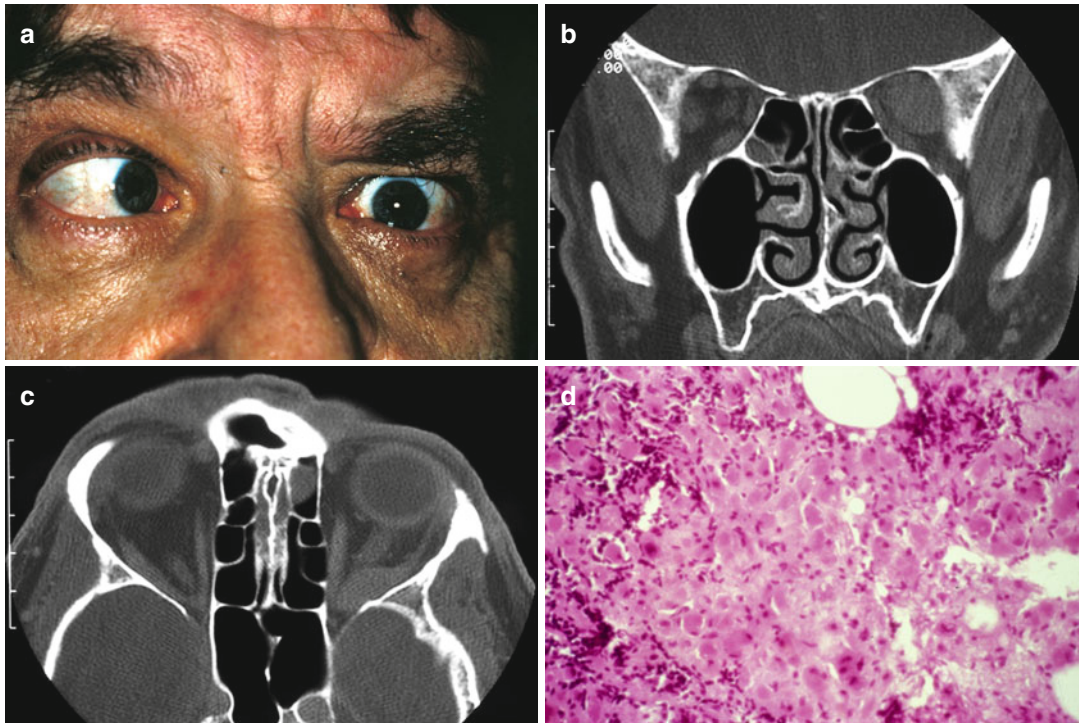

Fig. 13.8 Metastatic lung carcinoma. A 55-year-old male smoker presented with marked limitation of left eye abduction, slight left enophthalmos, and decrease of vision to counting fingers in the left eye (**a**). Coronal (**b**) and axial (**c**). CT scans show a homogenous posterior lateral rectus mass with compression of the optic nerve. Muscle is infiltrated with mixed small cell/large cell malignant cells with minimal cytoplasm and hyperchromatic nuclei (**d**)

surgery because of advanced disease of the orbit. Targeted therapy using hedgehog pathway and EGFR inhibitors shows significant promise in treatment of orbital and periocular BCC and cutaneous SCC, respectively. Such targeted therapy may be appropriate for patients who are not good candidates for surgery [24].

13.9 Orbital Metastases: Adults

13.9.1 Introduction

Approximately 8 % of all orbital neoplasia are metastatic in origin. Breast cancer (Fig. 13.7), lung cancer (Fig. 13.8), prostate cancer, and

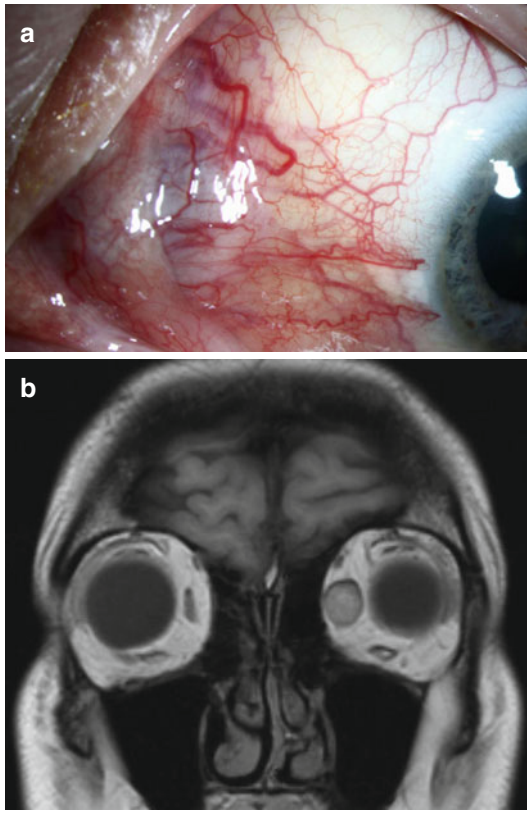

Fig. 13.9 Metastatic skin melanoma. Acute onset of painful proptosis and diplopia with congestion and bluish prominence of the medial rectus muscle insertion (**a**). MRI confirmed thickening of the medial rectus muscle (**b**). The patient had widespread metastatic cutaneous melanoma

melanoma are the most frequent primary tumors in adults that metastasize to the orbit (Fig. 13.9). In approximately 10 % of cases, the primary tumor remains unidentified. In the majority of cases (75 %), a diagnosis of preexisting primary tumor is known (Fig. 13.10), but in about 25 % of cases, the orbital tumor is the first presentation (Fig. 13.11) [25].

13.9.2 Clinical Features

Patients have more rapid onset of symptoms compared to other types of orbital neoplasia. Proptosis and motility disturbances are the most common presenting symptoms and signs. Pain is noted early in the course of the disease. Other symptoms and signs include a palpable mass, blepharoptosis, and decreased vision. Enophthalmos is present in 10 % of cases (most being metastasis from breast cancer). Clinical presentation of orbital metastatic disease can be categorized into mass effect, infiltrative (causing diplopia, enophthalmos), functional (neurological deficits), inflammatory (pain, chemosis, swelling), or silent (discovered on imaging or at surgery with no symptoms or signs) (Table 13.1) [26].

13.9.3 Diagnostic Evaluation

CT imaging may show a mass, bony changes (hyperostosis-prostate or hypostatic-thyroid), enlargement of muscle, or diffuse orbital tissue enlargement. Open orbital biopsy or needle biopsy confirms the diagnosis.

13.9.4 Treatment

Management may include radiotherapy, hormonal therapy, chemotherapy, or surgery. In some patients, control of local disease may limit progressive orbital pain, corneal exposure, and vision loss.

13.10 Orbital Metastases: Children

13.10.1 Introduction

Neuroblastoma, Ewing's sarcoma, Wilms' tumor, testicular embryonal sarcoma, ovarian sarcoma, and renal embryonal sarcoma may cause metastases to the orbit in children

13.10.1.1 Neuroblastoma

Neuroblastoma is the second most common (after rhabdomyosarcoma) orbital malignancy of childhood. Neuroblastoma arises from embryonic neural crest tissue of the postganglionic sympathetic nervous system. The most common site for primary tumor is in the abdomen, but the thorax, neck, or pelvis may also be affected. The

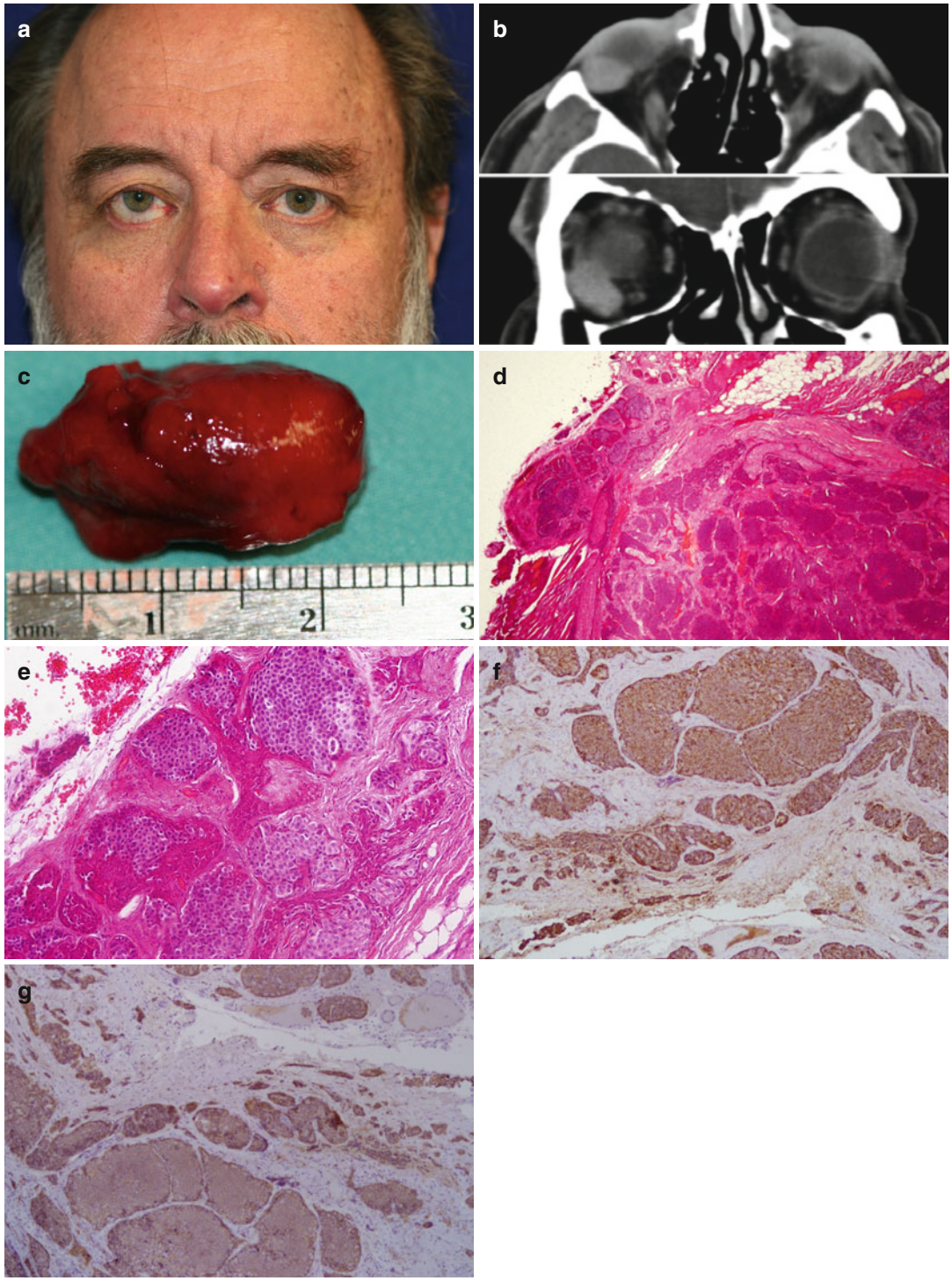

Fig. 13.10 Carcinoid tumor metastatic to the orbit. A 63-year-old male with a history of the carcinoid syndrome presented with double vision. Right proptosis and hyperglobus (**a**). Right inferolateral orbital mass causing hyperglobus and proptosis (**b**). Gross appearance after resection (**c**). The bulk of the lesion is made up of a cellular infiltrate that has a nesting pattern to it (**d**, H&E 4×). The cells themselves have a large nucleus with pleomorphism, nucleoli formation, and clumped chromatin. There are also scattered mitotic figures (**e**, H&E 20×). The tumor was positive for chromogranin (**f,** 10×) and synaptophysin (**g,** 10×) confirming neuroendocrine origin

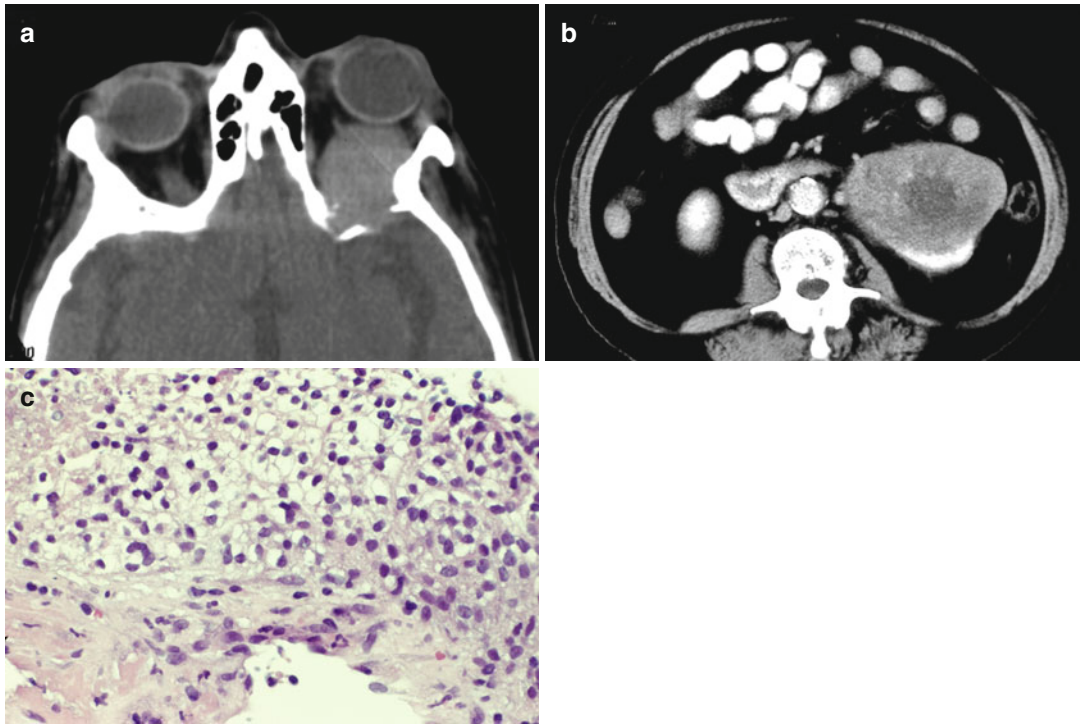

Fig. 13.11 Metastatic renal carcinoma. A 63-year-old female presented with proptosis, diplopia, and decreased vision in the left eye (**a**). Axial CT scans show a circumscribed homogenous orbital mass with bone destruction. Evaluation for primary tumor revealed a large mass replacing the right kidney (**b**). Fine needle aspiration biopsy of the kidney confirmed a clear cell renal carcinoma (**c**)

Table 13.1 Clinical features of orbital metastatic disease

Category	Feature
Mass effect	Visible or palpable mass
Infiltrative	Diplopia, exophthalmos, enophthalmos
Functional	Neurological deficits
Inflammatory	Pain, chemosis, swelling
Silent	Discovered on imaging or at surgery with no symptoms or signs

Modified from Goldberg et al. [26]

tumor presents anytime in the first two decades although the vast majority present before the age of 3 years [27].

There is sudden and rapid progression of proptosis, which may be unilateral or bilateral and accompanied by edema, ecchymosis, and ptosis. The differential diagnosis includes orbital cellulites, rhabdomyosarcoma, Ewing's sarcoma, medulloblastoma, and Wilms' tumor and lymphangioma. The superolateral orbit is most commonly involved.

There is a combination of bone and soft tissue involvement. There may be evidence of bone destruction with evidence of other cranial metastases. The patient may have Horner's syndrome, opsoclonus, myoclonus, and metastases to the iris or choroids. Aggressive combination chemotherapy and total body irradiation are used, but the prognosis remains poor.

13.10.1.2 Ewing's Sarcoma

Ewing's sarcoma is a highly malignant, small, round cell tumor of primitive mesenchymal cells in the bone marrow. These tumors may present as metastatic tumors or primary soft tissue orbital tumors [28]. Primitive neuroectodermal tumor of the orbit closely resembles Ewing's sarcoma [28]. The maxilla and the mandible are more commonly affected than the orbit. This tumor usually presents in the second decade of life. Orbital tumors present with rapidly progressing proptosis with or without orbital hemorrhage. The involved bone has a moth-eaten appearance.

Treatment includes radiotherapy and chemotherapy along with local resection. These tumors are quite radiosensitive. The 5-year survival rate is 80 % with surgery, radiation, and chemotherapy. Second primary osteogenic sarcoma may occur, so long-term follow-up is necessary.

References

1. Shields JA, Shields CL, Scartozzi R. Survey of 1264 patients with orbital tumors and simulating lesions: the 2002 Montgomery Lecture, part 1. Ophthalmology. 2004;111(5):997–1008.
2. Laforest C, Selva D, Crompton J, Leibovitch I. Orbital invasion by esthesioneuroblastoma. Ophthal Plast Reconstr Surg. 2005;21(6):435–40.
3. Loevner LA, Sonners AI. Imaging of neoplasms of the paranasal sinuses. Magn Reson Imaging Clin N Am. 2002;10(3):467–93.
4. Lyons CJ, McNab AA, Garner A, Wright JE. Orbital malignant peripheral nerve sheath tumors. Br J Ophthalmol. 1989;73:731–8.
5. Bhargava R, Parham DM, Lasater OE, et al. MR differentiation of benign and malignant peripheral nerve sheath tumors: use of the target sign. Pediatr Radiol. 1997;27:124–9.
6. Erzurum SA, Melen O, Lissner G, et al. Orbital malignant peripheral nerve sheath tumors. Treatment with surgical resection and radiation therapy. J Clin Neuroophthalmol. 1993;13:1–7.
7. Ordonez NG, Mackay B. Alveolar soft-part sarcoma: a review of the pathology and histogenesis. Ultrastruct Pathol. 1998;22:275–92.
8. Jordan DR, MacDonald H, Noel L, Carpenter B, Brownstein S, Munro S. Alveolar soft-part sarcoma of the orbit. Ophthalmic Surg. 1995;26:269–70.
9. Sherman N, Valvilala M, Pollock R, Romsdahl M, Jaffe N. Radiation therapy for alveolar soft-part sarcoma. Med Pediatr Oncol. 1994;22:380–3.
10. Mark RJ, Sercarz JA, Tran L, et al. Osteogenic sarcoma of the head and neck. The UCLA experience. Arch Otolaryngol. 1991;117:761–6.
11. Abramson DH, Ronner HJ, Ellsworth RM. Second tumors in non-irradiated bilateral retinoblastoma. Am J Ophthalmol. 1979;87:624–7.
12. Jacobiec FA, Howard GM, Jones IS, Tannenbaum M. Fibrous histiocytomas of the orbit. Am J Ophthalmol. 1974;77:333–45.
13. Folberg R, Cleaseby G, Flanagan JA, Spencer WH, Zimmerman LE. Orbital leiomyosarcoma after radiation therapy for bilateral retinoblastoma. Arch Ophthalmol. 1983;101:1562–5.
14. Font RL, Jurco III S, Brechner RJ. Postradiation leiomyosarcoma of the orbit complicating bilateral retinoblastoma. Arch Ophthalmol. 1983;101:1557–61.
15. Kaltreider SA, Destro M, Lemke BN. Leiomyosarcoma of the orbit. A case report and review of the literature. Ophthal Plast Reconstr Surg. 1987;3:35–41.
16. Jakobiec FA, Howard G, Rosen M, et al. Leiomyoma and leiomyosarcoma of the orbit. Am J Ophthalmol. 1975;80:1028–42.
17. Cai YC, McMenamin ME, Rose G, et al. Primary liposarcoma of the orbit: a clinicopathologic study of seven cases. Ann Diagn Pathol. 2001;5:255–66.
18. Tehrani AH, Heegaard S, Prause JU, et al. Liposarcoma metastatic to the orbit. Eur J Ophthalmol. 2003;13:108–12.
19. Jakobiec FA, Rini F, Char D, et al. Primary liposarcoma of the orbit. Problems in the diagnosis and management of five cases. Ophthalmology. 1989;96:180–91.
20. Costas A, Castro P, Munoz JM. Primary orbital liposarcoma: case report and review of the literature. Int J Oral Maxillofac Surg. 2001;30:170–2.
21. Cockerham KP, Kennerdell JS, Celin SE, Fechter HP. Liposarcoma of the orbit: a management challenge. Ophthal Plast Reconstr Surg. 1998;14:370–4.
22. Howard GR, Nerad JA, Carter KD, Whitaker DC. Clinical characteristics associated with orbital invasion of cutaneous basal cell and squamous cell tumors of the eyelid. Am J Ophthalmol. 1992;113:123–33.
23. Reifler DM, Hornblass A. Squamous cell carcinoma of the eyelid. Surv Ophthalmol. 1986;30:349–65.
24. Goldberg RA, Rootman J, Cline RA. Tumors metastatic to the orbit: a changing picture. Surv Ophthalmol. 1990;35:1–24.
25. Yin VT, Pfeiffer ML, Esmaeli B. Targeted therapy for orbital and periocular basal cell carcinoma and squamous cell carcinoma. Ophthal Plast Reconstr Surg. 2013;29(2):87–92.
26. Goldberg RA, Rootman J. Clinical characteristics of metastatic orbital tumors. Ophthalmology. 1990;97:620–4.
27. Levy WJ. Neuroblastoma. Br J Ophthalmol. 1957;41(1):48–53.
28. Dutton JJ, Rose Jr JG, DeBacker CM, Gayre G. Orbital Ewing's sarcoma of the orbit. Ophthal Plast Reconstr Surg. 2000;16(4):292–300.

Orbital Rhabdomyosarcoma

14

Natta Sakolsatayadorn and Julian D. Perry

Contents

N. Sakolsatayadorn, MD
Department of Ophthalmology, Faculty of Medicine Siriraj hospital, Mahidol University, Bangkok, Thailand
e-mail: nsakolsatayadorn@gmail.com

J.D. Perry, MD (✉)
Division of Ophthalmology, Cole Eye Institute, Cleveland Clinic Foundation, 9500 Euclid Avenue, Cleveland, OH 44195, USA
e-mail: perryj1@ccf.org

14.1 Introduction

Rhabdomyosarcoma (RMS) represents the most common orbital malignancy in children, and patients with this disease often present to the ophthalmologist. Because current therapeutic regimens offer an excellent chance for curing isolated orbital disease, prompt diagnosis and treatment are essential. Much of the success in reducing the morbidity and mortality over the past three decades has been through the collaborative efforts of the Intergroup Rhabdomyosarcoma Studies (IRS) formulated in the 1970s. Treatment of RMS with multiple modalities has transformed the dismal 25 % 3-year life expectancy of the 1960s to overall survival (OS) rates of higher than 90 % today [1, 2]. With such success, clinicians now have the opportunity to focus on minimizing the serious late sequelae of aggressive therapy.

At present, RMS is generally classified based on the histologic and biologic features of the tumor which help determine the treatment regimen. The two major subtypes are embryonal rhabdomyosarcoma (ERMS) and alveolar

J.D. Perry, A.D. Singh (eds.), *Clinical Ophthalmic Oncology*,
DOI 10.1007/978-3-642-40492-4_14,

Table 14.1 Familial cancer predisposition syndromes associated with RMS

Li-Fraumeni syndrome (TB53)
Neurofibromatosis type 1 (NF1)
Beckwith-Wiedemann syndrome (11p15 genes)
Costello syndrome (HRAS)
Noonan syndrome
Hereditary retinoblastoma syndrome (RB1)
Nevoid basal cell carcinoma syndrome (PTCH)
Rubinstein-Taybi syndrome (CREMMP)

Reproduced with permission from Xia et al. [12]

rhabdomyosarcoma (ARMS). The embryonal type is the most common and tends to occur in the head and neck region of infants and young children. This type typically shows less-aggressive behavior and provides a better prognosis. The morphological embryonal variants, such as spindle cell and botryoid type, are also highly curable. The alveolar type tends to affect older children and occurs more commonly in the extremities and trunk. It grows faster and requires more intensive treatment than ERMS.

Anaplastic rhabdomyosarcoma (formerly called pleomorphic RMS) is an uncommon type that occurs mostly in adults but may rarely occur in childhood.

14.2 Etiology

Most cases of RMS are sporadic occurrences, and its cause is still unknown. There is a slight predilection for males, with a 1.3–1.5:1 male to female ratio [3, 4]. No recognizable environmental, infectious, or biochemical influence in the pathogenesis of RMS exists; however, the malignancy has occurred secondarily in patients after radiotherapy for retinoblastoma and squamous cell carcinoma [5]. Epidemiological studies suggest that genetic predisposition may play an important role in RMS development [6–12] (Table 14.1). While no significant evidence of hereditary tendency for orbital rhabdomyosarcoma exists, the malignancy has been observed in siblings [2].

Table 14.2 Presenting symptoms of orbital rhabdomyosarcoma

Proptosis	80–100 %
Globe displacement	80 %
Eyelid and conjunctival swelling	60 %
Blepharoptosis	30–50 %
Palpable mass	25 %
Pain	10 %

14.3 Pathogenesis

Although RMS was once believed to arise from extraocular muscles, it is now accepted that the tumor originates from undifferentiated mesenchymal cells possessing the capacity to differentiate into striated muscle. Molecular genetic studies indicate that RMS arises by a distinct multistep process of molecular alterations. In addition to the primary mutations (PAX3/PAX7-FKHR gene fusions in ARMS and 11p15.5 allelic loss in ERMS), genetic alterations of other oncogenes and tumors suppressor genes occur as secondary events which may selectively collaborate with the primary alterations. These molecular changes result in high levels of exclusive products of the abnormal chromosome and ultimately contribute to tumorigenic behavior [13].

14.4 Clinical Features

The clinical features depend on the primary location. Most tumors are extraconal (37–87 % of cases), and more than two thirds of cases occupy the anterior or mid-orbit [14].

14.4.1 Symptoms

Orbital RMS is an aggressive tumor, and it commonly presents as rapidly progressive unilateral proptosis with periorbital soft tissue swelling. Lack of recognition and a confusing history of minor periorbital trauma often delay diagnosis (Table 14.2).

Table 14.3 Signs of orbital RMS

Proptosis/hypoglobus
Palpable mass
Lid edema or erythema
Chemosis, exposure keratopathy
Optic neuropathy or disc edema
Choroidal folds

14.4.2 Signs

Patients typically have nonaxial proptosis. The most typical location of the tumor is the superonasal quadrant of the orbit, and about half of embryonal rhabdomyosarcomas occur in this location, which causes hypoglobus and/or blepharoptosis. Abnormal extraocular motility is common. More anteriorly located tumors within the conjunctiva or eyelid tissues may produce periorbital soft tissue changes as eyelid edema, erythema, and conjunctival chemosis. The presentation often masquerades as an infectious or inflammatory process. Fundoscopic examination may show choroidal folds or optic disc edema with posterior orbital lesions (Table 14.3).

14.5 Diagnostic Evaluation

14.5.1 Imaging

When suspicion of RMS occurs, imaging should proceed urgently. Both computed tomography (CT) and magnetic resonance (MR) imaging can play a major role for provisional diagnosis, preoperative evaluation, staging, and follow-up. Each modality has different advantages. Computed tomography shows bony destruction with aggressive lesions better than MR imaging, and serial CT imaging studies may better show bone healing in response to treatment. Conversely, MR imaging demonstrates soft tissue extension better, especially intracranial and cavernous sinus involvement. MR imaging typically requires sedation or general anesthesia for younger patients to avoid motion artifact.

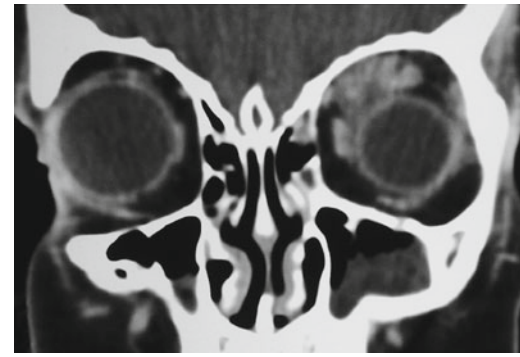

Fig. 14.1 Coronal computed tomographic imaging study of an alveolar rhabdomyosarcoma demonstrates a moderately well-defined superior nasal quadrant lesion that is isodense to the extraocular muscles. Adjacent bony destruction, although common in rhabdomyosarcoma, is not demonstrated in this study

On CT imaging, RMS typically appears as a well-circumscribed, extraconal, homogeneous mass with isodensity relative to extraocular muscle (Fig. 14.1). Calcification usually presents only in association with adjacent bony destruction. Heterogeneous areas may be seen in areas of tumor necrosis or hemorrhage. Signs of periorbital soft tissue swelling are expected, whether the tumor invades into the preseptal area or not. Contrast-enhanced studies show moderate to marked generalized enhancement. Bony erosion can be seen in 30–40 % of cases, especially in larger-sized tumors [14, 15].

On MR imaging, orbital RMS exhibits isointensity relative to muscle and brain parenchyma on T1-weighted studies and shows hyperintensity to these tissues on T2-weighted studies. Orbital structures may be encased by tumor extension. Moderate to marked uniform enhancement is seen on contrast-enhanced images (Fig. 14.2). In suspected paranasal sinus invasion, MR imaging can help differentiate trapped mucous secretion from tumor extension. Paranasal sinus invasion is seen in approximately 20 % of cases [14].

14.5.2 Tissue Diagnosis: Biopsy

Prompt open biopsy is preferred over fine-needle aspiration, which may provide inadequate tissue

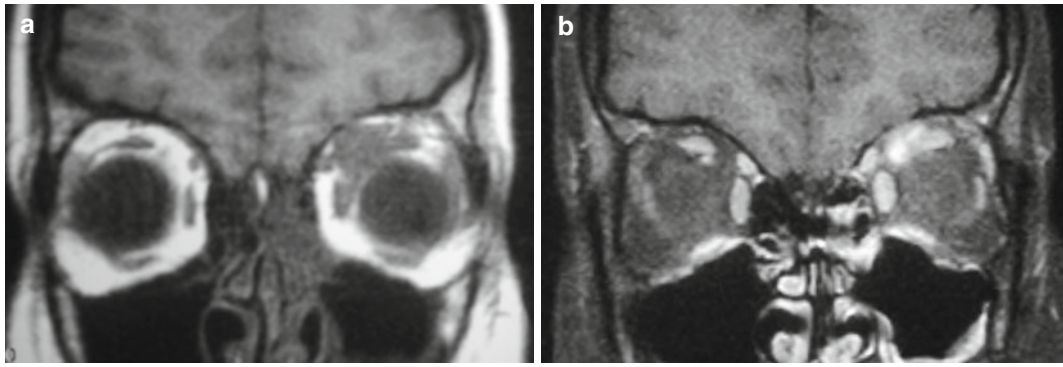

Fig. 14.2 T1-weighted MR imaging study shows the lesion is isointense to the extraocular muscles and hypointense to the orbital fat (**a**). Gadolinium-DTPA enhancement shows moderate enhancement (**b**)

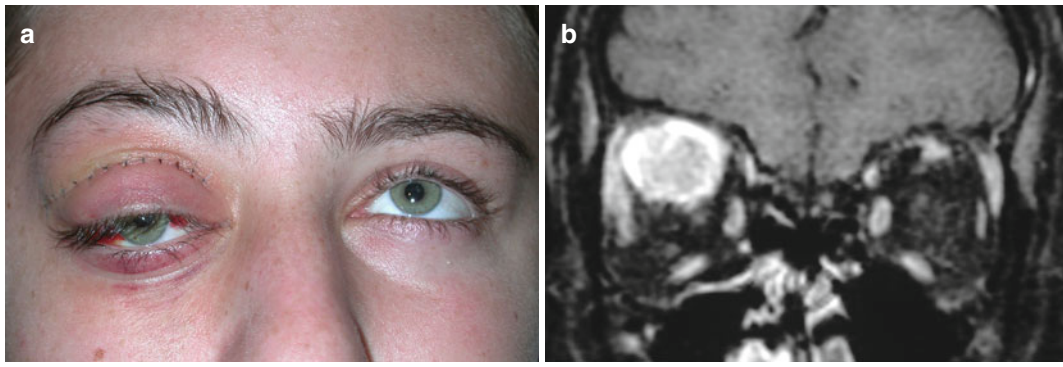

Fig. 14.3 Clinical appearance after orbital biopsy via anterior orbitotomy (**a**) for enhancing superior orbital mass (**b**)

for pathological and immunohistochemical studies (Fig. 14.3). The decisions for excisional versus incisional biopsy depend upon factors such as tumor site, size, adjacent orbital structures, extension, and visual function. Surgery should remove as much tumor load as possible but generally preserve visual structures and function, as RMS carries a reasonable prognosis with adjuvant treatment.

Metastasis tends spread hematogenously rather than via a lymphatic route. Lung and bone represent the most common metastatic targets of this disease. Spread to local lymph nodes occurs uncommonly, typically from more commonly anteriorly located tumors. Palpable nodes require biopsy with cytological confirmation for staging. Orbital RMS requires a full systemic and metastatic evaluation performed by the pediatric oncologist [16].

14.6 Salient Diagnostic Findings

14.6.1 Histology

Differentiation from other spindle cell tumors may present a significant challenge to the pathologist.

14.6.1.1 Light Microscope

Embryonic RMS is composed of small round cells to elongated or spindle-shaped cells which display various degrees of myogenic differentiation (Fig. 14.4). In abundant eosinophilic cytoplasm, bundles of actin and myosin filaments may produce cross striations with Masson trichrome staining which is seen in 20–60 % of tumors [14, 17].

Alveolar RMS tumor cells are small with a round nuclei and scant cytoplasm. Thin

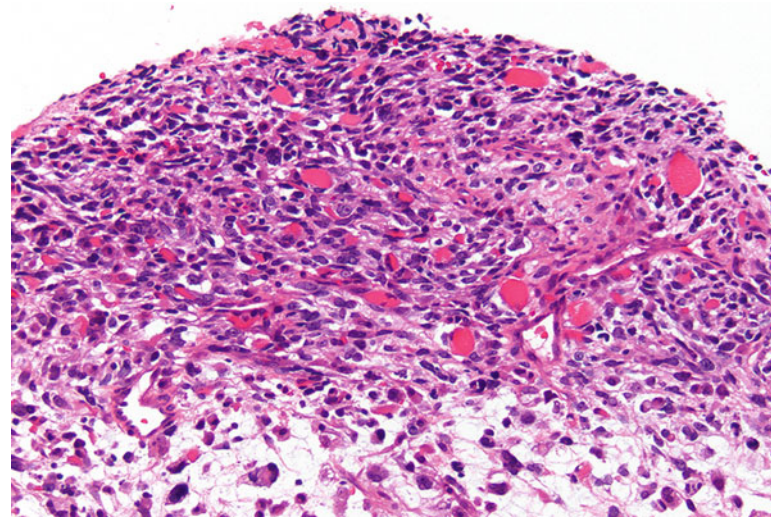

Fig. 14.4 Embryonal rhabdomyosarcoma with a combination of numerous small, primitive cells and larger cells with rhabdomyoblastic differentiation. The rhabdomyoblasts demonstrate eccentric nuclei and abundant densely pink cytoplasm (hematoxylin and eosin, 20×) (Courtesy of Thomas Plesec, MD, Cleveland, Ohio)

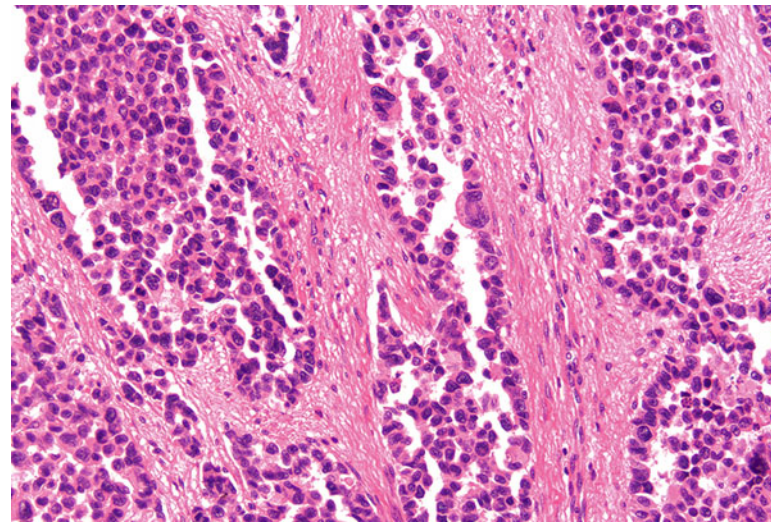

Fig. 14.5 Alveolar rhabdomyosarcoma with its characteristic nested or "alveolar" growth pattern. The nests are often lined by a single layer of malignant cells with discohesive cells lining the central zones (Courtesy of Thomas Plesec, MD, Cleveland, Ohio)

fibrovascular septae separate the tumor into round or ovoid spaces in a pattern reminiscent of lung alveoli (Fig. 14.5).

14.6.1.2 Immunohistochemistry

Numerous immunohistochemical markers identify the skeletal muscle-specific expression in an RMS tumor (Fig. 14.6). Desmin provides high sensitivity for tumors with skeletal differentiation, but it is not specific for RMS because it may also stain smooth muscle cells and occasionally myofibroblasts. Muscle-specific actin is seen in some cases of RMS. Vimentin staining assists in ruling out other small round cell tumors of childhood. Antibodies to myogenin and MyoD1 show high expression in more primitive cells (97 % sensitivity when combined) [18], but only faintly stain differentiated cell types. Caveolin-3 is a new marker that appears highly sensitive and specific for more differentiated RMS tumors and may help to detect residual tumor following chemotherapy. Table 14.4 lists commonly used stains. Unfortunately these stains are not reliable for subtyping RMS tumor [19].

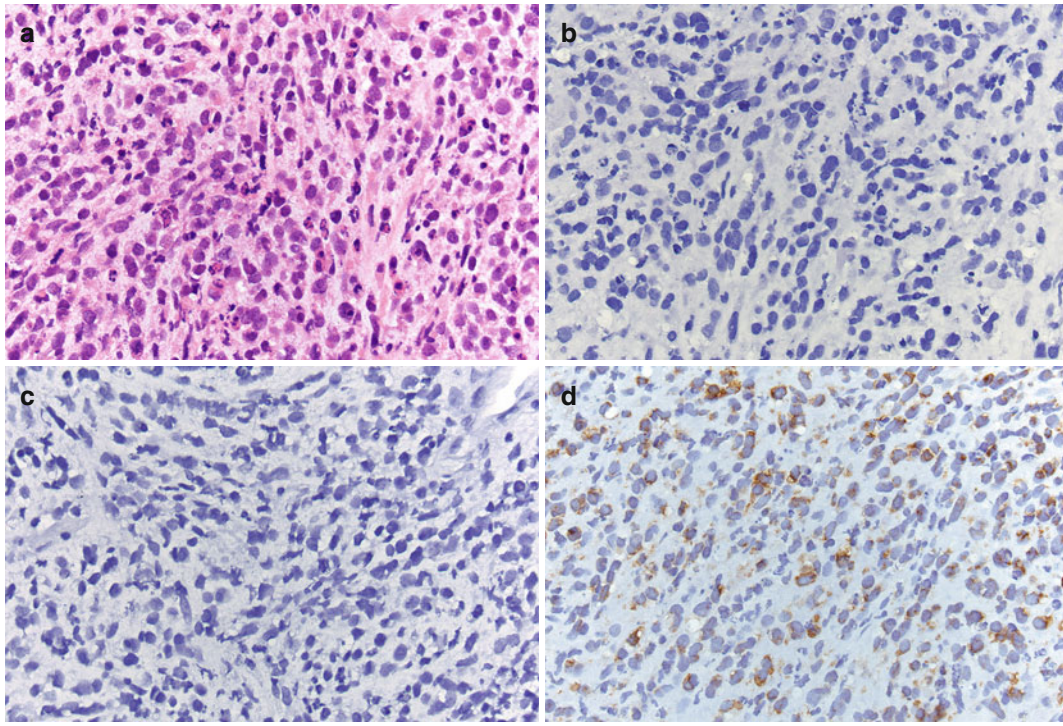

Fig. 14.6 Rhabdomyosarcoma (immunohistochemistry). This tumor is composed predominantly of small primitive cells with innumerable apoptotic bodies engendering a wide differential diagnosis, including carcinoma, lymphoma, and Ewing sarcoma in addition to rhabdomyosarcoma (**a**, hematoxylin and eosin, 20×). Leukocyte common antigen stain (LCA or CD45) is negative, which argues against lymphoma (**b**). Cytokeratin AE1/AE3 is a broad-spectrum keratin that is positive in most carcinomas. In this case, it is negative (**c**). Desmin is a sensitive marker of muscle differentiation, which is positive in this case (**d**). Myogenin (not pictured) is more specific for skeletal muscle differentiation, and it is also positive in this case (Courtesy of Thomas Plesec, MD, Cleveland, Ohio)

Table 14.4 Immunohistochemical markers of rhabdomyosarcoma

Desmin
Myoglobin
Myogenin
MyoD1
Vimentin
Caveolin-3
Muscle-specific actins

14.6.2 Molecular Analysis

Due to significant genetic differences between RMS types, cytogenetic studies assist in classifying the primary orbital tumor cells and detecting early disease recurrence.

Alveolar RMS cases often contain a unique chromosome translocation between the FKHR(FOX01A) gene on chromosome 13 either with the PAX3 gene on chromosome 2t(2;13)(q35;q14) or with the PAX7 gene on chromosome 1t(1;13)(p36;q14), which generates PAX3-FKHR and PAX7-FKHR fusion products, respectively. Approximately 20–30 % of alveolar RMS cases, however, lack these specific translocations (Fig. 14.7) [12, 18]. In contrast to the alveolar type, embryonal RMS does not show recurrent structural chromosome rearrangements, rather it often displays aneuploidy (a frequent allelic loss at chromosome 11p15.5 and a frequent chromosome gain of chromosome 8).

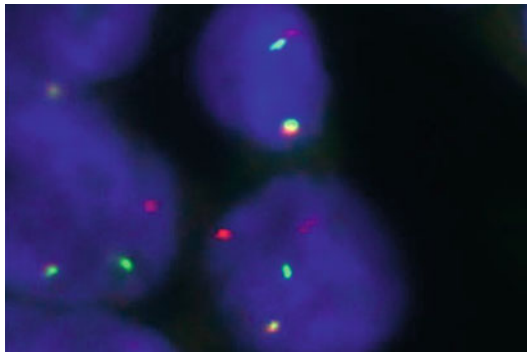

Fig. 14.7 Rhabdomyosarcoma (FISH). Dual-color break-apart fluorescence in situ hybridization (*FISH*) assay for the detection of *FOXO1* (13q14) rearrangements. Two blue- stained nuclei each demonstrate evidence of a *FOXO1* translocation as well as an intact chromosome. Split *red* and *green signals* indicate the translocation involving the *FOXO1* gene, whereas, when the gene is intact, the *red* and *green signals* are closely apposed and combine to create a *yellow signal* (Courtesy of Thomas Plesec, MD, Cleveland, Ohio)

14.7 Differential Diagnosis

Orbital RMS should be considered in the differential diagnosis of any child with proptosis and subacute edema. The rapidly progressive course and associated inflammatory signs can suggest both benign and malignant etiologies. Malignancies that can simulate RMS include neuroblastoma, leukemia or other metastases, lymphoma, and other sarcomas. Nonmalignant diseases include orbital cellulitis, dacryocystitis, idiopathic orbital inflammation, lymphangioma, capillary hemangioma, and dermoid cyst (Table 14.5).

14.8 Treatment

Current IRS treatment protocols for orbital RMS now consist of combined multimodal therapy including surgery (incisional or excisional biopsy, surgical debulking, or complete gross excision) followed by combinations of multiagent chemotherapy and/or radiation. Surgical margins, histology, and patient age contribute to the risk and regimen treatment stratification necessary to optimize outcome.

Table 14.5 Imaging helps distinguish lesions that may clinically simulate Orbital RMS

Benign lesion	Imaging characteristics
Subperiosteal hemorrhage	MRI: changing signal intensity of hemorrhage evolution, may present fluid level of blood product
Orbital cellulitis	Occur with adjacent paranasal sinusitis Contrast enhancement in distinguishing sinus secretion from enhanced tumor invasion, especially in MRI finding No bony erosion
Complicated dermoid cyst	Mostly located near zygomaticofrontal suture Cystic lesion with adjacent long-standing bone change effect
Lymphangioma	Reveal blood level in the larger cystic spaces "fluid-fluid level"
Malignant lesion	**Imaging clue**
Langerhans cell histiocytosis	Moth-eaten osteolytic lesion, arise in bone as origin
Chloroma (granulocytic sarcoma)	Frequent bilateral orbital lesion
Lymphoma	Lacrimal gland involvement Encase the globe
Metastasis of neuroblastoma	No definite clue Need tissue diagnosis or finding of primary tumor

14.9 Surgical

The surgical margin outcome determines the grouping classification assignment and influences the radiotherapy and chemotherapy regimen (Table 14.6). Therefore, the initial surgery should debulk as much tumor as possible with care to preserve vital orbital structures. Well-circumscribed, accessible lesions may allow for complete gross excision. More commonly, surgery results in significant gross residual tumor in order to preserve ocular function. The surgical approach to a RMS should preserve orbital periosteum, which may act as a barrier to local spread.

Table 14.6 IRSG grouping system

Group	Definition
I	Localized tumor, completely removed with pathologically clear margins, and no regional LN involvement
II	Localized tumor, grossly removed with (a) microscopically involved margins, (b) involved, grossly resected regional LN, or (c) both
III	Localized tumor, with gross residual disease after grossly incomplete removal, or biopsy only
IV	Distant metastases present at diagnosis

14.10 Chemotherapy

At present, all RMS patients receive some form of adjunctive chemotherapy. The regimen depends on the histologic type and grouping of the tumor (Table 14.7). The standard regimen is a combination of vincristine, actinomycin D, and cyclophosphamide (VAC). High-risk patients are considered for more additional treatment as topotecan or irinotecan. Some patients with low-risk disease may receive only VA.

14.11 Radiotherapy

The radiotherapy is essential for most cases except for completely resected localized lesions (group I). The radiation dose depends predominantly on the residual disease after the primary surgical resection. Low-dose radiation (40 Gy) for ERMS group II provides local tumor control rates of at least 90 %. For group III patients, radiation doses are more commonly 50 Gy. Modern radiotherapy techniques, including intensity-modulated radiotherapy (IMRT), fractionated stereotactic radiotherapy (FSRT), and proton radiotherapy, which deliver high doses to a definite target, may maintain outcomes while decreasing radiation-related side effects.

14.12 Follow-Up

After treatment, patients require serial comprehensive ocular examinations that measure visual acuity, proptosis, and extraocular motility. Examinations should evaluate for sequelae of radiation treatment, such as cataract, retinopathy, and keratopathy (Table 14.8). Imaging studyies should document new baseline status and residual tumor size. Follow-up should be every 3–4 months for the first year, then every 4–6 months for several years thereafter, and subsequently on a yearly basis with periodic orbital imaging. Secondary biopsy offers low yield with significant risk and should be reserved for patients with clinical indications of recurrence and changes on serial imaging studies [16].

14.13 Prognosis

In general, RMS's outcome depends on primary site, tumor size, local extension, presence of nodal and distal metastases, and histologic subtype including molecular analysis.

Isolated orbital involvement carries the best prognosis of all primary RMS locations, with an overall survival rate of 96 % and eye preservation rate of 86 % [20]. Five-year survival rates for ERMS increased during the period from 1976 to 2000 (60.9–73.4 %, respectively), whereas there was no significant improvement for 5-year survival rates of ARMS (40.1 and 47.8 %, respectively). Children who present between age 1 and 10 have a more favorable prognosis than infants or young adults. Histologic examination and molecular analysis contribute significantly to prognosis. For the more favorable embryonal tumors, prognosis improves with evidence of genetic hyperploidy. In contrast, less favorable alveolar tumors fare even worse with evidence of tetraploid DNA content [21]. Karyotype detection of chromosomal translocations indicates alveolar morphology, with the t(2;13) PAX3-FKHR fusion gene faring worse than those bearing t(1;13) PAX7-FKHR fusion gene [22]. In the rare instances where orbital disease is refractory to standard treatment, aggressive secondary surgery yields 3-year survival rates up to 70 % [23]. Patients with metastatic disease may benefit from myeloablative treatment with stem cell support. Survivors of previous treatment protocols now show the unfortunate side effects of radiotherapy, with over 70 % of eyes suffering some degree of vision loss [20]. Other common late sequelae include cataracts and facial hypoplasia.

Table 14.7 Orbital RMS: modified IRSG study V treatment protocol

	Risk (protocol)	Group	Age	XRT	Chemo treatment
ERMS	Low risk	I		–	VA
		II a		40 Gy	
		III		50 Gy	
		II b		40 Gy	VAC
		II c		40 Gy	
		III + node positive		50 Gy	
	Intermediate risk	IV	Age <10 year old	Local and distant RT	VAC ± Topo
	High risk		Age ≥10 year old		CPT-11 + VAC
ARMS	Intermediate risk	I, II, III		Local and distant RT	VAC + Topo
	High risk	IV			CPT-11 + VAC

ERMS embryonal, botryoid, or spindle cell rhabdomyosarcoma, *ARMS* Alveolar rhabdomyosarcoma, undifferentiated sarcoma, *XRT* radiotherapy, *VAC* vincristine, actinomycin D, cyclophosphamide, *Topo* topotecan, *CPT-11* irinotecan

Table 14.8 Late ocular sequelae of radiation therapy for orbital RMS

Cataract	82 %
Impaired vision in the treated eye	70 %
Orbital hypoplasia and asymmetry	59 %
Dry eyes	30 %
Ptosis/enophthalmos	28 %

Reproduced with permission from Raney et al. [20]

14.14 Future Research

14.14.1 New Propose Classification

Individuals with the PAX7 translocation are younger and have have longer event-free survival than those with the PAX3 translocation in the ARMS group and they seem to respond as well as the ERMS group. Adding chromosomal translocation and specific gene expression profiles to a risk-adapted classification scheme may allow some patients to receive less intensive treatment.

14.14.2 Improving the Standard Treatment

Chemotherapy and Radiation: The currently "ARST0331 protocol" study from IRS V for patients with low-risk ERMS, including most of the orbital RMS patients, is ongoing. The objectives are to maintain excellent survival rates while decreasing radiotherapy doses, decreasing the duration of vincristine and actinomycin D chemotherapy, and adding a total cumulative dose of cyclophosphamide. Limiting the use of these modalities should lower the risk of secondary malignancies and myelosuppression.

Gene and Signaling Pathway Study: Molecularly targeted agents (IGF1R inhibition, antiangiogenic approaches, and mTOR inhibition) are currently under investigation in combination with chemotherapy for patients with recurrent or metastatic RMS to provide less toxic systemic treatments and control the development of this malignant tumor as a vaccine therapy [13, 24].

Conclusion

RMS represents the most common childhood orbital malignancy. Despite recent advancements in treatment, it remains a potentially fatal disease, and current treatment regimens continue to carry significant morbidity. As the management of orbital RMS becomes increasingly complex, close collaboration between the ophthalmic surgeon, pediatric oncologist, and the radiation oncologist becomes necessary to optimize outcome.

References

1. Friedrich P, Ortiz R, Strait K, Fuentes S, Gamboa Y, Arambu I, Ah-Chu-Sanchez M, London W, Rodriguez-Galindo C, Antillon-Klussmann F, et al. Pediatric sarcoma in Central America: outcomes, challenges, and plans for improvement. Cancer. 2012; 119(4):871–9.
2. Howard GM, Casten VG. Rhabdomyosarcoma of the orbit in brothers. Arch Ophthalmol. 1963;70:319–22.
3. Dagher R, Helman L. Rhabdomyosarcoma: an overview. Oncologist. 1999;4(1):34–44.
4. Shields CL, Shields JA, Honavar SG, Demirci H. Clinical spectrum of primary ophthalmic rhabdomyosarcoma. Ophthalmology. 2001;108(12):2284–92.
5. Hasegawa T, Matsuno Y, Niki T, Hirohashi S, Shimoda T, Takayama J, Watanabe C, Kaneko A, Sano T, Sato M, et al. Second primary rhabdomyosarcomas in patients with bilateral retinoblastoma: a clinicopathologic and immunohistochemical study. Am J Surg Pathol. 1998;22(11):1351–60.
6. Gripp KW. Tumor predisposition in Costello syndrome. Am J Med Genet C Semin Med Genet. 2005;137C(1):72–7.
7. Gripp KW, Lin AE, Stabley DL, Nicholson L, Scott Jr CI, Doyle D, Aoki Y, Matsubara Y, Zackai EH, Lapunzina P, et al. HRAS mutation analysis in Costello syndrome: genotype and phenotype correlation. Am J Med Genet A. 2006;140(1):1–7.
8. Kerr B, Delrue MA, Sigaudy S, Perveen R, Marche M, Burgelin I, Stef M, Tang B, Eden OB, O'Sullivan J, et al. Genotype-phenotype correlation in Costello syndrome: HRAS mutation analysis in 43 cases. J Med Genet. 2006;43(5):401–5.
9. Moschovi M, Touliatou V, Papadopoulou A, Mayakou MA, Nikolaidou-Karpathiou P, Kitsiou-Tzeli S. Rhabdomyosarcoma in a patient with Noonan syndrome phenotype and review of the literature. J Pediatr Hematol Oncol. 2007;29(5):341–4.
10. Samuel DP, Tsokos M, DeBaun MR. Hemihypertrophy and a poorly differentiated embryonal rhabdomyosarcoma of the pelvis. Med Pediatr Oncol. 1999;32(1): 38–43.
11. Trahair T, Andrews L, Cohn RJ. Recognition of Li Fraumeni syndrome at diagnosis of a locally advanced extremity rhabdomyosarcoma. Pediatr Blood Cancer. 2007;48(3):345–8.
12. Xia SJ, Pressey JG, Barr FG. Molecular pathogenesis of rhabdomyosarcoma. Cancer Biol Ther. 2002;1(2): 97–104.
13. Belyea B, Kephart JG, Blum J, Kirsch DG, Linardic CM. Embryonic signaling pathways and rhabdomyosarcoma: contributions to cancer development and opportunities for therapeutic targeting. Sarcoma. 2012;2012:406239.
14. Chung EM, Smirniotopoulos JG, Specht CS, Schroeder JW, Cube R. From the archives of the AFIP: pediatric orbit tumors and tumor-like lesions: nonosseous lesions of the extraocular orbit. Radiographics. 2007;27(6):1777–99.
15. Mafee MF, Pai E, Philip B. Rhabdomyosarcoma of the orbit. Evaluation with MR imaging and CT. Radiol Clin North Am. 1998;36(6):1215–27. xii.
16. Shields JA, Shields CL. Rhabdomyosarcoma: review for the ophthalmologist. Surv Ophthalmol. 2003; 48(1):39–57.
17. Napolitano L, Howard J. Electron microscopic observations on non-specific lead staining in the small intestine of the cat after lipid or carbohydrate feeding. Anat Rec. 1968;160(1):25–35.
18. Davicioni E, Anderson MJ, Finckenstein FG, Lynch JC, Qualman SJ, Shimada H, Schofield DE, Buckley JD, Meyer WH, Sorensen PH, et al. Molecular classification of rhabdomyosarcoma–genotypic and phenotypic determinants of diagnosis: a report from the Children's Oncology Group. Am J Pathol. 2009; 174(2):550–64.
19. Fine SW, Lisanti MP, Argani P, Li M. Caveolin-3 is a sensitive and specific marker for rhabdomyosarcoma. Appl Immunohistochem Mol Morphol. 2005;13(3): 231–6.
20. Raney RB, Anderson JR, Kollath J, Vassilopoulou-Sellin R, Klein MJ, Heyn R, Glicksman AS, Wharam M, Crist WM, Maurer HM. Late effects of therapy in 94 patients with localized rhabdomyosarcoma of the orbit: report from the Intergroup Rhabdomyosarcoma Study (IRS)-III, 1984–1991. Med Pediatr Oncol. 2000;34(6):413–20.
21. Pappo AS, Crist WM, Kuttesch J, Rowe S, Ashmun RA, Maurer HM, Newton WA, Asmar L, Luo X, Shapiro DN. Tumor-cell DNA content predicts outcome in children and adolescents with clinical group III embryonal rhabdomyosarcoma. The Intergroup Rhabdomyosarcoma Study Committee of the Children's Cancer Group and the Pediatric Oncology Group. J Clin Oncol. 1993;11(10):1901–5.
22. Sorensen PH, Lynch JC, Qualman SJ, Tirabosco R, Lim JF, Maurer HM, Bridge JA, Crist WM, Triche TJ, Barr FG. PAX3-FKHR and PAX7-FKHR gene fusions are prognostic indicators in alveolar rhabdomyosarcoma: a report from the Children's Oncology Group. J Clin Oncol. 2002;20(11):2672–9.
23. Lawrence Jr W, Anderson JR, Gehan EA, Maurer H. Pretreatment TNM staging of childhood rhabdomyosarcoma: a report of the Intergroup Rhabdomyosarcoma Study Group. Children's Cancer Study Group. Pediatric Oncology Group. Cancer. 1997;80(6):1165–70.
24. Gosiengfiao Y, Reichek J, Walterhouse D. What is new in rhabdomyosarcoma management in children? Paediatr Drugs. 2012;14(6):389–400.

Enucleation for Ocular Tumors

15

Natta Sakolsatayadorn and Julian D. Perry

Contents

15.1 Introduction

Many studies over the past decade report a trend toward fewer enucleations, suggesting that improved treatments prevent end-stage eye disease. Interestingly, however, the incidence of enucleation for neoplasia has not decreased despite the more widespread use of globe-sparing techniques, such as chemotherapy and brachytherapy [1].

Enucleation represents the surgical removal of the globe from the orbit. The term "primary enucleation" is used to designate the first and the only treatment modality for an ocular tumor without any prior or adjunctive therapy. The goal of enucleation surgery for ocular malignancy is to prevent further local orbital spread of disease and to reduce the risk of regional spread and distant metastasis. For over a century, enucleation has played a major role in the treatment of ocular malignancy. In addition to eradicating malignancy, enucleation should also form the structural foundation to restore cosmesis and improve quality of life after what amounts to a devastating amputation to many patients (Table 15.1).

Table 15.1 Goals of enucleation

Remove malignancy with clear margins
Provide a healthy and comfort orbital socket without further complications
Restore quality of life and cosmesis

N. Sakolsatayadorn, MD
The Department of Ophthalmology,
Faculty of Medicine Siriraj Hospital,
Mahidol University, Bangkok, Thailand
e-mail: sinatta_s@mahidol.ac.th

J.D. Perry, MD (✉)
Division of Ophthalmology, Cole Eye Institute,
Cleveland Clinic Foundation, 9500 Euclid Avenue,
Cleveland, OH 44195, USA
e-mail: perryj1@ccf.org

J.D. Perry, A.D. Singh (eds.), *Clinical Ophthalmic Oncology*,
DOI 10.1007/978-3-642-40492-4_15, © Springer-Verlag Berlin Heidelberg 2014

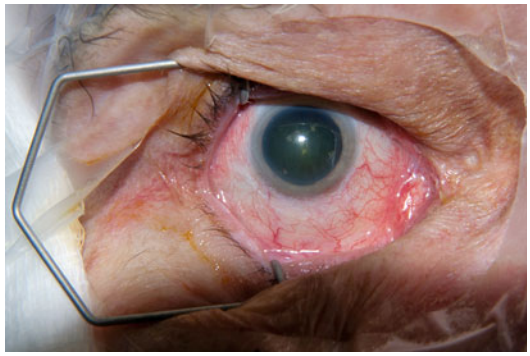

Fig. 15.1 As the preoperative external appearance is usually normal, presence of intraocular tumor should be confirmed by indirect ophthalmoscopy before proceeding (Reproduced with permission from Perry et al. [21])

15.2 Indications

The procedure is considered for extensive malignant ocular tumors refractory to other treatments, too advanced for more conservative therapies, or in patients who elect the procedure over other options. Surgery is generally reserved for advanced tumors that destroy visual function, cause intractable pain, or are unlikely to respond to further non-surgical therapy (Fig. 15.1).

The Collaborative Ocular Melanoma Study (COMS) includes the following indications for primary enucleation for choroidal melanoma:

- A medium-sized tumor (2.4–10 mm in thickness or up to 16 mm in basal diameter) with poor vision (<20/400) or no potential for visual recovery, with consideration of the functional status of the other eye and patient preference.
- A large-sized tumor (more than 10 mm in thickness or more than 16 mm in basal diameter) with neovascular glaucoma, optic nerve invasion, blind painful eye, localized extrascleral extension, or patient preference.

The indications for secondary enucleation for choroidal melanoma include failure of conservative therapy and ocular pain from radiation related complications, such as neovascular glaucoma.

For medium-sized tumors, patients choose a treatment option based on the expectation for vision preservation and the risk of radiation complications, since no survival or long-term quality of life advantages exist for one treatment over the other [2]. For large melanomas, no difference in survival exists between pre-radiation enucleation and primary enucleation [2–4]. The functional status of the fellow eye and patient preference represent important factors in the decision making process.

For intraocular tumors with limited extrascleral or orbital invasion, enucleation alone risks transecting the orbital component of the tumor and leaving residual disease within the orbit. Modified enucleation with partial tenonectomy or lateral orbitotomy with or without adjuvant therapy have theoretical advantages and avoid exenteration; however, current evidence does not suggest improved survival for any particular technique in these instances [5–8].

For retinoblastoma, enucleation is considered for extensive unilateral disease, neovascular glaucoma, or for an eye with advanced disease with no hope for useful vision. Eyes harboring other ocular tumors that fail to respond to conventional therapy or that develop secondary complications leading to a blind, painful eye may be considered for enucleation [9].

15.3 Preoperative Preparation

Preoperative consideration should be given to the decision for the procedure itself, the type of anesthesia, and the implant used to restore orbital volume after globe removal. Preoperative counseling provides information about advantages, disadvantages, alternatives, risks, and potential complications of enucleation, the orbital implant, and the prosthesis. Genetic counseling should be provided in cases where such information is available. Patients should be made aware that they may develop unexpected symptoms after enucleation, including strain with reading, changes in depth perception, visual hallucinations, and even depression and other unexpected consequences [10, 11]. The surgeon should encourage the patient to volunteer such symptoms and help provide them instruction on how to adapt the loss of an eye.

Given the psychological issues surrounding the loss of an eye, general anesthesia is often preferred over sedation. General anesthesia may allow for better analgesia and hemostasis. Local anesthesia with supplemental monitored

intravenous sedation may be more suitable in selected cases, such as those associated with medical risk factors for complications of general anesthesia [12]. In these cases, a supraorbital nerve, an infraorbital nerve, and a modified van Lint block may enhance patient comfort.

The ideal orbital implant should not only restore orbital volume and couple extraocular muscle movement to the prosthesis, it should also maximize biologic compatibility and minimize complications and cost.

Current orbital implants can be classified as integrated or nonintegrated. Nonintegrated implants are solid, with no capacity for tissue ingrowth or direct attachment to the surrounding orbital tissues. They become encapsulated over time. Extraocular muscle movement is coupled to prosthesis movement by the shape of the implant as it conforms to a concavity within the prosthesis. Nonintegrated orbital implant materials include polymethylmethacrylate (PMMA) and silicone and occur mostly in the shape of a sphere.

In contrast, integrated orbital implants contain pores and channels to allow for fibrovascular ingrowth, so the implant may accept a drilled-in motility peg to better couple implant movement to prosthesis movement. These implants are currently made from hydroxyapatite, porous polyethylene, and bioceramic materials. The rectus muscles are sutured directly to the implant or to an overlying wrapping material. Wrapping materials include donor sclera, autogenous fascia, and polyglycolic acid mesh; however, wrapping materials may increase infection rates and delay fibrovascular ingrowth [13]. Pegging rates have decreased significantly over the last decade, as surgeons have encountered complications from pegging, including mucous discharge, and excessive motility revealing the prosthesis edges. Serious complications from pegging, such as exposure, extrusion, and infection, can occur that may result in loss of the implant. Current pegging rates are under 10 % [14]. For unpegged implants, nonintegrated and integrated implants may provide similar motility when they are implanted using similar surgical techniques [15, 16]. As the use of integrated implants adds morbidity and additional cost without clear benefit in unpegged cases, some surgeons are using traditional nonintegrated, solid implants with increasing frequency [17, 18].

Most adult patients require at least a 20–22 mm spherical implant to replace 4.2–5.6 ml in volume, respectively, and to leave 2–2.5 ml for a prosthesis. Proper implant size leads toward a better aesthetic result and decreases socket complications. Alternatively, orbital implant size can be determined preoperatively or intraoperatively by using sizing algorithms (Table 15.2).

Given the smaller but growing orbital volume of pediatric patients (less than 5 years of age), determining suitable implant size can present challenges. Some surgeons suggest replacing 70 % of the enucleated eye volume with an implant and the remainder with the prosthesis. An implant 2 mm less in diameter than the axial length of the enucleated specimen or 1 mm less than the axial length of contralateral eye can be considered, which typically calls for implant sizes of 18–20. These algorithms tend to improve outcome and produce less socket complications (Table 15.3) [20]. In general, the largest implant that can be placed without undue wound tension should be used.

Table 15.2 Algorithm for implant size

Axial length[a] − 2 mm (− 1 mm in hyperopia)

[a]A-scan of the fellow eye, axial length (mm) = distance from the anterior cornea to the anterior aspect of the posterior sclera + 1 mm

Modified from Kaltreider and Lucarelli [19]

Table 15.3 Pediatric implant size (axial length − 2 mm = implant diameter) [20]

Axial length/ volume, mm/ml	Implant size/ volume, mm/ml	% Volume, implant	Prosthetic volume, ml	% Volume, prosthesis
16/2.1	14/1.4	67	0.7	33
18/3.0	16/2.1	70	0.9	30
20/4.2	18/3.0	71	1.2	29
22/5.6	20/4.2	75	1.4	25
24/7.2	22/5.6	78	1.6	22

Modified from Kaltreider et al. [20]

15.4 Technique

While enucleation techniques vary, certain principles apply. Whether employing general or local anesthesia, analgesia and improved hemostasis may be achieved with a retrobulbar or peribulbar block consisting of 3–4 ml of 1 % lidocaine with 1:100,000 epinephrine and 8.4 % sodium bicarbonate in a 1:10 ratio with 50 units per 10 ml of hyaluronidase. An additional 1 ml of the same solution can be injected beneath the conjunctiva. Penetration or perforation of the eye with the needle must be avoided during the block (Fig. 15.2).

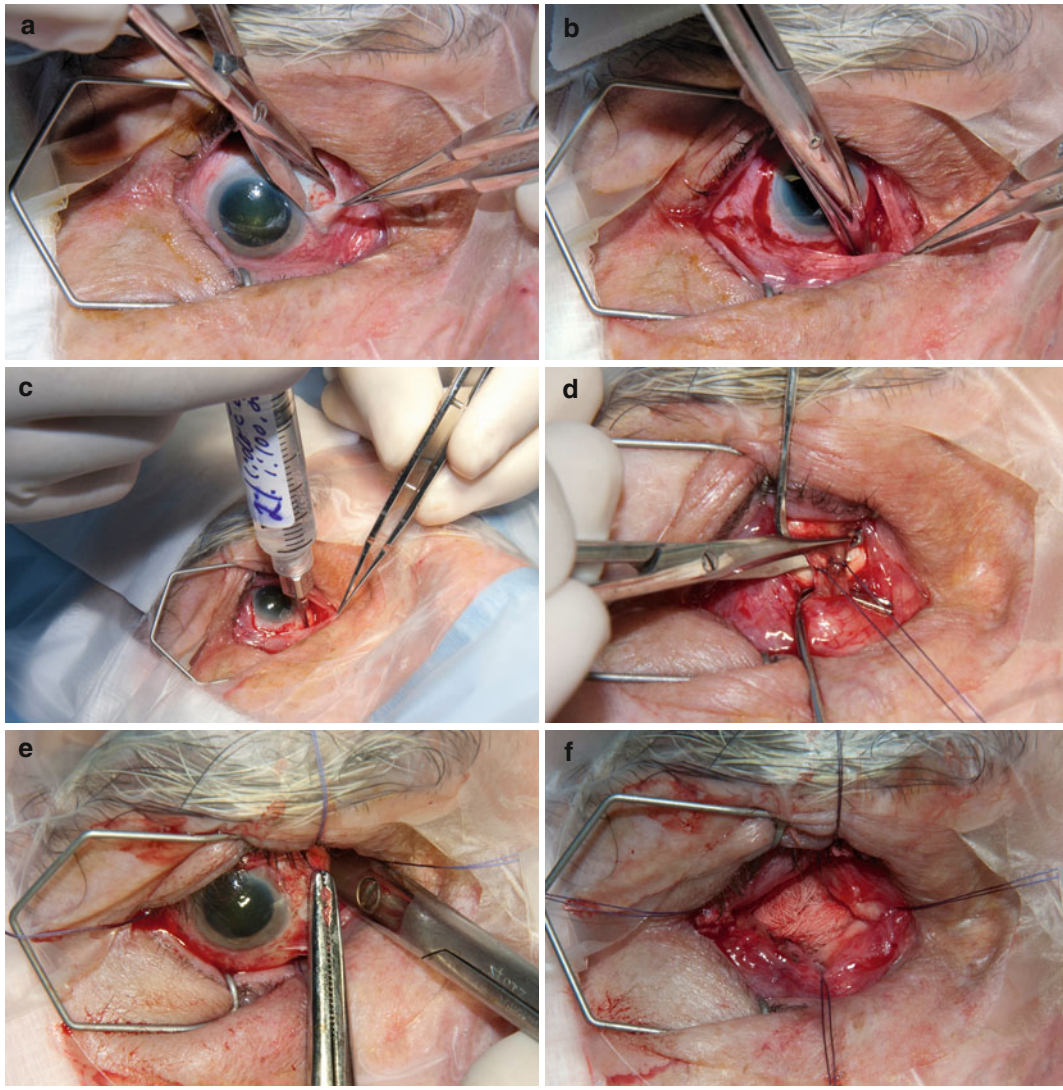

Fig. 15.2 Conjunctival peritomy (**a**) is followed by quadrantic dissection (**b**) and injection of local anesthetic (50:50 mixture of 2 % lignocaine with 1 in 100,000 epinephrine and 0.5 % bupivacaine) for hemostasis and postoperative analgesia (**c**). Recti muscle is then hooked and disinserted after tagging with 5-0 vicryl suture (**d**). Using a straight artery clamp applied to the medial rectus muscle stump with forward traction and slightly curved enucleation scissor inserted through the medial aspect, the optic nerve is identified by "strumming" (**e**). After resection of the optic nerve and delivery of the globe, the orbit is packed with a wet gauze (**f**). After 5–10 min hemostasis can be usually achieved by this method. A 22 mm unwrapped polyethylene implant is being inserted (**g**). All recti insertions are sutured to the implant in anatomical position (**h**) followed by meticulous closure of Tenon's layer (**i**) and conjunctiva (**j**). After insertion of a conformer, heavy patch is applied (**k**) (Reproduced with permission from Perry et al. [21])

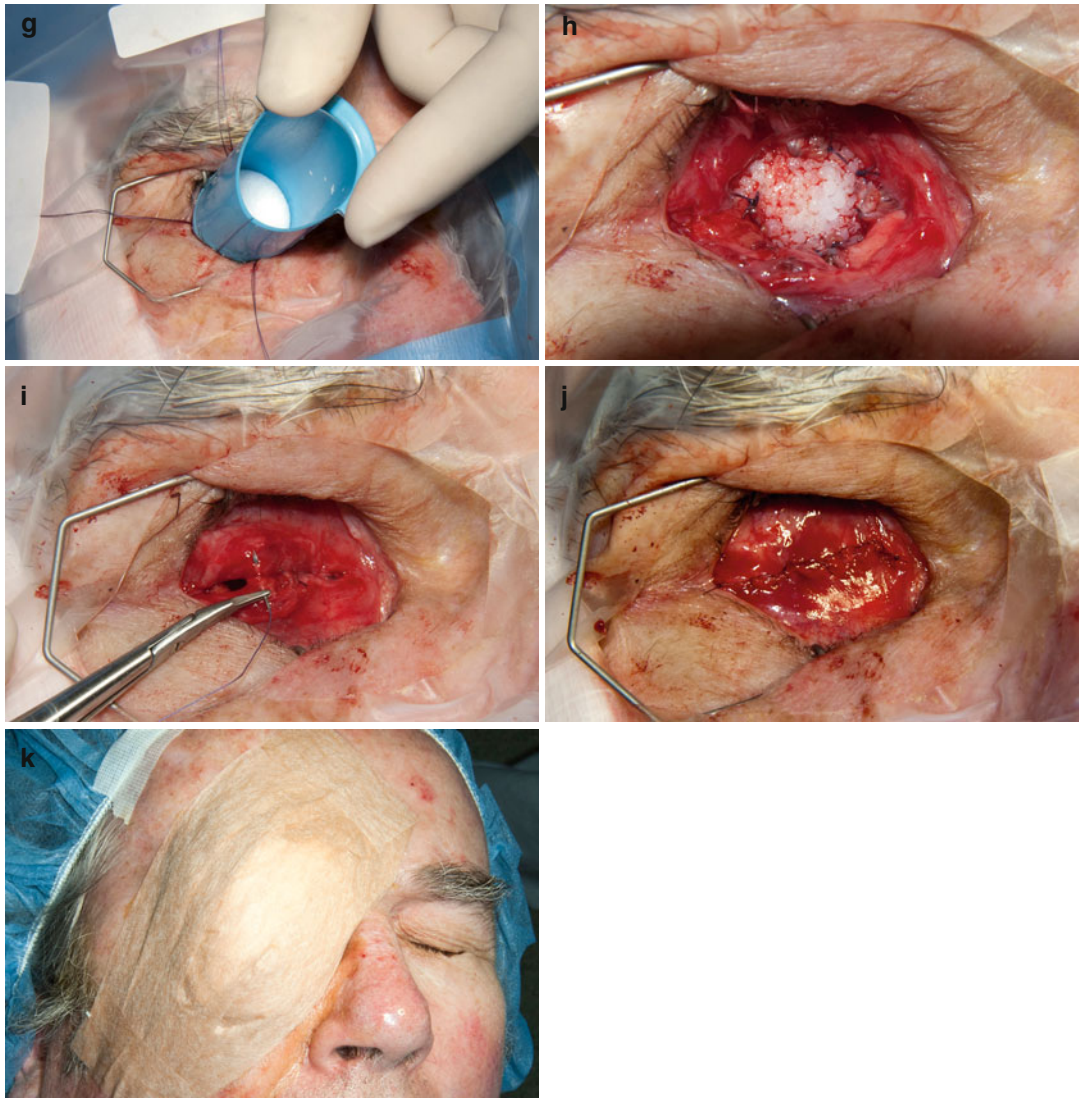

Fig. 15.2 (continued)

Blunt Westcott scissors are used to create a 360-degree peritomy. Conjunctiva and the Tenon layer are dissected from underlying sclera using Stevens scissors. Stevens scissors bluntly dissect each oblique quadrant and each rectus muscle is isolated on a muscle hook. The Tenon layer attachments to each rectus muscle are lysed and the muscle is secured on a double armed 6-0 polyglactin 910 suture through its insertion. Each muscle is disinserted from the globe using blunt Westcott scissors or Abley scissors.

The inferior oblique muscle insertion is identified and isolated with a muscle hook in the inferotemporal quadrant. The inferior oblique muscle may be cauterized prior to transection in order to minimize bleeding. The superior oblique muscle is identified in the superomedial quadrant and cut. Some surgeons secure the oblique muscles for later suturing to the implant.

After muscle disinsertion, some surgeons inject 2.5 cc of anesthetic solution into the sub-Tenon space of each oblique quadrant using a blunt irrigation tip. This may improve analgesia and hemostasis and displace the globe anteriorly to facilitate access to the optic nerve and reduce the risk of globe injury from the enucleation scissors.

A muscle hook is swept against the ocular surface to identify any remaining attachments that require dissection and a small incision is created in the posterior Tenon layer using Stevens scissors. A long curved hemostat may be introduced through the posterior Tenon layer incision to clamp the optic nerve in order to maintain hemostasis. The hemostat is inserted with the blades closed to palpate and strum the optic nerve prior to clamping. A hemostat or locking toothed forceps secures the medial rectus muscle stump to assist in gently retracting and elevating the globe. The optic nerve is transected using enucleation scissors, and the globe is removed using the hemostat or forceps on the medial rectus stump. Some surgeons do not clamp the optic nerve because the clamp may diminish the space to apply the enucleation scissors, and because clamping may introduce crush artifact to the optic nerve aspect of the specimen. After transection of the nerve, the optic nerve stump is cauterized with bipolar cautery under direct visualization using malleable retractors. Thermal trauma of the orbital soft tissues may cause a loss of orbital volume, so cautery should be minimized and performed only in the area of the optic nerve stump under direct visualization.

An injector or a periosteal elevator with modest posterior digital pressure is used to place the implant. For wrapped implants, windows can be created just posterior to each rectus muscle attachment. Otherwise, the muscles can be sutured directly to or over the implant. Direct attachment of the vertical rectus muscles to each other may lead to fornix insufficiency. Porous polyethylene allows for direct suturing of the rectus muscles to the implant. For unwrapped solid implants, suturing each rectus muscle to the adjacent rectus muscle suture using a 4-0 polyglactin 910 suture creates a physiologic attachment of the extraocular muscles over the implant with a diameter of approximately 10 mm. The anterior Tenon layer is closed using a running 4-0 polyglactin 910 suture. The conjunctiva is closed using a running 6-0 plain gut suture.

Antibiotic ointment and a small plastic conformer are placed into the socket and temporary tarsorrhaphy is performed. A pressure patch is placed up to 1 week (Fig. 15.3).

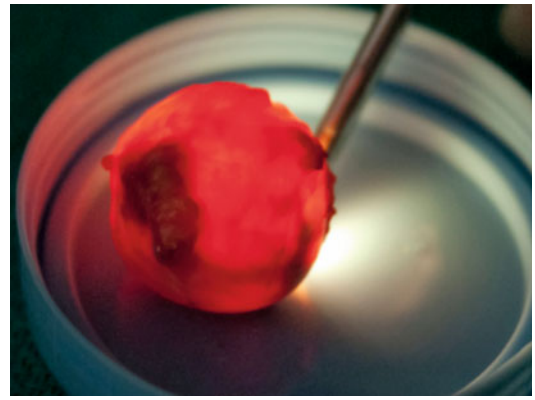

Fig. 15.3 Enucleated globe should be examined to document the length of the optic nerve stump, presence or absence of gross extraocular extension. Using transillumination, tumor can be easily located in preparation to retrieve fresh tissue for diagnostic, prognostic, or research purposes (Reproduced with permission from Perry et al. [21])

15.5 Results and Complications

15.5.1 Tumor Recurrence

In choroidal melanoma, tumor recurrence after enucleation is 1.1–14.6 %, and it can present up to 20 years following surgery. Patients with extrascleral extension discovered clinically, at surgery, or in the pathology laboratory, should receive periodic orbital imaging, such as CT scan, MR imaging, or positron emission tomography (PET scan) (Fig. 15.4) [22, 23].

15.5.2 Complications

Despite advances in operative techniques and improvements in orbital implants, postoperative complications continue to occur. Complication rates of 4–28 % have been reported [24, 25].

In the early postoperative period, local complications common to all surgeries, such as pain, swelling, and hemorrhage, may occur (Table 15.4). Early conjunctival wound dehiscence may also occur [26]. While conjunctival wound dehiscence may occur more commonly in patients with a history of preoperative radiation (8 % vs. 4 %) [24], this complication is often the result of poor technique. Proper implant sizing,

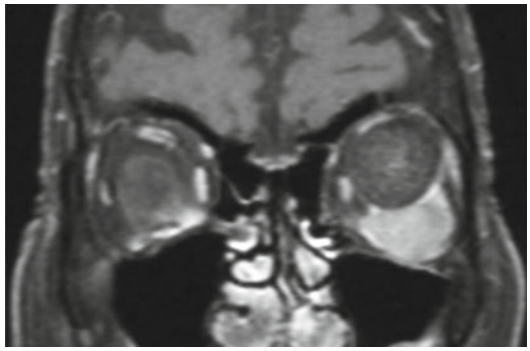

Fig. 15.4 Three years after an eventful enucleation for all large choroidal melanoma, this patient presented with displacement of the prosthesis. MRI (T1, post contrast, fat suppressed) showed enhancing orbital mass. Orbital recurrence of melanoma was confirmed by orbital fine-needle aspiration biopsy. Review of histopathology of the enucleated globe revealed evidence of extension into vortex vein without extrascleral or orbital extension

Table 15.4 Perioperative and immediate postoperative complications

Pain that prolonged hospitalization	1–2 %
Hemorrhage	1 %
Eyelid swelling	4 %

Modified from The Collaborative Ocular Melanoma Study (COMS) [25]

Table 15.5 Long-term complications of enucleation

Structure	Complication
Ocular surface	Chronic discharge, pyogenic granuloma, giant papillary conjunctivitis, conjunctival cyst
Implant	Exposure, extrusion, migration, infection, volume insufficiency
Eyelid	Laxity, malposition (ectropion, entropion, blepharoptosis)
Fornix	Foreshortening, socket contraction
Optic nerve	Phantom eye syndrome (visual hallucination and phantom eye pain)

posterior implant placement, and efforts to minimize wound tension minimize this complication. Early infection is uncommon and occurs equally between radiated and non-radiated eyes. Long-term complications can involve the surface, implant, eyelid, or the fornices (Table 15.5).

Significant overlap exists between these complications, and many can be avoided with proper surgical technique and implant sizing and placement. In the COMS large tumor trial, patients who received pre-enucleation radiation had an overall complication rate of 8 %, whereas patients who did not receive radiation had a complication rate of 4 % [25].

Additional complications of pegged implants include chronic discharge, visible prosthesis edges on extreme gaze, peg malposition, peg cracking, and an audible peg click [27]. Reports on overall complication rates vary widely for porous and nonporous implants and for pegged and unpegged implants. However, general trends among the various implant choices exist. While porous implants may not extrude as often as solid implants because of fibrovascular ingrowth, they likely incur a higher exposure rate versus silicone implants, and nearly all exposures will ultimately require surgical repair. Reported exposure rates range from 0 to 33.3 % for porous implants [28, 29]. A recent survey revealed an overall exposure rate of only 3 %, with the vast majority of events occurring with porous implants rather than solid implants [27]. A meta-analysis of exposure rates of enucleation implants demonstrated a 1.3 % rate with silicone, a 4.9 % rate with coralline hydroxyapatite, and an 8.1 % rate with porous polyethylene [30]. For pegged implants, all complication rates are greater, including pyogenic granuloma formation (14 %), exposure (6 %), infection (5 %), and peg malposition (5 %) [27].

Most exposed and extruded implants are chronically infected and will require surgical intervention to remove the avascular portion of the implant (and possibly the entire implant) and place vascularized tissue over the new/revised implant. Free mucous membrane implants placed directly over the exposed implant without removing the avascular and chronically infected portion rarely survive. Tarsoconjunctival flaps may be placed over the exposure after debriding the implant, but these flaps may produce fornix foreshortening. Dermis fat grafts may be placed over the debrided implant as well. Volume insufficiency can be addressed with deep orbital wedge implants or replacement of a small implant with a larger one. Injections of hyaluronic acid filler substances and free fat grafts have also been used to augment orbital volume. Fornix insufficiency can be addressed with free mucous membrane grafts

or allografts. Dermis fat grafts can simultaneously address volume and conjunctival insufficiency.

Phantom eye syndrome is increasingly recognized to be frequent and persistent even several years after enucleation. Visual hallucination and phantom eye pain (penetrating, shooting, or superficial) may be present in 42 and 23 % of cases, respectively [31].

15.6 Follow-Up

An anophthalmic socket patient requires lifelong follow-up, with the aim to address three major issues: comfort (a healthy socket with adequate structure allows for comfortable retention of an ocular prosthesis), cosmesis (symmetry of eyelid position, prosthesis projection, soft tissue contour, and prosthetic movement is never perfect, but can be maximized with additional surgery or revision of the prosthesis if needed; aging changes and the altered ligamentous structures after enucleation often produce cosmetic issues that may benefit from additional surgery), and disease recurrence (follow-up should include examination of the eye socket for signs of disease recurrence in addition to evaluating socket fornices, volume, implant, and eyelid position) [32].

Conclusion

Enucleation still represents the treatment of choice for a variety of ocular malignancies and tumors. Enucleation removes malignancy with clear margins to reduce metastasis and improve survival and allow for the comfortable retention of an ocular prosthesis to restore cosmesis. Understanding the principles of enucleation surgery should improve functional and aesthetic results while minimizing complications.

References

1. Setlur VJ, Parikh JG, Rao NA. Changing causes of enucleation over the past 60 years. Graefes Arch Clin Exp Ophthalmol. 2010;248(4):593–7.
2. Melia M, Moy CS, Reynolds SM, Hayman JA, Murray TG, Hovland KR, Earle JD, Kurinij N, Dong LM, Miskala PH, et al. Quality of life after iodine 125 brachytherapy vs enucleation for choroidal melanoma: 5-year results from the Collaborative Ocular Melanoma Study: COMS QOLS report no. 3. Arch Ophthalmol. 2006;124(2):226–38.
3. Jampol LM, Moy CS, Murray TG, Reynolds SM, Albert DM, Schachat AP, Diddie KR, Engstrom Jr RE, Finger PT, Hovland KR, et al. The COMS randomized trial of iodine 125 brachytherapy for choroidal melanoma: IV. Local treatment failure and enucleation in the first 5 years after brachytherapy. COMS report no. 19. Ophthalmology. 2002;109(12):2197–206.
4. Fine SL, Hawkins BS. The investigators' perspective on the collaborative ocular melanoma study. Arch Ophthalmol. 2007;125(7):968–71.
5. De Potter P, Shields JA, Shields CL, Santos R. Modified enucleation via lateral orbitotomy for choroidal melanoma with orbital extension: a report of two cases. Ophthal Plast Reconstr Surg. 1992;8(2):109–13.
6. Fusetti S, Parrozzani R, Urban F, Gurabardhi M, Ferronato G, Midena E. Modified enucleation for choroidal melanoma with large extrascleral extension. Orbit. 2010;29(2):70–5.
7. Singh AD, Jacques R, Rundle PA, Mudhar HS, Rennie IG. Combined enucleation and orbitotomy for choroidal melanoma with orbital extension. Eye (Lond). 2006;20(5):615–7.
8. Blanco G. Diagnosis and treatment of orbital invasion in uveal melanoma. Can J Ophthalmol. 2004;39(4):388–96.
9. Moshfeghi DM, Moshfeghi AA, Finger PT. Enucleation. Surv Ophthalmol. 2000;44(4):277–301.
10. Amaro TA, Yazigi L, Erwenne C. Depression and quality of life during treatment of ocular bulb removal in individuals with uveal melanoma. Eur J Cancer Care (Engl). 2010;19(4):476–81.
11. Coday MP, Warner MA, Jahrling KV, Rubin PA. Acquired monocular vision: functional consequences from the patient's perspective. Ophthal Plast Reconstr Surg. 2002;18(1):56–63.
12. Yen KG, Elner VM, Musch DC, Nelson CC. Periocular versus general anesthesia for ocular enucleation. Ophthal Plast Reconstr Surg. 2008;24(1):24–8.
13. Gayre GS, Lipham W, Dutton JJ. A comparison of rates of fibrovascular ingrowth in wrapped versus unwrapped hydroxyapatite spheres in a rabbit model. Ophthal Plast Reconstr Surg. 2002;18(4):275–80.
14. Viswanathan P, Sagoo MS, Olver JM. UK national survey of enucleation, evisceration and orbital implant trends. Br J Ophthalmol. 2007;91(5):616–9.
15. Custer PL, Kennedy RH, Woog JJ, Kaltreider SA, Meyer DR. Orbital implants in enucleation surgery: a report by the American Academy of Ophthalmology. Ophthalmology. 2003;110(10):2054–61.
16. Colen TP, Paridaens DA, Lemij HG, Mourits MP, van Den Bosch WA. Comparison of artificial eye amplitudes with acrylic and hydroxyapatite spherical enucleation implants. Ophthalmology. 2000;107(10):1889–94.

17. Perry JD, Tam RC. Safety of unwrapped spherical orbital implants. Ophthal Plast Reconstr Surg. 2004;20(4):281–4.
18. Wells TS, Harris GJ. Direct fixation of extraocular muscles to a silicone sphere: a cost-sensitive, low-risk enucleation procedure. Ophthal Plast Reconstr Surg. 2011;27(5):364–7.
19. Kaltreider SA, Lucarelli MJ. A simple algorithm for selection of implant size for enucleation and evisceration: a prospective study. Ophthal Plast Reconstr Surg. 2002;18(5):336–41.
20. Kaltreider SA, Peake LR, Carter BT. Pediatric enucleation: analysis of volume replacement. Arch Ophthalmol. 2001;119(3):379–84.
21. Perry JD, Singh AD, Mehta MP. Enucleation for choroidal melanomas. In: Ryan SJ, editor. Retina. St. Louis: Elsevier; 2011.
22. Shields JA, Augsburger JJ, Dougherty MJ. Orbital recurrence of choroidal melanoma 20 years after enucleation. Am J Ophthalmol. 1984;97(6):767–70.
23. Asensio Sanchez VM, Alonso M, Sierra JM. Positron emission tomography in the diagnosis of orbital relapse of choroidal melanoma. Arch Soc Esp Oftalmol. 2005;80(2):113–5.
24. Tataru CP, Pop MD. Enucleation in malignant choroidal melanoma – results in 15 years of using a new material in the prosthesis of the orbital cavity. J Med Life. 2012;5(2):185–8.
25. The Collaborative Ocular Melanoma Study (COMS) randomized trial of pre-enucleation radiation of large choroidal melanoma III: local complications and observations following enucleation COMS report no. 11. Am J Ophthalmol. 1998;126(3):362–72.
26. Sami D, Young S, Petersen R. Perspective on orbital enucleation implants. Surv Ophthalmol. 2007;52(3):244–65.
27. Su GW, Yen MT. Current trends in managing the anophthalmic socket after primary enucleation and evisceration. Ophthal Plast Reconstr Surg. 2004;20(4):274–80.
28. Nunery WR, Heinz GW, Bonnin JM, Martin RT, Cepela MA. Exposure rate of hydroxyapatite spheres in the anophthalmic socket: histopathologic correlation and comparison with silicone sphere implants. Ophthal Plast Reconstr Surg. 1993;9(2):96–104.
29. Nunery WR, Cepela MA, Heinz GW, Zale D, Martin RT. Extrusion rate of silicone spherical anophthalmic socket implants. Ophthal Plast Reconstr Surg. 1993;9(2):90–5.
30. Custer PL, Trinkaus KM. Porous implant exposure: incidence, management, and morbidity. Ophthal Plast Reconstr Surg. 2007;23(1):1–7.
31. Rasmussen ML. The eye amputated - consequences of eye amputation with emphasis on clinical aspects, phantom eye syndrome and quality of life. Acta Ophthalmol. 2010;88 Thesis 2:1–26.
32. Shields CL, Shields JA. Retinoblastoma management: advances in enucleation, intravenous chemoreduction, and intra-arterial chemotherapy. Curr Opin Ophthalmol. 2010;21(3):203–12.

Orbital Exenteration

16

Suresh Sagili and Raman Malhotra

Contents

S. Sagili, FRCOphth
R. Malhotra, MBChB, FRCOphth (✉)
Corneoplastic Unit, Queen Victoria Hospital,
East Grinstead, West Sussex RH193DZ, UK
e-mail: raman.malhotra@qvh.nhs.uk

16.1 Introduction

Orbital exenteration is defined as removal of all the orbital contents including the periorbita and eyelids. The aim of exenteration is to achieve local control of disease extending to the orbit while preserving normal tissues whenever possible to optimize surgical rehabilitation. Subtotal exenteration (eyelid sparing, conjunctiva sparing) is a modification of exenteration to aid healing and cosmetic rehabilitation. If the bone of the orbit is invaded, an "extended" exenteration is required that includes resection of the diseased bone. The ethmoids, maxillary wall, and zygomatic bone are commonly resected in extended orbital exenteration.

16.2 Indications

Orbital invasion by periocular cutaneous malignant tumors (basal cell carcinoma, sebaceous gland carcinoma, squamous cell carcinoma, and melanoma) remains the most common indication for orbital exenteration [1, 2]. Other indications include tumors arising in the conjunctiva, orbit, globe, or paranasal sinuses.

16.2.1 Eyelid Malignant Tumors

Basal cell carcinoma (BCC) is the most common malignant skin tumor accounting for approximately 90 % in most series [3, 4], squamous cell

J.D. Perry, A.D. Singh (eds.), *Clinical Ophthalmic Oncology*,
DOI 10.1007/978-3-642-40492-4_16, © Springer-Verlag Berlin Heidelberg 2014

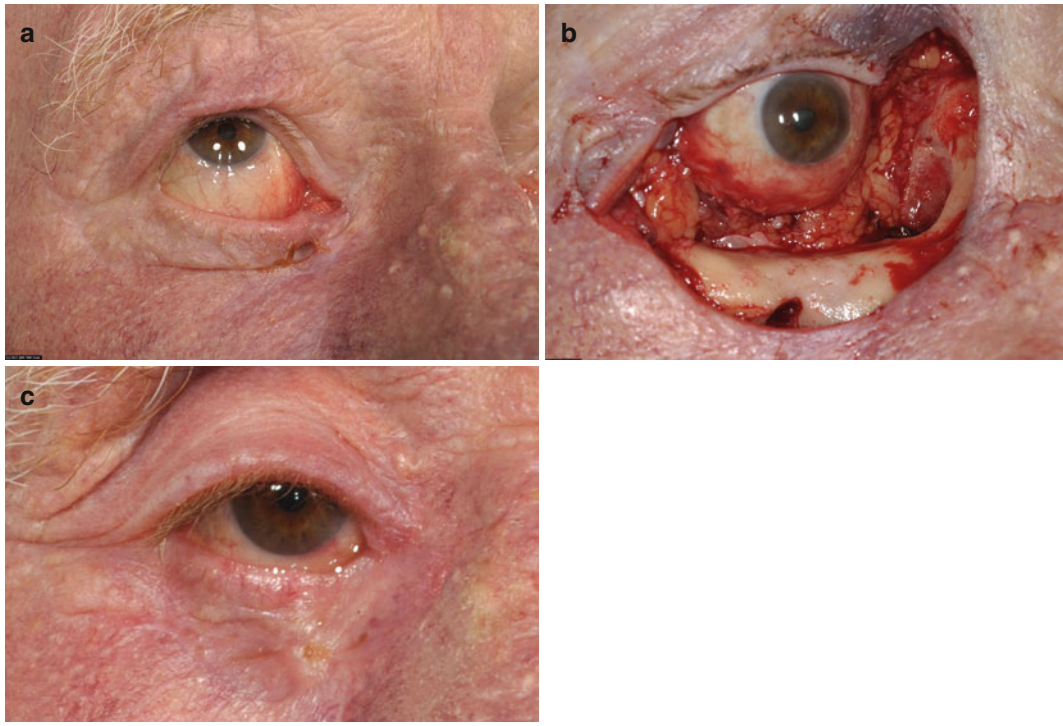

Fig. 16.1 Recurrent lower eyelid BCC invading the anterior orbit (**a**). Anterior *orbitectomy* was performed (globe sparing) to excise the tumor along with anterior orbital tissue and lacrimal sac with periosteum (**b**). The defect was closed using a midline forehead pericranial periosteal flap and skin graft. Appearance 4 months later (**c**)

carcinoma (SCC) and sebaceous gland carcinoma (SGC) each comprising approximately 4–6 % of cases. The reported incidence of orbital invasion by periocular cutaneous BCC and SCC is 1.6–2.5 and 5.9 %, respectively [5, 6]. Recurrent tumor, medial canthal location, infiltrative and morpheic histologic growth patterns, and perineural invasion are known risk factors for orbital invasion by BCC. Orbital invasion usually presents as mass effect (globe displacement, ptosis) or signs of tissue infiltration (restricted ocular motility, enophthalmos, immobile eyelids, fixation of the tumor to bone) [5].

Once the diagnosis of orbital invasion is made, the treatment modality should be individualized and chosen with consideration of the extent of orbital involvement, visual function, and the patient's general health. Exenteration may be combined with adjunctive radiotherapy in cases in which margins are not clear or in high-risk aggressive tumors with perineural invasion (PNI).

Although orbital invasion by BCC has been traditionally managed by exenteration, an alternative conservative (non-exenterating) excision may be considered in selected cases in early stages of anterior orbital invasion [5]. In selected cases, when there is only anterior orbital involvement or in patients with a single eye, local excision (Fig. 16.1) with or without radiotherapy and close follow-up with regular scans (preferably magnetic resonance imaging, MRI) is a possible alternative option (globe-sparing excision). Madge et al. reported a 20 case series of medial canthal BCCs, complicated by anterior orbital invasion, managed using globe-sparing surgical techniques rather than exenteration [5]. There was one recurrence in this series in a patient with previously recurrent disease. Surgical technique involved en bloc excision of visible tumor plus a clinically tumor-free margin. Bone was removed as part of an en bloc specimen in five patients. The lacrimal sac was removed in every patient.

Frozen-section histologic examination was used for margin control in eight patients (40 %) and rapid paraffin in nine patients (45 %). A combination of techniques (frozen section then paraffin, Mohs' surgery then paraffin section) was used in three patients to address cutaneous and then deeper orbital margins, respectively. The decision to exenterate or to pursue a conservative surgical excision should be made after a full discussion with the individual patient and taking into consideration the level of vision in each eye.

Orbital invasion has been reported in 6–45 % of SGC cases and orbital exenteration may help reduce the potential for metastasis and improve survival [7, 8]. Presence of conjunctival intraepithelial (pagetoid) spread in SGC of eyelids has been reported to traditionally carry a higher likelihood for requiring orbital exenteration [9].

16.2.2 Conjunctival Malignant Tumors

The most common conjunctival tumors that require exenteration are melanoma and squamous cell carcinoma. McKelvie et al. reported orbital invasion in 15 % of cases with conjunctival squamous cell neoplasia and performed orbital exenteration in all these cases [10]. Conjunctival squamous cell carcinoma, particularly the rare variants, mucoepidermoid or spindle cell carcinomas, tends to invade the orbit, and in such cases, orbital exenteration generally achieves tumor control [11]. Nowadays, however, with the advent of topical chemotherapy, there has been a paradigm shift in the management of ocular surface squamous neoplasia with only advanced invasive lesions requiring exenteration.

Shield et al. [12] recommended orbital exenteration in extensive recurrent conjunctival melanoma and in cosmetically unacceptable or non-resectable neoplasm without demonstrable metastasis. In cases of advanced conjunctival melanoma, they recommended an eyelid-sparing exenteration, which provides more rapid healing of the socket. Recently however, adjunctive brachytherapy and topical chemotherapy have been reported to achieve high rates of local tumor control in conjunctival melanoma, obviating the need for exenteration [13].

16.2.3 Intraocular Malignant Tumors

The management of choroidal melanoma with extrascleral extension has been a subject of controversy with some authors proposing orbital exenteration whenever extrascleral extension is demonstrated and others reporting it to be of no value in increasing survival [12, 14]. Although extrascleral extension of choroidal melanoma is associated with an increased risk of metastasis, there has been no clinically significant difference noted in survival probabilities of patients undergoing early exenteration compared to enucleation alone, on extended follow-up [14, 15]. Poor prognosis in these patients is due to the increased risk of metastasis associated with extrascleral extension. Anterior extrascleral extension can be treated by local resection with enucleation or scleral reinforcement after local radiation therapy. Advanced extension may be dealt with by enucleation with resection of all visible orbital melanoma followed by radiation [16].

The indication for exenteration is now becoming obsolete in the management of retinoblastoma [17]. Retinoblastoma invading the orbit can now be managed with neoadjuvant chemotherapy followed by enucleation.

16.2.4 Orbital Malignant Tumors

The primary modality of treatment of orbital rhabdomyosarcoma is combined radiotherapy and chemotherapy. Orbital exenteration may be indicated in cases of incomplete tumor regression or in cases of recurrence after treatment with chemotherapy and radiotherapy [18].

According to the American Joint Committee on Cancer Tumor Node Metastasis definition, stage T3 or more adenoid cystic carcinoma of the lacrimal gland (tumor between 2.5 and 5 cm in greatest dimension) is an indication for orbital exenteration [19]. Adenoid cystic carcinoma of

the lacrimal gland is known to invade bone as well as demonstrate perineural infiltration. Therefore, these tumors are managed with orbital exenteration including removal of bone from the lacrimal gland fossa (part of the orbital roof and lateral wall), followed by radiotherapy [20].

16.2.5 Paranasal Sinus Malignant Tumors

Tumors arising in the paranasal sinuses and nose may also require exenteration, and the indications include involvement of the orbital apex, unresectable full-thickness invasion through periorbita into posterior orbital fat, extension into the extraocular muscles, and invasion of the bulbar conjunctiva or sclera [21]. As the eyelids are rarely involved by tumors arising from paranasal sinuses, an eyelid-sparing exenteration can usually be performed in these cases.

Dhiwakar et al. [22] recommend exenteration in all patients with invasive sino-orbital aspergillosis involving retrobulbar tissues and the orbital apex. However, Pushker et al. [23] have recently questioned the need for orbital surgery in the management of orbital aspergillosis reporting control of infection with antifungal agents alone.

16.2.6 Miscellaneous Diseases

Orbital exenteration has been reported in the management of advanced or poorly controlled benign orbital disease associated with chronic periorbital pain and no functional vision [24]. In these cases, an eyelid-sparing exenteration can be performed.

16.3 Preoperative Preparation

A multidisciplinary team approach is necessary in planning the management of cases with malignant tumors invading the orbit. A maxillofacial or head and neck surgeon, plastic surgeon, neurosurgeon, pathologist, radiologist, and an oncologist may be involved in the management of these cases. As it is a disfiguring procedure with prolonged rehabilitation, preoperative counseling is important in deciding on the timing and best surgical approach.

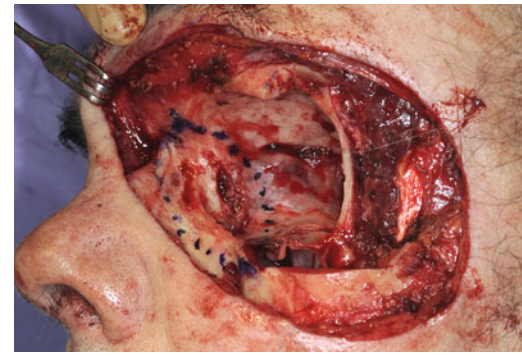

Fig. 16.2 Extended exenteration with partial excision of lateral orbital wall and temporalis muscle. The lacrimal sac fossa and medial maxilla surrounding this area are outlined for excision based upon radiological evidence of extension into the proximal nasolacrimal duct

The surgical technique is dependent upon the location and extent of the tumor. The eyelids may be preserved in tumors placed posteriorly within the orbit and in selected cases with periocular skin involvement. If macroscopic changes suspicious of bone invasion are identified at the time of surgery, frozen-section examination of the periorbita may be helpful in identifying tumor infiltration. If it is positive, an extended exenteration (Fig. 16.2) is required with wide margin removal of adjacent bone up to normal-looking bone cortex. The resected bone should be sent for decalcification and pathological analysis.

Computerized tomography (CT) scanning should be performed to evaluate the bony details of the orbit. The image acquisition protocol should include fine cuts (1–3 mm), coronal and axial views with bone and soft tissue windows. MRI with contrast is required to identify the extent of tumor invasion into and beyond the orbit. MRI with contrast is also useful in helping to identify perineural invasion. Antiplatelet agents should be discontinued preoperatively if considered appropriate. Arrangements should be made for cross-matched blood in patients with low hemoglobin levels. A pathologist should be consulted in advance for the potential need for

frozen-section evaluation of cutaneous resection margins. The anesthetist should be warned that the dissection and excision of the orbital apex can provoke the oculocardiac reflex, inducing a severe bradycardia and, occasionally, brief asystole.

16.4 Technique

General anesthesia is preferable due to potential for inadequate analgesia during posterior excision with the use of regional and local anesthesia combined with intravenous sedation. In all cases, adjunctive regional anesthesia, 5–10 ml of 0.5 % bupivacaine with 1:200,000 units of adrenaline, is given as a peribulbar injection. In addition, a further 10–12 ml of 0.5 % bupivacaine with 1:200,000 units of adrenaline is given as a series of subcutaneous injections around the orbital margin and as specific nerve blocks around the supratrochlear, supraorbital, infratrochlear, anterior ethmoidal, infraorbital, zygomaticofacial, and zygomaticotemporal nerves.

16.4.1 Total Exenteration (Exenteration Including the Eyelids)

The skin incision is marked around the orbital margin. The eyebrow is normally preserved unless involved in the malignant tumor. The eyelid margins are sutured together with a 4-0 silk suture. Skin and subcutaneous tissues are incised using a No. 15 blade and the dissection is carried down to the periosteum of the orbital rim. Hemostasis is achieved with a bipolar cautery. The periosteum at the orbital margin is then incised with a No. 15 blade (Fig. 16.3). The periosteum is elevated from the margins of the orbit and subperiosteal dissection into the orbit is carried out using a periosteal elevator. Malleable retractors such as Davis brain spatulas, Bernstein nasal, or Sewell orbital retractors are placed around the orbit to retract the soft tissues (Fig. 16.3). The periosteum is elevated from the orbital walls, beginning superotemporally in a spiral configuration, circumnavigating the anterior orbit before continuing the dissection more posteriorly. The periosteum should be kept intact to avoid any prolapse of orbital fat. Periosteal elevation along the orbital roof should be performed carefully to avoid the risk of damage to the dura mater through dehiscences in the bone (Fig. 16.4). The use of monopolar cautery should be avoided along the orbital roof and apex as it can result in cerebrospinal fluid leak in the presence of bony defects. The dissection is then continued inferotemporally and the lateral canthal tendon is incised. The zygomaticotemporal and zygomaticofacial vessels are cauterized and the dissection is then continued across the floor of the orbit. Bleeding from the bone can be managed with bone wax. The subperiosteal dissection

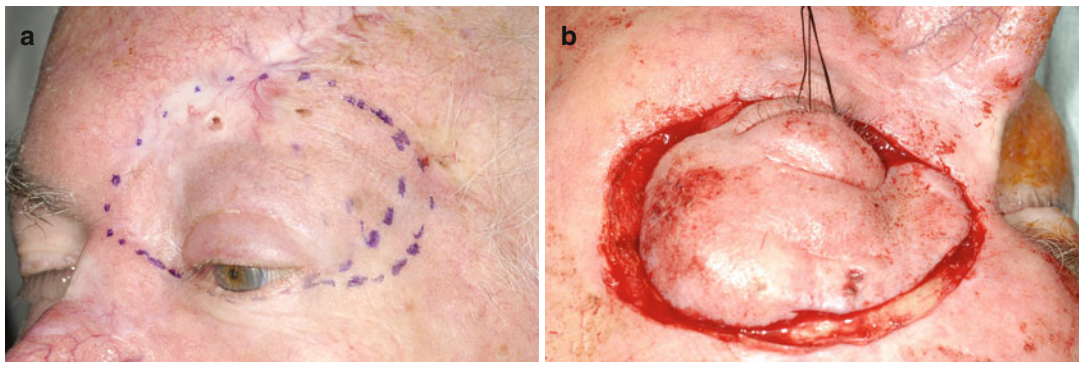

Fig. 16.3 Skin incision is marked for total exenteration (**a**), and skin, subcutaneous tissue, and periosteum are incised (**b**). Periosteum is elevated (**c**) from the margins of the orbit and subperiosteal dissection into the orbit is carried out along the lateral wall of the orbit (**d**). Exenterated orbit (**e**)

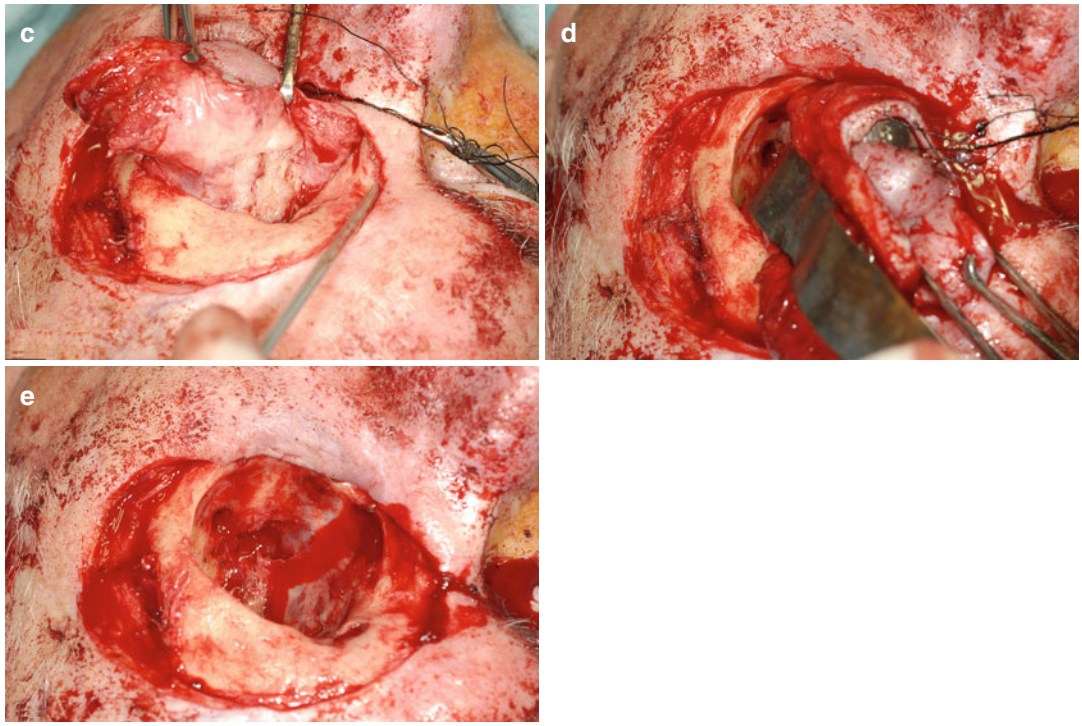

Fig. 16.3 (continued)

then continues from the superolateral orbit towards the superomedial orbit. The supraorbital and supratrochlear vessels are cauterized using bipolar cautery.

At the medial canthus, the angular vessels are cauterized using bipolar cautery and the medial canthal tendon is incised. The subperiosteal dissection is then carried along the lacrimal fossa beyond the posterior lacrimal crest. The proximal nasolacrimal duct (NLD) is incised at the entrance of its foramen and hemostasis is usually achieved using both monopolar and bipolar cautery.

The periorbita is carefully raised from the medial orbital wall, avoiding fracture of the lamina papyracea. The anterior and posterior ethmoidal vessels are identified at their respective foramina and are cauterized. Once the dissection has approached the apex of the orbit, a curved clamp is placed deeply within the orbit, just anterior and close to the apex enclosing the muscles, nerves, and vessels. Tissues anterior to the clamp are excised. Intracranial arterial avulsion during orbital exenteration has been reported due to variable communications between the ophthalmic artery and other intracranial vascular structures [25]. Therefore, judicious traction on orbital apical soft tissue should be used during exenteration to minimize the risk of intracranial injury. Where macroscopic or radiological evidence of bone involvement exists, the affected bone is removed with rongeurs or a saw (extended exenteration). The skin and muscle are approximated medially and laterally at the orbital rim to reduce the skin aperture before assessing the defect to reconstruct.

16.4.2 Subtotal Exenteration

In subtotal exenteration, the orbital tissues are preserved including eyelid skin, orbicularis muscle, and conjunctiva to achieve rapid healing and early cosmetic rehabilitation. Subtotal exenteration can be further classified into eyelid-sparing exenteration and eyelid- and conjunctiva-sparing exenteration.

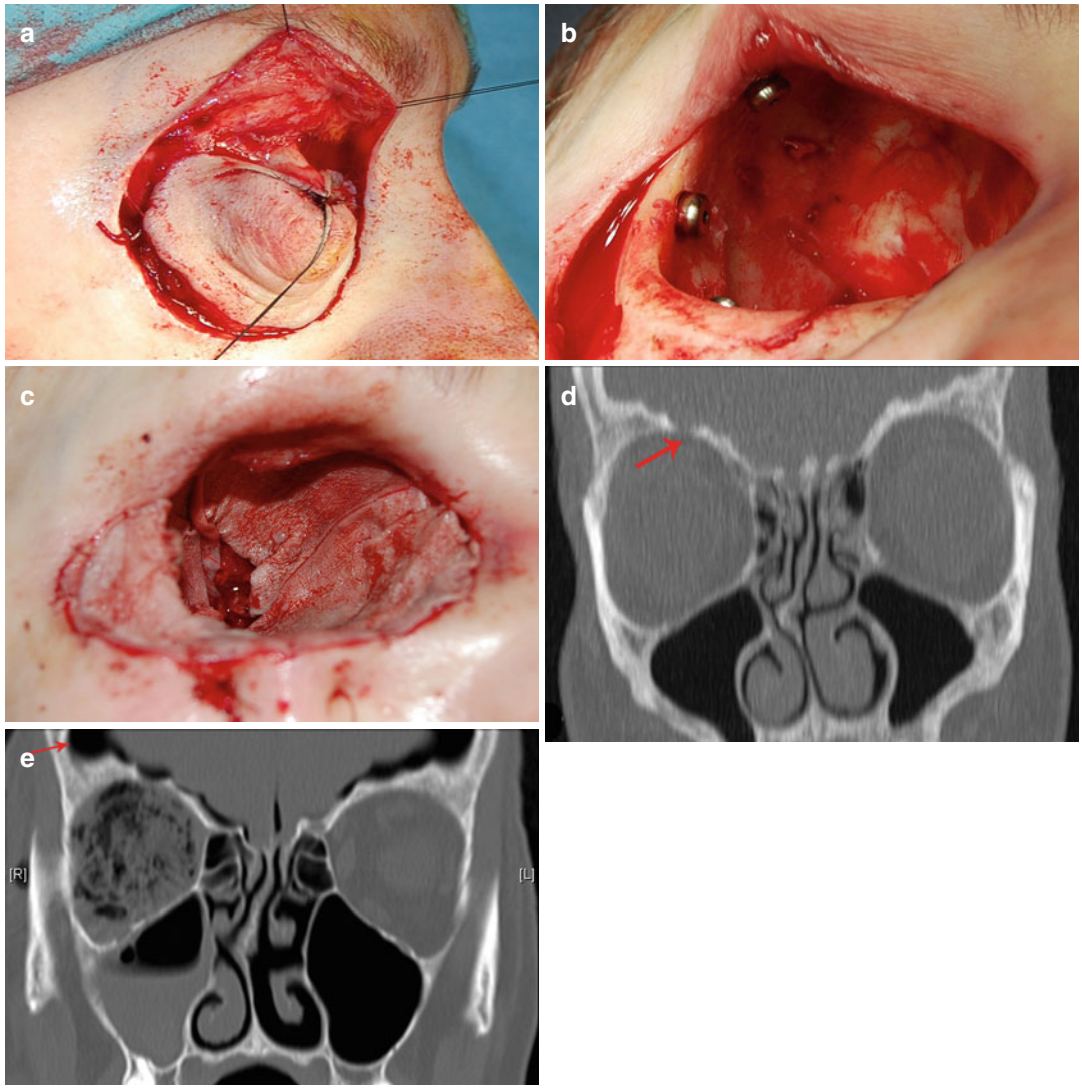

Fig. 16.4 Orbital exenteration was performed for a lower eyelid sebaceous gland carcinoma invading the orbit (**a**). Osseointegration (**b**) was performed at the time of exenteration and the socket was lined with split-thickness skin graft (**c**). Breach in the thin orbital roof occurred during surgery in a thin aspect of the orbital roof that can be seen in the preoperative CT scan (**d**, *arrow*), which resulted in CSF leak and a pathognomonic pneumocranium (**e**, *arrow*) postoperatively

16.4.2.1 Eyelid-Sparing Exenteration

Incisions are made 1 mm from the lashes in the upper and lower lids (Fig. 16.5). Dissection is preferably deep to the orbicularis muscle, but it can be at a more superficial level between the skin and orbicularis muscle if tumor clearance would be compromised by a deeper level of dissection. At the orbital rim, the periosteum is incised 360° and the exenteration proceeds as described for total exenteration above. The skin–muscle flaps preserved from the eyelids are sutured together (Fig. 16.5). A drain may be placed in the socket; however, this is not usually necessary. Antibiotic ointment is instilled. A simple dressing is placed over the skin lining of the socket and a pressure bandage is applied. Healing is significantly shorter following eyelid-sparing exenteration. The socket deepens relatively

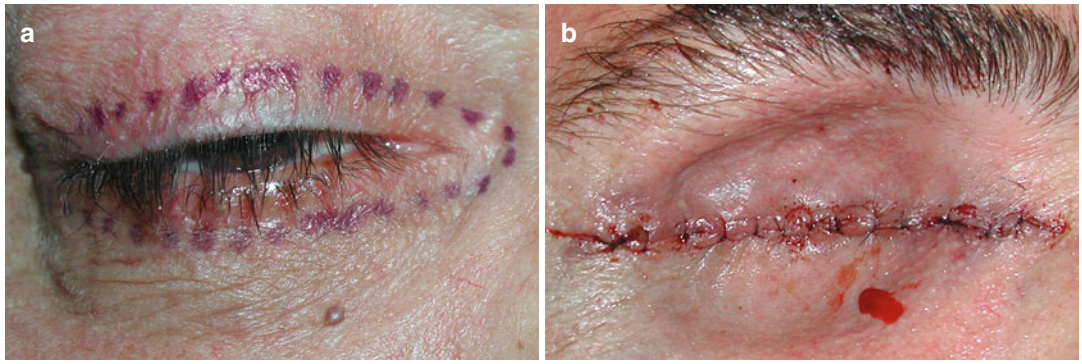

Fig. 16.5 Sub- and supraciliary skin incision marked for eyelid-sparing exenteration (**a**). The skin–muscle flaps preserved from the eyelids are sutured together after exenteration (**b**)

quickly postoperatively in order to allow fitting of a prosthesis.

16.4.2.2 Eyelid- and Conjunctiva-Sparing Exenteration

Conjunctiva-sparing exenteration has been reported by Goldberg et al. [1] and may be suitable in selected cases, taking into consideration the location of the tumor (localized invasion in one quadrant of the orbit) and biological behavior of the disease process. Looi et al. described an eyelid- and conjunctiva-sparing exenteration procedure with temporalis muscle transfer and dermis fat graft [26]. They reserved this procedure for selected cases with histologically benign orbital lesions that exhibit local aggressive clinical behavior or for malignant lesions with no significant conjunctival, eyelid, lacrimal gland, or posterior orbit involvement.

Preservation of eyelids and the conjunctiva allows early rehabilitation and fitting of an ocular prosthesis (prosthetic shell). The basic requirements for a conjunctiva-sparing exenteration socket to maintain a prosthetic shell are (1) orbital tissue volume to support the prosthesis, (2) a mucous membrane surface with fornices to accommodate the prosthesis, and (3) eyelids to hold the prosthesis within the socket [1].

A limbal peritomy is performed and the dissection is carried out in the subconjunctival plane to the orbital rim. A subperiosteal dissection is then carried out posteriorly into the orbit thus preserving the uninvolved conjunctiva. Goldberg et al. recommended preserving approximately 50 % of the conjunctival surface and then using a mucous membrane-free graft (buccal mucosa, hard palate mucosa, or nasal turbinate mucosa) to reconstruct the residual defect in the fornix [1]. A dermis fat graft is sutured to the deep orbital remnants to augment the orbital volume.

16.5 Reconstruction of the Orbital Cavity

Orbital reconstruction can be divided into three groups: *local*, healing by secondary intention (laissez-faire), split-thickness skin graft, or dermis fat graft; *locoregional*, advancement flaps, regional pedicle flaps, temporalis muscle transfer, frontalis rotational flap, or temporoparietal fascial flap; and *distal,* microvascular free flaps.

16.5.1 Local Reconstruction Techniques

16.5.1.1 Laissez-Faire

The traditional approach after excision is to allow healing by spontaneous granulation and epithelialization [27]. If the socket is to be left to heal by secondary intention or if a split-thickness skin graft is used (see below), antibiotic ointment is instilled and either an Aquacel® dressing (ConvaTec Ltd) or an Allevyn Cavity® dressing

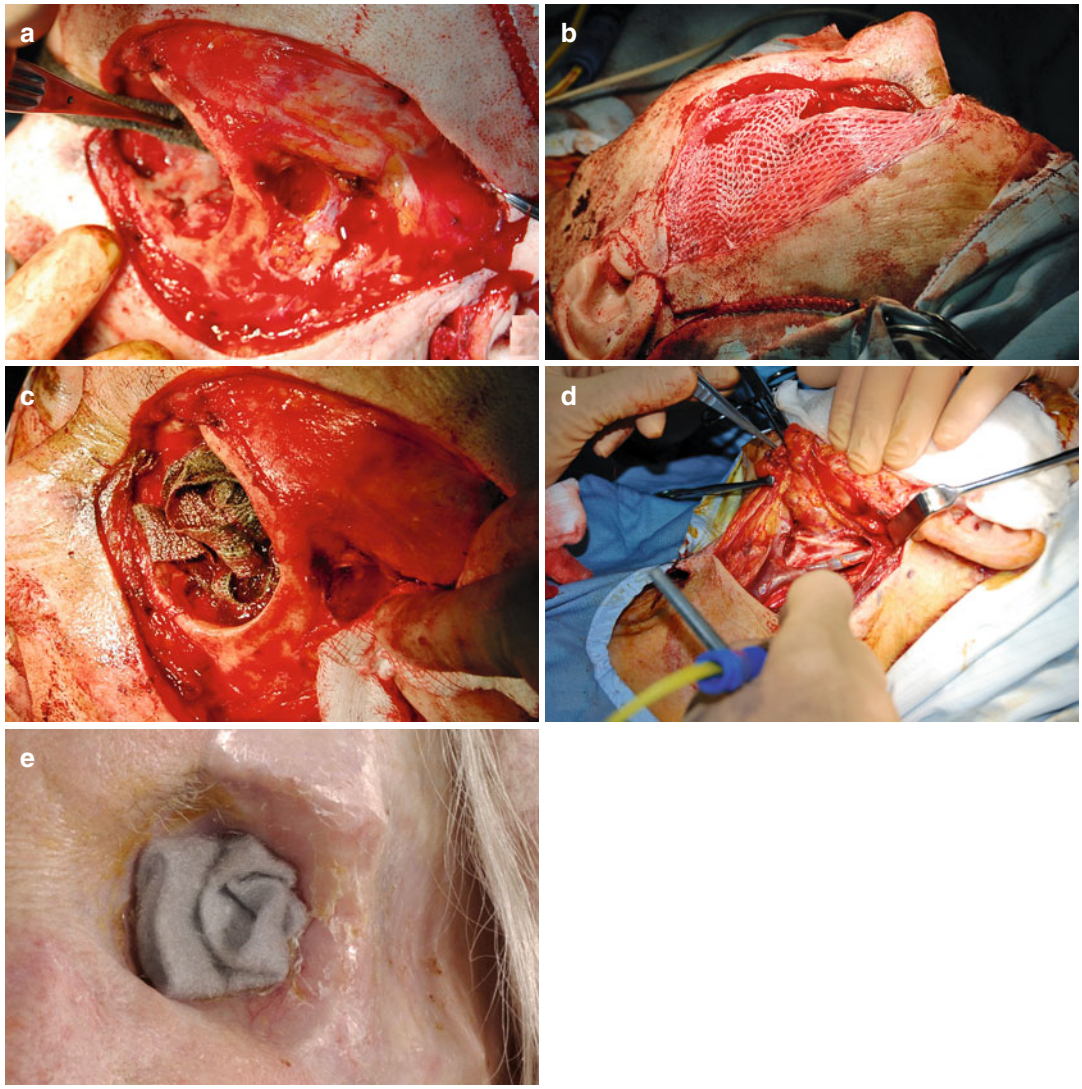

Fig. 16.6 Orbital exenteration defect (**a**), following excision of a large 8 cm diameter malignant melanoma of the eyelid (Breslow thickness greater than 4 mm and Clark's level V). Neck dissection was performed at the same time. The socket was dressed with Whitehead's varnish soaked in ribbon gauze and allowed to heal by laissez-faire (**b**, **c**). The temple defect was covered with a fenestrated split-thickness skin graft (**d**). This patient remains alive and well 4 years since excision (**e**)

(manufactured by Smith & Nephew United, Inc. of Largo, FL) is placed into the socket and a sterile dressing (eye pads) is applied [28]. The purpose of a deep cavity dressing is to provide an antibacterial role and stimulus for granulation and hemostasis. To this effect, a cheaper alternative for a deep cavity dressing (Fig. 16.6) in individuals without a history of iodine sensitivity is the traditional Whitehead's varnish (compound iodoform paint BPC). It consists of iodoform, benzoin, starch, natural balsams, and solvent ether. In addition to its disinfectant action, the iodoform provides some anesthesia when applied to mucous membranes and has been shown to reduce pain on split-thickness skin graft donor sites [29, 30].

The dressing is removed 5–6 days postoperatively. The socket is cleaned and dressed daily for

2 weeks and the frequency of the wound care is gradually reduced. The wound can be left exposed and camouflaged with a plastic eye shield (Cartella shield) once the discharge has ceased. Complete healing of the socket can take up to 3–4 months. An orbital prosthesis is fitted when the socket has completely healed. Laissez-faire is an easier, quicker option that allows recurrences to be detected potentially early (an advantage in the past before improved imaging became available) and provides a comparable color match to the surrounding skin when granulation is complete. Historically, this was considered particularly useful in the elderly patients not suitable for more lengthy reconstructive procedures. The disadvantages of secondary healing of an exenterated orbit include the need for regular dressing changes, delayed healing, potentially greater likelihood of persistent sino-orbital fistulas, prolonged postoperative socket care, and delayed facial rehabilitation. The Manchester orbital exenteration wound assessment tool (MOEWAT) has been reported to be useful in tracking changes in wound healing, postoperatively [31]. MOEWAT uses eight parameters as indices for the assessment and tracking of wound progress and wound healing (body mass index, bone exposure, wound appearance, fistula/sinus, exudates, wound margin, pain, and conjunctive therapies).

16.5.1.2 Split-Thickness Skin Graft

Split- or full-thickness skin grafts can be used for reconstruction when an open cavity is desired; when there is no need to isolate the orbital cavity from the sinonasal, oral, or intracranial cavities; and when radiation therapy is not given preoperatively or postoperatively. A split-thickness skin graft is preferred and provides the greatest coverage. It is usually harvested from the thigh with a dermatome and placed directly onto the bone in order to line as much of the socket as possible (Fig. 16.7). The edges of the graft are usually sutured to the skin edges around the socket. The use of a skin graft shortens the healing period. It helps reduce undue wound contracture and maintains a deeper socket in comparison to that usually achieved by secondary healing in order to enable easy fitting of an orbital prosthesis. It also facilitates easy examination of the socket where the possibility of tumor recurrence may exist. This approach however requires a separate donor site. The skin graft may fail in patients who are at risk of poor healing, including diabetic patients and those who have previously received radiotherapy.

Split-thickness skin grafts may be used in conjunction with and placed over pericranial periosteal flaps. A large periosteal flap may be harvested from the forehead and placed directly over the bony cavity and, in particular, any bony defect of the orbital roof or medial wall. Pericranial periosteal flaps, being a vascular structure, help accelerate the take of split-thickness skin grafts and also osseointegration thus reducing the time taken for prosthetic rehabilitation (Fig. 16.7) [32].

16.5.1.3 Dermis Fat Graft

A dermis fat graft from the abdominal wall can be used to fill the defect after subtotal eyelid-sparing exenteration. The remaining eyelid skin is closed over the graft. The dermis fat graft derives its blood supply from any residual posterior orbital tissues and the eyelid skin and orbicularis muscle anteriorly. Alternatively, a myocutaneous flap may also be advanced over the graft to provide further blood supply to the dermis fat graft [33].

Locoregional flaps and microvascular free flaps provide early rehabilitation. These act as effective barriers for separating the orbit from adjacent structures particularly if an extended orbital exenteration is performed. A locoregional and even distal free flap is of potential benefit in patients receiving postoperative adjunctive radiation therapy. In addition to providing soft tissue coverage over the orbital bones, locoregional flaps and microvascular free flaps allow isolation of the orbit from the nasal cavity, paranasal sinuses, and cranial cavity to help prevent fistulas. Locoregional flaps have the advantage of being derived from areas anatomically adjacent to the orbit and require less socket care than for sockets managed by laissez-faire or split-thickness skin grafts [27].

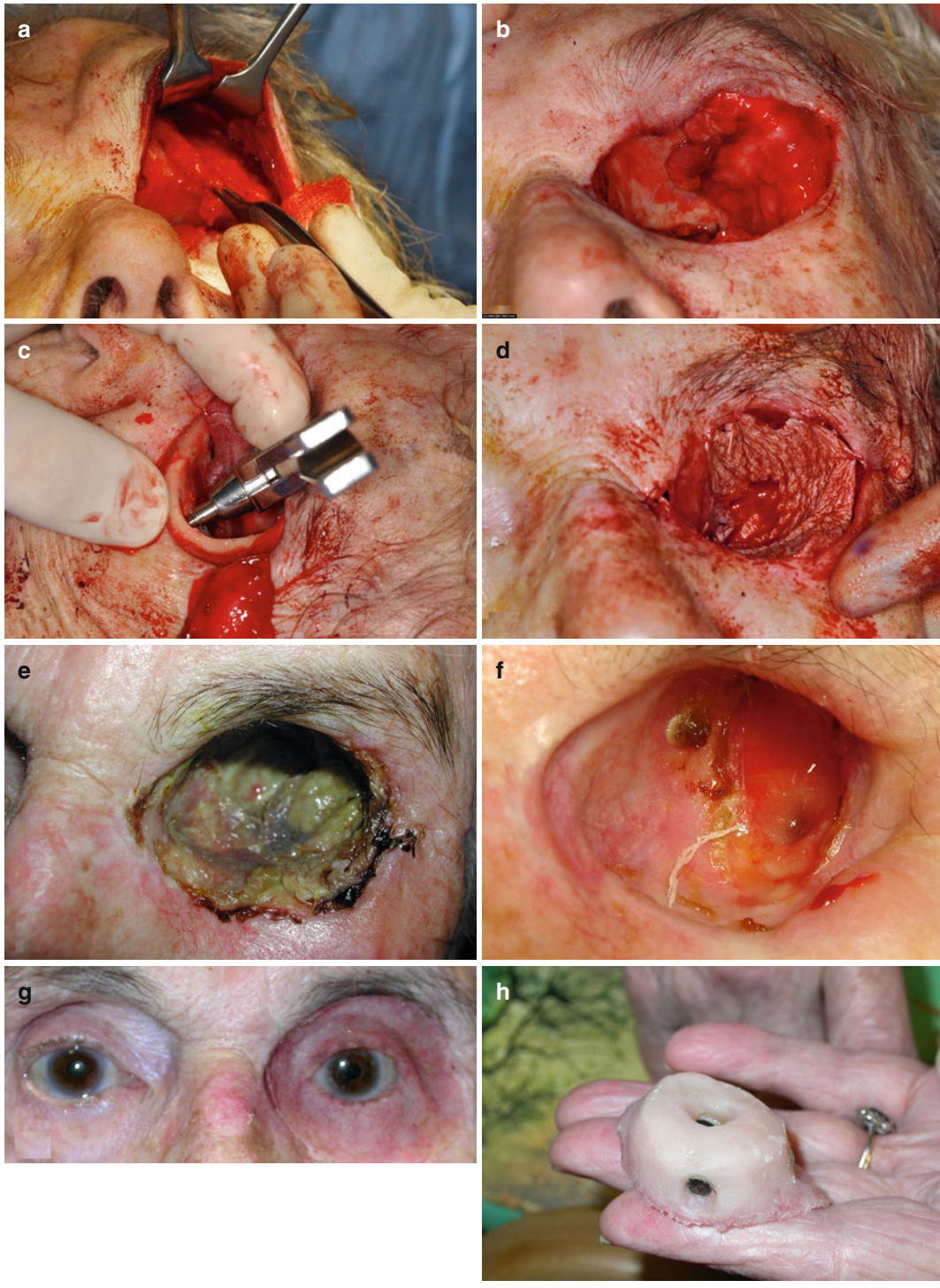

Fig. 16.7 This patient had previously undergone orbital radiotherapy for an incompletely excised basal cell carcinoma which subsequently recurred, requiring exenteration. Pericranial flap fashioned from the forehead to line the exenterated orbit (**a**, **b**). Osseointegrated implants inserted at the time of exenteration (**c**). Split-thickness skin graft placed over the pericranial flap to line the orbit (**d**). Three weeks post exenteration with split-thickness skin graft placed over a pericranial flap (**e**). Nine months later, the socket has still not healed completely and there is incomplete keratinization (**f**). Magnets cast into the posterior surface of the prosthesis (**h**). Prosthesis covering the exenterated left orbit (**g**)

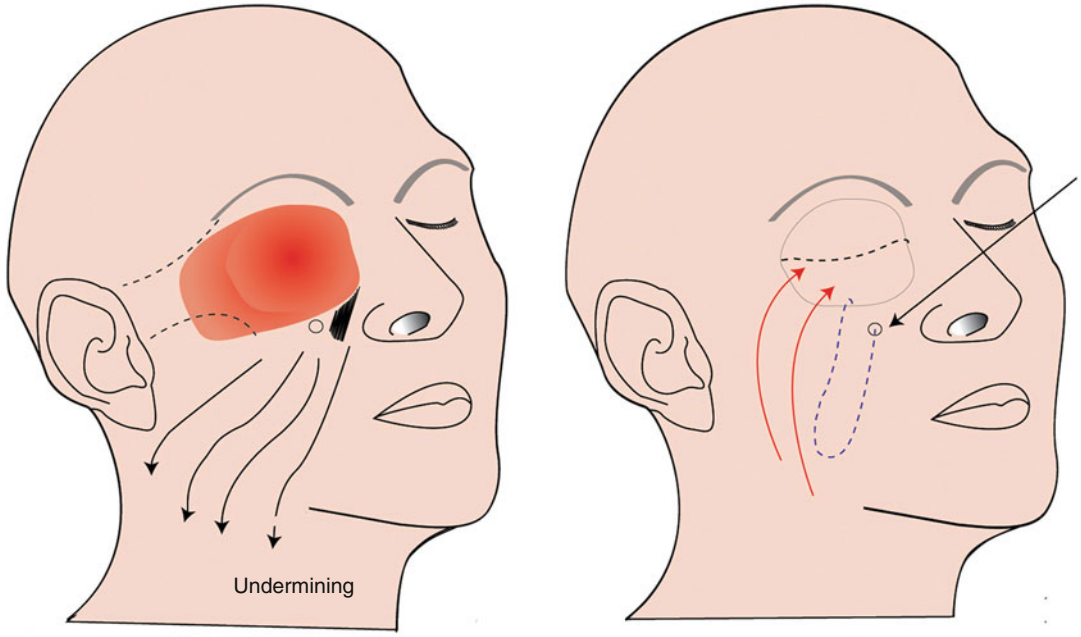

Fig. 16.8 Following total exenteration, subcutaneous cheek dissection (to avoid injury to the facial nerve) is carried out to a level just below the oral commissure and 2–3 cm below the angle of the mandible (**a**). To facilitate sufficient vertical advancement of the cheek flap, a point for deep fixation of the flap is created using deep sutures to the inferior orbital rim with using 4-0 Vicryl® sutures and where periosteum is not present, using the infraorbital canal as a bone tunnel (**b**, *arrow*). The cheek flap is padded with the cheek supported upwards for 3–7 days

16.5.2 Locoregional Reconstruction Techniques

16.5.2.1 Cheek Advancement Flap

Our preferred technique of direct closure with cheek advancement is a modification of the cervicofacial flap and offers a one-stage, reliable, and safe method of reconstruction following orbital exenteration [34]. Reconstruction of the exenterated orbit using cheek advancement represents an evolution of the flap repair described by Robin Beare in 1969 [35]. This technique was later reported by Mercer [36] as the "cervicofacial" flap. This is of particular benefit in cases of neglected tumor where the patient is reluctant or unable to attend regular hospital appointments and thus rehabilitation with minimal postoperative intervention is necessary. Subcutaneous cheek dissection (thus avoiding injury to the facial nerve) to a level just below the oral commissure and 2–3 cm below the angle of the mandible is performed. The cheek flap is fixed with deep sutures to the inferior orbital rim using 4-0 Vicryl® sutures and where periosteum is not present, using the infraorbital canal as a bone tunnel and a point for deep fixation of the cheek (Fig. 16.8). This simple cheek advancement avoids creating a secondary defect, and because it involves less dissection and additional skin incisions in comparison to a cervicofacial or other regional flaps, it is an easier procedure to perform with fewer facial scars. It may pull the brow inferiorly; however, this is not a problem if a prosthesis is being fitted and may be corrected by way of a direct supra-brow lift with insertion of the excised skin as a graft, directly below the brow hair. Extensive dissection into the cervical region is avoided and it can be used in conjunction with additional methods such as pericranial or skin transposition flaps. It does not preclude osseointegration if required either at the time of repair or at a later date, and as such, we would recommend it as a useful option in repairing the exenterated orbit. Other locoregional options

include a cheek fasciocutaneous V-Y flap [37] or the use of a galeal flap [38], pericranial flap [32], local transposition skin flaps from the forehead, and temporalis muscle flap.

16.5.2.2 Temporalis Muscle Transfer

The temporalis fascia and muscle are split and the muscle is released from the zygomatic arch and lateral orbital rim. The temporalis muscle flap is then transposed into the orbit through a bony opening made in the lateral wall and covered by a skin graft or remnant eyelids [39]. This procedure adds volume to the orbit and covers small bony defects and any dural tears. Disadvantages include contour problems in the temporal fossa and rarely, compromised mastication.

Temporal myocutaneous flap based on the superficial temporal artery is rotated deep to the tissues of forehead and below the supraorbital rim into the orbit [27]. The donor site defect is closed with a full-thickness skin graft or direct closure. An advantage of this flap is its application to make the socket deformity shallower in a patient not keen on wearing a prosthesis. However, the procedure leaves a secondary depression in the temple. The temporal branch of the facial nerve may also be damaged, resulting in a brow ptosis.

16.5.3 Distal Reconstruction Technique (Free Flap)

A microvascular free flap is particularly useful for the reconstruction of large defects from an extended exenteration. Microvascular free-tissue transfer is a technique that involves the harvest of the patient's own soft tissues and/or bone from remote anatomical sites. These flaps, along with their defined vasculature, are then used to reconstruct the defect. Blood supply to the flap is reestablished at the reconstructed site by anastomosis of the artery and vein to recipient vessels (the superficial temporal artery and vein).

Commonly used microvascular flaps include the rectus abdominis free flap [40], latissimus dorsi, radial forearm, or lateral arm flap [27].

A free flap can help minimize the severe cosmetic disfigurement of an extended exenteration with exposed sinus cavities. Unlike a locoregional flap, free flaps are not limited by the flap size or pedicle length and provide ample volume to fill the orbital defect while minimizing the morbidity associated with local flaps. They also have the advantage of providing healthy tissue in the case of previously irradiated sites. However, these procedures are difficult to perform and extremely time-consuming. There is a risk of flap failure and donor site morbidity. If the flap is too bulky, as can occasionally be the case, it may prevent the successful wearing of an orbital prosthesis. Cavity obliteration techniques were traditionally considered to hamper clinical surveillance of the operative site; however, imaging techniques have advanced reducing the likelihood of missing a recurrence.

16.6 Complications (Table 16.1)

16.6.1 Intraoperative Persistent Hemorrhage

Persistent hemorrhage may occur either at the orbital apex or at the proximal nasolacrimal duct. Basic principles in managing persistent bleeding include maintaining the operating table in a reverse Trendelenburg position to reduce venous congestion in the head. This also helps reduce mean arterial pressure at the level of the orbit. The role of the anesthetist in managing surgical

Table 16.1 Complications following exenteration

Intraoperative	Hemorrhage
	Exposure of dura
	CSF leak
	Intracranial arterial avulsion
Postoperative	Fistula formation into the paranasal sinuses, the nose, or the nasolacrimal duct
	Infection (bacterial/fungal)
	Orbital abscess
	Graft necrosis/eschar formation
	Nonhealing ulcers
	Chronic discharge and exposed bone
	Cerebrospinal fluid leak and pneumocranium

blood loss has grown greatly in the last few decades. Apart from physical maneuvers and local agents to control intraoperative bleeding, controlled hypotension has also been increasingly utilized, especially with the advent of newer pharmacologic agents that are safer, more predictable, and more effective [41]. Balanced rather than purely hypotensive anesthesia is advisable [42]. A safe approach is to aim to keep the mean arterial pressure above 75 % of the patient's normal value and to eliminate tachycardia [41–43].

Application of direct pressure or compression with sterile cotton gauze at the bleeding site can often control the bleeding. A bipolar cautery or monopolar cautery can then be used to cauterize any bleeding vessels. However, it is important to avoid the use of monopolar cautery along the orbital roof as it can cause a CSF leak in the presence of a bony defect. Adrenaline-soaked packs can also be applied to cause vasoconstriction. Bleeding from the bone can be controlled by application of bone wax and the bleeding caused by emissary vessels can be controlled by dry bone drilling. Excessive hemorrhage following the transaction of the orbital tissues at the orbital apex may be managed by clamping of the residual stump, by use of bipolar cautery, and by applying pressure. Injudicious use of monopolar cautery should be avoided at the orbital apex. For persistent cavity bleeds, it is useful to consider the application of hot packs at approximately 50 °C. This is a traditional practice in maxillofacial and head and neck surgery. Since the last century, hot-water irrigation has been used in obstetrics to reduce predelivery and post-delivery bleeding [44]. Hot-water irrigation is also well established as an effective treatment modality for intractable posterior epistaxis [45, 46]. The mechanism behind its effectiveness remains unclear; however, based upon rabbit studies, hot-water nasal irrigation above 46 °C achieved vasodilation and mucosal edema with subsequent narrowing of the intranasal lumen. Severe changes, including epithelial necrosis, occurred with temperatures beyond 52 °C [47]. It is also possible that an increase in temperature may increase the speed of the clotting cascade.

16.6.2 Management of Cerebrospinal Fluid (CSF) Leak

The reported incidence of CSF leaks during orbital exenteration is 1.6–16.7 % [48]. De Conciliis noted that dural exposure occurred in 20.5 % of exenterations and 30.8 % of extended exenterations which included excision of one or more orbital walls [49]. Furthermore, in that study, 60 % of CSF leaks and 75 % of dural exposures occurred in extended exenterations involving resection of one or more orbital walls. De Conciliis et al. were able to predict dural exposure in 50 % of the cases based on clinical data CT findings [49]. Hence, preoperative evaluation is invaluable in predicting and preparing for management of CSF leaks, helping to alert the surgeon to proceed with caution where pathology has infiltrated or thinned posterior or superior bone (Fig. 16.4). A temporary CSF leak may also be seen at the time of cutting the optic nerve at the apical stump [48].

Diagnosis of a CSF leak at the time of surgery can be made when leakage of clear fluid is seen in areas at high risk for encountering dura. However, when CSF and blood are mixed together, diagnosis may be difficult. CSF separates from blood when placed on filter paper and produces a ring or *halo* sign. This is not however exclusive to CSF and can lead to false-positive results. Glucose content can be analyzed rapidly; however, this is also unreliable as glucose in CSF cannot be distinguished from that in blood, tears, or nasal secretions. Hence, measuring glucose from the discharge is generally of little value in the preoperative setting. Beta-2 transferrin assay is a marker protein specific to CSF. It has high sensitivity and specificity, can be performed rapidly, and is the test of choice if available. Primary repair with 5-0 or 6-0 polyglactin or braided nylon should be performed to create a watertight seal when there is adequate exposure and the edges of the dural laceration can be readily apposed. An onlay graft, commonly a layer of fat, temporalis muscle, or fascia, may then be placed over the exposed dura to further ensure a watertight barrier [50]. Tisseel fibrin glue (Baxter Healthcare Corp., Deerfield, IL) has been used

with favorable results in CSF leaks to the orbit [51]. Although often used in conjunction with an onlay graft to further seal the repair, using an adhesive alone has also been reported to be adequate in very small dural defects without tissue loss [48]. Cyanoacrylate glue applied to a dry surgical field has also been effective in closure of CSF leaks. Bone wax has also been described in situations where the leak arises from the depth of a relatively small bony defect [52]. The aim is to fill the bone defect preventing CSF leakage into the orbit while the dura seals itself. However, bone wax should be used with caution as Bolger et al. reported three cases of CSF leaks that were associated with bone wax [53]. Large fistulas can be managed with a pericranial flap or a temporalis muscle flap [54]. CSF leaks identified postoperatively can be managed conservatively. A pneumocranium on CT scan is pathognomonic (Fig. 16.4e). Conservative management includes avoiding straining activities such as nose-blowing or coughing, use of stool softeners, and elevating the head to reduce CSF pressure. Prophylactic antibiotics are often used in cases of CSF leaks; however, their use remains controversial. Surgical repair should be considered when the leak does not settle conservatively [48].

16.6.3 Management of Sino-orbital Fistula

The incidence of sino-orbital fistulas ranges from 5 to 23 % and commonly involves the ethmoid sinus. The risk factors for developing sino-orbital fistulas are prior radiotherapy, sinus disease, and intraoperative penetration of the sinus. Fistulas occur more commonly in sockets left to granulate and are less common in sockets lined by skin graft [55]. Late presentation of fistulas may be due to bony erosion from tumor recurrence and orbital examination and imaging should be considered. Small asymptomatic fistulas can be managed conservatively with socket hygiene and small symptomatic fistulas can be closed directly. Large fistulas are repaired with grafts or flaps. Commonly used grafts include skin, mucous membrane, temporalis muscle/fascia, fascia lata, or pericranium. Commonly used flaps include skin flaps, myocutaneous flaps, free flaps, and pericranial flaps [56]. Pericranial flap is our preferred option as it is flexible, thin, vascular, and acts as a tough barrier between the orbit and sinus. The use of uncinate flaps and middle turbinate flaps has also been described to close fistulas from the nasal side [57].

Infections in the orbit can be treated with topical and/or systemic antibiotics. Graft necrosis can be either managed conservatively (allowed to granulate) or treated with a repeat skin graft. Chronic nonhealing ulcers can be debrided and treated with a skin graft or flap. Yassur et al. have reported the use of becaplermin gel (recombinant human platelet-derived growth factor) for the treatment of chronic orbital ulcer after exenteration [58].

16.7 Cosmetic Rehabilitation

Rehabilitation usually involves a prosthesis; however, patients may prefer to wear a patch or dark glasses. An essential part of the surgical decision-making process is the reconstruction and rehabilitation of the exenterated socket. Whenever feasible, a decision should be made before surgery as to whether the patient will wear a patch, an oculofacial prosthesis, or an ocular prosthesis (prosthetic shell). Oculofacial prosthesis can be mounted on the glasses (Fig. 16.9), fixed with tissue glue, or attached by magnets or clips to titanium osseointegrated implants (Fig. 16.7g, h). Spectacle-mounted prostheses prevent the spectacles ever being removed in public. Patients often lose confidence with these methods and tend to abandon their prosthesis for a patch [1].

16.7.1 Titanium Osseointegrated Implants

Nerad et al. first described osseointegrated implants as a means of fixing oculoplastic prosthesis [59]. This was described as a two-stage procedure (first, insertion of the titanium implants and, second, placement of the transcutaneous

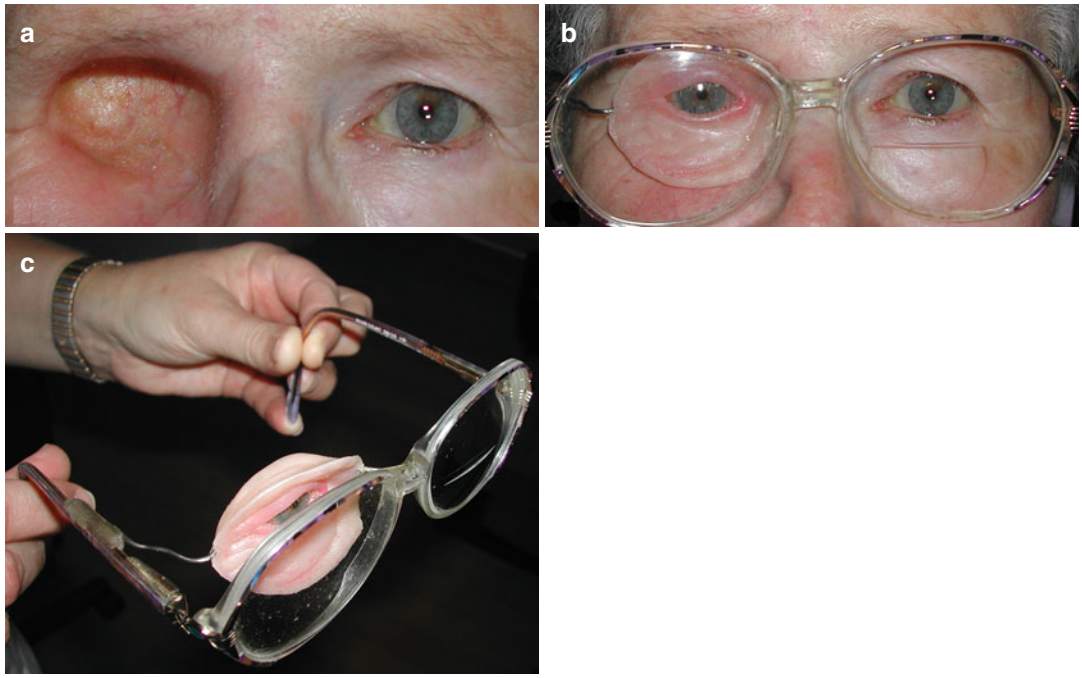

Fig. 16.9 Spectacle-mounted prosthesis (**b**, **c**) as a simple option for cosmetic rehabilitation of the exenterated orbit (**a**)

abutments). Transcutaneous abutments were traditionally placed 4 months after the insertion of titanium implants, under local anesthesia. A series of bars or magnetic devices are then attached to the abutments, which allow firm fixation of the prosthesis. The insertion of titanium implants was not performed at the time of exenteration because of the risk of necrosis, of the skin grafts, when placed over an avascular structure (titanium). However, this can now be performed at the time of exenteration [60]. Cameron et al. [32] described the use of pericranial graft to facilitate the placement of osseointegrated implants at the time of exenteration. The pericranial flap, being a highly vascular tissue, improves the take of a split skin graft. This technique allows reliable alignment of the prosthesis and good retention. Removal and reattachment of the prosthesis by the patient are also relatively easy. The prosthesis can be made light in weight. The edge of the prosthesis can also be made to blend with the surrounding skin more easily and the cosmetic results can be excellent for the carefully selected patient. The ideal patient is relatively young, highly motivated, with good hygiene, will comply with long-term aftercare of the implants, and will attend long-term follow-up appointments. This technique is time-consuming and expensive, however. The implants must be kept meticulously clean to avoid inflammation or infection. There is a small risk of losing the implants in previously irradiated orbits [59].

16.7.2 Ocular Prosthesis (Prosthetic Shell)

Prosthetic shell can be fitted in a selected group of patients where the eyelids and conjunctiva are spared during orbital exenteration. The basic requirements for a conjunctiva-sparing exenteration socket to maintain a prosthetic shell are orbital tissue volume to support the prosthesis, a mucous membrane surface with fornices to accommodate the prosthesis, and eyelids to hold the prosthesis within the socket [1]. If approximately 50 % of the patient's conjunctival surface can be saved, then a mucous membrane-free graft (buccal mucosa, hard palate mucosa, or nasal turbinate mucosa) can be used to reconstruct the

fornix. If split-thickness skin is used instead, then the patient may be bothered by persistent discharge and a smelly "mixed socket."

16.8 Prognosis

The success of the surgery depends on obtaining tumor-free margins at the time of surgery. It is not always possible to achieve complete clearance of a tumor with exenteration and incomplete clearance has been reported in up to 38 % of total and 17 % of subtotal exenterations by Goldberg et al. [1]. The lower percentage of incomplete clearance with subtotal exenteration in this study was due to the fact that the cases with locally invasive malignancy were treated with subtotal exenteration and the cases with widespread tumor invasion were treated with total exenteration.

Bartley et al. reported an 88.6 % survival at 1 year and a 56.8 % survival at 5 years in patients with no residual tumor after exenteration [7]. Their reported 1-year survival was 55.0 % and the 5-year survival was 25.8 % in patients with metastasis or residual tumor after exenteration. Rahman et al. reported an overall survival of 93 % at 1 year, 57 % at 5 years, and 37 % at 10 years [15]. They reported that achieving tumor-free margins after exenteration did not influence the long-term survival. Hence, the presence of clear surgical margins should not be regarded as an indication of cure as clear excision margins may prevent local recurrence, but they do not always prevent micrometastasis to lymph nodes or distant organs.

Perineural invasion is associated with increased incidence of incomplete clearance and recurrence resulting in worse prognosis particularly in squamous cell carcinoma and lacrimal gland adenoid cystic carcinoma. In cases of tumor-positive margins, other treatment modalities such as radiation or chemotherapy may play a role in prolonging survival. Williams et al. reported a 5-year survival of 50 % in patients with radiological (CT/MRI) evidence of perineural invasion, compared with 86 % survival in patients with no radiological evidence of perineural invasion [61].

References

1. Goldberg RA, Kim JW, Shorr N. Orbital exenteration: results of an individualized approach. Ophthal Plast Reconstr Surg. 2003;19:229–36.
2. Ben Simon GJ, Schwartz RM, Douglas R, Fiaschetti D, McCann JD, Goldberg RA. Orbital exenteration: one size does not fit all. Am J Ophthalmol. 2005;139:11–7.
3. Tyers AG. Orbital exenteration for invasive skin tumors. Eye. 2006;20:1165–70.
4. Howard GR, Nerad JA, Carter KD, Whitaker DC. Clinical characteristics associated with orbital invasion of cutaneous basal cell and squamous cell tumors of the eyelid. Am J Ophthalmol. 1992;113:123–33.
5. Madge SN, Khine AA, Thaller VT, Davis G, Malhotra R, McNab A, O'Donnell B, Selva D. Globe-sparing surgery for medial canthal Basal cell carcinoma with anterior orbital invasion. Ophthalmology. 2010;117:2222–8.
6. Donaldson MJ, Sullivan TJ, Whitehead KJ, Williamson RM. Squamous cell carcinoma of the eyelids. Br J Ophthalmol. 2002;86:1161–5.
7. Bartley GB, Garrity JA, Waller RR, Henderson JW, Ilstrup DM. Orbital exenteration at the Mayo Clinic 1967–1986. Ophthalmology. 1989;96:468–73.
8. Cook Jr BE, Bartley GB. Treatment options and future prospects for the management of eyelid malignancies: an evidence-based update. Ophthalmology. 2001;108:2088–98.
9. Chao AN, Shields CL, Krema H, Shields JA. Outcome of patients with periocular sebaceous gland carcinoma with and without intraepithelial invasion. Ophthalmology. 2001;108:1877–83.
10. McKelvie PA, Daniell M, McNab A, Loughnan M, Santamaria JD. Squamous cell carcinoma of the conjunctiva: a series of 26 cases. Br J Ophthalmol. 2002;86:168–73.
11. Shields JA, Shields CL, Demirci H, Honavar SG, Singh AD. Experience with eyelid-sparing orbital exenteration: the 2000 Tullos O. Coston Lecture. Ophthal Plast Reconstr Surg. 2001;17:355–61.
12. Shields JA, Shields CL. Massive orbital extension of posterior uveal melanoma. Ophthal Plast Reconstr Surg. 1991;7:238–51.
13. Damato B, Coupland SE. An audit of conjunctival melanoma treatment in Liverpool. Eye (Lond). 2009;23:801–9.
14. Kersten RC, Tse DT, Anderson RL, et al. The role of orbital exenteration in choroidal melanoma with extrascleral extension. Ophthalmology. 1985;92:436–43.
15. Rahman I, Maino A, Cook AE, Leatherbarrow B. Mortality following exenteration for malignant tumors of the orbit. Br J Ophthalmol. 2005;89:1445–8.
16. Lin KL, Tena LB, Finger PT. Orbital brachytherapy for extrascleral extension of choroidal melanoma. Br J Ophthalmol. 2006;90:1438–9.

17. Meel R, Radhakrishnan V, Bakhshi S. Current therapy and recent advances in the management of retinoblastoma. Indian J Med Paediatr Oncol. 2012;33:80–8.
18. Raney B, Huh W, Hawkins D, Hayes-Jordan A, Million L, Rodeberg D, Teot L, Anderson J, for the Soft Tissue Sarcoma Committee of the Children's Oncology Group, Arcadia, CA. Outcome of patients with localized orbital sarcoma who relapsed following treatment on Intergroup Rhabdomyosarcoma Study Group (IRSG) Protocols-III and -IV, 1984–1997: a report from the Children's Oncology Group. Pediatr Blood Cancer. 2012. doi:10.1002/pbc.24289. [Epub ahead of print]
19. Ahmad SM, Esmaeli B, Williams M, Nguyen J, Fay A, Woog J, Selvadurai D, Rootman J, Weis E, Selva D, McNab A, DeAngelis D, Calle A, Lopez A. American Joint Committee on Cancer classification predicts outcome of patients with lacrimal gland adenoid cystic carcinoma. Ophthalmology. 2009; 116:1210–5.
20. Williams MD, Al-Zubidi N, Debnam JM, Shinder R, DeMonte F, Esmaeli B. Bone invasion by adenoid cystic carcinoma of the lacrimal gland: preoperative imaging assessment and surgical considerations. Ophthal Plast Reconstr Surg. 2010;26:403–8.
21. Suárez C, Ferlito A, Lund VJ, Silver CE, Fagan JJ, Rodrigo JP, Llorente JL, Cantù G, Politi M, Wei WI, Rinaldo A. Management of the orbit in malignant sinonasal tumors. Head Neck. 2008;30:242–50.
22. Dhiwakar M, Thakar A, Bahadur S. Invasive sino-orbital aspergillosis: surgical decisions and dilemmas. J Laryngol Otol. 2003;117:280–5.
23. Pushker N, Meel R, Kashyap S, Bajaj MS, Sen S. Invasive aspergillosis of orbit in immunocompetent patients: treatment and outcome. Ophthalmology. 2011;118:1886–91.
24. Rose GE, Wright JE. Exenteration for benign orbital disease. Br J Ophthalmol. 1994;78:14–8.
25. Gonzalez LF, Bilyk JR. Intracranial arterial avulsion during orbital exenteration. Orbit. 2012;31:190–3.
26. Looi A, Kazim M, Cortes M, Rootman J. Orbital reconstruction after eyelid- and conjunctiva-sparing orbital exenteration. Ophthal Plast Reconstr Surg. 2006;22:1–6.
27. Levin PS, Ellis DS, Stewart WB, Toth BA. Orbital exenteration. The reconstructive ladder. Ophthal Plast Reconstr Surg. 1991;7:84–92.
28. Cooper J. Wound management following orbital exenteration surgery. Br J Nurs. 2009;18(6):S4.
29. Stanley D, Emerson DJ, Daley JC. Whitehead's varnish and Jelonet–a better dressing for skin graft donor sites than Jelonet alone. Ann R Coll Surg Engl. 1988;70:369–71.
30. Lim M, Lew-Gor S, Sandhu G, Howard D, Lund VJ. Whitehead's varnish nasal pack. J Laryngol Otol. 2007;121:592–4.
31. Cooper J. The MOEWAT as a proposed method of evaluating orbital exenteration wounds. J Wound Care. 2011;20(478):480–3.
32. Cameron M, Gilbert PM, Mulhern MG, Sneddon KJ. Synchronous reconstruction of the exenterated orbit with a pericranial flap, skin graft and osseointegrated implants. Orbit. 2005;24:153–8.
33. Shore JW, Burks R, Leone Jr CR, McCord Jr CD. Dermis-fat graft for orbital reconstruction after subtotal exenteration. Am J Ophthalmol. 1986;102:228–36.
34. Sira M, Malhotra R. Reconstruction of orbital exenteration defects by primary closure using cheek advancement. Br J Ophthalmol. 2013;97(2):201–5.
35. Beare R. Flap repair following exenteration of the orbit. Proc R Soc Med. 1969;62:1087–90.
36. Mercer DM. The cervicofacial flap. Br J Plast Surg. 1988;41:470–4.
37. Moretti E, Ortiz S, Gómez García F, Barrovechio JC, Valvo C. Complete mobilization of the cheek zone for orbit exenteration. J Craniofac Surg. 2005;16:823–8.
38. Zwahlen RA, Grätz KW, Obwegeser JA. The galea fascia flap in orbital reconstruction: innovative harvest technique. Eur J Surg Oncol. 2006;32:804–7.
39. Reese AB, Jones IS. Exenteration of the orbit and repair by transplantation of the temporalis muscle. Am J Ophthalmol. 1961;51:217–27.
40. Pryor SG, Moore EJ, Kasperbauer JL. Orbital exenteration reconstruction with rectus abdominis microvascular free flap. Laryngoscope. 2005;115:1912–6.
41. Degoute CS. Controlled hypotension: a guide to drug choice. Drugs. 2007;67(7):1053–76.
42. Nair S, Collins M, Hung P, Rees G, Close D, Wormald PJ. The effect of beta-blocker premedication on the surgical field during endoscopic sinus surgery. Laryngoscope. 2004;114(6):1042–6.
43. Petrozza PH. Induced hypotension. Int Anesthesiol Clin. 1990;28:223–9.
44. Hansen TB. Hot water irrigation to obtain haemostasis [Danish]. Bull Midwifes (Copenh). 1890;3:8–10.
45. Novoa E, Schlegel-Wagner C. Hot water irrigation as treatment for intractable posterior epistaxis in an outpatient setting. J Laryngol Otol. 2012;126:58–60.
46. Stangerup S, Dommerby H, Siim C, Kemp L, Stage J. New modification of hot-water irrigation in the treatment of posterior epistaxis. Arch Otolaryngol Head Neck Surg. 1999;125:686–90.
47. Stangerup SE, Thomsen HK. Histological changes in the nasal mucosa after "hot-water-irrigation": an animal experimental study. Rhinology. 1996;34:14–7.
48. Limawararut V, Valenzuela AA, Sullivan TJ, McNab AA, Malhotra R, Davis G, Jones N, Selva D. Cerebrospinal fluid leaks in orbital and lacrimal surgery. Surv Ophthalmol. 2008;53:274–84.
49. de Conciliis C, Bonavolonta G. Incidence and treatment of dural exposure and CSF leak during orbital exenteration. Ophthal Plast Reconstr Surg. 1987;3:61–4.
50. Ebersold MJ. Five things oculoplastic surgeons should know about neurosurgery. Ophthal Plast Reconstr Surg. 2000;16:247–9.
51. Goldberg RA, Weinberg DA, Shorr N, et al. Maximal, threewall, orbital decompression through a coronal approach. Ophthal Surg Lasers. 1997;28:832–43.

52. Graham SM, Brown CL, Carter KD, et al. Medial and lateral orbital wall surgery for balanced decompression in thyroid eye disease. Laryngoscope. 2003;113:1206–9.
53. Bolger WE, Tadros M, Ellenbogen RG, et al. Endoscopic management of cerebrospinal leak associated with the use of bone wax in skull-base surgery. Otolaryngol Head Neck Surg. 2005;132:418–20.
54. Schaefer SD, Soliemanzadeh P, Della Rocca DA, et al. Endoscopic and transconjunctival orbital decompression for thyroid-related orbital apex compression. Laryngoscope. 2003;113:508–13.
55. Rahman I, Cook AE, Leatherbarrow B. Orbital exenteration: a 13 year Manchester experience. Br J Ophthalmol. 2005;89:1335–40.
56. Mehta V, Alon EE, Buchbinder D, Urken ML. Novel use of unilateral galeopericranial flaps for closure of sino-orbital cutaneous fistulas. Laryngoscope. 2011; 121:777–81.
57. Limawararut V, Leibovitch I, Davis G, Rees G, Goldberg RA, Selva D. Sino-orbital fistula: a complication of exenteration. Ophthalmology. 2007; 114:355–61.
58. Yassur I, Hirschbein MJ, Karesh JW. Clinicopathologic reports, case reports, and small case series: 0.01 % becaplermin gel for the treatment of a chronic orbital ulcer after exenteration. Arch Ophthalmol. 2001;119:1858–9.
59. Nerad J, Carter KD, LaVelle WE, et al. The osseointegration technique for the rehabilitation of the exenterated orbit. Arch Ophthalmol. 1991;109: 1032–8.
60. Greig AV, Jones S, Haylock C, Joshi N, McLellan G, Clarke P, Kirkpatrick WN. Reconstruction of the exenterated orbit with osseointegrated implants. J Plast Reconstr Aesthet Surg. 2010;63:1656–65.
61. Williams LS, Mancuso AA, Mendenhall WM. Perineural spread of cutaneous squamous and basal cell carcinoma: CT and MR detection and its impact on patient management and prognosis. Int J Radiat Oncol Biol Phys. 2001;49:1061–9.

Principles of Orbital Surgery

17

David H. Verity and Geoffrey E. Rose

Contents

D.H. Verity, MD, MA, BM BCh, FRCOphth (✉)
G.E. Rose, BSc, MBBS, MS, DSc, MRCP, FRCS, FRCOphth
Orbital Clinic, Moorfields Eye Hospital, 162 City Road, London EC1V 2PD, UK
e-mail: david.verity@moorfields.nhs.uk; geoffrey.rose@moorfields.nhs.uk

17.1 Introduction

Over the past 50 years, the management of orbital disease has increasingly been recognised as a discipline in its own right. While in the early 1940s orbital surgery was considered to lie firmly within the realm of the neurosurgeon [1], in recent decades surgery has moved away from transcranial approaches to the orbit towards a variety of increasingly refined regional approaches that utilise incisions along the relaxed skin tension lines or the conjunctiva. However, where disease extends beyond the bony confines of the orbit into the cranium, pterygopalatine fossa, or paranasal sinuses, multidisciplinary management with a neurosurgeon and maxillofacial or head-and-neck surgeon may be required. This chapter covers special preoperative, intraoperative, and postoperative considerations in patients undergoing orbital surgery and illustrates a series of practical approaches to the orbital contents.

J.D. Perry, A.D. Singh (eds.), *Clinical Ophthalmic Oncology*,
DOI 10.1007/978-3-642-40492-4_17, © Springer-Verlag Berlin Heidelberg 2014

17.2 Anatomical Limitations: The 'Conoid of View, in Orbital Surgery

The bony orbit is tetrahedral in shape, its walls protecting the orbital soft tissues whose volume is about 28 ml. Unless the bony wall(s) is displaced or removed, all surgical approaches to the orbit are limited by the anterior orbital opening (generally less than 3 cm) and the extent to which the globe can be displaced. Thus, for an apical lesion, the maximum theoretical 'conoid of view' is about 50º by 30º, although in practical terms soft tissues typically tend to obscure the operative field and limit the view even further, with the surgeon's view sometimes being monocular. A wider 'conoid', although increasingly 'oblique' with deeper orbital structures, facilitates both surgical access and the surgeon's view. This can be achieved either by placing the incision closer to the lesion (e.g. using a lateral canthotomy for lateral lesions) or by displacing the orbital wall laterally (as is performed in a bone-swinging lateral orbitotomy).

17.3 Orbital Surgery: Risks to Visual Functions

Operating on delicate tissues within the confined space of the bony orbit carries risks of tissue injury [2]. While impairment of motor and facial sensory nerves can be reversible, visual loss due to ischaemic optic neuropathy – presumed due to vasospasm – rarely recovers. This risk depends upon both the difficulty of surgical access and the space available for tissue displacement while operating. Although risk 'zones' are discussed (Tables 17.1 and 17.2), it should be remembered that the surgeon's experience is a significant factor across all such zones, with more posterior lesions presenting the greatest challenge and requiring greater expertise.

Surgery for lesions alongside the globe in the anterior one-third of the orbit, where the conoid of view is wide, carries significantly less risk for iatrogenic nerve damage (Table 17.1) than for surgery in the posterior third of the orbit (Table 17.2), where the conoid of view is reduced and structures are viewed more obliquely. These considerations frequently influence management, with a judicious 'wait and watch' approach being acceptable for some posterior lesions suspected of being benign and where the natural history (and risk to vision) remains uncertain.

Table 17.1 Risks of surgery in the anterior third of the orbit

1. General risks:
Visual loss (low)
Diplopia
2. Specific risks:
Orbital roof: Sensory changes corresponding to frontal nerve and/or supratrochlear nerve
Superonasal quadrant: Sensory changes, diplopia (injury to trochlea or superior oblique tendon)
Medial orbit: Risk to lacrimal outflow apparatus (watery eye), risk of medial orbital wall fracture
Orbital floor: Sensory changes (infraorbital nerve)
Lateral orbit: Mydriasis (causing photophobia, early presbyopia), reduced aqueous tear production (rare)

Table 17.2 Risks of surgery in the middle and posterior thirds of the orbit

Irreversible visual loss, partial or complete
Diplopia
Ptosis
Periocular paraesthesia or anaesthesia

17.4 Preoperative Counselling

The risks to sight, ocular alignment, and periocular sensation must be discussed with all patients prior to surgery. Unfortunately, the risks cannot be defined with great precision (unlike, e.g., the specific risks in cataract surgery) due to wide interindividual variations both in the extent and severity of disease and in orbital soft tissue or bony anatomy. However, the patient can be advised on certain risks depending on the location of disease (Table 17.3): for example, approaches to the orbital roof carry a small risk of injury to the frontal nerve but a minute risk to vision and ocular alignment, whereas surgery in the anterior superomedial quadrant risks injury to the trochlea and secondary diplopia. In contrast,

Table 17.3 Peroperative risks in orbital surgery

Compromised visualisation of orbital structures
Fat prolapse into the surgical field
Orbital haemorrhage
Tissue injury:
Manipulation of the orbital tissues and thermal injury from diathermy (both increasing the risk of postoperative visual loss due to vasospasm at the orbital apex [2])
Sustained pressure on the globe and ocular ischemia
Ocular surface exposure

surgery for posterior lesions carries a much greater risk to orbital functions, because access to the posterior orbit affords the surgeon a narrow conoid of view and limited space for tissue manipulation. For apical lesions whose behaviour and imaging suggest a 'benign' pathology (such as an apical cavernous haemangioma), periodic documentation of visual functions is acceptable and intervention considered only where there is clear evidence of progression. Where the history, clinical behaviour, or imaging indicates a malignant process, however, the risks of surgery may be outweighed by those of *not* operating, that is, by the risk of regional or systemic spread of an undiagnosed malignant neoplasm.

17.5 Peroperative Medical and Anaesthetic Considerations

Orbital surgery can be performed with local and regional blocks under deep sedation (especially for more anterior procedures, such as lacrimal gland biopsy). However, unless the risks are considered unacceptable, the use of general anaesthesia is often preferred as it permits better control of systemic blood pressure during surgery. In all patients, pre-existing medical conditions, including systemic hypertension, hypo- or hyperthyroidism, and diabetes, should be as well controlled as possible, and patients should be assessed by an anaesthetist familiar with the specific anaesthetic requirements for orbital surgery. Preoperative investigations will be determined by the medical history of the patient and the nature of the proposed surgery but will often include a full blood count, urea and electrolytes, thyroid function tests, clotting studies, and an ECG.

When medically appropriate, hypotensive anaesthesia improves the operative field by reducing arterial and venous bleeding: this can be achieved with either a volatile anaesthetic agent (e.g. isoflurane or sevoflurane) or with total intravenous anaesthesia (TIVA) using a combination of propofol and remifentanil. There is much evidence to support the use of TIVA: it often confers a smooth recovery from anaesthesia and also is associated with a lower incidence of postoperative nausea and vomiting. These qualities of TIVA are highly desirable for orbital surgery, where a postoperative surge in orbital perfusion pressure can be hazardous and particularly where day-case surgery is being performed [3]. Remifentanil is a powerful, extremely short-acting synthetic opiate that not only prevents intraoperative coughing (without the need for intraoperative muscle relaxants) but also reduces the hypertensive response to pain [4]. As remifentanil is rapidly metabolised on ceasing the infusion (it having a context-sensitive half-life of about 3 min), it is essential that an intraoperative analgesic is also given, with intravenous paracetamol usually being the first choice. The peroperative use of platelet-inhibiting anti-inflammatory analgesics such as diclofenac and ibuprofen is controversial and, considering the risks of orbital haemorrhage, are best avoided. Postoperative pain, also a risk factor for hypertension and, thereby, for orbital haemorrhage, should be pre-empted with longer-acting peroperative opiates, such as morphine or fentanyl. Regional infiltration with a long-acting local anaesthetic, such as bupivacaine, should also be considered where possible as it further reduces the need for postoperative analgesia and, therefore, the risk of postoperative nausea and vomiting. Finally, where surgery involves placement of an orbital implant – for example, after ocular evisceration or enucleation or with fracture repairs – parenteral dexamethasone, in combination with a 5HT-3 receptor antagonist (such as ondansetron), can also be used to reduce the incidence of nausea and vomiting.

Table 17.4 Antiplatelet agents, warfarin, and orbital surgery

Antiplatelet agent	Minimum cessation prior to surgery
All versions of amino-salicylic acid (ASA):	4 weeks
Nonsteroidal medications	3 weeks
Other antiplatelet drugs (e.g. clopidogrel)	2 weeks
Warfarin – target INR for orbital surgery is <1.5	3–4 days
Herbal remedies	4 weeks
Spices containing ajoenes (garlic, ginger, gingko, ginseng)	4 weeks

Table 17.5 The six principle approaches to the orbit

1. Upper eyelid skin-crease approach
2. Swinging lower eyelid approach (2 variants)
3. Lateral canthotomy approach
4. Bone-swinging lateral orbitotomy
5. Transconjunctival retrocaruncular approach
6. Conjunctival peritomy approach

Numerous drugs affect haemostasis and carry a significant risk of haemorrhage in orbital surgery [5]. These include antiplatelet agents (typically for cardiovascular indications), numerous variants of nonsteroidal medications, and herbal remedies and spices. The orbital surgeon should document a thorough drug history as well as seek the advice of a physician before discontinuing such drugs prior to surgery (Table 17.4). Depending on the indication, cessation of antiplatelet agents and warfarin can cause significant comorbidity and, in certain circumstances, a low molecular weight heparin may need to be given over the peroperative period [6]. Irrespective of the other risk factors for haemorrhage, a surgeon should always consider placing a vacuum drain for 12–24 h when operating on all but the most anterior of orbital lesions.

17.6 The Six Essential Orbitotomies: An Overview

The six approaches described here (Table 17.5) generally permit access to each region of the orbit. When disease is ill-defined or straddles different areas, combinations of these approaches may aid in visualisation and dissection. While the approach can often be determined preoperatively, if inadequate access is afforded by the initial approach, additional adjoining approaches can be added. The choice of orbitotomy is largely determined by the location and depth of the access required: for example, where incisional biopsy is intended, a trans-lid approach (either via the upper lid skin crease or inferior conjunctiva) is often adequate. In contrast, to increase the surgeon's conoid of view for intact excision of a deeper lesion, it might be necessary to utilise a lower lid swinging flap or bone-swinging lateral orbitotomy, these approaches giving wider access to the orbital depths.

17.7 Anterior Orbitotomy: Upper Eyelid Skin-Crease Approach

The upper two-thirds of the orbit are readily accessible through the upper eyelid approach, this healing with no visible scar and providing access as far back as the superior orbital fissure and orbital apex (Fig. 17.1). Surgery involves an incision through the upper lid skin crease, dividing the orbicularis muscle along the length of the incision and placing the skin/muscle flaps on traction (a 2/0 silk suture is convenient for this). For lacrimal gland masses, the incision is placed in the lateral aspect of the skin crease and – with blunt dissection of the suborbicularis plane – the arcus marginalis is exposed at the superolateral orbital rim. With a Desmarres retractor elevating the incision edge and brow tissues and a 16 mm malleable retractor displacing the lacrimal gland and orbital septum inferomedially, the arcus marginalis is opened for about 15–20 mm immediately inferior to the lateral orbital rim, this exposing the preaponeurotic fat pad and the outer face of the orbital lobe of the lacrimal gland. The latter is readily mobilised from its fossa (unless there has been marked chronic inflammation), and a large specimen may be harvested from its external surface using an E11 blade. Haemostasis is achieved by applying diathermy directly to the cut surfaces, the gland is repositioned within the orbit, orbital fat redraped in the region, and the skin closed with a

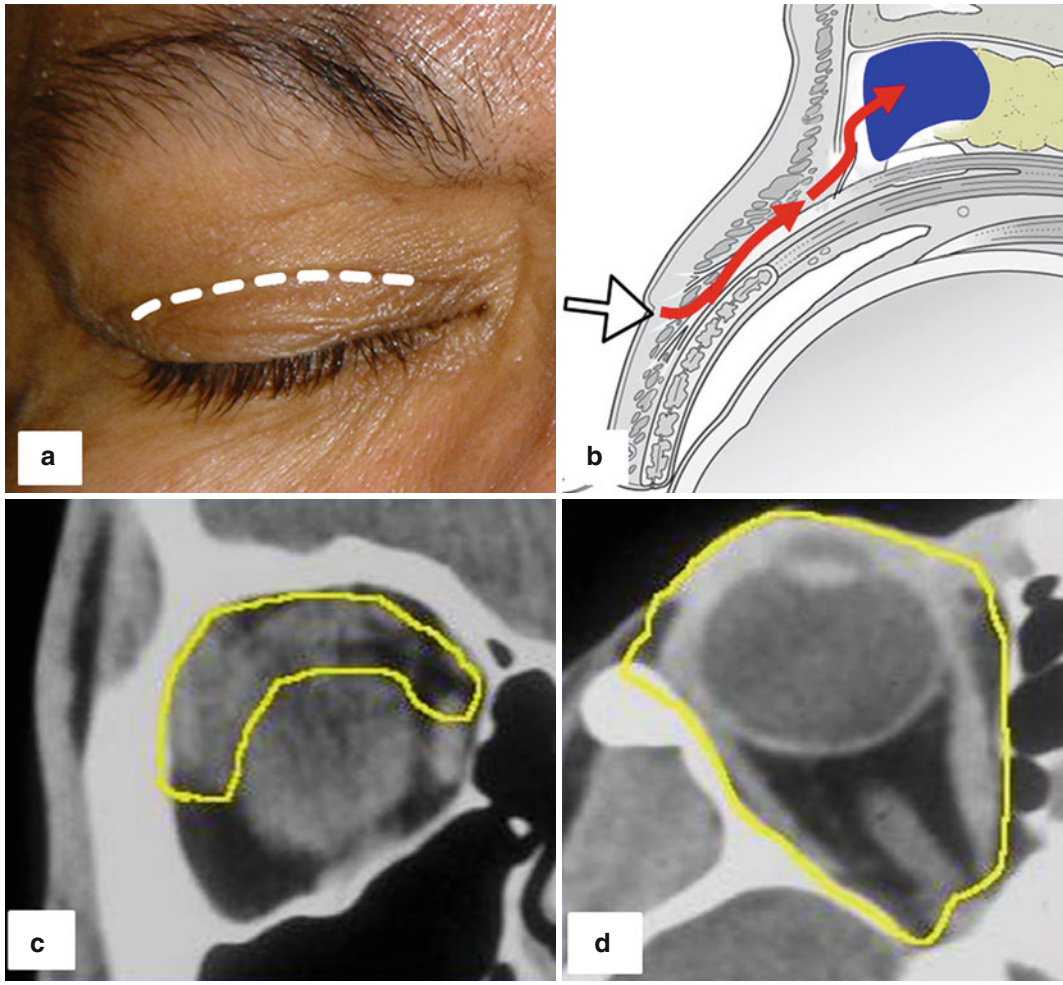

Fig. 17.1 Anterior orbitotomy – upper eyelid skin-crease approach incision (*dotted line*) (**a**). Schematic route to the postseptal space. *Arrow* demonstrates skin crease (**b**) and areas of the orbit that can be reached by this approach (**c** and **d**)

running 6/0 nylon suture or, in a child, with an 8/0 soluble suture. A topical ocular antibiotic is applied and a non-adherent dressing applied with firm padding for 12–24 h – a drain being unnecessary. The patient should be evaluated 10–14 days postoperatively with review of the histopathology and, in the adult, removal of the non-absorbable surface suture.

Frequently, biopsy of the lacrimal gland is inappropriately performed via the conjunctival fornix, this being more straightforward than the orbitotomy approach described above. However, such surgery is inadvisable because it carries a *major* risk of dry eye due to inadvertent injury to the lacrimal ductules, and moreover, the palpebral lobe is often spared the underlying disease process.

For non-lacrimal masses, the orbital septum should be opened near the lesion and a few millimetres below the arcus marginalis, to avoid damage to the levator apparatus. Access to the orbital *roof* is achieved by spreading the connective tissue septa *above* the preaponeurotic fat pads with blunt-ended scissors, taking care to avoid injury to the frontal neurovascular complex. In contrast, gentle blunt dissection *beneath* the preaponeurotic fat pads and across the surface of the levator muscle provides access to the levator complex or to the upper intraconal space (for lesions lying above or medial to the optic nerve) [7].

Using blunt-ended scissors to open up the soft tissues and placing 16 mm malleable retractors either side of the scissors, the orbital depths are exposed after applying diathermy to the tissue septa overlying the area of interest. This manoeuvre is repeated several times, with the assistant gently retracting the surrounding tissues to maintain a clear view of the area in question. Where the intention is to excise intact a well-defined mass, any adjacent bridging vascular pedicles are divided after gentle diathermy until the entire surface of the mass has been cleared from adjacent tissues and can be removed without tissue drag. For incisional biopsy of an ill-defined lesion, the mass is gripped firmly (crush artefact being minimised by avoiding repeated grasping) and a large biopsy obtained either with an E11 blade or with tissue scissors. After obtaining haemostasis, a vacuum drain is placed for all surgery within the deep orbit – this reduces serum accumulation at the orbital apex and, thereby, minimises the risk of visual loss; the drain trocar is passed through the eyebrow to avoid a visible scar.

17.8 Anterior Orbitotomy: Swinging Lower Eyelid Approach

Although the inferior two-thirds of the orbit can be reached by several routes, the previously popular 'tear-trough' skin incision has largely been abandoned due to the creation of a visible scar, the risks of fistula formation, and risk of lower eyelid retraction due to adhesions to the underlying bone. Although the subciliary blepharoplasty incision remains a reliable approach where skin reduction is required during orbital surgery, the conjunctival approach often gives wider exposure with less tissue manipulation while avoiding the above risks.

Thus, the contemporary approach to the lower two-thirds of the orbit is the lower lid swinging flap [8, 9], of which there are two types (Fig. 17.2). The first is the 'high' flap, this providing immediate access to the *preseptal* plane and thence to the inferior orbital rim, from which exceptional access is gained to the orbital floor and medial wall. The second, giving wide access to the extraconal and intraconal spaces, is the 'low' flap, in which the conjunctival incision is placed low in the depths of the inferior fornix. This incision directly enters the *postseptal* extraconal fat, from which – with gentle tissue spreading and the use of retractors – the orbital contents can be reached. Understanding the fundamental difference between these two approaches and their rationale (these not developed in the original description) [9] is essential when planning an approach through the lower eyelid.

17.8.1 The 'High' Variant of the Swinging Lower Eyelid Approach

For both variants, the lower lid is first disconnected from the lateral orbital rim using a slightly downward-directed lateral canthotomy and cantholysis. The conjunctiva is then opened along its full horizontal extent at a millimetre below the tarsus, taking care to avoid inadvertent injury to the canaliculus. The cornea is protected by approximating the cut edge of the inferior conjunctiva to the upper lid margin with a widely spaced 4/0 nylon loop on a bow; this suture also keeps the septum taut and aids subsequent opening of the preseptal (post-orbicularis) plane. After separating the septum and orbicularis, the inferior orbital rim and suborbicularis fat pad (just below the rim) are exposed with firm sweeps of a cotton bud and the periosteum opened at the orbital rim to expose the inferior extraperiosteal space. A 16 mm malleable retractor is used to raise the periosteum off the floor, taking care to diathermy and divide the artery that crosses from the infraorbital canal to the orbit.

Such an approach is typically used for the repair of orbital fractures; exposure of the whole medial orbital wall is readily achieved, and the conjunctival incision can be continued into the retrocaruncular line and temporary division of the origin of the inferior oblique muscle where necessary. After closure of the orbital periosteum with interrupted 5/0 soluble sutures, the lower eyelid swinging flap is repaired in a layered fashion using a 6/0 soluble suture; this involves a

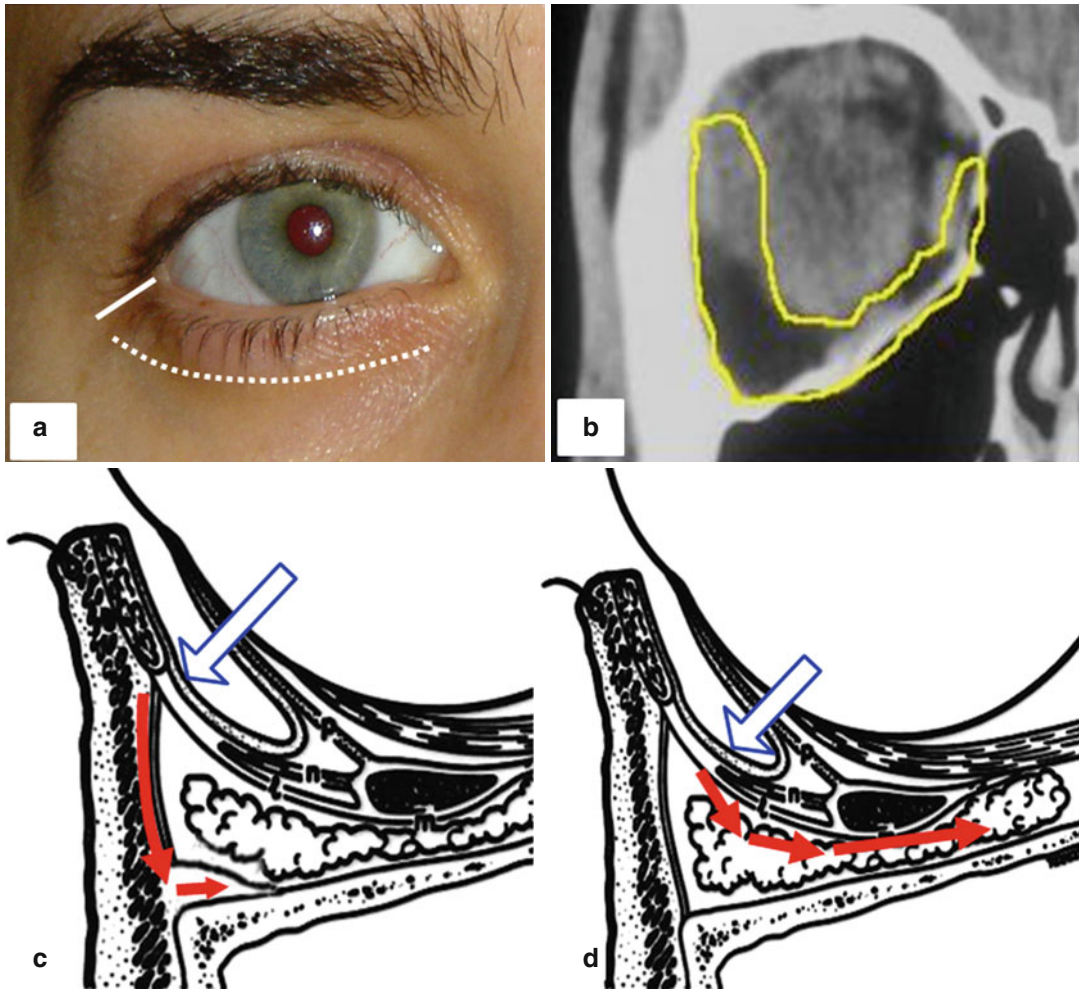

Fig. 17.2 Anterior orbitotomy – swinging lower eyelid approach. Figure showing lateral canthotomy and conjunctival incision (**a**, *dotted line*) and the area of the orbit that can be reached (**b**). The 'high' (**c**, *arrow*) and 'low' (**d**, *arrow*) variants are shown

single suture to close the lateral aspect of the conjunctiva, alignment of the grey line and lash lines, suturing of the cut end of the lower tarsus to the upper limb of the canthal tendon, closure of the orbicularis muscle, and finally closure of the skin.

17.8.2 The 'Low' Variant of the Swinging Lower Eyelid Approach

The postseptal route offered by the 'low' lower lid swinging flap affords good access to the lateral, inferior, and even medial extraconal space, allowing the orbital surgeon to remove large tumours from these regions. Masses overlying an expanded inferior orbital fissure can be debulked as far posteriorly as the pterygopalatine fossa, and intraconal lesions can be excised after entering the intraconal fat space between the inferior and lateral recti, these muscles being the most widely spaced. This route also permits access to tumours of the optic nerve; for example, in cases of a painful, blind exophthalmos due to an optic nerve tumour (without intracranial extension), the entire intraorbital portion of the nerve may be removed with this versatile approach. Similarly, the more oblique approach to the inferior rectus

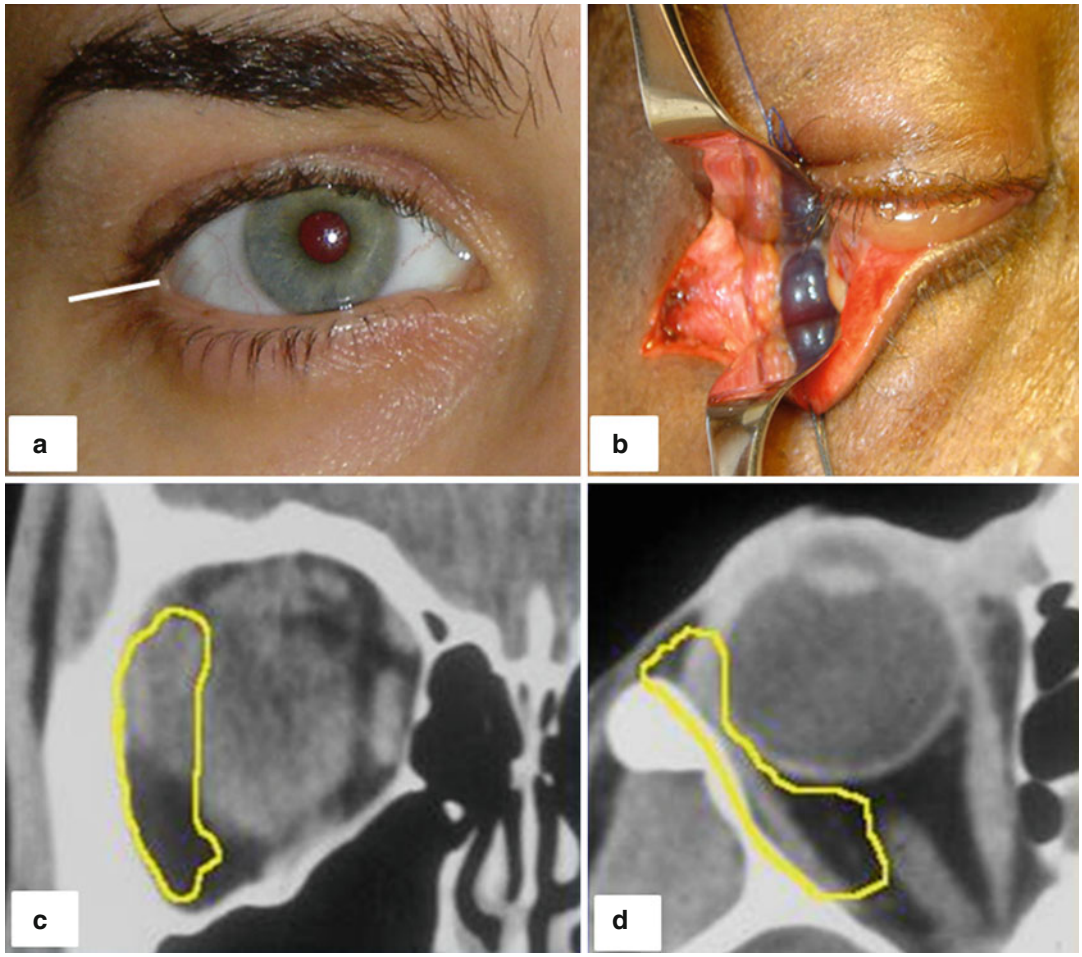

Fig. 17.3 Anterior orbitotomy: lateral canthotomy approach. Skin incision (**a**). Patient undergoing removal of a vascular lesion (note superior and inferior placement of paddle retractors (**b**) and areas of the orbit that can be reached through this approach (**c**, **d**)

(as compared with a conjunctival approach which gives an 'end-on' view of the muscle) markedly facilitates representative biopsy of the belly of this muscle.

17.9 Anterior Orbitotomy: Lateral Canthotomy Approach

Exposure of the lateral half of the orbit can be achieved through a lateral canthotomy incision, this having several advantages over other approaches including a short operative time, no perceptible scar, and no disruption of the attachments of the upper or lower limbs of the lateral canthal tendon (Fig. 17.3). This approach is particularly useful where a diffuse process, such as lymphoma or idiopathic inflammation, involves multiple tissues and where biopsy of muscle, fat, and lacrimal gland is required.

In this approach, the outer canthus is divided horizontally to the orbital rim and traction sutures placed through the upper and lower eyelids. The tissues are spread and retracted to expose the lateral extraperiosteal fat plane, with division of the lower forniceal conjunctiva further enhancing access if required. The incision is readily closed with 6/0 soluble sutures aligning the lid margins and uniting the upper and lower limbs of the tendon and skin closure with the same suture.

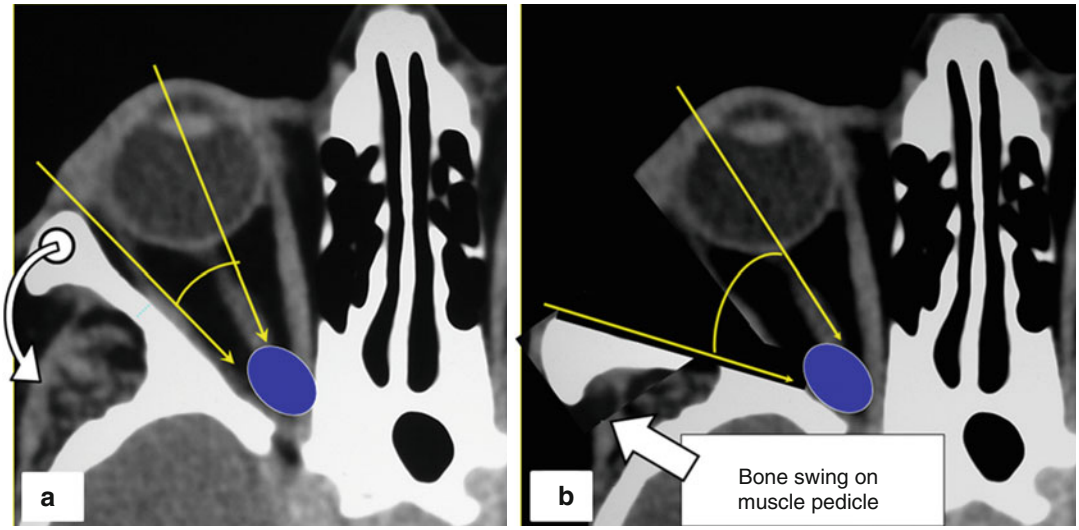

Fig. 17.4 Lateral orbitotomy with bone mobilisation. Schematic showing bone mobilisation on a temporalis flap (**a**), thereby reducing the surgical path length and widening the 'conoid of view' (*arrows*) of the orbital apex (**b**). *Arrows* demonstrate the 'conoid of view' with each approach

17.10 Lateral Orbitotomy with Bone Mobilisation

In the lateral orbitotomy approach, the surgical 'conoid of view' is significantly widened by swinging the lateral orbital wall outwards on the temporalis muscle, thereby shortening the surgical path length and improving access to the orbital apex (Fig. 17.4). With increasing usage of the 'low' lower lid swinging flap, the need to use this approach for the removal of retrobulbar lesions has declined significantly. However, lateral orbitotomy remains an important approach for removal of large lacrimal gland pleomorphic adenomas (where the wider exposure reduces the risk of tumour disruption during isolation of the posterior pole of the gland) and for removing lesions tightly wedged into the orbital apex (where the approach reduces surgical path length and improves tumour visualisation). Although past techniques were based on the Stallard-Wright extended brow incision [9, 10], nowadays an upper lid skin-crease incision with infero-lateral extension across the horizontal raphe is preferred (Table 17.6) [11]. Furthermore, the previous techniques with lateral wall removal risked ischaemic necrosis of the bone, whereas the contemporary method of swinging the bone on a temporalis muscle flap avoids this risk, retains the good access, and speeds the surgical closure.

Table 17.6 Advantages of the extended upper lid skin-crease lateral orbitotomy approach compared to previous brow approaches

The surgeon can plan a skin-crease incision approach and extend this intraoperatively into a lateral orbitotomy approach if necessary
Excellent access to the superior and lateral orbit [8]
Shorter, aesthetically acceptable incision than a sub-brow incision
No thinning of the brow hairs
Less brow soft-tissue atrophy

Surgery involves extending a lateral two-thirds upper eyelid skin-crease incision for about 10–15 mm into the *infero*-lateral rhytid. The periosteum is incised widely at about 6–7 mm outside the rim, from the lateral one-third of the upper rim to the level of the inferior orbital rim. The periosteum is then raised off the bone in an anterior direction, over the lateral orbital rim, and posteriorly across the lateral orbital wall taking care to diathermy and divide the zygomatico-temporal perforating vessels.

Using a high-frequency oscillating saw, two parallel anteroposterior cuts are made through the lateral wall, the upper cut being at the level of

Table 17.7 Clinical and radiological features of pleomorphic adenoma

Gradually progressive lid fullness and hypoglobus
Painless (pain implying malignant transformation)
Hard palpable mass in the lacrimal fossa
CT characteristics
Well-defined lesion
Indentation of the globe
Smooth expansion of the lacrimal gland fossa
Preservation of cortical bone

the superficial temporal line and the lower just above the level of the zygomatic arch. Two 10–15 mm relieving incisions are made as 'extensions' of these bony cuts – one being upwards to mobilise the superficial temporal fascia and the other inferiorly into the temporalis muscle – to create a 'muscle hinge' upon which the bone can later be out-fractured. A pair of 2 mm drill holes is placed in the rim either side of each of the osteotomies, and the same drill is used to 'score' the internal face of the lateral wall about 1 cm behind the rim, this creating a fault line which aids subsequent out-fracturing of the rim. With a large retractor placed between the lateral wall and periosteum to protect the orbital contents, the lateral rim is out-fractured on the temporalis muscle hinge and the ragged bone edge of the lateral orbital wall cropped backwards both to increase access to the orbital apex and to ease repositioning of the mobilised rim at the end of surgery. Venous haemorrhage from the exposed sphenoidal marrow space, if significant, can be treated with bone wax, and access to the orbit is then gained by opening the periosteum behind the arcus marginalis.

This approach is commonly performed for intact excision of large pleomorphic adenomas (Chap. 10) of the lacrimal gland (this diagnosis strongly suggested on clinical and radiological grounds (Table 17.7 and Fig. 17.5) or for resection of small apical masses or very large intraconal tumours. Following meticulous haemostasis, the laterally displaced bone fragment is swung back into position and secured with 4/0 absorbable sutures passed through each pair of drill holes. A vacuum drain is placed after bone-swinging lateral orbitotomy, with the drain passing out through the lateral eyebrow. The periosteum and deep tissues are closed, in layers, with the same 4/0 soluble suture and the skin incision closed with a running 6/0 nylon suture along its length.

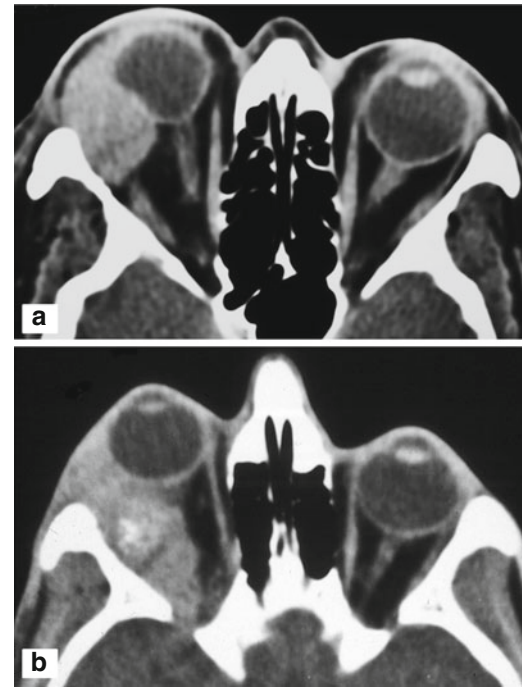

Fig. 17.5 Computed tomography (*CT*) is the imaging of first choice for investigating the patient with orbital disease. A well-defined solid lesion is shown which indents the globe (**a**) which, taken with the clinical history of a gradually enlarging painless mass, is most likely to be a pleomorphic adenoma that requires intact excision – either through a skin-crease orbitotomy or through a bone-swinging lateral orbitotomy. In contrast, a pervasive lesion which cloaks the globe (without indentation) and which has spread along the lateral orbital wall and invaded the superior ophthalmic fissure. With an acute history of painful lid swelling and exophthalmos, this lesion is likely to be a malignant lacrimal gland neoplasm and requires urgent biopsy through an upper lid skin-crease orbitotomy (**b**)

17.11 Transconjunctival Retrocaruncular Approach to the Medial Orbit

The transconjunctival retrocaruncular (transcaruncular) approach provides excellent access to the medial orbit, ethmoid sinuses, the medial half of the orbital floor, and the extraconal structures

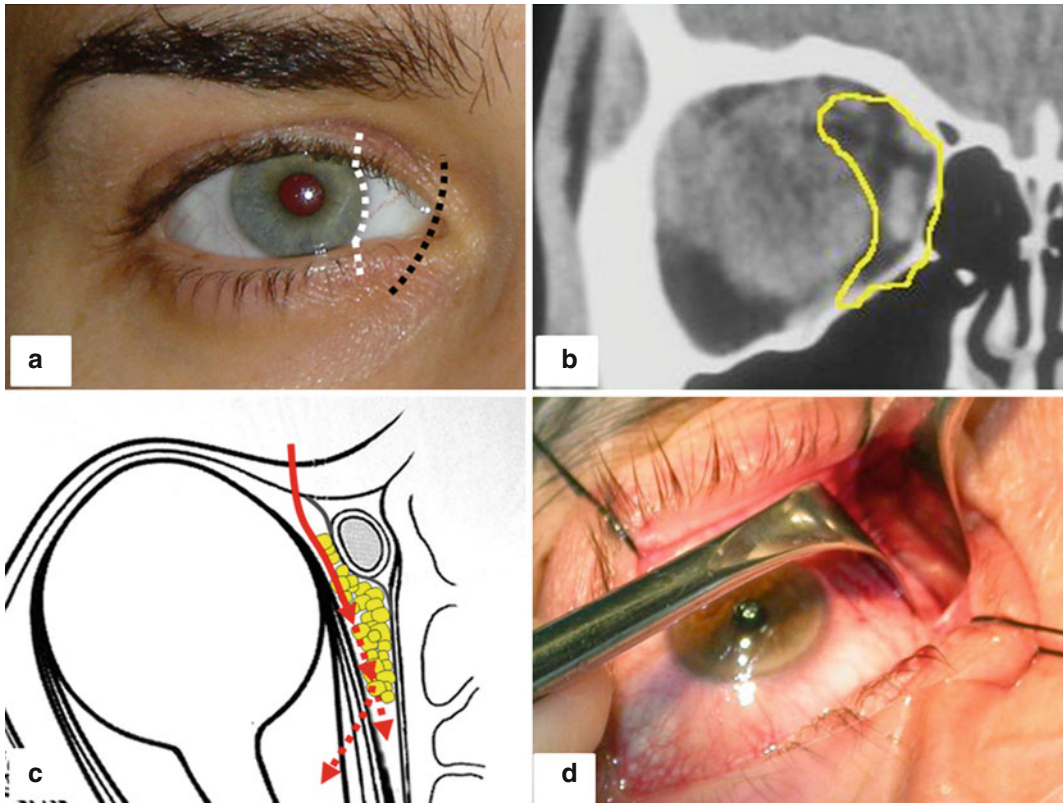

Fig. 17.6 Conjunctival approaches to the orbit. Image showing a peritomy approach (*white dotted line*) and a retrocaruncular transconjunctival approach (**a**, *black dotted line*). The region which can be accessed is shown (**b**), while the schematic (**c**) shows the surgical path taken by the retrocaruncular approach. The lids are separated with traction sutures, while two paddle retractors are placed within the medial orbit, one retracting the globe laterally and the other protecting the lacrimal sac (**d**)

within the medial part of the orbit (Fig. 17.6) [12]. The approach leaves the lacrimal sac undisturbed, is rapid, and leaves no visible scar and as such is vastly superior to the previously popular Lynch incision. It is particularly valuable where an infero-medial orbital decompression is required for compressive optic neuropathy but is also useful for draining medial orbital collections and removing medial orbital masses.

The medial ends of the eyelids are distracted with 2/0 silk traction sutures, and discrete points of diathermy are applied to the conjunctiva on the back edge of the caruncle and continued in an arc about 5 mm superiorly and 10 mm inferiorly along the fornices. These points define an incision mark at a safe distance from the two canaliculi; the conjunctiva is then opened along this line with tissue scissors, and with the lacrimal sac protected by an 11 mm malleable retractor, the posterior lacrimal crest is exposed by blunt dissection with the scissors directed 45º posteromedially. The plane of dissection remains intraperiosteal for removing or biopsying lesions in the medial orbit. For access to the ethmoid air cells (for medial wall decompression or fracture repair), the extraperiosteal space should be entered about 5 mm posterior to the posterior lacrimal crest, and the medial periosteum is reflected laterally with a 16 mm retractor. This approach affords good access of the orbital apex, from the ethmoidal neurovascular bundles superiorly down to the orbital floor medial to the infraorbital nerve. To prevent fat prolapse, the conjunctival incision should be closed with two 7/0 absorbable sutures, one at the upper and one at the lower border of the caruncle.

17.12 The Conjunctival Peritomy Approach

Although this approach might appear to be easier than those described previously, the view of deep orbital structures tends to be much more oblique ('end-on') than that achieved with the eyelid approaches, this often leading to biopsies of inadequate size, biopsies with marked crush artefact, or non-representative samples from the periphery of the true pathology. Despite these limitations, however, the transconjunctival peritomy can still be useful for masses abutting the globe or for retrobulbar lesions [13]. Access to the parabulbar space is achieved through a conjunctival peritomy of up to 180º (with radial relieving incisions to improve access further), and the deep retrobulbar space is reached by fenestrating the posterior Tenon's fascia at the appropriate site. The peritomy is readily closed with 2 or 3 tacking 8/0 soluble sutures at the limbus.

17.13 Early Postoperative Management and Counselling

Several manoeuvres may reduce accumulation of fluid and inflammatory mediators deep in the orbit. A vacuum drain may be positioned within the orbital depths, the operated orbit may be padded moderately firmly, and the patient can be nursed in a semi-recumbent position. Good postoperative blood pressure control and adequate prevention of coughing, retching, or straining may minimise the risk of postoperative haemorrhage. With surgery in the mid-orbit or apex, intraoperative parenteral glucocorticoids reduce the exudation of inflammatory mediators and offer neuroprotection. A rapidly tapering postoperative course of oral steroid can also be given. Intraoperative and postoperative antibiosis may be used for prolonged procedures and surgeries involving the paranasal sinus cavities to reduce the risk of infection.

In over 30 years of experience, the authors have never seen mydriasis or visual loss caused by a *painless* acute haemorrhage [2]: the only instance of acute haemorrhage causing optic neuropathy (interestingly, due to palpebral artery haemorrhage after eyelid surgery) was associated with both extreme and increasing pain that could not be ignored. Our current recommendation is, therefore, to monitor the patient for severe and increasing pain for 12 h after surgery, rather than the conventional teaching of frequent monitoring of pupillary reactions and vision. Arterial orbital haemorrhage leads to a 'rock-hard' orbit and optic nerve ischemia, and in such cases, any sutured closure should be released as a matter of urgency, the hematoma drained, and – if necessary – the operative site reexplored to perform diathermy haemostasis and for placement of a corrugated drain.

The orbital vacuum drains are removed once they have stopped draining, this typically being within 8–12 h in most patients. Unless there is any suggestion of slow postoperative orbital bleeding, the anticoagulated patient can restart anticoagulants a day or two after surgery.

Following discharge, usually 1 day after surgery, patients are encouraged to pursue all normal activities, with the exception of vigorous sporting activities, heavy lifting, or inverted yoga positioning – all of which significantly increase orbital venous pressure and which should, therefore, be avoided for 2–3 weeks. In addition, patients are advised not to fly or dive for about 10–14 days after *any* orbital surgery that involves the paranasal sinuses, this including repair of orbital floor fractures or decompression of the medial wall or orbital floor.

Patients are advised that following deep orbital surgery, eyelid swelling, ptosis, and diplopia are not uncommon and can take weeks or months to settle fully. The risk of significant diplopia – and its potential impact on lifestyle and livelihood – should be clearly discussed at the outset and surgery planned accordingly. Certain self-employed patients considering aesthetic orbital decompression might reasonably opt for lateral wall decompression alone to minimise the risk of incapacitating short-term diplopia, but the risk of residual exophthalmos, and thus the need for further orbital decompression, should be clearly understood before surgery.

Table 17.8 Orbital disease: Principles of surgical management

The preoperative medical risks for surgery should be recognised and treated
Dedicated orbital imaging – typically CT – is required to determine the location and extent of disease
The decision to biopsy a lesion or excise a mass intact is determined on the basis of the history, as well as the clinical and imaging characteristics:
Biopsy:
Pervasive lesions
Lesions straddling surgical boundaries
Where complete excision poses an unacceptable risk to vision
Intact excision:
Well-defined lesions
Probable pleomorphic adenoma (this based on the history and CT findings)
Thorough explanation of the surgical risks to visual functions, these based on preoperative morbidity, location of lesion, and surgical approach
Sound knowledge of the six key orbitotomy approaches and their indications
Maximise width of access (conoid of view)
Minimise surgical path length
Meticulous haemostasis and careful tissue handling
Prompt recognition and treatment of early postoperative haemorrhage

17.14 Summary

The surgical principles in managing orbital disease include a detailed understanding of the preoperative surgical risks (such as uncontrolled hypertension or thyrotoxicosis), obtaining dedicated orbital imaging (with CT being preferred, except where there is optic nerve disease or intracranial extension of disease), determining whether an incisional biopsy or intact excision is required, and providing comprehensive preoperative counselling to the patient (Table 17.8). With the six fundamental orbitotomies described, it is possible to deal with all solely orbital disease, with almost no need to resort to dated approaches such as lid-split orbitotomy or the bicoronal flap approach. Where disease straddles the craniofacial compartments, however, such patients are best treated by surgeons familiar with periorbital surgery, and this can involve more extensive approaches (such as midfacial degloving, lateral rhinotomy, or bicoronal flap) – with the most complex cases often involving different surgeons with overlapping areas of expertise [14, 15].

References

1. Dandy W. Results following the transcranial attack of orbital tumours. Arch Ophthalmol. 1941;25:191–6.
2. Rose GE. The "devil's touch"; visual loss and orbital surgery. A synopsis of the Mustardé Lecture, 2006. Orbit. 2007;26:147–58.
3. Chatterjee S, Rudra A, Sengupta S. Current concepts in the management of postoperative nausea and vomiting. Anesthesiol Res Pract. 2011;2011:748031. doi:10.1155/2011/748031.
4. Thompson JP, Rowbotham DJ. Remifentanil–an opioid for the 21st century. Br J Anaesth. 1996;76:341–3.
5. Hass AN, Penne RB, Stefanyszyn MA, Flanagan JC. Incidence of postblepharoplasty orbital haemorrhage and associated visual loss. Ophthal Plast Reconstr Surg. 2004;20:426–32.
6. Douketis JD, Spyropoulos AC, Spencer FA, Mayr M, Jaffer AK, Eckman MH, Dunn AS, Kunz R, American College of Chest Physicians. Perioperative management of antithrombotic therapy: antithrombotic therapy and prevention of thrombosis, 9th ed: American College of Chest Physicians evidence-based clinical practice guidelines. Chest. 2012;141:e326S–50.
7. Pelton RW, Patel BC. Superomedial lid crease approach to the medial intraconal space: a new technique for access to the optic nerve and central space. Ophthal Plast Reconstr Surg. 2001;17:241–53.
8. De Riu G, Meloni SM, Gobbi R, Soma D, Baj A, Tullio A. Subciliary versus swinging eyelid approach to the orbital floor. J Craniomaxillofac Surg. 2008;36:439–42.
9. McCord Jr CD, Moses JL. Exposure of the inferior orbit with fornix incision and lateral canthotomy. Ophthalmic Surg. 1979;10:53–63.
10. McNab AA, Wright JE. Lateral orbitotomy – a review. Aust N Z J Ophthalmol. 1990;18:281–6.
11. Harris GJ, Logani SC. Eyelid crease incision for lateral orbitotomy. Ophthal Plast Reconstr Surg. 1999;15:9–16.
12. Shorr N, Bayliss HI, Goldberg RA, Perry JD. Transcaruncular approach to the medial orbit and orbital apex. Ophthalmology. 2000;107:1459–63.
13. Cho KJ, Paik JS, Yang SW. Surgical outcomes of transconjunctival anterior orbitotomy for intraconal orbital cavernous hemangioma. Korean J Ophthalmol. 2010;24:274–8.
14. Saeed P, van Furth WR, Tanck M, Freling N, van der Sprenkel JW, Stalpers LJ, van Overbeeke JJ, Mourits MP. Surgical treatment of sphenoorbital meningiomas. Br J Ophthalmol. 2011;95:996–1000.
15. Shriver EM, Ragheb J, Tse DT. Combined transcranial-orbital approach for resection of optic nerve gliomas: a clinical and anatomical study. Ophthal Plast Reconstr Surg. 2012;28:184–91.

Orbital Implants

18

David R. Jordan and Stephen R. Klapper

Contents

18.1 Introduction

Loss of an eye to tumor, trauma, or end-stage ocular disease is devastating. There is a loss of binocular vision with reduced peripheral visual field and loss of depth perception. Job limitations may arise and affected individuals may experience a sense of facial disfigurement. Because eye contact is such an essential part of human interaction, it is extremely important for the patient with an artificial eye to maintain a natural, normal appearing prosthetic eye. In the past two decades, there have been numerous developments and refinements in anophthalmic socket surgery with respect to implant material and design, implant wrapping, implant-prosthesis coupling, and socket volume considerations. It is now possible than ever before to provide the anophthalmic patient with an artificial eye that looks and moves almost as naturally as a normal eye.

18.2 Porous Orbital Implants

18.2.1 Hydroxyapatite Implants

In the effort to design a biocompatible, integrated orbital implant, Perry (1985) introduced coralline (sea coral) hydroxyapatite (HA) spheres (Bio-Eye, Integrated Orbital Implants, San Diego, CA) [1]. The HA implants represented a new generation of buried, integrated spheres with a regular system of interconnecting pores that allowed host fibrovascular ingrowth (Fig. 18.1) [1, 2].

D.R. Jordan, MD, FRCSC, FACS (✉)
University of Ottawa Eye Institute, #104, 340 McLeod Street, Ottawa, ON K2P 1A4, Canada
e-mail: jordan1897@rogers.com

S.R. Klapper, MD, FACS (✉)
Klapper Eyelid and Facial Surgery, 13430 North Meridian Street, Suite 364, Carmel, IN 46032, USA
e-mail: steve@klapperplasticsurgery.com

J.D. Perry, A.D. Singh (eds.), *Clinical Ophthalmic Oncology*,
DOI 10.1007/978-3-642-40492-4_18, © Springer-Verlag Berlin Heidelberg 2014

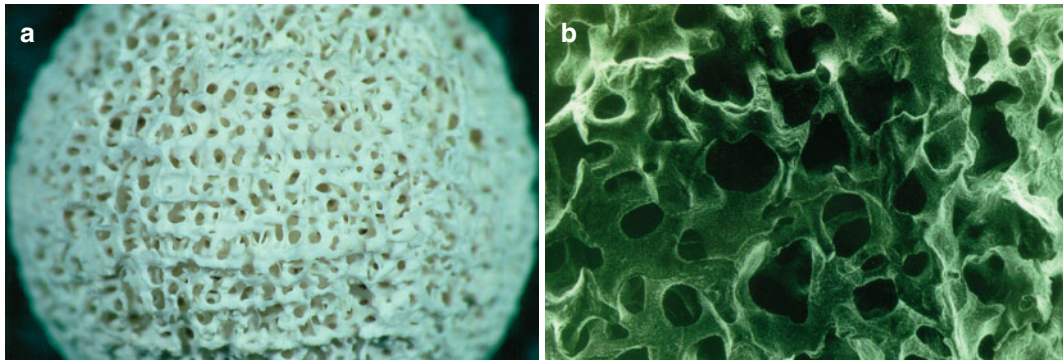

Fig. 18.1 The porous architecture of the Bio-Eye™ hydroxyapatite implant is well visualized (**a**). Scanning electron microscopy illustrating the porous architecture of a Bio-Eye™ (**b**, 222×10)

Implant fibrovascularization potentially reduced the risk of migration, extrusion, and infection [3]. The HA implant also allowed secure attachment of the extraocular muscles, which in turn lead to improved implant motility [1, 2]. By drilling into the HA implant, inserting a peg and coupling the peg to the prosthetic eye, an improved range of movement as well as fine darting prosthetic eye movements (commonly seen during close conversational speech) were seen. This allowed a more lifelike quality to the artificial eye.

Although HA implants represented a significant advance in anophthalmic surgery, experience with HA over the last two decades has expanded our understanding of the limitations of HA. Reported complications are not uncommon and include implant exposure, conjunctival thinning, socket discharge, pyogenic granuloma formation, implant infection, and persistent pain or discomfort [4–8]. Implant exposure problems continue to deter some surgeons from using HA implants, but this complication appears to be related more to surgical implantation technique (including HA implant wrap selection) and host factors than properties related to HA spheres [3].

The introduction of HA as an orbital implant significantly raised the costs associated with enucleation, evisceration, and secondary orbital implant procedures. The Bio-Eye™ HA implant may cost over $600 (US) more than traditional silicone or polymethylmethacrylate (PMMA) spherical implants ($15–$50 US). Additional expenses associated with HA placement include an implant wrap material, assessment of implant vascularization with a confirmatory magnetic resonance (MR) imaging study, a secondary drilling procedure with peg placement, and prosthesis modification. In the search for porous orbital implants with a reduced complication profile and diminished surgical and postoperative costs, numerous alternative implant materials have been introduced around the world.

18.2.2 Synthetic Porous Implants

Synthetic porous polyethylene (MEDPOR®, Porex Surgical Inc., Newnan, GA, USA) implants were introduced almost two decades ago for use in the orbit and have been widely accepted as an alternative to the Bio-Eye™ HA [9–12]. Porous polyethylene implants although less biocompatible than HA [13] are typically well tolerated by orbital soft tissue. They have a smoother surface than HA implants which permits easier implantation and potentially less irritation of the overlying conjunctiva following placement (Fig. 18.2). These implants have a high tensile strength yet are malleable which allows sculpting of the anterior surface of the implant. They may be used with or without a wrapping material, and the extraocular muscles can be sutured directly onto the implant, although most surgeons may find this difficult without predrilled holes. Porous polyethylene implants are available in spherical, egg, conical, and mounded shapes (quad

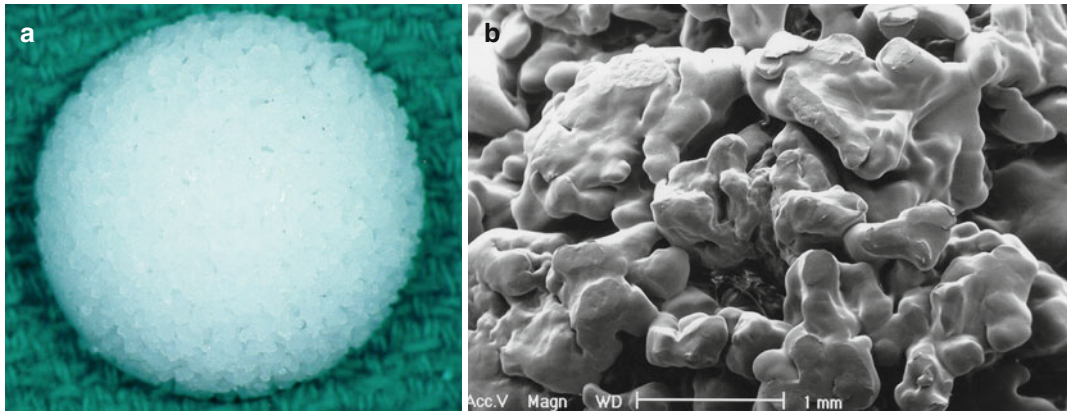

Fig. 18.2 On gross examination, the porous polyethylene implant appears to have more of a channel system than pores (**a**). Scanning electron microscopy of a porous polyethylene implant (222×10) illustrating the smooth surface of the architecture as well as the channel system (**b**). Reproduced with permission from Perry [1]

implant) [10–12]. The anterior surface can also be manufactured with a smooth, nonporous surface to prevent abrasion of the overlying tissue (e.g., MEDPOR® smooth surface tunnel implant, SST™) while retaining a larger pore size posteriorly to facilitate fibrovascular ingrowth. The addition of Bioglass (US biomaterials Corp, Alachua, FL, USA) to the MEDPOR® implant may help stimulate early vascular ingrowth and reduce complications such as exposure, migration, and extrusion [14]. The MEDPOR® implant costs vary depending upon what model is used and the number ordered. It may be up to approximately $200 (US) less than the Bio-Eye™ HA sphere.

18.2.3 Synthetic Hydroxyapatite Implants

Synthetic HA implants developed by FCI (Issy-les-Moulineaux, Cedex, France) have an identical chemical composition to that of the Bio-Eye™, although scanning electron microscopy (SEM) has revealed decreased pore uniformity and interconnectivity and the presence of blind pouches [15]. Central implant fibrovascularization in a rabbit model still appears to occur in a similar manner in both the Bio-Eye™ and FCI_3 implants [16]. The synthetic FCI_3 implant has gained in popularity in many parts of the world over the past 15 years; however, it is not yet available in the USA. The problems and complications associated with the synthetic FCI_3 implant are similar to that of the Bio-Eye™ [17]. It is less expensive than the Bio-Eye (approximately 480 US dollars)

Other forms of HA implants in use around the world include the Chinese HA and the Brazilian HA implants [18, 19]. Although less expensive than the Bio-Eye™, these implants have impurities or poor porous structure that offer little advantage. Other implant designs continue to surface, some of which are of little added value [20] while others have only been in use for a short time and there advantages/disadvantages are not yet apparent [21].

18.2.4 Ceramic Implants

Aluminum oxide (Al_2O_3) is a ceramic implant biomaterial that has been used in orthopedic surgery and dentistry for more than 30 years. Spherical and Egg-Shaped Bioceramic Orbital Implants (FCI, Issy-les-Moulineaux, Cedex, France) have been available in North America for over a decade. Aluminum oxide is a porous, inert substance and has been suggested as a standard reference material in studies of implant biocompatibility [22]. These implants permit host fibrovascular ingrowth similar to the Bio-Eye™

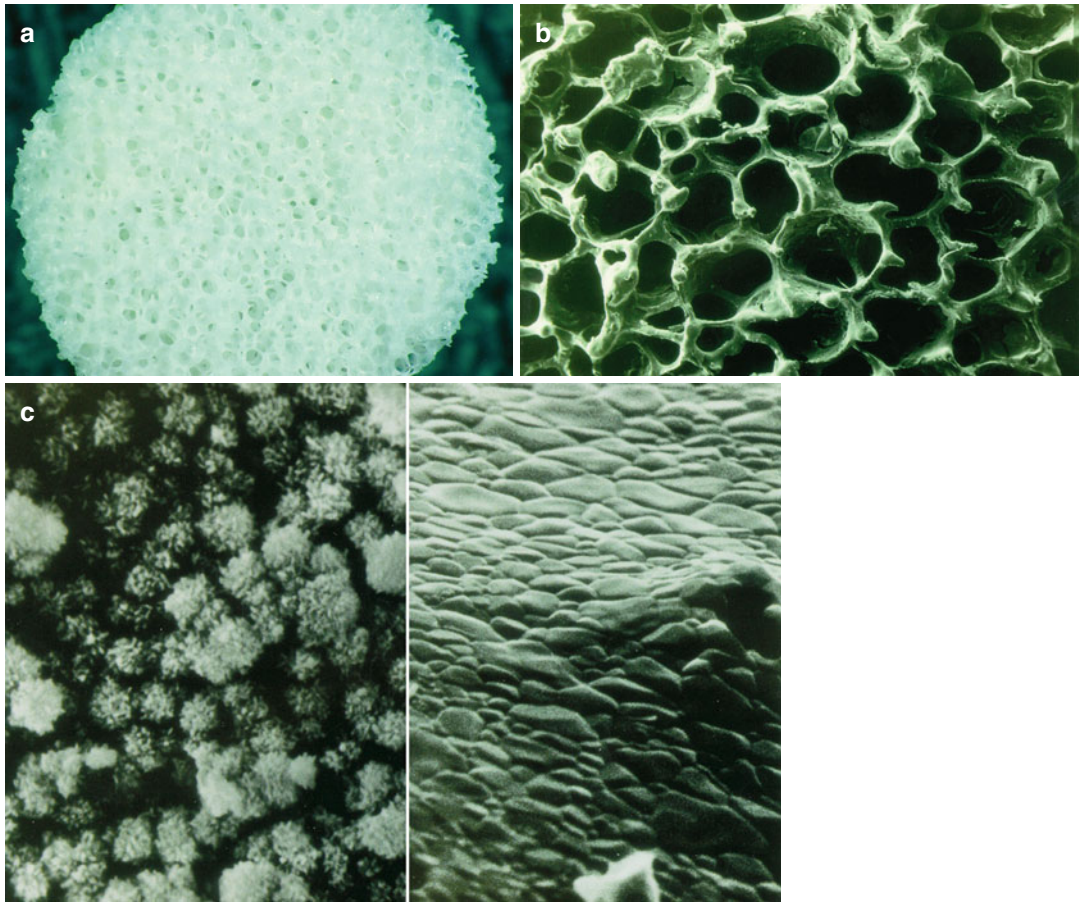

Fig. 18.3 The porous architecture of an aluminum oxide (Bioceramic) implant is well visualized (**a**). Scanning electron microscopy illustrating the more uniform porous architecture of the aluminum oxide orbital implant (**b**, 222×10). On high power scanning electron microscopy (230×10^3), the solid component of the Bio-Eye™ (**c**, *left*) has a rough appearing microcrystalline structure compared to the smooth microcrystalline structure of the aluminum oxide (Bioceramic) implant (**c**, *right*)

[23, 24]. Human fibroblasts and osteoblasts proliferate more rapidly on aluminum oxide than HA suggesting it is a more biocompatible substance than HA [13, 22]. The Bioceramic implant is lightweight and has a uniform pore structure and excellent pore interconnectivity (Fig. 18.3a, b) [15]. The microcrystalline structure is smoother than the rough surfaced Bio-Eye™ (Fig. 18.3c). Although sockets with the aluminum oxide implants may initially be quieter than those with HA, the same complications as other porous implants (e.g., exposure) may be seen [25]. Long-term follow-up is important with any porous implant as late complications (years after implantation) are known to occur [25–28]. As with the other available porous orbital implants, aluminum oxide is less expensive than the Bio-Eye™ ($450 US vs. $650 US).

18.3 Implant Selection

There continues to be little consensus regarding orbital implant material and design preference [29]. Surgeons have their own preferences regarding use of spherical versus shaped implants, wrapped versus unwrapped implants, and pegged versus unpegged implants. Implant cost, hospital budgets, and marketing pressures also play a role in implant selection.

When deciding upon an implant to use, these authors divide the various implants into three useful categories:

(a) Porous spheres that may potentially be pegged (HA – coralline or synthetic, porous polyethylene, aluminum oxide)
(b) Quasi-integrated implants (Universal implant, Quad MEDPOR®)
(c) Standard nonporous sphere (polymethylmethacrylate, silicone)

If the patient is healthy and between the ages of 15 and 65 years, a porous implant (e.g., Bioceramic implant) that can potentially be pegged is our first choice [25, 26]. If a peg is not being remotely considered, the advantage of using a porous spherical implant is diminished, as the movement associated with a non-pegged porous orbital implant is equal to that of a wrapped nonporous spherical implant [30–33]. In light of widespread disappointment with pegging of porous implants and no motility advantage of unpegged porous over nonporous spherical implants, some authors feel more consideration should be given to techniques that are equally effective, less costly, and perhaps more reliable [34]. Direct fixation of extraocular muscles to a solid silicone sphere, by using nonabsorbable sutures knotted beneath the muscles, provides implant stability and prosthesis motility comparable to those non-pegged porous implants, with equal or less risk of implant exposure and infection [34]. However, the advantage of fibrovascular ingrowth and potentially diminished risk of implant migration remain reasons to consider using a porous implant [14, 35].

A quasi-integrated implant such as the Universal (PMMA) or MEDPOR® Quad implant is an alternative consideration to the porous or nonporous spherical implant as the mounded surface of the implant offers improved motility over a standard sphere as a result of the coupling that occurs between the mounds on the implant and the posterior surface of the prosthesis [12]. The implant placement is operator and technique sensitive. As a result, it is technically more difficult for those only doing occasional enucleations or secondary implantation surgery.

A standard PMMA sphere, wrapped, centered within the muscle cone and attached to the four rectus muscles is another alternative if pegging is not a consideration. A standard sphere placed into the orbit, without a wrap and without connection to the rectus muscles, is the least desirable choice as it offers little movement and the implant is prone to migration.

In a young child (less than 5 year), we prefer either a wrapped sphere (PMMA, silicone) centered within the muscle cone and connected to the four rectus muscles and inferior oblique muscle or a PMMA mounded implant (Universal, MEDPOR® Quad). Implant exchange with a porous orbital implant that can potentially be pegged is considered at a later age (>15 year). In the aging individual (>65 year), the authors do not use porous orbital implants and prefer a standard sphere (PMMA, silicone) wrapped and centered in the muscle cone and connected to the rectus muscles or a PMMA mounded implant (Universal, MEDPOR® Quad).

18.4 Volume Considerations

Removal of an eye following enucleation or evisceration creates an orbital soft tissue volume deficiency. Insufficient volume replacement results in an abnormally deep superior sulcus, upper eyelid ptosis, and enophthalmos and may require a larger than desirable prosthesis [36–40].

Approximately 70–80 % of the volume of an individual's normal globe should be replaced with the orbital implant [38]. This generally allows for a prosthetic volume that is approximately 2 ml [36]. Larger prostheses often result in progressive lower eyelid laxity and malposition due to the weight of the prostheses on the eyelid. Larger prostheses may also have limited socket excursion [37].

Several authors have reported that the variability of axial length and globe volume is significant with globe volumes varying between 6.9 and 9.0 ml [38–40]. Proper implant volume may be determined either preoperatively or intraoperatively (enucleation cases) from the axial length

of the eye or by determining the volume of fluid the enucleated eye displaces in a graduated cylinder [38–40]. Kaltreider has shown that the axial length minus 2 mm (or A-scan minus 1 mm) approximates the implant diameter for optimal volume replacement in emmetropic and myopic individuals (Chap. 15) [38, 41]. Custer suggested a graduated cylinder be used to measure the volume of fluid displaced by an enucleated eye. The volume of the globe minus 2 ml gives the ideal implant size to use [39]. Individualization of the implant size is important in optimizing orbital volume replacement and in achieving the best possible esthetic result [37, 38, 40, 41].

18.5 Orbital Implant Wrapping

Placement of an HA implant or Bioceramic implant within the soft tissue of the eye socket is facilitated by a smooth wrapping material which diminishes tissue drag [1]. In addition, the wrap facilitates precise fixation of the extraocular muscles to the implant surface [1]. Implant wraps may also provide a barrier function over the spiculated porous implant surface [1, 26] although there is some debate whether covering the anterior surface of the implant with an avascular material is helpful in preventing implant exposure [42–44]. The advantages of placing an unwrapped implant include simplification of the procedure, decreased operating room time, reduced cost, avoidance of a second surgical site for harvesting autogenous wrap, and a decreased risk of disease transmission [29, 43, 44].

If a wrap is used, human donor sclera has traditionally been the first choice [1, 2]. The use of human donor material however has fallen out of favor recently with both surgeons and patients due to the potential risk of transmission of HIV, hepatitis B or C, and prions (Creutzfeldt -Jakob disease) [45]. Although we are not aware of any reports of disease transmission from donor sclera, segments of the human immunodeficiency virus(HIV)-1 genome have been identified in preserved human sclera [46]. Creutzfeldt-Jakob disease transmission from dural and corneal transplants has been reported [47–49]. In addition, seronegative organ and tissue donors may transmit HIV [50]. Many eye banks charge a substantial fee to provide donor sclera.

Specially processed human donor pericardium, fascia lata, and sclera are marketed as safe alternative implant wraps to preserved human donor tissues (Biodynamics International (USA), Inc., Tampa, FL). These wraps have the convenience of a long (up to 5 years) shelf life; however, they are currently priced at levels that may exceed the cost of the implant itself.

Processed bovine pericardium (Peri-Guard® or Ocu-Guard™ Supple, BioVascular Inc., Saint Paul, MN, USA) is FDA approved and also available as an implant wrap material [51, 52]. Although there have been only few cases of bovine spongiform encephalopathy (BSE) in American cattle to date, reports of infected cattle in Alberta, Canada, have surfaced in the past decade, and the potential for the disease to occur with possible prion transmission still exists [45].

Autologous temporalis fascia [53], fascia lata [54], rectus abdominis sheath [55], and posterior auricular muscle complex graft [56] have been tried as orbital implant wrapping materials. Use of these tissues requires a second operative site, prolonged operative time, and a potentially increased risk of morbidity.

Microporous expanded polytetrafluoroethylene (e-PTFE) (Gore-Tex, W.L. Gore & Associates, Flagstaff, AZ) has also been advocated as an implant wrapping material (Oculo-Plastik, Montreal, Quebec, Canada); however, complications with its use have made it undesirable [57–59].

Undyed polyglactin 910 mesh (Vicryl mesh, Ethicon, Somerville, NJ, USA) is a bioabsorbable synthetic material and is our preference as a wrapping material for porous orbital implants [60, 61]. Vicryl mesh eliminates the risk of infectious disease transmission, does not require a second surgical site, is readily available, is simple to use, and is inexpensive. Vicryl mesh-wrapped HA implants have been shown to permit rapid implant fibrovascularization in an animal model [61, 62] and may provide a potential advantage of permitting fibrovascular ingrowth over the entire implant surface unlike implants completely wrapped in sclera [63]. We have reported a 2.1 % incidence of implant exposure in 187 consecutive

patients receiving Vicryl mesh-wrapped HA orbital implants [64]. Addition of a small scleral cap (15 mm × 15 mm) over the anterior surface of the Vicryl mesh-wrapped implant may reduce implant exposure even further [26]. Oestreicher et al. also reported a low exposure incidence using a similar bioabsorbable wrapping material composed of polyglycolic acid (Dexon mesh style No. 8, non-stretch, medium-weight closed tricot, Davis & Geck, Manati, Puerto Rico) [7]. Despite our success with polyglactin 910 mesh as an implant wrap material, some surgeons continue to believe that it is associated with a higher rate of implant exposure [59, 60]. It remains the view of these authors that high exposure rates with Vicryl mesh-wrapped implants is a technique-related problem that can be significantly minimized with correct implant insertion and meticulous tension-free wound closure [65, 66]. We also now routinely place a 13–15 mm diameter cap of donor sclera over the anterior surface of the mesh-wrapped implant as added insurance against implant exposure [26].

18.6 Pegging Porous Orbital Implants

Infrared oculography has demonstrated significant objective improvement in horizontal gaze after motility peg placement [26]. Despite the improved motility, many surgeons and patients still elect to avoid peg placement due to the satisfactory results without pegging and the possibility of pegging-related complications [34, 67–72]. Although pegging has declined dramatically over the past few years, we believe that a precise and meticulous technique [73] in the appropriately selected individual can be very successful. Johnson [74] and others [26, 27] have also shown largely positive results, validating the efficacy of pegging porous orbital implants (e.g., hydroxyapatite, Bioceramic) with minor risk of serious complications.

Proper care of the artificial eye and regular follow-up visits with the ocularist and ophthalmic plastic surgeon are important. Watching for small problems (e.g., exposure around the peg) and management of these small issues at an early stage can often avoid more serious problems with the peg and implant later. If the patient is unlikely, unable, or unwilling to keep their follow-up visits, pegging should be avoided. The authors do not feel children (roughly less than age 15 year), adults over the age of 65 year, or individuals of any age with a chronic illness (collagen vascular disease, sarcoidosis, diabetes, immunosuppressive therapy, etc.) should be considered for pegging.

Peg systems were generally designed for peg placement once fibrovascularization of the implant has been completed. Implant fibrovascularization is believed to diminish the risks of implant infection, exposure, and migration [9, 63]. Drilling into an avascular area of the implant may predispose the implant to infection [75]. Gadolinium-enhanced MR imaging is currently the recommended method of assessing the extent of implant vascularization [76]. Fibrovascular ingrowth may occur at varying rates in different patients. Implant drilling and peg placement is generally deferred until 10–12 months after HA implant insertion.

Several titanium peg systems are currently available for use with porous orbital implants. Titanium is more biocompatible and better tolerated by human soft tissue than the original peg systems made of polycarbonate [77]. The FCI peg system utilizes a hydroxyapatite-coated titanium sleeve [73]. The HA coating potentially allows for stronger interface bonding with the orbital fibroblasts than the uncoated P-K system supplied for use with the Bio-Eye™. The MEDPOR® Motility Coupling Post (MCP) (Porex Surgical, College Park, GA, USA) is a titanium screw that can be screwed directly into porous polyethylene implants [78, 79]. Some authors have advocated primary placement of the MCP at the time of implant insertion [80, 81]. This practice, however, remains controversial and most surgeons defer implant pegging for more than 6 months after implant placement.

18.7 Summary

Anophthalmic surgery is no longer simply about replacing a diseased eye with an orbital implant. Ophthalmic surgeons and oculariists are now

more than ever focused on restoring a patient's appearance and prosthetic motility to as near normal as possible. Although evisceration surgery has recently increased in popularity and favored by many surgeons because of the simplicity of the technique, less disruption to the socket anatomy and excellent cosmetic results, enucleation is still required in patients with known or potentially occult ocular malignancies as well as blind, painful, and/or unsightly eyes with opaque media and unknown or unclear past ocular histories [82].

References

1. Perry AC. Advances in enucleation. Ophthal Plast Reconstr Surg. 1991;4:173–82.
2. Dutton JJ. Coralline hydroxyapatite as an ocular implant. Ophthalmology. 1991;98:370–7.
3. Nunery WR, Heinz GW, Bonnin JM, Martin RT, Cepela MA. Exposure rate of hydroxyapatite spheres in the anophthalmic socket: histopathologic correlation and comparison with silicone sphere implants. Ophthal Plast Reconstr Surg. 1993;9:96–104.
4. Goldberg RA, Holds JB, Ebrahimpour J. Exposed hydroxyapatite orbital implants: report of six cases. Ophthalmology. 1992;99:831–6.
5. Kim YD, Goldberg RA, Shorr N, Steinsapir KD. Management of exposed hydroxyapatite orbital implants. Ophthalmology. 1994;101:1709–15.
6. Remulla HD, Rubin PAD, Shore JW, Sutula FC, Townsend DJ, Woog JJ, Jahrling KV. Complications of porous spherical orbital implants. Ophthalmology. 1995;102:586–93.
7. Oestreicher JH, Liu E, Berkowitz M. Complications of hydroxyapatite orbital implants: a review of 100 consecutive cases and a comparison of Dexon mesh (polyglycolic acid) with scleral wrapping. Ophthalmology. 1997;104:324–9.
8. Jordan DR, Brownstein S, Jolly SS. Abscessed hydroxyapatite orbital implants: a report of two cases. Ophthalmology. 1996;103:1784–7.
9. Blaydon SM, Shepler TR, Neuhaus RW, White WL, Shore JW. The porous polyethylene (Medpor) spherical orbital implant: a retrospective study of 136 cases. Ophthal Plast Reconstr Surg. 2003;19:364–74.
10. Karesh JW, Dresner SC. High density porous polyethylene (Medpor) as a successful anophthalmic implant. Ophthalmology. 1994;101:1688–96.
11. Rubin PAD, Popham J, Rumeldts S, et al. Enhancement of the cosmetic and functional outcomes of enucleation with the conical orbital implant. Ophthalmology. 1998;105:919–25.
12. Anderson RL, Yen MT, Lucci LM, et al. The quasi-integrated porous polyethylene orbital implant. Ophthal Plast Reconstr Surg. 2002;18:50–5529.
13. Mawn LA, Jordan DR, Gilberg S. Proliferation of human fibroblasts in vitro after exposure to orbital implants. Can J Ophthalmol. 2001;36:245–51.
14. Ma Y, Schou KR, Maloney-Schou M, Harwin FM, Ng J. The porous polyethylene/Bioglass spherical orbital implant: a retrospective study of 170 cases. Ophthal Plast Reconstr Surg. 2011;27:21–7.
15. Mawn L, Jordan DR, Gilberg S. Scanning electron microscopic examination of porous orbital implants. Can J Ophthalmol. 1998;33:203–9.
16. Jordan DR, Munro SM, Brownstein S, Gilberg SM, Grahovac SZ. A synthetic hydroxyapatite implant: the so-called counterfeit implant. Ophthal Plast Reconstr Surg. 1998;14(4):244–9.
17. Jordan DR, Bawazeer A. Experience with 120 synthetic hydroxyapatite implants ($FCI_{3)}$. Ophthal Plast Reconstr Surg. 2001;17:184–90.
18. Jordan DR, Pelletier C, Gilberg SM, Brownstein S, Grahovac SZ. A new variety of hydroxyapatite: the Chinese implant. Ophthal Plast Reconstr Surg. 1999;15(6):420–4.
19. Jordan DR, Hwang I, McEachren TM, Brownstein S, Gilberg SM, Grahovac SZ, Mawn L. Brazilian hydroxyapatite implant. Ophthal Plast Reconstr Surg. 2000;16:363–9.
20. Jordan DR, Brownstein S, Gilberg S, Matthew B, Mawn L, Khouri L. Investigation of a bioresorbable orbital implant. Ophthal Plast Reconstr Surg. 2002;18:342–8.
21. Klett A, Guthoff R. Deckung von Orbitaimplantaten mit muskelgestielter autologer sklera. Ophthalmologe. 2003;100:449–52.
22. Christel P. Biocompatibility of alumina. Clin Orthop. 1992;282:10–8.
23. Jordan DR, Mawn L, Brownstein S, McEachren TM, Gilberg SM, Hill V, Grahovac SZ, Adenis JP. The bioceramic orbital implant: a new generation of porous implants. Ophthal Plast Reconstr Surg. 2000;16:347–55.
24. Jordan DR, Gilberg S, Mawn LA. The bioceramic orbital implant: experience with 107 implants. Ophthal Plast Reconstr Surg. 2003;19:128–35.
25. Jordan DR, Klapper SK, Gilberg SM, Dutton JJ, Wong A, Mawn L. The bioceramic implant: evaluation of implant exposures in 419 implants. Ophthal Plast Reconstr Surg. 2010;26:80–2.
26. Wang JK, Lai PC, Liao SL. Late exposure of the bioceramic orbital implant. Am J Ophthalmol. 2009;147:162–70.
27. Karslioglu SK, Buttanri IB, Fazil K, Serin D, Akbaba M. Long-term outcomes of pegged and unpegged bioceramic orbital implants. Ophthal Plast Reconstr Surg. 2012;28:264–7.
28. Jordan DR, Gilberg SM, Bawazeer A. The coralline hydroxyapatite orbital implant (Bio-Eye™): experience with 170 patients. Ophthal Plast Reconstr Surg. 2004;20(1):69–71.
29. Su GW, Yen MT. Current trends in managing the anophthalmic socket after primary enucleation and evisceration. Ophthal Plast Reconstr Surg. 2004;20(4):274–80.

30. Guillinta P, Vasani SN, Granet DB, Kikkawa DO. Prosthetic motility in pegged versus unpegged integrated porous orbital implants. Ophthal Plast Reconstr Surg. 2000;19:119–22.
31. Custer PL, Kennedy RH, Woog JJ, Kaltreider SA, Meyer DA. Orbital implants in enucleation surgery, a report by the American Academy of Ophthalmology. Ophthalmology. 2003;110:2054–61.
32. Custer PL, Trinkaus KM, Fornoff J. Comparative motility of hydroxyapatite and alloplastic enucleation implants. Ophthalmology. 1999;106:513–6.
33. Colen TP, Paridaens DA, Lemij HG, et al. Comparison of artificial eye amplitudes with acrylic and hydroxyapatite spherical enucleation implants. Ophthalmology. 2000;107:1889–94.
34. Wells T, Harris GJ. Direct fixation of extra-ocular muscles to a silicone sphere: a cost sensitive, low-risk enucleation procedure. Ophthal Plast Reconstr Surg. 2011;27:364–7.
35. Trichopoulas N, Augsburger JJ. Enucleation with unwrapped porous and non-porous implants: a 15 year experience. Ophthal Plast Reconstr Surg. 2005; 21:331–6.
36. Kaltreider SA. The ideal ocular prostheses. Analysis of prosthetic volume. Ophthal Plast Reconstr Surg. 2000;16(5):388–92.
37. Kaltreider SA. The ideal ocular prosthesis: analysis of prosthetic volume. Ophthal Plast Reconstr Surg. 2000;16:388–92.
38. Kaltreider SA, Lucarelli MJ. A simple algorithm for selection of implant size for enucleation and evisceration. Ophthal Plast Reconstr Surg. 2002;18: 336–41.
39. Custer PL, Trinkaus KM. Volumetric determination of enucleation implant size. Am J Ophthalmol. 1999; 128:489–94.
40. Thaller VT. Enucleation volume measurement. Ophthal Plast Reconstr Surg. 1997;13:18–20.
41. Kaltreider SA, Jacobs JL, Hughes MO. Predicting the ideal implant size before enucleation. Ophthal Plast Reconstr Surg. 1999;15(3):37–43.
42. Perry JD. Hydroxyapatite implants (letter). Ophthalmology. 2003;110:1281.
43. Long JA, Tann TM, Bearden WH, Callahan MA. Enucleation: is wrapping the implant necessary for optimal motility. Ophthal Plast Reconstr Surg. 2003; 19(3):194–7.
44. Suter AJ, Molteno AC, Becin TH, et al. Long term follow-up of bone derived hydroxyapatite orbital implants. Br J Ophthalmol. 2002;86: 1287–992.
45. Nunery WR. Risk of prion transmission with the use of xenografts and allografts in surgery. Ophthal Plast Reconstr Surg. 2003;17:389–94.
46. Seiff SR, Chang Jr JS, Hurt MH, Khayam-Bashi H. Polymerase chain reaction identification of human immunodeficiency virus-1 in preserved human sclera. Am J Ophthalmol. 1994;118:528–9.
47. Long CJ, Heckman JG, Neunderfer B. Creutzfeldt-Jakob disease via dural and corneal transplants. J Neurol Sci. 1998;160:128–39.
48. Hogan RN, Brown P, Heck E, Cavanagh H. Risk of prion disease transmission from ocular donar tissue transplantation. Cornea. 1999;18:2–11.
49. Heckman JG, Lang CJ, Petruch F, et al. Transmission of Creutzfeldt-Jakob disease via a corneal transplant. J Neurol Neurosurg Psychiatry. 1997;63:388–90.
50. Simonds RJ, Holmberg SD, Hurwitz RL, Coleman TR, Bottenfield S, Conley LJ, Kohlenberg SH, Castro KG, Dahan BA, Schable CA, Rayfield MA, Rogers MF. Transmission of human immunodeficiency virus type 1 from a seronegative organ and tissue donor. N Engl J Med. 1992;326:726–32.
51. Arat YO, Shetlar DJ, Boniuk M. Bovine pericardium versus homologous sclera as a wrapping for hydroxyapatite orbital implants. Ophthal Plast Reconstr Surg. 2003;19:189–93.
52. Gayre GS, DeBacker CM, Lipham W, Tawfik HA, Holck DEE, Dutton JJ. Bovine pericardium as a wrapping for orbital implants. Ophthal Plast Reconstr Surg. 2001;17:381–7.
53. Pelletier C, Gilberg S, Jordan DR. Use of Temporalius fascia for management of exposed hydroxyapatite implants. Ophthal Plast Reconstr Surg. 1998;14: 198–203.
54. Naugle Jr TC, Fry CL, Sabatier RE, Elliot LF. High leg incision fascia lata harvesting. Ophthalmology. 1997;104:1480–8.
55. Kao SCS, Chen S. The use of rectus abdominis sheath for wrapping of the hydroxyapatite orbital implants. Ophthalmic Surg Lasers. 1999;30:69–71.
56. Naugle Jr TC, Lee AM, Haik BG, Callahan MA. Wrapping hydroxyapatite orbital implants with posterior auricular muscle complex grafts. Am J Ophthalmol. 1999;128:495–501.
57. Karesh JW. Polytetrafluoroethylene as a graft material in ophthalmic plastic and reconstructive surgery: an experimental and clinical study. Ophthal Plast Reconstr Surg. 1987;3:179–85.
58. Choo PH, Carter SR, Crawford JB, Seiff SR. Exposure of expanded polytetrafluoroethylene-wrapped hydroxyapatite orbital implant: a report of two patients. Ophthal Plast Reconstr Surg. 1999;15:77–8.
59. Kao L. Polytetrafluoroethylene as a wrapping material for a hydroxyapatite orbital implant. Ophthal Plast Reconstr Surg. 2000;16:286–8.
60. Jordan DR, Allen LH, Ells A, Gilberg S, Brownstein S, Munro S, Grahovac S, Raymond F. The use of vicryl mesh (polyglactin 910) for implantation of hydroxyapatite orbital implants. Ophthal Plast Reconstr Surg. 1995;11:95–9.
61. Jordan DR, Ells A, Brownstein S, Munro S, Grahovac S, Raymond F, Allen LH. Vicryl-mesh wrap for the implantation of hydroxyapatite orbital implants: an animal model. Can J Ophthalmol. 1995;30:241–6.
62. Klapper SR, Jordan DR, Punja K, Brownstein S, Gilberg SM, Mawn L, Grahovac SZ. Hydroxyapatite implant wrapping materials: analysis of fibrovascular ingrowth in an animal model. Ophthal Plast Reconstr Surg. 2000;16:278–85.
63. Gayre GS, Lipham W, Dutton JJ. A comparison of rates of fibrovascular ingrowth in wrapped versus

unwrapped hydroxyapatite spheres in a rabbit model. Ophthal Plast Reconstr Surg. 2002;18:275–80.
64. Jordan DR, Klapper SR, Gilberg SM. The use of vicryl mesh in 200 porous orbital implants. Ophthal Plast Reconstr Surg. 2003;19:53–61.
65. Custer PL. Enucleation: past, present, and future. Ophthal Plast Reconstr Surg. 2000;16:316–21.
66. Custer PL. Reply to Dr. D.R. Jordan's letter on polyglactin mesh wrapping of hydroxyapatite implants. Ophthal Plast Reconstr Surg. 2001;17: 222–3.
67. Jordan DR, Chan S, Mawn L, Gilberg SM, Brownstein S, Hill V. Complications associated with pegging hydroxyapatite orbital implants. Ophthalmology. 1999;106:505–12.
68. Edelstein C, Shields CL, DePotter P, Shields JA. Complications of motility peg placement for the hydroxyapatite orbital implant. Ophthalmology. 1997;104:1616–21.
69. Lin CJ, Lio SL, Jou JR, Kao SC, Hou PK, Chen MS. Complications of motility peg placement for porous hydroxyapatite orbital implants. Br J Ophthalmol. 2002;86:394–6.
70. Jordan DR. Spontaneous loosening of hydroxyapatite peg sleeves. Ophthalmology. 2001;108:2041–4.
71. Cheng MS, Liao SL, Lin L. Late porous polyethylene implant exposure after motility coupling post placement. Am J Ophthalmol. 2004;138:420–4.
72. Lee SY, Jang JW, Lew H, Kim SJ, Kim HY. Complications in motility peg placement for hydroxyapatite orbital implants in anophthalmic socket. Jpn J Ophthalmol. 2002;46:103–7.
73. Jordan DR, Klapper SR. A new titanium peg system for hydroxyapatite orbital implants. Ophthal Plast Reconstr Surg. 2000;16:380–7.
74. Johnson RLC, Ramstead CL, Nathoo N. Pegging the porous orbital implant. Ophthal Plast Reconstr Surg. 2011;27:74–5.
75. Ainbinder DJ, Haik BG, Tellado M. Hydroxyapatite orbital implant abscess: histopathologic correlation of an infected implant following evisceration. Ophthal Plast Reconstr Surg. 1994;10:267–70.
76. Klapper SR, Jordan DR, Ells A, Grahovac SZ. Hydroxyapatite orbital implant vascularization assessed by magnetic resonance imaging. Ophthal Plast Reconstr Surg. 2003;19:46–52.
77. Cook S, Dalton J. Biocompatibility and biofunctionality of implanted materials. Alpha Omegan. 1992;85:41–7.
78. Choi JC, Iwamoto MA, Bstandig S, Rubin PA, Shore J. Medpor motility coupling post: a rabbit model. Ophthal Plast Reconstr Surg. 1999;15:190–201.
79. Rubin PAD, Fay AM, Remulla HD. Primary placement of motility coupling post in porous polyethylene orbit implants. Arch Ophthalmol. 2000;118:826–32.
80. Hsu WC, Green JP, Spilker MH, Rubin PAD. Primary placement of a titanium motility post in a porous polyethylene orbital implant. Ophthal Plast Reconstr Surg. 2003;16:370–9.
81. Tawfik HA, Dutton JJ. Primary peg placement in evisceration with the spherical porous polyethylene orbital implant. Ophthalmology. 2004;111:1401–6.
82. Timothy NH, Feilich DE, Linberg JV. Perspective: evisceration versus enucleation, the ocularists standpoint. Ophthal Plast Reconstr Surg. 2003;19(6):417–20.

Ocular Prosthesis

19

Darrel W. Hardin

Contents

19.1 Introduction

An ocularist is a trained technician skilled in the arts of fitting, shaping, and painting ocular prostheses. In addition to creating it, the ocularist shows the patient how to handle and care for the prosthesis and provides long-term care through periodic examinations. In this chapter, the steps in construction of custom designed prosthesis are outlined. Cosmetic rehabilitation following exenteration is discussed elsewhere.

19.2 Historical Perspective

The first ocular prostheses were made by Roman and Egyptian priests as early as the fifth century B.C. In those days, artificial eyes were made of painted clay attached to cloth and worn outside the socket. It took many centuries for the first in-socket artificial eye to be developed. At first, these were made of gold with colored enamel. Then, in the later part of the sixteenth century, the Venetians started making artificial eyes out of glass. These early glass eyes were crude, uncomfortable to wear, and very fragile. Even so, the Venetians continued making them and kept their methods secret until the end of the eighteenth century when German glassblowers developed superior techniques and the center for glass eye making moved to Germany. Shortly thereafter, glass eye making was introduced in the United States.

D.W. Hardin
Ocular and Facial Prosthetics, Darrell W. Hardin Inc., 34950 chardon Road Ste 103, Willoughby Hills, OH 44094, USA

Ohio Optical Dispensers Board, 77 South High Street 16th Floor, Columbus, OH 43215, USA
e-mail: ping1960@att.net

J.D. Perry, A.D. Singh (eds.), *Clinical Ophthalmic Oncology*,
DOI 10.1007/978-3-642-40492-4_19,

19.3 Recent Developments

During World War II, the imported German glass used for glass prostheses became unavailable in the United States. As a result of this shortage, the US Government in conjunction with a number of American firms popularized the techniques for making artificial eyes out of acrylic plastic. The popularity of this method has continued to increase over the years, and today the vast majority of patients wear ocular prostheses made of acrylic.

19.4 Steps in Construction of Artificial Eye

It is recommended to wait for 6 weeks following enucleation to allow complete healing prior to fitting of prosthesis.

Socket impression is obtained by inserting the impression tray into the socket and then injecting alginate through a syringe into the tip of the impression tray (Fig. 19.1a). This fills the socket with the impression material, which hardens in

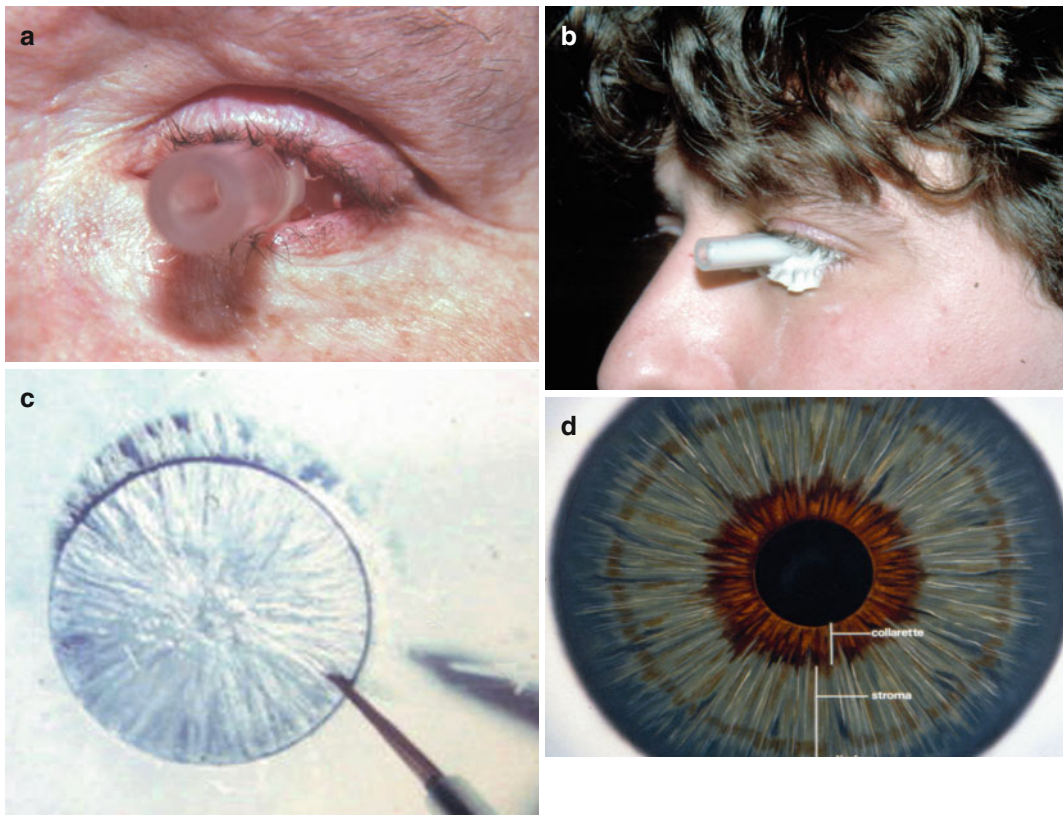

Fig. 19.1 Socket impression being obtained by inserting the impression tray into the socket (**a**). Alginate is injected through a syringe into the tip of the impression tray (**b**). Blank iris disc (**c**) and after it has been painted reproducing stroma and collarette (**d**). Appearance after lamination of corneal button (**e**). The iris cornea button recessed in the wax shape (**f**). Finished prosthesis after drawing of veins and pigment (**g**)

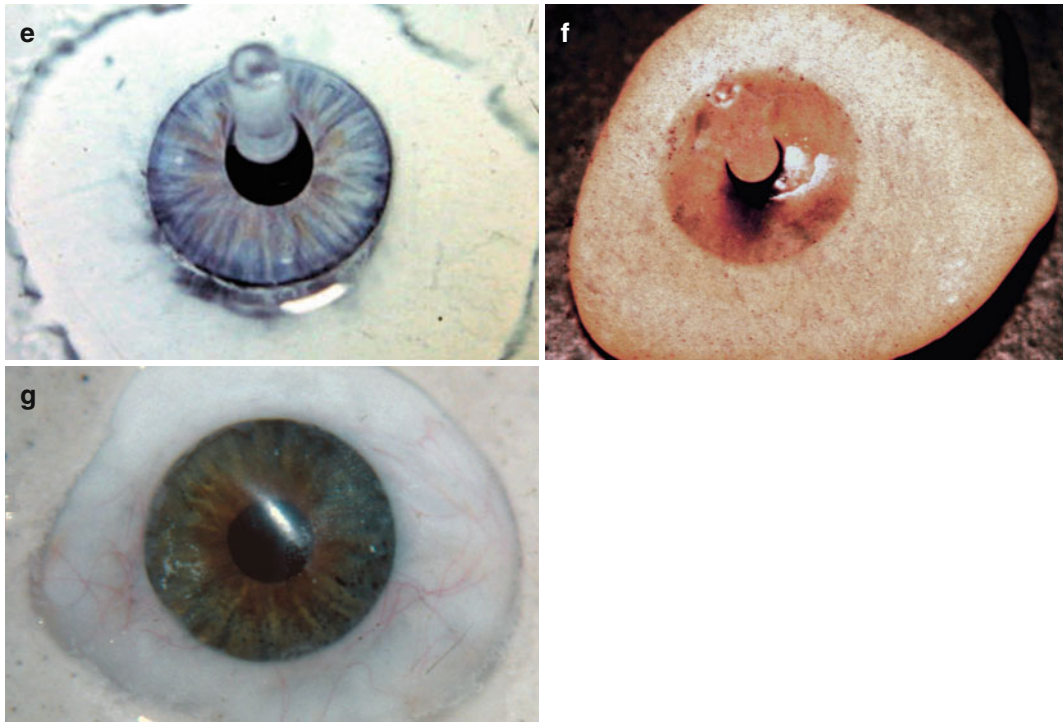

Fig. 19.1 (continued)

roughly 2 min (Fig. 19.1b). Impression is then poured in stone to make the first two-piece mold. After removing from stone, each piece of mold is then tinfoiled and burnished. Special resinated wax is poured into the cavity and allowed to cool. Iris disc (sized 10 mm through 13.5 mm) and cornea button are then selected with proper three-dimensional pupil (sizes 2–7 mm) (Fig. 19.1c). Iris disc is then hand painted (1,200–1,500 brush strokes), copying colors of existing eye to reproduce anatomy of stroma and collarette (Fig. 19.1d). After iris disc has dried, the corneal button is laminated in place (Fig. 19.1e). Wax shape is removed from mold, and the mold is discarded. The wax piece is trimmed, smoothed, and inserted in the socket. Thorough examination is done to check the fit. At this time, wax can be increased or decreased depending on the need. While in the socket, the pupil center is marked. The wax piece is removed from socket, and the area where the iris is to set is carved. The iris/cornea button is then recessed in the wax shape (Fig. 19.1f). After smoothening, the wax mold is reinserted in the socket; at this time the gaze is adjusted.

Upon completion of previous steps, a new mold is poured into a microwavable, two-piece flask, upper and lower unit. Wax shape is removed, and iris button is retrieved, placed in the mold, and packed with acrylic. After curing, eye is removed, trimmed, and polished. The eye is tried in socket and checked once again for proper fit and iris placement. Eye is removed and cut down for veining and pigmenting of

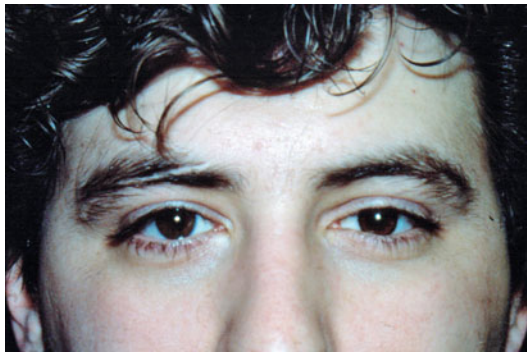

Fig. 19.2 Well-fitting prosthesis offering excellent cosmetic outcome

prosthesis. Veins are placed in position, reproducing pattern of existing eye (silk veins). Pigment (color) is placed in the same manner as veins. Prosthesis is cured for four additional hours. After curing, prosthesis is thoroughly examined and compared with patient's exiting eye for accuracy (adjustment or correction of pigmentation is completed at this time). Mold is tinfoiled and burnished. Prosthesis is placed in mold and packed with clear acrylic, which encapsulates pigmentation and adds proper anterior curvature (Fig. 19.1g). Prosthesis is removed, trimmed, and polished prior to final fitting and assessment for positioning (Fig. 19.2).

The patient is then given instructions for care and for a follow-up in 3–6 months after they receive the prosthesis or anytime if they have questions or problems.

Conclusions

Given low complication rates following enucleation and custom designing of prosthesis, excellent cosmetic appearance can be achieved in the vast majority of cases. With proper fit, maintenance, and cleaning, the prosthesis provides years of comfort and usefulness.